

Carbon Hydrogen Bond Activation of Aldehydes by Rhodium (III) Porphyrins

by

LAU Cheuk Man

Thesis Submitted to the Department of Chemistry
in Partial Fulfilment of the Requirements for the Degree of
Master of Philosophy
in
Chemistry

Thesis/Assessment Committee:

Professor SHING Kung Ming Tony, Chair

Professor CHAN Kin Shing, Committee Member

Professor NG Kee Pui Dennis, Committee Member

Professor LAU Chak-po, External Examiner

© The Chinese University of Hong Kong

July 2005

The Chinese University of Hong Kong holds the copyright of this thesis. Any person(s) intending to use a part or whole of the materials in the thesis in a proposed publication must seek copyright release from the Dean of the Graduate School.



Table of Contents

	Page
Table of Contents	i
Acknowledgements	iii
Abbreviations	iv
Structural Abbreviations for Porphyrin Complexes	v
Abstract	vi
Chapter 1 Introduction	
1.1 General Introduction	1
1.2 Activation of Carbon-Hydrogen Bond (CHA) by Transition Metal	2
1.2.1 Application of CHA by Transition Metals	3
1.2.2 Thermodynamic in CHA by Transition Metals	5
1.2.3 Types of Carbon-Hydrogen Activations	6
1.3 Carbon-Hydrogen Bond Activation of Aldehydes	14
1.3.1 Catalytic Application of CHA of Aldehydes by Transition Metals	14
1.3.2 Stability of Intermediate M(COR)	15
1.3.3 Issue in Selectivity	16
1.4 Structural Features of Rhodium Porphyrins	23
1.5 Objective of the work	24
Chapter 2 Carbon-Hydrogen Activation of Aldehydes by Rh(tp)Cl and Rh(tp)Me	
2.1 Introduction	26
2.2 CHA of Aldehydes by Rh(tp)Cl	27
2.2.1 Preparation of Rh(tp)Cl	27
2.2.2 Solvents Screening	27
2.2.3 Results and Discussion	30
2.3 CHA of Aldehydes by Rh(tp)Me	33
2.3.1 Preparation of Rh(tp)Me	34
2.3.2 Results and Discussion	35
2.4 Mechanistic Studies	37
2.4.1 CHA of Aldehydes by Rh(tp)Cl	37
2.4.2 CHA of Aldehydes by Rh(tp)R	42
2.5 Comparison of the $\nu(\text{C}=\text{O})$	48
2.6 X-ray Data	49

2.7 Summary	50
Chapter 3 CHA of Aldehydes by Rh(ttp)CH₂CH₂OH and Rh(ttp)⁺X⁻	
3.1 Introduction	52
3.2 CHA of Aldehydes by Rh(ttp)CH ₂ CH ₂ OH	53
3.2.1 Results and Discussion	53
3.2.2 Mechanistic Studies	61
3.3 CHA of Aldehydes by Rh(ttp) ⁺ X ⁻	65
3.4 Summary	67
Conclusion	68
Experimental	69
Reference	93
Appendix I Crystal Data and Processing Parameters	99
List of Spectra	141
Spectra	143

Acknowledgement

I would like to express my most sincere gratitude to my supervisor, Prof. Kin Shing Chan, for his invaluable advice, guidance and enthusiasm in my postgraduate studies throughout these consecutive years. Also, he inspired me much in learning how to utilize fundamental chemical knowledge in my research.

I should also like to give thanks to all members of the Department of Chemistry for their help and technical support in all circumstances.

Special thanks should be given to Mr Siu Kwan Yeung for communication of his preliminary results and assistance on laboratory techniques.

Thanks are also given to all my dear current and former group members in Room 357: Dr Kin Wah Mak, Dr Man Kin Tse, Dr Fuk Yee Kwong, Mr Timothy Tin Lok Tam, Mr Chi Wai Lai, Mr Michael Yu, Mr Tse Ho Lai, Mr Peng Fai Chui, Ms Li-rong Zhang and Mr Xin Zhu Li for their encouragement and helpful discussion. Without their help, I think I would not be able to finish the course of my study.

July, 2005.

Cheuk Man Lau

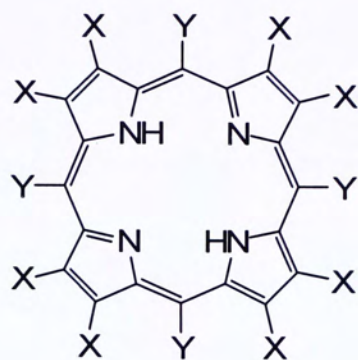
Department of Chemistry

The Chinese University of Hong Kong

Abbreviations

δ	: chemical Shift	MHz	: megahertz
Anal	: analytical	min	: minute (s)
Bn	: benzyl	mL	: milliliter (s)
B.D.E.	: bond dissociation energy	mmol	: milimole (s)
br s	: broad singlet (NMR)	MS	: mass spectrometry
^t Bu	: <i>tert</i> -butyl	NMR	: nuclear magnetic resonance
Calcd.	: calculated	oep	: octaethylporphyrin
d	: day (s)	Por	: porphyrin dianion
d	: doublet (NMR)	ppm	: part per million
DMF	: <i>N,N</i> -dimethylformamide	PPh ₃	: triphenylphosphine
E	: entropy	Ph	: phenyl
Et	: ethyl	PhCN	: benzonitrile
FABMS	: fast atom bombardment mass spectrometry	Py	: pyridine
g	: gram (s)	q	: quartet (NMR)
G	: Gibbs free energy	r.t.	: room temperature
GCD	: gas chromatography detector	s	: second (s)
h	: hour (s)	s	: singlet (NMR)
HRMS	: highest resolution mass spectrometry	ttp	: tetratolyporphyrin
Hz	: Hertz	tmp	: tetramesitylporphyrin
IR	: infrared	THF	: tetrahydrofuran
<i>J</i>	: coupling constant	t	: triplet (NMR)
m	: multiplet (NMR)	TLC	: thin-layer chromatography
M ⁺	: molecular ion	TMS	: tetramethylsilane
M	: Molarity	μ L	: microliter (s)
Me	: methyl		
mg	: milligram (s)		

Structural Abbreviations for Porphyrins



Nomenclature of Porphyrins

Abbreviations	Porphyrin	X	Y
H ₂ (ttp)	tetratolyporphyrin	H	4-CH ₃ C ₆ H ₄
H ₂ (tmp)	tetramesitylporphyrin	H	2,4,6-(CH ₃)C ₆ H ₂
H ₂ (oep)	octaethylporphyrin	Et	H

Abstract

Selective aldehydic carbon-hydrogen bond activation (CHA) of aryl and alkyl aldehydes was found in several rhodium porphyrins, Rh(tp)Cl, Rh(tp)Me and Rh(tp)CH₂CH₂OH to give aryoyl and acyl rhodium porphyrin complexes (RCORh(tp)).

Both Rh(tp)Cl and Rh(tp)Me reacted with aldehydes in solvent-free conditions at 200°C. Rh(tp)Cl reacted with aldehydes to give both CHA products and reduction products in a manner of the classical electrophilic activation of hydrocarbons, while much cleaner reaction occurs with Rh(tp)Me. Successful CHA in mild, aerobic conditions at 50°C in THF were achieved with Rh(tp)CH₂CH₂OH. Rate acceleration was accomplished with the addition of PPh₃ to Rh(tp)CH₂CH₂OH

摘要

芳基醛及烷基醛的醛碳氫鍵 (Aldehydic C-H Bond) 可被數個類型的卟啉銠絡合物 ($\text{Rh}(\text{ttp})\text{Cl}$, $\text{Rh}(\text{ttp})\text{Me}$ 及 $\text{Rh}(\text{ttp})\text{CH}_2\text{CH}_2\text{OH}$) 選擇性地活化，繼而產生酰基卟啉銠複合物 ($\text{RCORh}(\text{ttp})$)。

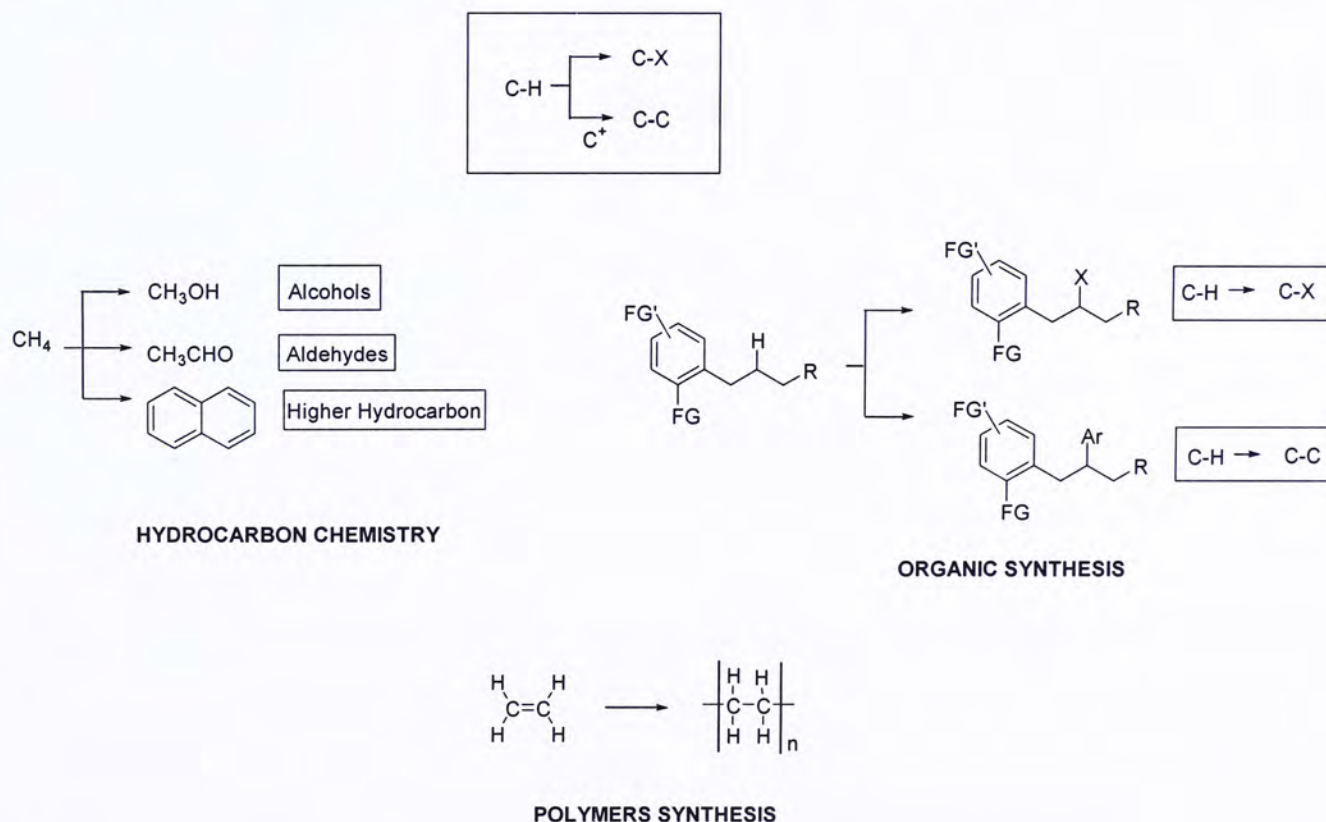
在無溶劑高溫條件下， $\text{Rh}(\text{ttp})\text{Cl}$ 及 $\text{Rh}(\text{ttp})\text{Me}$ 可與醛反應。 $\text{Rh}(\text{ttp})\text{Cl}$ 透過典型親電活化 (electrophilic activation) 產生醛碳氫鍵複合物及還原產物 (reduction product)，而 $\text{Rh}(\text{ttp})\text{Me}$ 反應則相對比較乾淨。在溫和有氧情況下，醛碳氫鍵可被 $\text{Rh}(\text{ttp})\text{CH}_2\text{CH}_2\text{OH}$ 成功活化，其反應速度可因加入 PPh_3 而得到改善。

Chapter 1 Introduction

1.1 General Introduction

1.1.1 Hydrocarbons

The ultimate source of hydrocarbons in nature is the fossil fuels (including coal, petroleum and natural gas), which are regarded as the major and the commonest energy source in our daily life. About two-thirds of the coal mined today is burnt in power stations to generate electricity, while petroleum and natural gas are burnt to supply energy. Besides energy supply, the hydrocarbons could also be functionalized into various chemicals, plastics, alcohols for our daily use (Scheme 1.1).¹

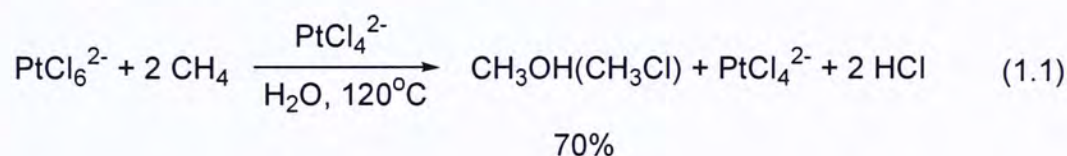


Scheme1.1 C-H bonds Functionalization.

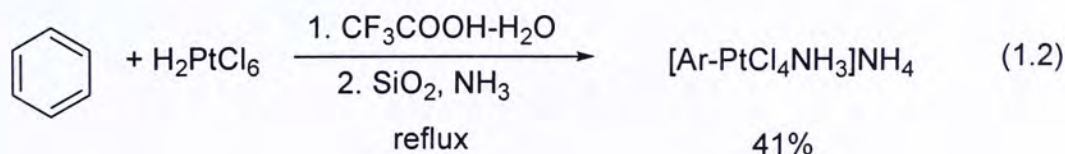
1.2 Activation of Carbon-Hydrogen Bond (CHA) by Transition Metals

Generally, functionalization of hydrocarbons consists of two essential problems: (1) activation of the hydrocarbons, and (2) functionalization once it has been activated. It is also desirable to carry out functionalization in catalytic and selective manners under mild conditions.

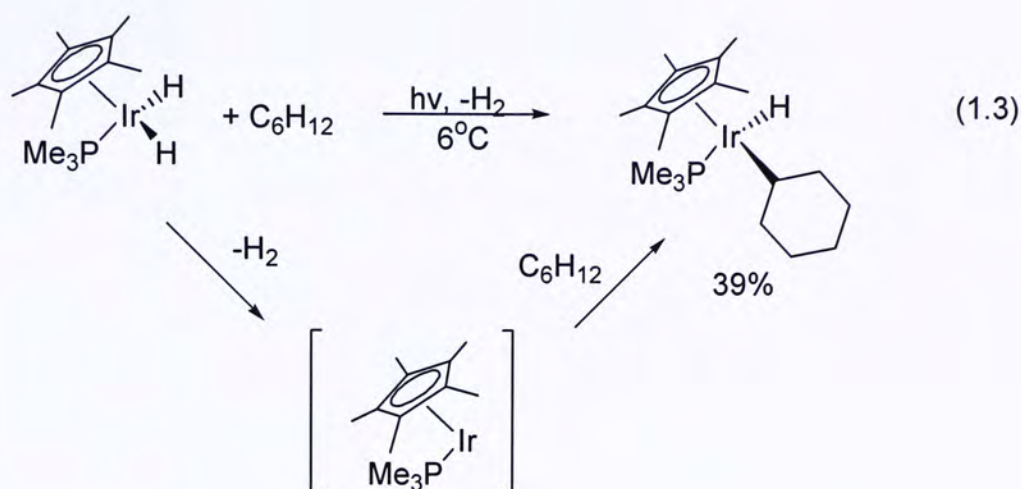
Early examples on CHA of alkanes were reported by Shilov. The addition of Pt(IV) to the aqueous reaction of PtCl_4^{2-} with methane leads to the production of methanol and methyl chlorides. It illustrates an “electrophilic” CHA. (eq. 1.1)²



Later in 1980's, Shilov and Bergman observed activation of aromatic C-H bonds to metal centers. Shilov reported that H_2PtCl_6 reacted with arenes to afford the anionic σ -aryl Pt(IV) complexes (eq. 1.2).³



Bergman demonstrated the first examples of intermolecular oxidative addition of arene C-H bonds to give stable alkyl iridium hydrides (eq. 1.3).⁴ The iridium dihydride $\text{Cp}^*\text{Ir}(\text{H})_2\text{PMe}_3$ ($\text{Cp}^* = \eta^5\text{-C}_5\text{Me}_5$) was irradiated in cyclohexane solution to produce the complex $\text{Cp}^*(\text{PMe}_3)\text{Ir}(\text{H})(\text{C}_6\text{H}_{11})$ in satisfactory yield via the intermediate of $\text{Cp}^*\text{Ir}(\text{PMe}_3)$. The $\text{Cp}^*\text{Ir}(\text{PMe}_3)$ metal fragment also preferred to cleave the stronger C-H bonds ($\text{aryl} > 1^\circ > 2^\circ > 3^\circ$).⁵

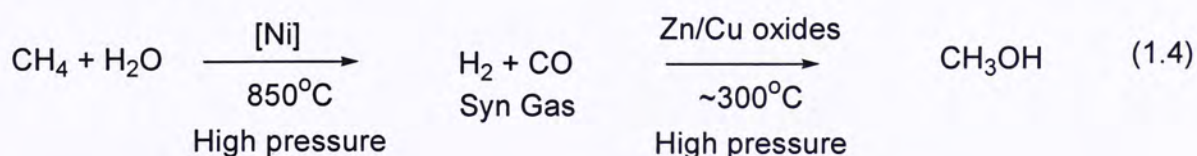


1.2.1 Application of CHA by Transition Metals

CHA by transition metal carried out in catalytic manner allows the conversion of hydrocarbons into value-added derivatives. The following two catalytic processes illustrate the industrial importance.

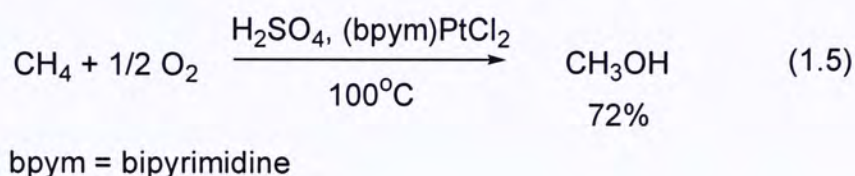
(1) Production of methanol (CH₃OH) from methane (CH₄) via CH activation

Methanol is a clean and effective energy source; in addition, it is a good and important raw material for higher hydrocarbons. In current technologies, methanol is produced from the natural gas (CH₄). Natural gas generates into carbon monoxide (CO) and hydrogen (H₂) (syn-gas) which are then converted to methanol through Fischer-Tropsch chemistry (eq. 1.4).^{6, 7}



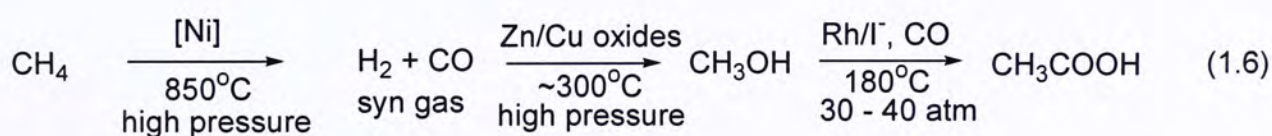
However, such process is energy intensive and proceeds at high temperatures (850 °C). Hence a modified direct method in functionalizing the C-H bond in a more efficient

and cost-effective manner is desirable. Recently, Periana et al developed a direct, low-temperature (100°C), oxidative conversion of methane to methanol in 72% one-pass yield at 81% selectivity based on methane by using the Pt complex as catalyst (eq. 1.5).⁸

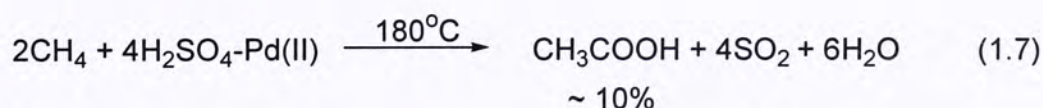


(2) Production of acetic acid (CH₃OOH) from methane (CH₄) via CH activation

Acetic acid is currently synthesized from methane in a three-step capital-intensive and energy-intensive process based on the high-temperature conversion of methane into syn gas; then, conversion of syn gas to methanol; finally carbonylation of the methanol to acetic acid via the Monsanto process or Cativa process (eq. 1.6).^{6,7,11} Hence, recent research efforts are being directed at a more direct and less expensive method.

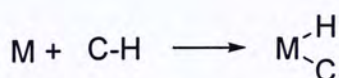


In the development of oxidative conversion of methane to its derivatives, Periana also observed the direct, one-step, selective oxidative condensation of two methane molecules to acetic acid at 180°C in liquid sulfuric acid in low yields (~ 10%) based on methane by Pd(II) complexes (eq. 1.7).⁹



1.2.2 Thermodynamic in CHA by Transition Metals

The CHA is believed to be controlled by the thermodynamic of the product formation. By considering the bond dissociation energy (BDE)¹⁰ of bonds being broken and made, the thermodynamic of CHA is estimated. The C-H bond energy in methane is 105 kcal mol⁻¹, the C-C bond energy is about 89 kcal mol⁻¹ in ethane;¹⁰ the BDE of activated M-C bond for late transition metals is about 60 kcal mol⁻¹ and the M-H bond has the BDE of 60 kcal mol⁻¹.⁴⁷ In the simplest form, a metal reacts with a C-H bond to form both the M-C and M-H bonds. The estimated ΔH_{298} is about -16 kcal mol⁻¹ and ΔG_{298} is about -6 kcal mol⁻¹. Therefore the C-H bond activation by transition metal is thermodynamically favorable (Figure 1.1).¹²



$$\Delta H^0 \sim (M-H) + (M-C) - (C-H)$$

$$\Delta G = \Delta H - T\Delta S$$

$$\begin{aligned} \Delta H_{298}(\text{estimated}) &= (M-H) + (M-C) - (C-H) - (M) \\ &= (-60 \text{ kcal mol}^{-1}) + (-60 \text{ kcal mol}^{-1}) - (-104 \text{ kcal mol}^{-1}) - 0 \text{ kcal mol}^{-1} \\ &= -16 \text{ kcal mol}^{-1} \end{aligned}$$

where ΔS is negative $\sim 35\text{eu}$

$$\begin{aligned} \text{hence, } \Delta S_{298}(\text{estimated}) &= (298\text{K})(35\text{eu})/1000 \\ &= 10 \text{ kcal mol}^{-1} \text{ (Ref 13)} \end{aligned}$$

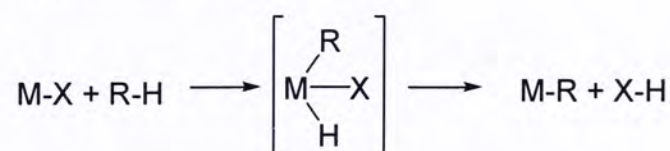
$$\begin{aligned} \Delta G_{298}(\text{estimated}) &= \Delta H_{298}(\text{estimated}) - \Delta S_{298}(\text{estimated}) \\ &= -16 \text{ kcal mol}^{-1} - (-10 \text{ kcal mol}^{-1}) \\ &= -6 \text{ kcal mol}^{-1} \end{aligned}$$

Figure 1.1 Estimated ΔH_{298} for C-H activation by transition metals

1.2.3 Types of Carbon-Hydrogen Bond Activations

C-H activation by transition metal complexes can be divided into five categories: (A) C-H bonds can be activated by oxidative addition at a single metal center, in which the interaction usually involves a 3-centered cyclic transition state. (B1). Electrophilic activation *or* (B2) sigma-bond metathesis, which involves electron deficient early transition metals (d^0) and f-elements. In such reactions, metals are known to form metal alkyls with strong M-C bonds, and it is usually considered to occur through a four-centered cyclic transition states. (C) C-H bonds can be activated via homolytic or radical process, which involves the metalloradical to initiate the reaction. Finally, CHA can be achieved by (D) reversible addition of C-H bond across M=X bonds (X = heteroatom or alkylidene). This process also involves a four-centered cyclic transition state (Scheme 1.2).^{12, 76}

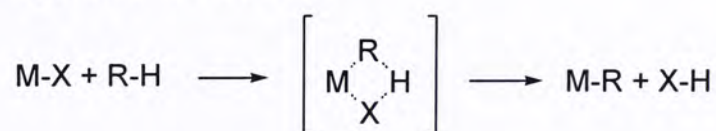
(A) Oxidative Addition



(B1) Electrophilic Activation



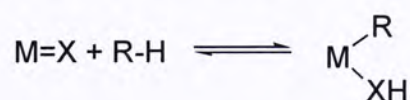
(B2) Sigma Bond Metathesis



(C) Homolytic or Radical process



(D) Reversible addition of C-H bond across M=X

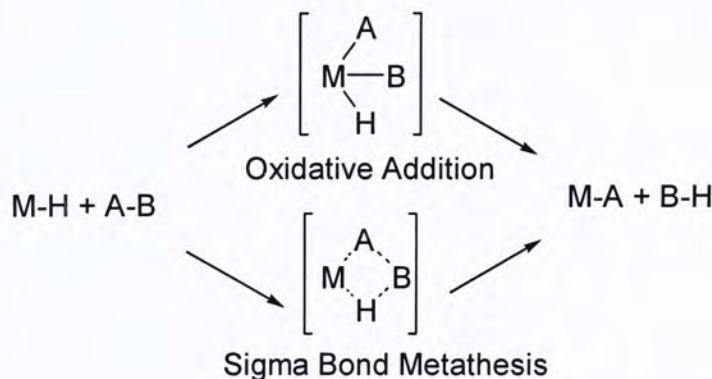


Scheme 1.2 Five basic C-H activation pathways

(1) Oxidative Addition and Electrophilic Activation (or Sigma Bond Metathesis) of C-H bonds

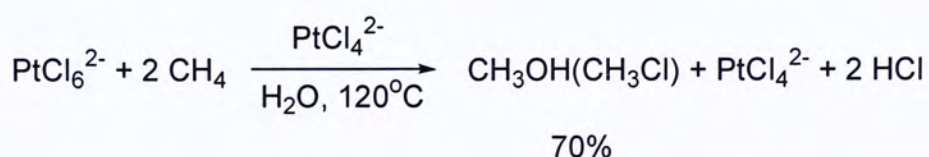
Oxidative addition and sigma-bond metathesis are bimolecular processes. Therefore they follow the second order rate law ($k_2[M][AB]$).¹⁴ Oxidative addition is the addition of A-B to a metal M. The metal center is formally oxidized by two electron loss. The metal goes from n to $n+2$ oxidation states. However, when the transition metal is at its highest oxidation state (e.g. Ir(V)) or lacks of low lying d -electrons (d^0), sigma-bond metathesis will proceed and occur through a four-centered cyclic transition state. Only the isolation of intermediate is possible to establish the oxidative addition pathway. Oxidative addition and sigma bond metathesis are compared in Table 1.1.¹⁴

Table 1.1 Comparison between oxidative addition and sigma bond metathesis.

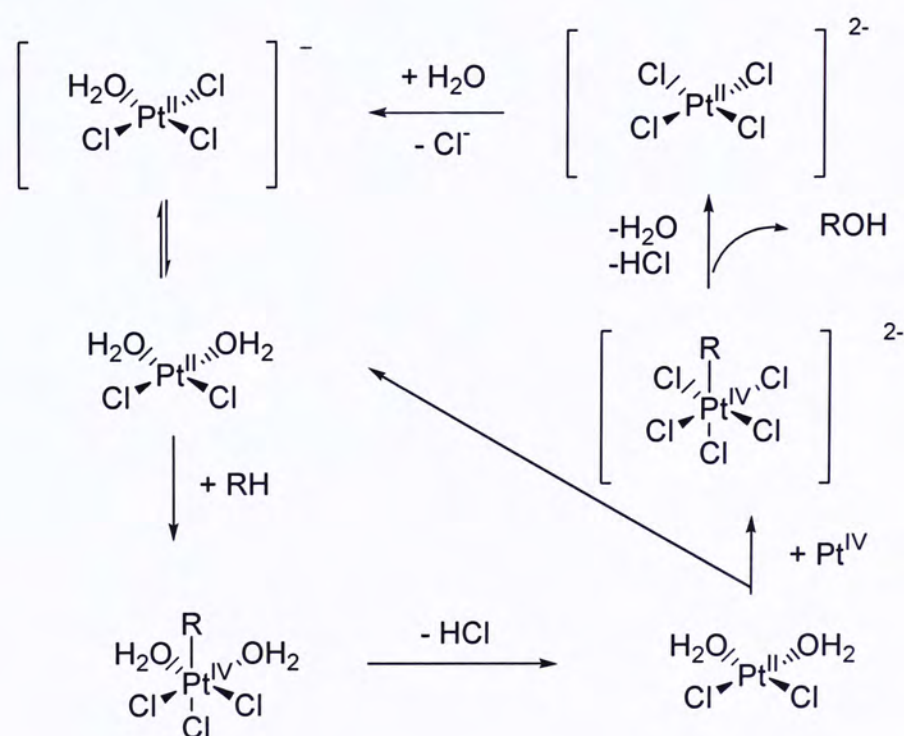


	Oxidative addition	sigma-bond metathesis
Reaction type	Bimolecular	Bimolecular
Oxidation state for [M]	n to $n+2$ (Ir ³⁺ to Ir ⁵⁺ is possible) ^{23,24}	Unchanged (Sc ⁺² to Sc ⁺⁴ is impossible)
Kinetic rate law	$k_2[M][AB]$ (2 nd order)	$k_2[M][AB]$ (2 nd order)
ΔS^\ddagger (eu)	-35 ¹³	-36 ^{15 - 17}
Oxidative Addition Intermediate	Yes	No

C-H activation with Pt(II) observed by Shilov in 1970s gives an example of oxidation addition. CHA of alkanes catalyzed by Pt complex, which Pt(II) is oxidized into Pt(IV). The reaction continuously reacts in a cycle to yield the products at mild conditions. Scheme 1.2 illustrates the mechanism with the oxidative addition as the key elementary step.²

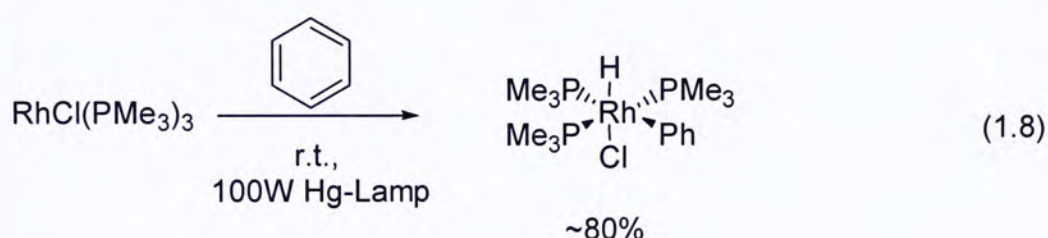


Proposed Mechanism

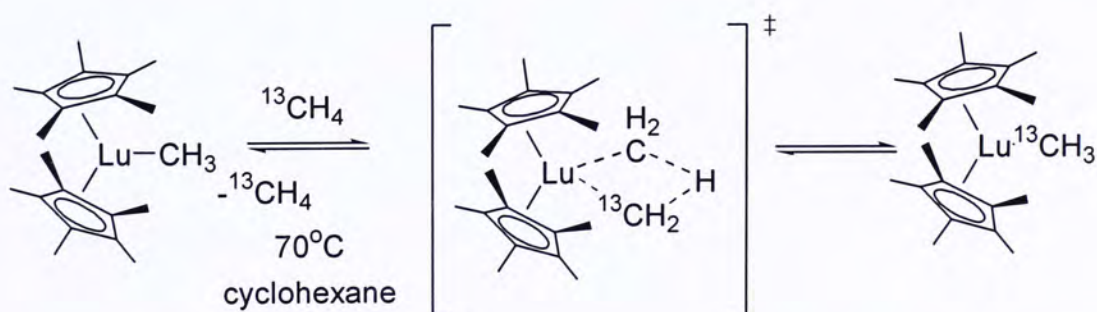


Scheme 1.2. C-H activation of Pt(II) and alkane.

Other low valent transition metals are also used in the oxidative addition of arenes C-H bonds. One of the most typical examples is the intermolecular addition of arene C-H bonds to give stable alkyl iridium hydrides reported by Bergman as discussed in section 1.2.⁴ Other examples of oxidative addition of C-H bonds have also been reported recently (eq. 1.8).¹⁸

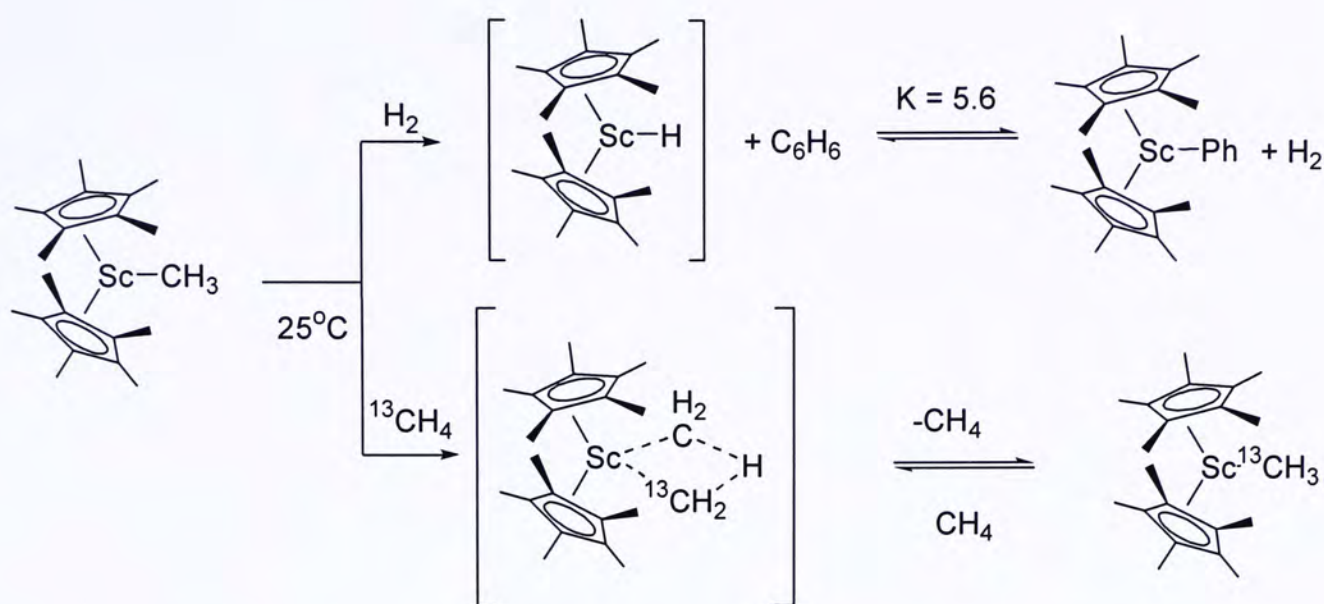


Usually sigma bond metathesis happens in high valent early transition metals since these metals lack the d -electrons (d^0). Watson reported that $\text{Cp}^*_2\text{LuCH}_3$ exchanged its methyl ligand with $^{13}\text{CH}_3\text{-H}$ at 70°C in cyclohexane solution (Scheme 1.3).¹⁹



Scheme 1.3 $\text{Cp}^*_2\text{LuCH}_3$ exchanges with $^{13}\text{CH}_4$ via sigma bond metathesis.

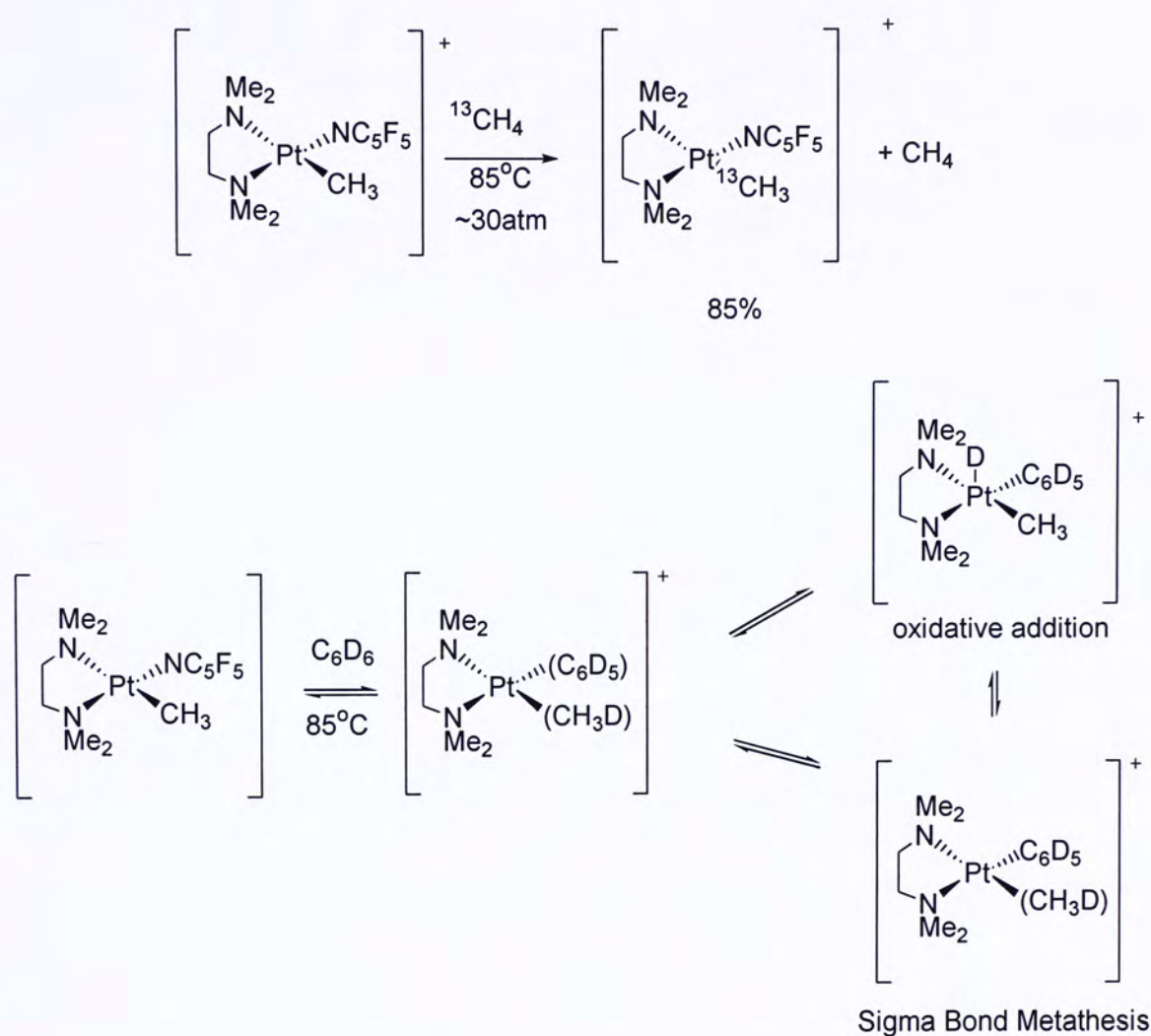
Bercaw also reported the exchange of $^{13}\text{CH}_3$ with the scandocene complex (Cp^*ScMe) (Scheme 1.4).²⁰ In the presence of hydrogen, the $[\text{Cp}^*_2\text{ScPh}]$ was generated. $[\text{Cp}^*_2\text{ScH}]$ further reacted with benzene to give Cp^*_2ScPh in an equilibrium with $K_{\text{eq}} = 5.6$ at 25°C . A sigma bond metathesis mechanism was suggested.



Scheme 1.4 Electrophilic activation of C-H bonds by scandocene complex.

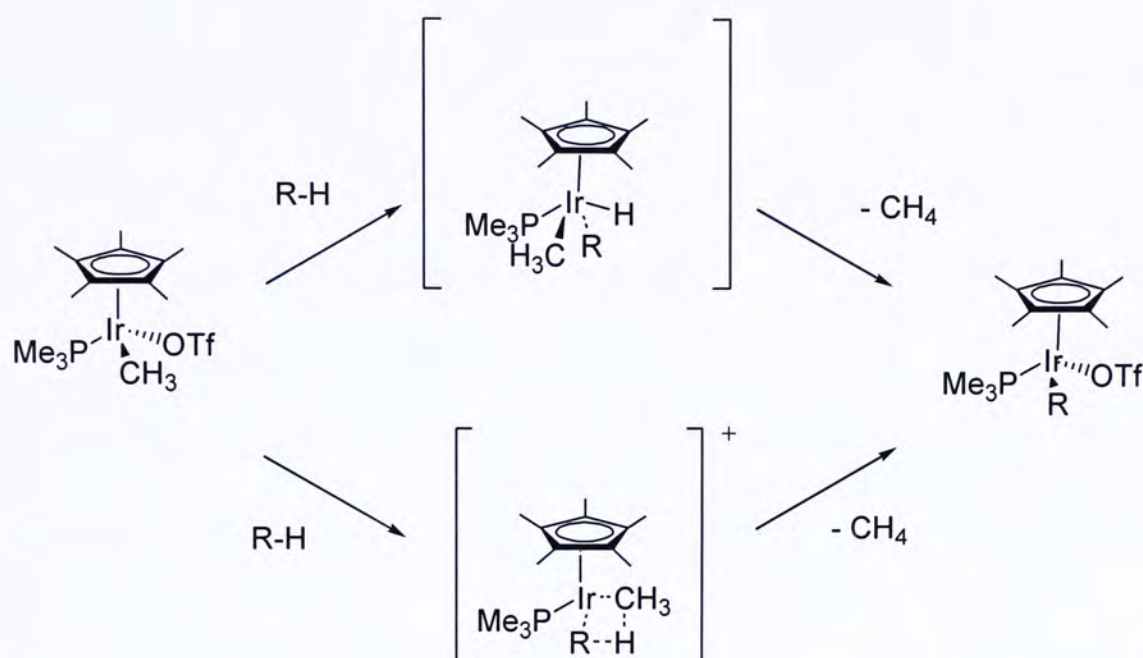
(C) Differentiation between the Oxidative Addition and Sigma Bond Metathesis

In most cases, it is rather difficult to distinguish between oxidative addition and sigma bond metathesis if the metal has easily accessible higher oxidation state. One favorite example was reported by Bercaw and Labinger on the oxidation of methane to Pt^{II} complex. The $[(\text{tmeda})\text{Pt}(\text{CH}_3)(\text{NC}_5\text{F}_5)]^+$ was treated with 30 atm $^{13}\text{CH}_4$, an exchange of methyl group was observed between the Pt^{II} complex and methane. When the $[(\text{tmeda})\text{Pt}(\text{CH}_3)(\text{NC}_5\text{F}_5)]^+$ was heated in C_6D_6 , the methane isotopomers CH_4 , CH_3D , CH_2D_2 and CHD_3 were observed in the ^1H NMR after several days. The observation of H/D exchange was interpreted in terms of the oxidative addition of C-H bond to give Pt^{IV} dialkyl hydride and the formation of Pt^{II} sigma-complex (Scheme 1.5).²¹



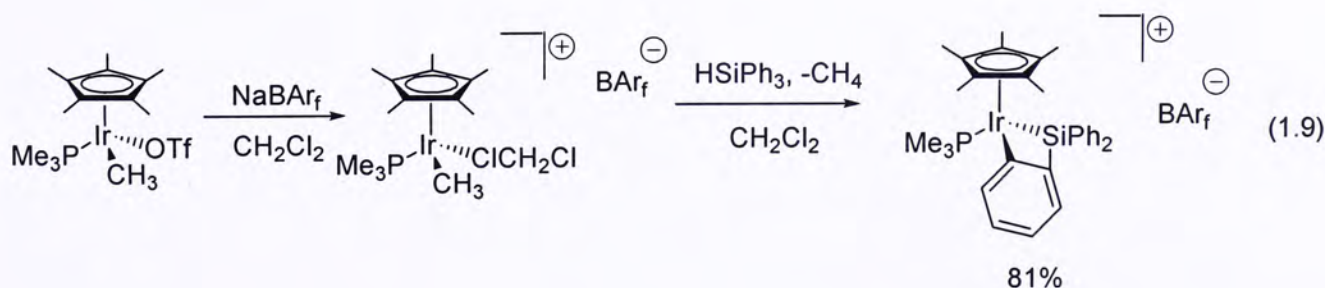
Scheme 1.5 C-H activation at cationic Pt(II) center.

Bergman also reported the reaction of $\text{Cp}^*(\text{PMe})\text{Ir}(\text{III})\text{MeOTf}$ ($\text{Me} = \text{CH}_3$, $\text{OTf} = \text{OSO}_2\text{CF}_3$) with alkanes; two possible mechanistic pathways: oxidative addition and sigma-bond metathesis were proposed (Scheme 1.6).²⁵



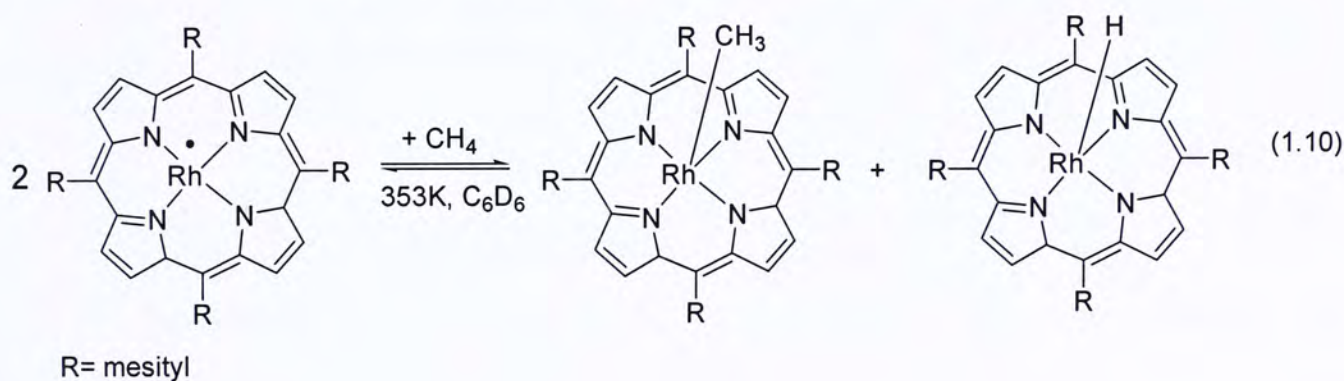
Scheme 1.6 C-H activation of iridium (III) complexes via Ir(V) as intermediate.

In order to distinguish the mechanistic pathway, reaction between the $[\text{Cp}^*(\text{PMe}_3)\text{Ir}(\text{Me})(\text{CH}_2\text{Cl}_2)[\text{BAR}_f]]$ ($\text{BAR}_f = \text{B}(\text{C}_6\text{F}_5)_4$) with tertiary silane was carried out, and Ir(V) complex was formed in 81% yield, which it was further characterized by X-ray analysis. Indeed other stable organometallic Ir(V) complexes had been reported by Perutz²³ and Maitilis.²⁴ The literature precedent Ir(V) complexes lend strong support to the oxidative addition mechanism via Ir(V) oxidation state (eq. 1.9).²⁵ In addition, a theoretic study also strongly supported oxidative addition over sigma-bond metathesis in this case.²²



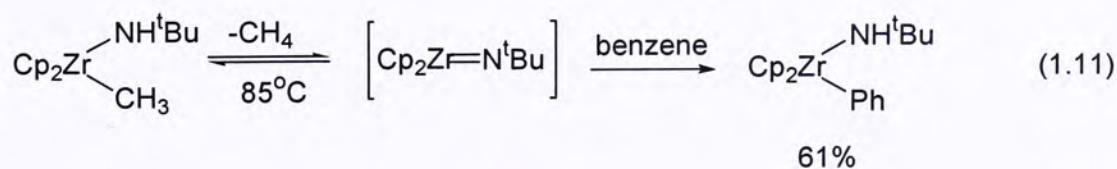
(2) Homolytic or Radical Activation of C-H bond

Wayland demonstrated the CHA by rhodium (II) porphyrin complexes which are the typical examples of such metalloradical reactions.²⁶⁻²⁹ The monomeric metalloradical, Rh(tmp) (tmp = tetramesitylporphyrin), activates methane via a 4-centered, transition state to give Rh(tmp)Me and Rh(tmp)H. Usually, this type of C-H activation is kinetically controlled by the size and shape of the substrate (eq. 1.10).



(3) Reversible Addition of C-H bond across M-X bonds

When the metal complex with a double bonded heteroatom reacts with the hydrocarbons, equilibrium of the exchange of the metal complex and the C-H activated products observed. This could be illustrated by Bergman's study on the C-H addition to a zirconium-nitrogen double bond complex with the imido complex as intermediate. After loss of methane from the zirconium complex, the imido complex is generated and activates the C-H bond of benzene (eq 1.11).³⁰

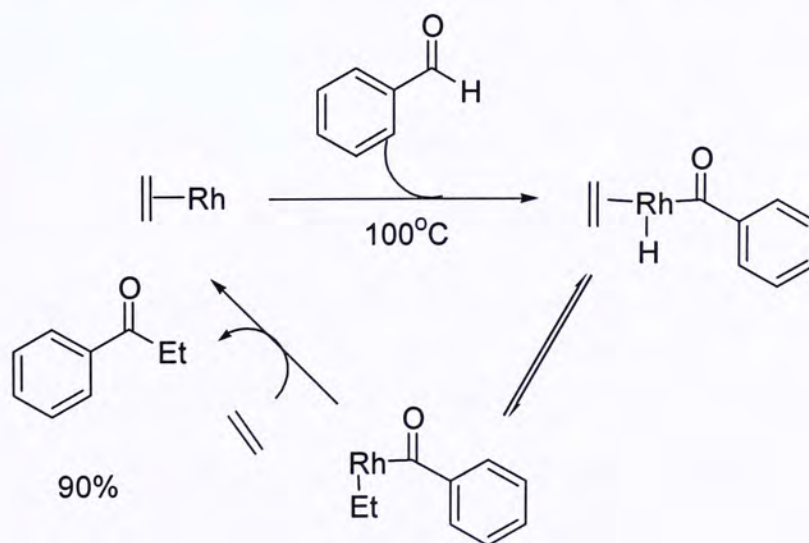


1.3 Carbon-Hydrogen Bond Activation of Aldehydes

The aldehydic C-H bond is a reactive C-H bond. It readily reacts with transition metal complexes. In general, the aldehydic C(O)-H_α bond is fairly weak and its bond energy is about 88.7 kcal mol⁻¹. While the aromatic C-H bond energy is about 112.9 kcal mol⁻¹ and the bond energy of the aliphatic C-H_β is around 98 kcal mol⁻¹.^{10, 31} Owing to this weak C-H bond, CHA of aldehydes is selective. Hence aldehydic CHA is used in preparation of organic compounds in a catalytic manner. The following examples show the catalytic application of the aldehydic CHA.

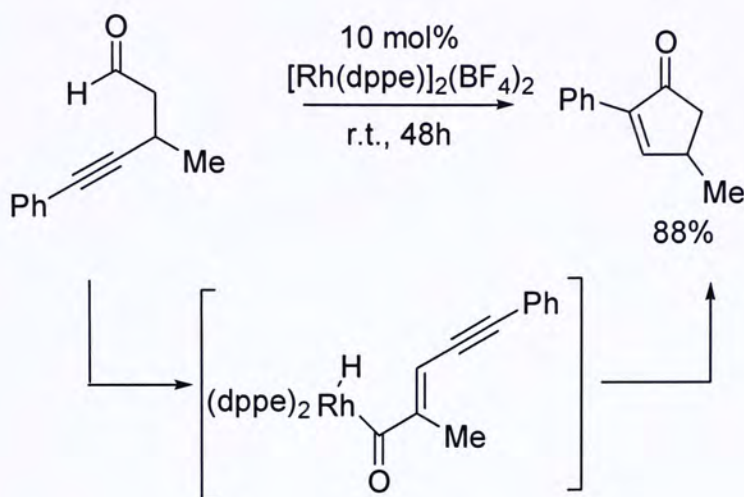
1.3.1 Catalytic Application of CHA of Aldehydes by Transition Metals

Milstein reported the catalytic application of aldehydic CHA in the intermolecular hydroacylation of olefin. The indenyl complex $[(\eta^5\text{-C}_9\text{H}_7)\text{Rh}(\eta^5\text{-C}_2\text{H}_4)_2]$ is a catalyst for intermolecular hydroacylation - the addition of aldehydes to alkenes (Scheme 1.7).³²



Scheme 1.7 Catalytic Hydroacylation of Olefin

Similar report by Fu on the synthesis of cyclopentenones by intramolecular hydroacylation catalyzed by rhodium(I) complex, it also shows a selective aldehydic C-H activation (Scheme 1.8).³³

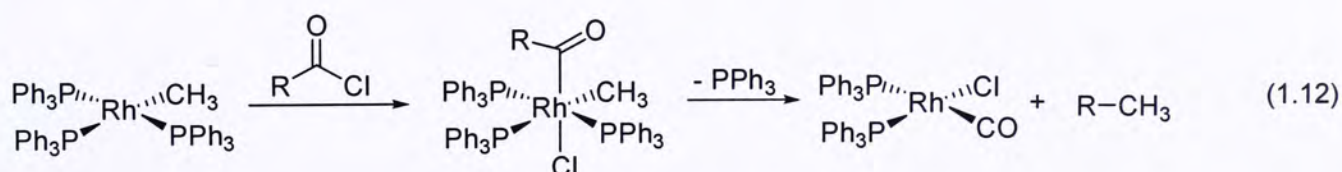


Scheme 1.8 Catalytic Intramolecular Hydroacylation of cyclopentenones

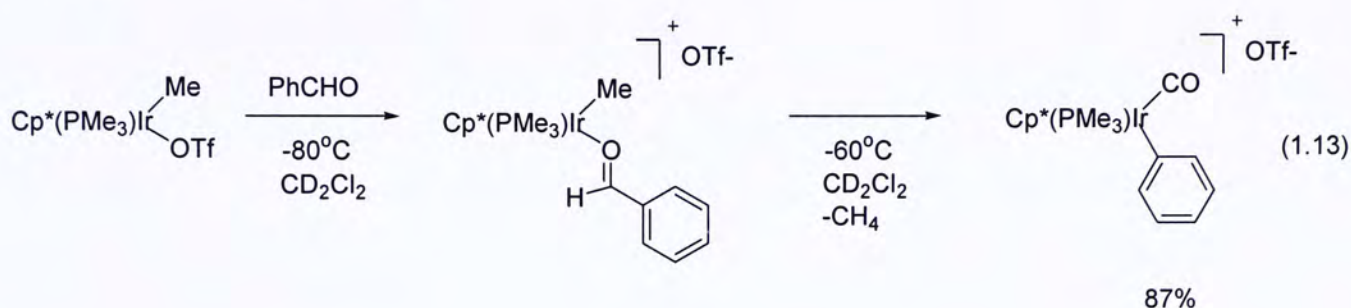
1.3.2 Stability of Intermediate M(COR)

Transition metals, such as Fe, Ru, Os, Pt, Rh and Ir, react with aldehydes to form the hydridoacylmetal complex, $M(H)(COR)$, which is useful in studying catalytic processes such as the decarbonylation of aldehydes and the hydroformylation of olefins. Usually, metal acyl hydride $M(COR)$ is unstable. The instability is generally due to their propensity either to decarbonylate or to reductive-eliminate.

For example the oxidative addition of the carbonyl group to Wilkinson's catalyst $RhCl(PPh_3)_3$, the intermediate product $(M(CO)R)$ further undergoes facile decarbonylation (eq. 1.12).⁷



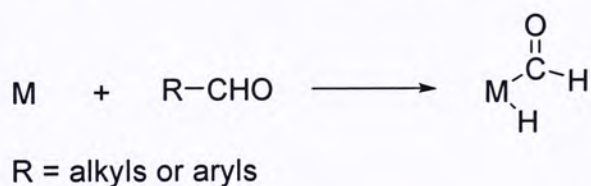
Similarly in CHA of aromatic aldehyde, MCOAr formed commonly undergoes facile decarbonylation. For example, $\text{Cp}^*(\text{PMe}_3)\text{Ir}(\text{Me})\text{OTf}$ reacts with benzaldehyde and gives the hydrocarbonyl carbonyl salt $[\text{Cp}^*(\text{PMe}_3)\text{Ir}(\text{Ph})(\text{CO})][\text{OTf}]$ instead of the benzoyl-iridium complex (Equation 1.13).³⁴



1.3.3 Issues in Selectivity

Thermodynamically, carbon-hydrogen bond activation of aldehydes at the aldehydic position is the most favorable in both aryl aldehydes and aliphatic aldehydes (Table 1.2). However, CHA at the aromatic C-H and aliphatic C-H bonds are also possible. The selectivity of the CHA of aldehydes will be discussed in the following section.

Table 1.2 Estimation on the thermodynamics of CHA of aldehydes by transition metals.



$$\Delta H^0 \sim (\text{M}-\text{H}) + (\text{M}-\text{C}) - (\text{C}-\text{H})$$

$$\Delta G = \Delta H - T\Delta S$$

where ΔS is negative $\sim 35\text{eu}$

$$\begin{aligned} \text{hence, } \Delta S_{298}(\text{estimated}) &= (298\text{K})(35\text{eu})/1000 \\ &= 10 \text{ kcal mol}^{-1} \text{ (Ref 13)} \end{aligned}$$

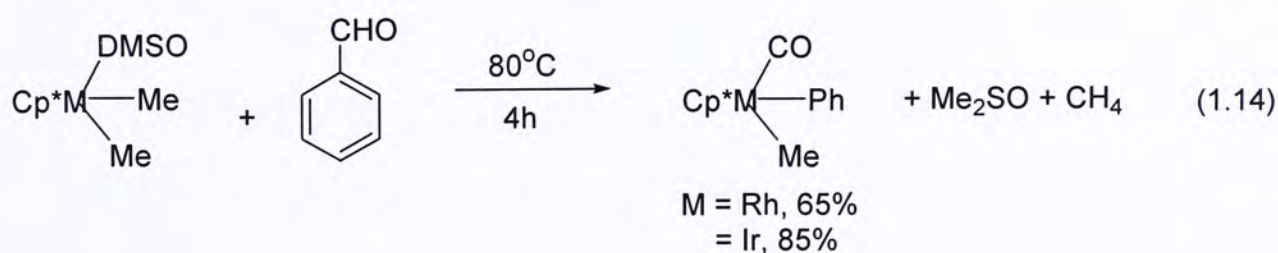
	BDE (kcal mol ⁻¹) ^{10,31}	ΔH_{298} (estimated) (kcal mol ⁻¹)	ΔG_{298} (estimated) (kcal mol ⁻¹)
C(O)-H_α ^a	88	-32	-23
C-H_{Ar} ^b	112	-18	-8
C-H_β	98	-22	-13

^a: BDE of M-C(O)R ~ 62 kcal mol⁻¹, ^b: BDE of M-Ph ~ 70 kcal mol⁻¹ (Ref 47).

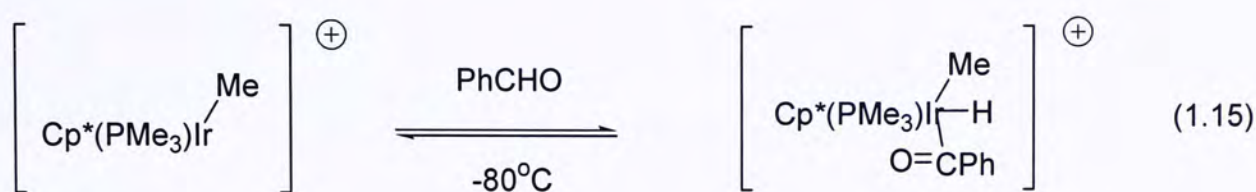
(1) CHA of Aryl Aldehydes (ArCHO)

The BDE of the aromatic C-H bond is 112 kcal mol⁻¹, while the BDE of the aldehydic C(O)-H_α bond is about 88 kcal mol⁻¹. In accordance with bond strengths, transition metals react with the aldehyde and produce the C(O)-H_α activation products as the major products while CHA at other position is rarely observed.

One of the examples of the aldehydic CHA was reported by Maitlis. The neutral complexes Cp^{*}M(Me)₂(DMSO) (M = Rh, Ir) react with aldehyde in cyclohexane at 80°C to yield the aldehydic CHA products. (eq. 1.14).³⁵

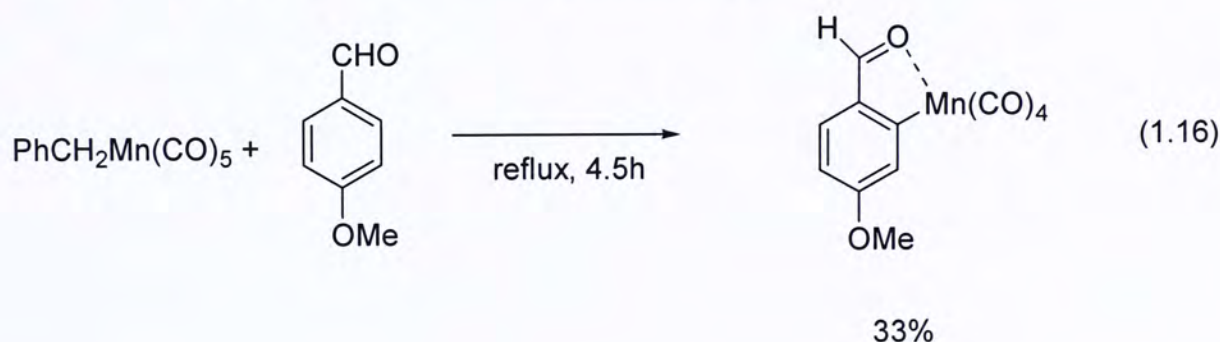


A recent example of the reaction between Cp^{*}(PMe₃)Ir(Me)OTf and benzaldehyde was reported by Bergman. An aldehydic C-H bond activation complex was observed in ¹H NMR, however the mechanism (oxidative addition or sigma bond metathesis) was not successful determined as the reaction was too rapid to monitor (eq. 1.15).³⁴

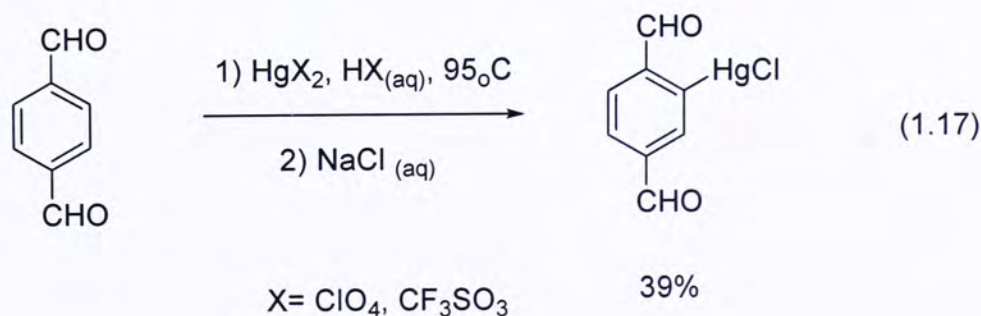


Though most examples show that aldehydic CHA is more favorable, there are few cases on *ortho*-CH activation. These examples show the important role of the weak coordination of oxygen to the metal center, which assists the C-H activation.

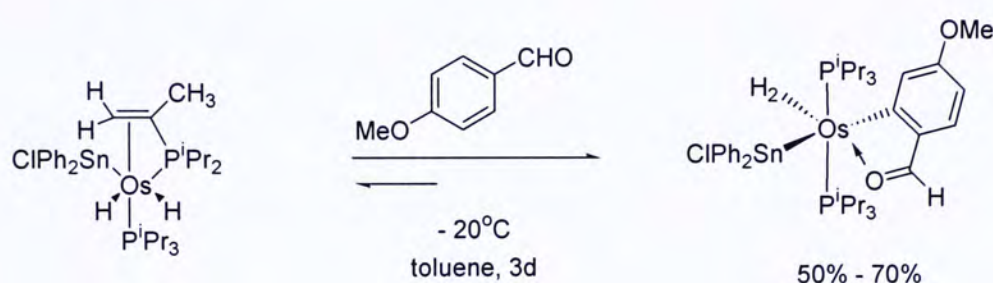
Generally, the *ortho*-CHA of aldehyde is performed by 14-valence-electron transition metals, e.g. Mn, Hg, Os. The earliest stoichiometric example is the reaction between $\text{PhCH}_2\text{Mn}(\text{CO})_5$ and *p*-methoxybenzaldehydes (eq. 1.16).³⁶



Later, Vicente and Abad found that HgCl_2 also reacted with 4-methoxybenzaldehyde to give the *ortho*-formylaryl complex (eq. 1.17). The reaction most likely operates through an electrophilic aromatic substitution ($\text{S}_{\text{E}}\text{Ar}$) pathway.³⁷

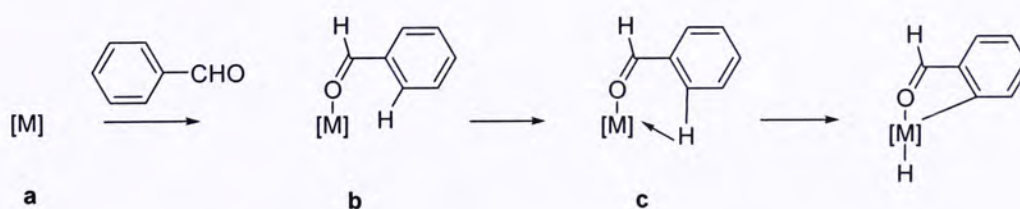


A chemoselective aromatic CHA of an aryl aldehyde occurs on osmium complex. The osium(VI) dihydride complex reacts with the 4-methoxybenzaldehyde to form the *ortho* aromatic CHA product (Scheme 1.9). The $\text{OsH}_4\text{Cl}(\text{SnPh}_3)(\text{P}^i\text{Pr}_3)_2$ is a synthon for the 14-valence electron monohydride, $\text{OsH}(\text{SnClPh}_2)(\text{P}^i\text{Pr}_3)_2$, which activates an *ortho*-CH bond of aromatic ketones.³¹



Scheme 1.9 Selective *ortho*-CHA by Osmium Complex

In the above cases, the selective *ortho*-CHA all happens in the 14-valence-electron metals. The addition of aldehyde to metal centers should involve the elementary steps shown in Scheme 1.11. Initially the formyl oxygen coordinates to the metal center. Then the cleavage of the closest *ortho*-CH bond takes place in two steps: (1) The *ortho*-M-C bond is formed (intermediate **c**), and being driven by the change in π bonds of the conjugated system. (2) Then intermediate **c**, which contains the *ortho*-M-C bond and the agostic C-H bond, is transferred to the metal to form the product (Scheme 1.10).³¹

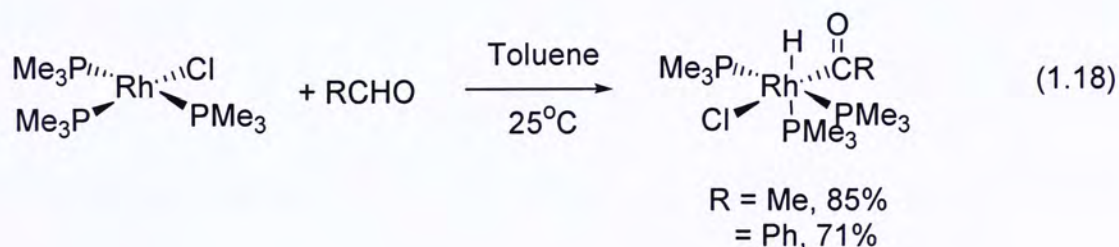


Scheme 1.10 The proposed mechanism

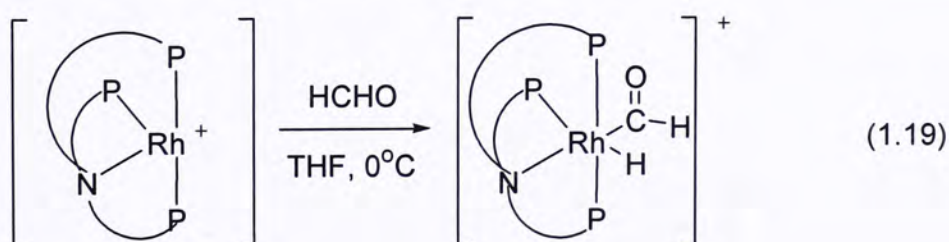
According to this mechanism, the *ortho* -CH addition of aryl aldehydes requires 2 empty valence orbitals in the metallic fragment to promote the activation. Hence, it is not surprising that 16-valence-electron complexes do not activate the *ortho* -CH bonds.

(2) CHA of Aliphatic Aldehydes (RCHO)

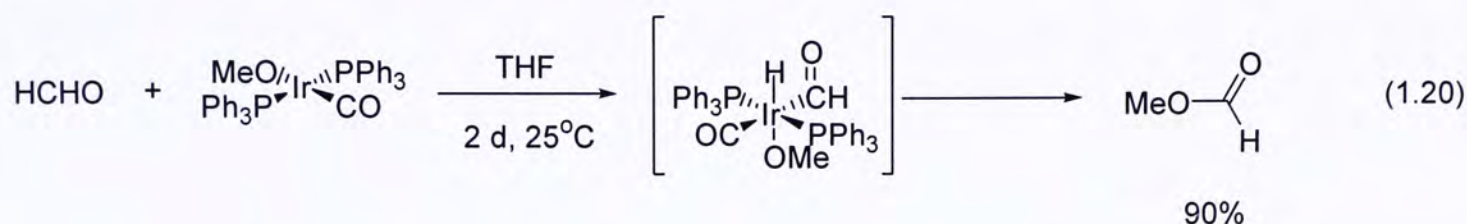
CHA of the aliphatic aldehydes by transition metals usually give hydridoacylmetal complexes. Since hydridoacylmetal complexes have been postulated as intermediates in a number of transformations, thus, various studies have been carried out. One of the examples is the oxidation addition of MeCHO to RhCl(PMe₃)₃ and stable *cis*-hydroacylrhodium complex, *cis*-HRh(COMe)(PMe₃)₃Cl, is formed at room temperature (eq. 1.18).³⁸



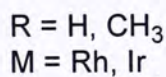
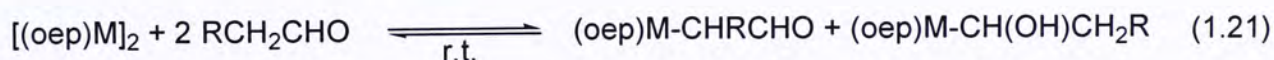
The tripodal rhodium (I) complex also react with the aldehydic C-H bonds to yield the stable Rh(III) *cis*-hydroacyl complexes (eq. 1.19).³⁹



In the case of Ir(I) complexes, *cis*-addition of the aldehydic C-H bond to the metal center was observed instead. The reaction of formaldehyde with the ROIr(CO)(PPh)₂, (R = Me, ⁱPr, ⁿPr, ^tBu) leads to the formation of esters (eq. 1.20).⁴⁰



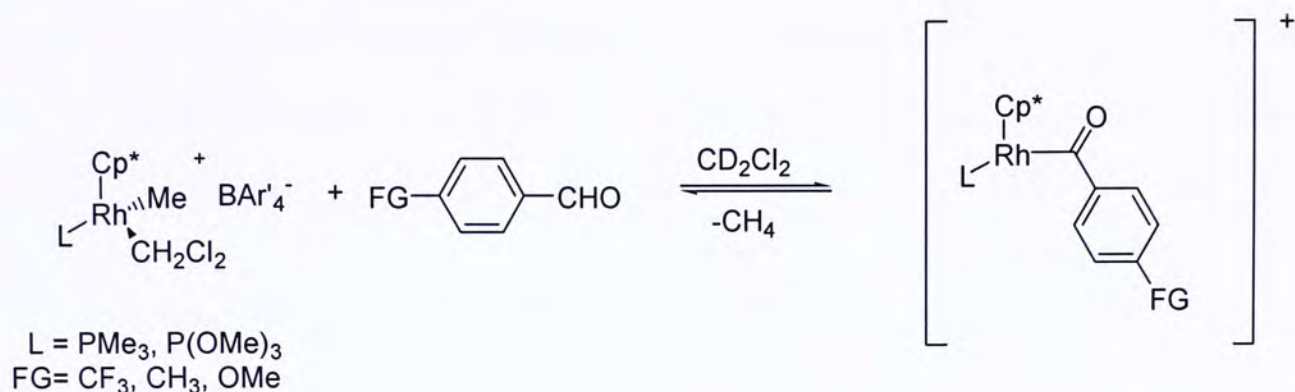
CHA of the aliphatic C-H_β is rare since the reaction of the aldehydic C-H activation produces a more kinetically favorable products M(COR), yet the CHA of C-H_β is still kinetically feasible. This can be illustrated by Wayland's report on the C-H_β activation of ethanal and propanal by [(oep)M]₂ (M = Rh and Ir). Both β-formyl complexes (oep)M-CH₂RCHO and α-hydroxyalkyl complexes (oep)M-CH(OH)CH₂R are formed in approximately equal quantities (eq. 1.21).⁴⁶ The unusual formation of the β-formyl complexes (oep)M-CH₂RCHO is due to a radical process. [(oep)M]₂ initially adds to the enol isomers of aldehydes and subsequently β-hydride elimination occurs to give the aldehydic CHA product.⁴⁶



(B) CHA of Aryl Aldehydes by Rh(III) and Ir (III) complexes

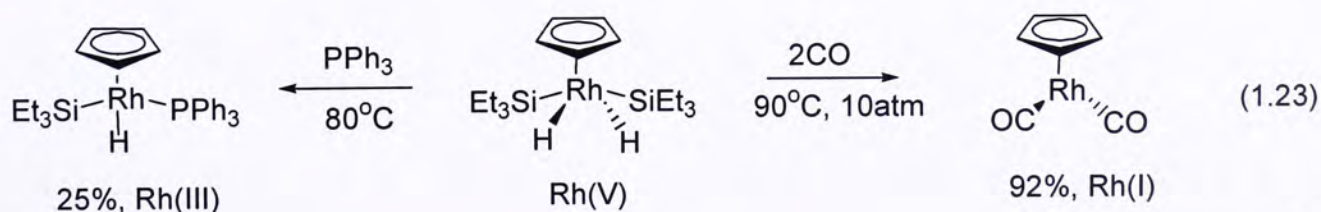
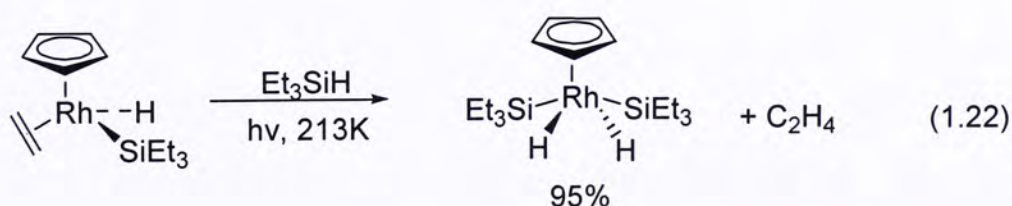
Recently activation of aldehydic C-H by Cp*Rh(PMe₃)(Me)(CH₂Cl₂)⁺ was reported by Bergman and Brookhart.⁴¹ The cationic rhodium (III) methyl complex reacted with the *p*-substituted benzaldehydes. The aldehyde adducts were produced via a dissociative process of the coordinated dichloromethane (Scheme 1.11).⁴¹ However, the

mechanistic pathways and the possible existence of Rh(V) intermediate still remain unclear, therefore further investigation is needed.



Scheme 1.11 The cationic rhodium (III) methyl complexes react with the p-substituted benzaldehydes

Organometallic Rh(V) complexes are rare but yet they still exist. Perutz et al reported the formation and isolation of Rh(V) hydrides via photochemical oxidative addition reactions at low temperature (eq. 1.22).²³ Later Maitlis et al reported the reactivity of the $[\eta^5\text{-C}_5\text{Me}_5\text{Rh(V)(H)}_2(\text{SiEt}_3)_2]$. Further ligand substitution with PPh_3 and CO triggers the reduction of Rh(V) to Rh(III) and Rh(I) respectively (eq. 1.23).²⁴ Hence, the organometallic and catalytic chemistry of rhodium should not be limited to +1 to +3 oxidation states.



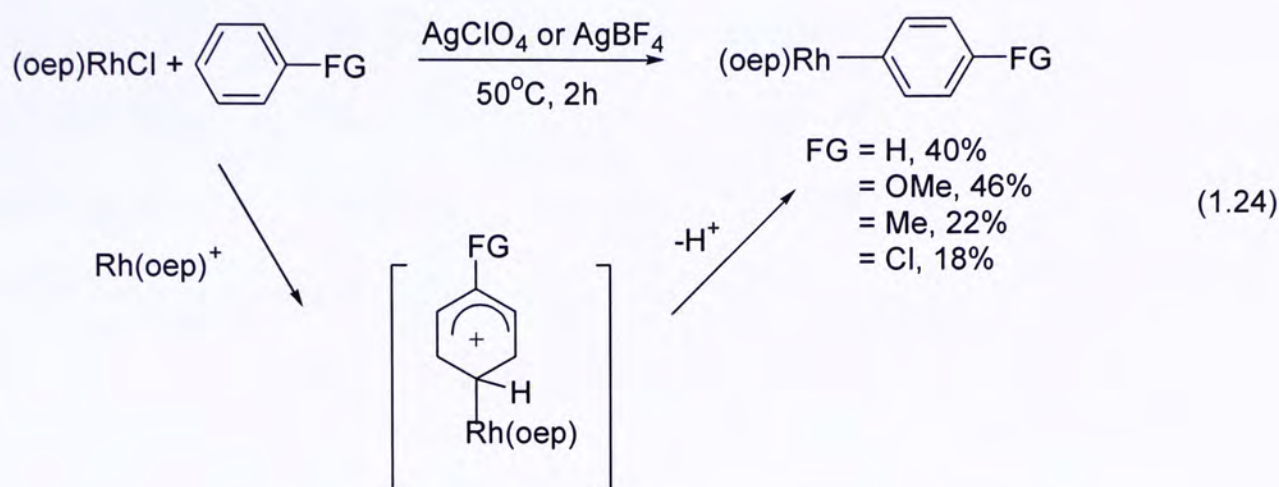
1.4 Structural Features of Rhodium Porphyrins

The rigid porphyrin nucleus consists of four pyrrole-rings which are joined by four methine bridges to give a macrocycle. The macrocycle is highly conjugated and there are 22- π electrons, but only 18 of them are included in the delocalization pathway. This conforms with Hückel's rule for aromaticity. This aromaticity can be shown by ^1H NMR spectroscopy. The shielded NH protons in porphyrins appear at very high field whereas the outer, *meso*-protons appear at very low field.⁴² Usually porphyrin ligand is planar in geometry.

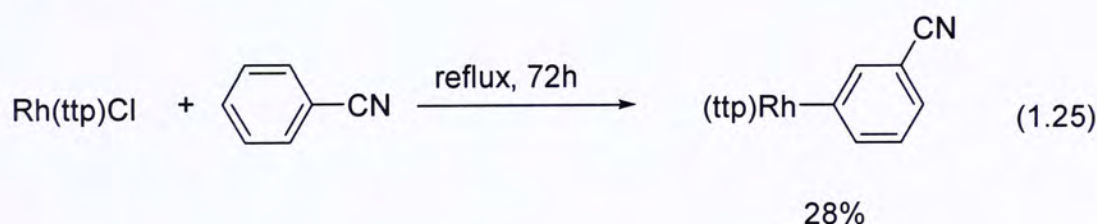
When porphyrin ligands bind metal ions, the resultant metaloporphyrins can act as Lewis acid. The metal occupies the center of the porphyrin hole and is coordinated by the four nitrogen atoms of the pyrroles through the four lone pairs.

The rhodium center in porphyrin complexes can exist in +1, +2, and +3 oxidation states. The +1 oxidation state is found in anionic species, $\text{Rh}(\text{por})^-$ (Rh^{I} , d^8), which functions as strong nucleophiles. The +2 oxidation state of rhodium species ($\text{Rh}^{\text{II}}(\text{por})$, d^7), act as metalloradicals. While the +3 oxidation state is found in cationic species, $\text{Rh}(\text{por})^+$ (Rh^{III} , d^6), which are strong Lewis acids and electrophiles.⁴²⁻⁴⁴

The electrophilic $\text{Rh}(\text{por})^+$ (Rh^{III}) cationic species react with the C-H bonds of arenes to give aryl rhodium complexes. In 1986, Ogoshi reported a highly regioselective CHA of arene by rhodium (III) porphyrin via the electrophilic aromatic metalation under mild conditions.⁴⁴ (Octaethylporphyrinato)rhodium (III) chloride, (oep) RhCl , reacts with arenes in the presence of silver salts, AgClO_4 or AgBF_4 to yield the *p*-substituted aryl complexes (eq. 1.24).



Chan et al. also reported the CHA of arenes by rhodium (III) porphyrin chlorides.⁴⁵ Rh(tpp)Cl reacted with refluxing benzonitrile to form the meta-cyanophenyl rhodium porphyrins, via likely electrophilic aromatic substitution in view of the meta-substituted product (eq. 1.25).



1.5 Objective of the work

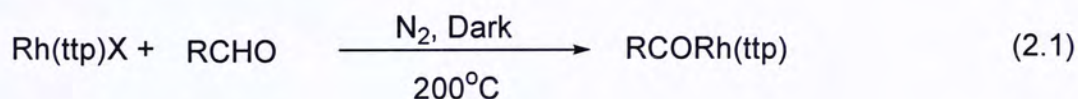
Although aldehydes can be easily activated by most transition metals at the aldehydic position or at the *ortho*- position on the arene, there is no example on the CHA of aldehyde by rhodium (III) porphyrin complexes. There are still uncertainties on the position of activation. In addition, examples of C-H activation by Rh(III) and Ir(III) are mechanistically interesting, whether oxidative addition or sigma bond metathesis would be more favorable is still unknown.

Therefore the objective of my work is to examine the reactions of Rh(III)(por)X (X = Cl, Me, OTf, BF₆, CH₂CH₂OH) with the aryl aldehydes, (1) to determine the activation position of the C-H bonds and (2) to attempt to address the possible mechanism and the nature of the Rh(V) intermediate.

Chapter 2 Carbon-hydrogen Activation of Aldehydes by Rh(ttp)Cl and Rh(ttp)Me

2.1 Introduction

Rhodium tetratolylporphyrin chloride Rh(ttp)Cl **1** and rhodium porphyrin methyl Rh(ttp)Me **10** were found to react smoothly with aldehydes in solvent-free conditions at 200°C with selective aldehydic carbon-hydrogen bond activation to give the acyl rhodium porphyrins (eq. 2.1). This contrasts from the report by Chan et al. on electrophilic aromatic substitution reaction (S_EAr) between Rh(ttp)Cl **1** and benzonitrile in giving the meta-cyanophenyl rhodium porphyrin.⁴⁵



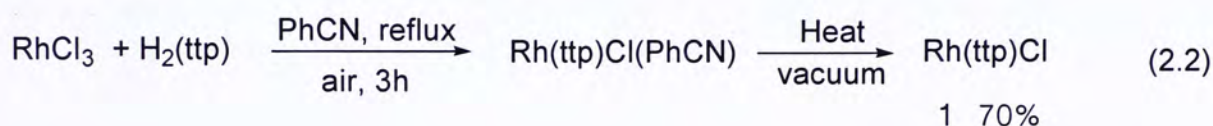
X = Cl, Me
R = alkyl, aryl

In order to gain more understanding of the selectivity and mechanistic features of this CHA, systematic studies were carried out with Rh(ttp)X (X = Cl, Me, OTf, BF₆, CH₂CH₂OH).

2.2 CHA of Aldehydes by Rh(ttp)Cl

2.2.1 Preparation of Rh(ttp)Cl

RhCl₃·xH₂O reacted with H₂(ttp) in benzonitrile at refluxing temperature for 3 hours to give Rh(ttp)Cl(PhCN). Purified Rh(ttp)Cl(PhCN) was further heated at 80°C under vacuum for one day to remove the coordinated PhCN and Rh(ttp)Cl **1** was obtained in 70% yield (eq. 2.2).⁴⁵ Then Rh(ttp)Cl **1** was used in the CHA of aldehydes and preparation of other starting materials.



2.2.2 Solvents Screening

Since aromatic protons and aldehydic protons are reactive, a suitable solvent had to be sought. Rh(ttp)Cl **1** was screened with various solvents. The polarities, dielectric constants, viscosities of the solvents and aldehydes, and the solubility of Rh(ttp)Cl **1** are listed in Table 2.1.

Table 2.1 Solvent parameters of solvents and aldehydes.

Entry	Benzaldehyde / Solvents	m.p. (°C)	b.p. (°C)	Polarity (μ)	Dielectric constant (ϵ)	Viscosity (mPas)	Solubility of Rh(ttp)Cl ^a
1	Benzaldehyde	26	179	3.00	17.85	1.55	Good
2	4-Chlorobenzaldehyde ^{b, c}	46	214	-	-	-	Not soluble
3	4-Cyanobenzaldehyde ^{b, c}	98	133 ^e	-	-	-	Not soluble
4	4-Fluorobenzaldehyde ^c	-10	181	-	-	-	Good
5	4-Methoxybenzaldehyde ^c	-1	248	-	22.00	4.10 ^g	Good
6	4- <i>N,N</i> -dimethylaminobenzaldehyde ^{b, c}	71	176 ⁱ	-	-	-	Not soluble
7	4-Tertbutylbenzaldehyde ^c	-	100 ^j	-	-	-	Good
8	4-Toluenaldehyde ^c	-6	204	-	-	-	Good
9	4-Trifluoromethylbenzaldehyde ^c	0	66 ^d	-	-	-	Good
10	Heptanal	-42	150	-	9.07	0.98 ^f	Fair
11	Pivaldehyde	6	75	2.86	-	1.37	Poor
12	Propanal	-81	48	2.72	18.52	1.36	Poor
13	Acetamide	80	222	3.68	67.69	1.43	Good
14	Benzene	6	80	0	2.28	1.50	Good
15	Dibutyl ether	-124	92	1.17	3.08	1.40	Good
16	Cyclohexane	7	81	-	2.02	0.94 ^h	poor
17	Diglyme	-68	162	1.97	7.23	1.41	Good
18	1,4-Dioxane	12	101	0	2.22	1.42	Good
19	<i>n</i> -Heptane	-91	98	-	1.92	1.39	Poor
20	<i>N</i> -Methyl-2-pyrrolidinone	-24	202	4.10	32.55	1.47	Good
21	Tetrachloroethene	-70	130	0	2.27	1.51	Poor
22	1,2,4-Trichlorobenzene ^c	16	214	-	-	-	Good

Data are obtained from Ref 48.

^a: visual inspection at room temperature, ^b: solid, ^c: data obtained from Ref. 49, ^d: obtained at 13mmHg, ^e: obtained at 12 mmHg, ^f: obtained at 15°C, ^g: obtained at 25°C, ^h: obtained at 20°C, ⁱ: obtained at 17 mmHg, ^j: obtained at 6 mmHg.

Rh(ttp)Cl **1** dissolved in most of the aldehydes and solvents at room temperature. Rh(ttp)Cl **1** reacted with the solvents in one day at refluxing temperature. Surprisingly, all solvents in Table 2.1 reacted with Rh(ttp)Cl **1**. Unknowns Rh(ttp) alkyls and aryls were observed in ^1H NMR as revealed by the up-field signals from - 5.00 to - 0.57 ppm. Even inert hydrocarbons such as cyclohexane and *n*-heptane reacted with Rh(ttp)Cl **1** to give *c*-hexylRh(ttp) and *n*-heptylRh(ttp) respectively by ^1H NMR analysis. In addition, if 100 equivalents of PhCHO were added (Table 2.2), unknown complex was still observed from ^1H NMR analysis together with PhCORh(ttp) **2**. Since the aim of these experiments was to find out a suitable solvent, therefore products were not isolated and identified (Table 2.2). In order to avoid the reaction with solvent, solvent-free conditions were used.

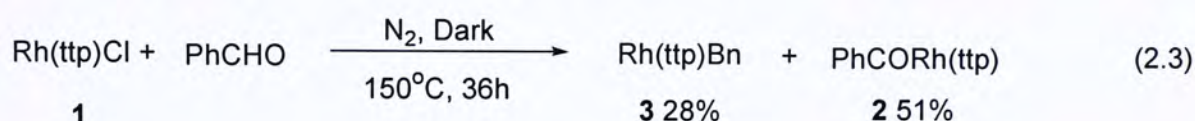
Table 2.2 Screening for inert solvent for Rh(ttp)Cl **1**.

$\text{Rh(ttp)Cl } \mathbf{1} + \text{PhCHO } 100 \text{ equiv.} + \text{solvent} \xrightarrow[\text{temp, 24h}]{\text{Dark, N}_2}$			
Entry	Solvent	Temp ($^{\circ}\text{C}$)	Reaction rate
1	Benzene	110	Moderate
2	Dibutyl ether	150	Moderate
3	Diglyme	150	Moderate
4	1,4-Dioxane	150	Moderate
5	<i>N</i> -Methyl-2-pyrrolidinone	150	Slow
6	Tetrachloroethene	150	Slow
7	1,2,4-Trichlorobenzene	150	Moderate

2.2.3 Results and Discussion

2.2.3.1 Temperature effect on CHA of aldehydes by Rh(ttp)Cl

When Rh(ttp)Cl **1** reacted with benzaldehyde at 200°C for 1 day, selective aldehydic CHA product PhCORh(ttp) **2** was formed in 79% yield. Interestingly by lowering the reaction temperature from 200°C to 150°C, a reduction product Rh(ttp)Bn **3** was observed (eq. 2.3). Therefore the product formation is temperature dependent.



The temperature effect on CHA of Rh(ttp)Cl **1** with benzaldehyde was further examined (Table 2.3). Below 150°C no reaction occurred. At 150°C both reduction product Rh(ttp)Bn **3** and CHA product PhCORh(ttp) **2** were produced at the same time. Upon prolonged heating, Rh(ttp)Bn **3** slowly disappeared with increased yield of PhCORh(ttp) **2**. Similar results were observed at 180°C and 200°C. At 200°C only the CHA product **2** was formed in 79% yield after 1 day. PhCORh(ttp) **2** was thermally stable as no decarbonylated product, Rh(ttp)Ph was observed. It appeared that PhCORh(ttp) **2** and Rh(ttp)Bn **3** were generated in a parallel manner. In addition Rh(ttp)Bn **3** seemed to further react with PhCHO to give PhCORh(ttp) **2**. Regardless of the detailed reaction pathways, optimal reaction conditions for synthesizing PhCORh(ttp) **2** were found to require 200°C and 1 day.

Table 2.3 Temperature effect on CHA of benzaldehyde by Rh(ttp)Cl **1**

$ \begin{array}{c} \text{Rh(ttp)Cl} + \text{PhCHO} \xrightarrow[\text{Temp, Time}]{\text{N}_2, \text{Dark}} \text{Rh(ttp)Bn} + \text{PhCORh(ttp)} + \text{HCl} \\ \mathbf{1} \qquad \qquad \qquad \mathbf{3} \qquad \qquad \mathbf{2} \end{array} $					
Entry	Temp (°C)	Time (h)	Yield (%)		Total Yield (%)
			Rh(ttp)Bn 3	PhCORh(ttp) 2	2 + 3
1	70	2	0	0	0
2	120	2	0	0	0
3	130	24	0	0	0
4	150	24	5	38	43
5		36	28	51	79
6	180	48	17	43	60
7	200	0.5	18	28	46
8		24	0	79	79

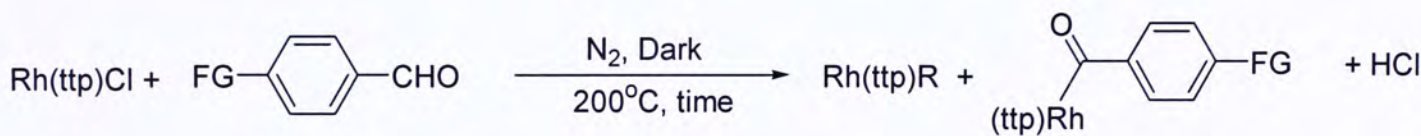
2.2.3.2 CHA of Aryl Aldehydes

CHA of *para*-substituted aryl aldehydes by Rh(ttp)Cl **1** were carried out in optimized conditions. Aldehydic CHA products were isolated as the only product in moderate to good yield at 200°C (Table 2.4). All rhodium aroyl complexes were thermally stable at 200°C. No decarbonylation was observed. Substrates bearing alkyl carbon-hydrogen bond such as 4-MeC₆H₄CHO and 4-^tBu-C₆H₄CHO gave small amounts of alkyl CHA products of (4-CHOC₆H₄CH₂)Rh(ttp) **6** and (4-CHOC₆H₄C(Me)₂CH₂)Rh(ttp) **8** in about 1 hour. However, upon heating, **6** and **8** disappeared with increasing yields of the corresponding major aroyl rhodium complexes **7** and **9** respectively. These alkyl CHA products might either undergo thermal decomposition or further react with the aryl aldehydes to give the aroyl complexes.

Pronounced substituent effect of the aryl aldehydes on the product selectivity was noted. The electron rich 4-MeOC₆H₄CHO produced no aldehydic CHA product but only

Rh(ttp)Me **10** in 11% yield. Furthermore, only those aryl aldehydes in liquid states at room temperature reacted with Rh(ttp)Cl **1** to yield the aldehydic CHA products. The electron withdrawing group (F and CF₃) reacted faster than electron donating substituents (Me and ^tBu) based on the disappearance of the Rh(ttp)Cl **1** by the TLC analysis. Solid *para*-substituted aryl aldehydes such as those of NMe₂, CN and Cl did not react or give complex mixture. 4-N(Me)₂C₆H₄CHO did not give any Rh(ttp)Me **10**. Hence limitation for preparation of some of the rhodium aroyl complexes exists.

Table2.4 CHA of *para*-substituted aryl aldehydes with Rh(ttp)Cl **1**



Entry	FG	Time (h)	Yield (%)	
			Rh(ttp)R	(4-FGC ₆ H ₄ CO)Rh(ttp)
1	H	24	-	2 (79)
2	F	24	-	4 (45)
3	Cl	24	-	none ^b
4	CF ₃	24	-	5 (50)
5	CN	24	-	none ^a
6	Me	1	(4-CHOC ₆ H ₄ CH ₂)Rh(ttp) 6 (4)	7 (20)
7		24	-	7 (57)
8	^t Bu	1	(4-CHOC ₆ H ₄ C(Me) ₂ CH ₂)Rh(ttp) 8 (2)	9 (17)
9		24	-	9 (38)
10	OMe	24	Rh(ttp)Me 10 (11)	-
11	NMe ₂	24	-	none ^a

^a: complex mixture; ^b: no reaction, only Rh(ttp)Cl remained by TLC and ¹H NMR analysis.

2.2.3.3 CHA of Aliphatic Aldehydes

Aliphatic aldehydes also reacted with Rh(tpp)Cl **1**. However poor results were obtained. Low-yielding aldehydic CHA products or complex mixture of products were formed (Table 2.5). Aliphatic aldehydes with α -acidic protons heptanal gave a complex mixture **11** at 200°C. EtCHO gave a very low yield of EtCORh(tpp) **12** at 100°C. However, the pivaldehyde produced a slightly higher yield of ^tBuCORh(tpp) **13** in 24%. All rhodium acyl complexes were thermally stable at 200°C. No decarbonylation was observed.

Table 2.5 CHA of aliphatic aldehydes by Rh(tpp)Cl **1**

$$\text{Rh(tpp)Cl} + \text{R-CHO} \xrightarrow[\text{Temp, Time}]{\text{N}_2, \text{ Dark}} \text{RCORh(tpp)}$$

1

Entry	R	Temp (°C)	Time (h)	Yield (%)
1	C ₇ H ₁₅	200	24	11 Oily product mixture
2	C ₂ H ₅	100	48	12 (3)
3	^t Bu	200	48	13 (10)

2.3 CHA of aldehydes by Rh(tpp)Me

Since Rh(tpp)Cl **1** was reduced by aldehydes to produce reduction products Rh(tpp)Bn **3**, as side products or intermediates, the yield of CHA products would suffer. Hence the electron richer complex, Rh(tpp)Me **10** was used. Reduction potential of Rh(tpp)Me **10** ($E_{1/2} = -1.43 \text{ V}$)⁵⁴⁻⁵⁵ is more negative than that of Rh(tpp)Cl **1** ($E_{1/2} = -1.01 \text{ V}$)⁵⁰⁻⁵³ and therefore more difficult to reduce.

Moreover, CHA of aldehydes by Rh(tpp)Me **10** was envisioned to generate the methane (CH₄) which has equally good driving force with that of Rh(tpp)Cl **1**, as the BDEs of Me-H and Cl-H are nearly the same (Table 2.6),

Table 2.6 Estimation on the thermodynamics of CHA of aldehydes by Rh(tpp)Cl **1** and Rh(tpp)Me **10**

$$\text{M-X} + \text{PhCHO} \longrightarrow \text{PhCOM} + \text{H-X}$$

X = Cl, Me

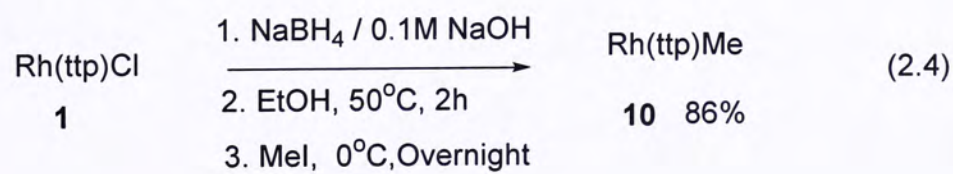
$$\Delta H^0 \sim (\text{M-C}) + (\text{H-X}) - (\text{C-H}) - (\text{M-X})$$

$$\Delta S_{298}(\text{estimated}) = 13 \text{ kcal mol}^{-1} \text{ (Ref. 78)}$$

	BDE (M-X) (kcal mol ⁻¹) ⁷⁷	BDE (H-X) (kcal mol ⁻¹)	ΔH ₂₈₉ (estimated) (kcal mol ⁻¹) ⁷⁸	ΔG ₂₉₈ (estimated) (kcal mol ⁻¹)
Cl	70	104 ⁴⁷	-6	7
Me	35	105 ¹⁰	-42	-29

2.3.1 Preparation of Rh(tpp)Me **10**

Rh(tpp)Me **10** was synthesized by reductive alkylation of Rh(tpp)Cl **1** with NaBH₄/MeI in 86% yield (eq. 2.4).⁵⁷



2.3.2 Results and Discussion

2.3.2.1 Optimization of Reaction Conditions

The optimal temperature of aldehydic CHA of prototypical PhCHO with Rh(tpp)Me **10** was investigated (Table 2.7). At 100°C, only 12% yield of CHA product was obtained and 40% yield of starting materials was recovered after 2 days. When temperature was increased to 200°C, fast and complete reaction occurred. PhCHO reacted with Rh(tpp)Me **10** to afford PhCORh(tpp) **2** in 82% yield within 0.5 h. No Rh(tpp)Bn **3** was formed. Hence the optimal temperature was found to be 200°C.

Table 2.7 Optimization of temperature for CHA with Rh(tpp)Me **10**.

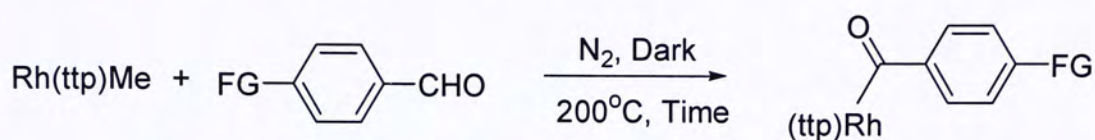
$\text{Rh(tpp)Me } \mathbf{10} + \text{PhCHO} \xrightarrow[\text{Temp, Time}]{\text{N}_2, \text{Dark}} \text{PhCORh(tpp) } \mathbf{2} + \text{Rh(tpp)Me } \mathbf{10} + \text{CH}_4$				
Entry	Temp (°C)	Time (h)	2 Yield (%)	10 Recovered (%)
1	100	48	12	40
2	200	0.5	82	0

2.3.2.2 CHA of Aryl Aldehydes

CHA of aryl aldehydes by Rh(tpp)Me **10** was carried out in optimized conditions at 200°C in a solvent-free conditions. CHA products were cleanly and selectively produced without any reduction product formed. Rh(tpp)Me **10** reacted faster than Rh(tpp)Cl **1** with various aryl aldehydes. Most of the substrates gave aldehydic CHA products at moderate to good yield. 4-Methoxybenzaldehyde also yielded the rhodium aroyl complex **16** successfully and selectively in 56%. However, 4-N(Me)₂C₆H₄CHO gave complexes of unidentified products. PhCHO appeared to be the most reactive

substrate among all the aryl aldehydes. Both electron deficient aldehyde (CF₃) and electron rich aldehyde (OMe) reacted more slowly (Table 2.8).

Table 2.8 CHA of different para-substituted aryl aldehydes by Rh(ttp)Me **10**.



Entry	FG	Time (h)	Yield (%)
1	H	0.5	2 (82)
2	F	8	4 (76)
3	Cl	24	17 (53)
4	CF ₃	16	5 (54)
5	Me	16	7 (73)
6	^t Bu	48	9 (39)
7	OMe	16	16 (56)
8	NMe ₂	60	Unknown

2.3.2.3 CHA of aliphatic aldehydes

Improved aldehydic CHA was also obtained for the aliphatic aldehydes. CHA products of aliphatic aldehydes were successfully prepared from Rh(ttp)Me **10** in moderate yields (Table 2.9)

Table 2.9 CHA of aliphatic aldehydes by Rh(ttp)Me **10**.

$$\text{Rh(ttp)Me} + \text{RCHO} \xrightarrow[\text{Temp, Time}]{\text{N}_2, \text{Dark}} \text{RCORh(ttp)} + \text{CH}_4$$

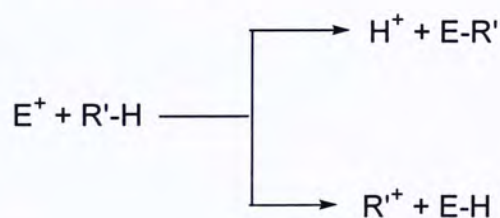
10

	R	Temp (°C)	Time (h)	Yield (%)
1	C ₇ H ₁₅	200	48	13 (41)
2	C ₂ H ₅	100	24	14 (60)
3	^t Bu	200	48	15 (37)

2.4 Mechanistic studies

2.4.1 CHA of Aldehydes by Rh(ttp)Cl

In hydrocarbon chemistry, carbocations react with hydrocarbons in parallel electrophilic CHA reactions to generate (1) the new C-C bond and protons; (2) alkanes and new carbocations (Scheme 2.1).¹

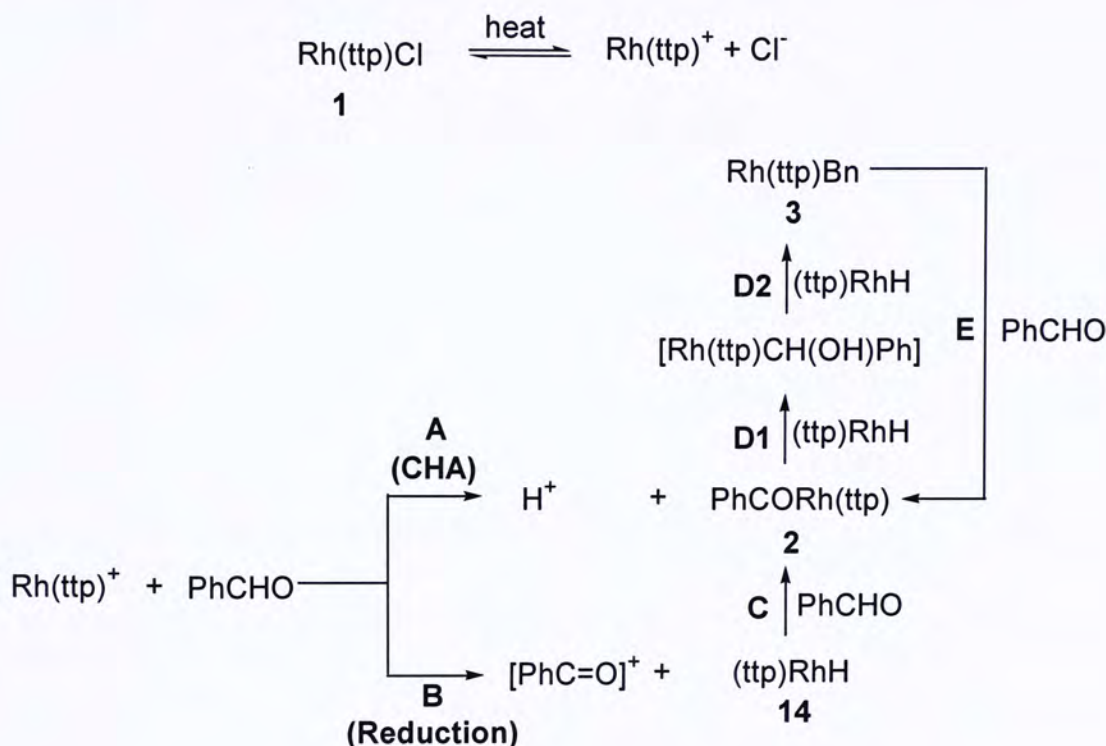


E = R, Rh(por)

Scheme 2.1 Parallel Electrophilic Activation by Carbocation and Rh(por)⁺

Rh(ttp)Cl **1** likely dissociates into the electrophilic Rh(ttp)⁺ and Cl⁻ at 200°C and reacts with benzaldehyde like carbocations in a parallel manner (1) Aldehydic CHA (acyl rhodium porphyrin complex and proton) (**A**); and (2) reduction reaction (Rh(ttp)H **14** and acylium ion (PhC=O)⁺) (**B**). Consequently, Rh(ttp)H **14** will further react with PhCHO and give PhCORh(ttp) **2**. On the other hand, a successive reduction of PhCORh(ttp) **2** by Rh(ttp)H **14** would finally yield the Rh(ttp)Bn **3** (**D**). In addition, the gradual

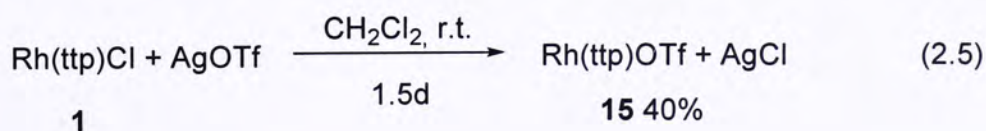
disappearance of Rh(ttp)Bn **3** during the reaction might be due to further reaction of Rh(ttp)Bn **3** with PhCHO to afford PhCORh(ttp) **2** (**E**) (Scheme 2.2). Hence further experiments were carried to test the proposed mechanism.



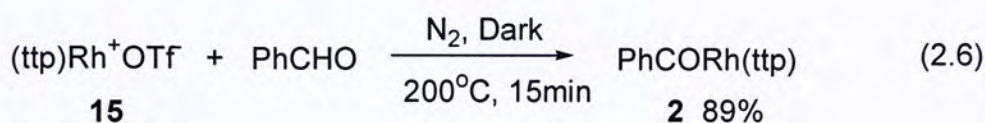
Scheme 2.2 Proposed Parallel CHA of Aldehydes by Rh(ttp)Cl **1**

Pathway A and B - Rh(ttp)⁺. In the CHA of arenes reported by Ogoshi,⁴⁴ Rh(III) porphyrin cationic species Rh(oep)X (oep = octaethylporphyrin; X = OCl₄⁻, BF₄⁻, PF₆⁻) reacted with arenes. As aldehydic CHA by Rh(ttp)Cl **1**, Rh(ttp) cation likely formed as intermediate. Therefore, a more reactive Rh(ttp)OTf **15** was prepared to examine the CHA chemistry.

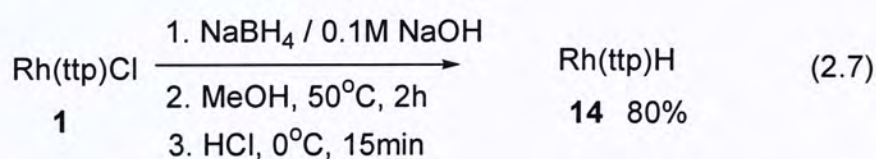
Rh(ttp)OTf **15** was prepared from reaction of Rh(ttp)Cl **1** with 1.2 equiv. of AgOTf in dichloromethane at room temperature in 1.5 days. The crude Rh(ttp)OTf **15** was purified by a quick column chromatography and 40% yield was obtained (eq. 2.5).⁴⁴



Rh(ttp)OTf **15** reacted with the benzaldehyde at 200°C (eq. 2.6). Aldehydic CHA product PhCORh(ttp) **2** was formed rapidly in 89% yield within 15 min. Rh(ttp)OTf **15** also reacted with 4-methoxybenzaldehyde at 200°C in 15 min to give a mixture which contained Rh(ttp)Me **10** and 4-MeOC₆H₄CORh(ttp) **16** by ¹H NMR analysis. No reduction product of Rh(ttp)Bn **3** was observed. The result supports the intermediacy of Rh(ttp) cationic species in the CHA of PhCHO by Rh(ttp)Cl **1**.



Pathway C and D - Rh(ttp)H **14.** To produce CHA product, Rh(ttp)H **14** was synthesized according to literature method.⁵⁸ Rh(ttp)Cl **1** was reduced by NaBH₄ and then protonated by HCl to give Rh(ttp)H **14** in 80% yield. The freshly prepared Rh(ttp)H **14** was then vacuum-dried (eq. 2.7).



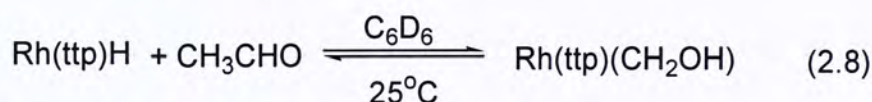
When Rh(ttp)H **14** reacted with PhCHO at 50°C for 2 days, neither CHA product nor reduction product was observed both by TLC and crude ¹H NMR analysis. However, when the temperature was increased to 200°C, Rh(ttp)Bn **3** and Rh(ttp)COPh **2** were formed in 4% and 35% yields respectively within 0.5 h. Hence, the formation of Rh(ttp)H **14** through pathway **B** is substantiated. Moreover, Rh(ttp)H **14** appeared to be an intermediate which (1) reacted with PhCHO to give PhCORh(ttp) **2** (**C**) and (2) reduced PhCORh(ttp) **2** into Rh(ttp)Bn **3** (**D**)(Table 2.10).

Table 2.10 CHA of aryl aldehydes by Rh(tpp)H **14**

$$\text{Rh(tpp)H} + \text{FG}-\text{C}_6\text{H}_4-\text{CHO} \xrightarrow[\text{Temp, Time}]{\text{N}_2, \text{Dark}} \text{Rh(tpp)R} + \text{(tpp)Rh}-\text{C(=O)}-\text{C}_6\text{H}_4-\text{FG}$$

Entry	FG	Temp (°C)	Time (h)	Yield (%)	
				Rh(tpp)R	
1	H	50	48	Rh(tpp)Bn 3 (trace)	2 (trace)
2	H	200	0.5	Rh(tpp)Bn 3 (4)	2 (35)
3	OMe	50	48	Rh(tpp)Me 10 (0)	16 (0)
4	OMe	200	0.5	Rh(tpp)Me 10 (15)	16 (21)

The reduction of RCHO by Rh(por)H is also precededented. Rh(tpp)H was reported to react with acetaldehyde in *d*₆-benzene in sealed NMR tube experiment, Rh(tpp)(CH₂OH) was observed from the ¹H NMR (eq. 2.8).⁵⁸

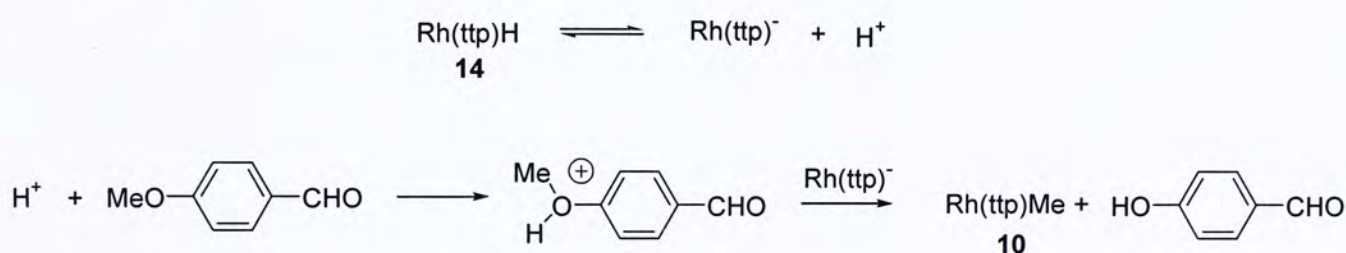


Similarly, when benzaldehyde reacted with Rh(tpp)H **14**, both PhCORh(tpp) **2** and reduction product BnRh(tpp) **3** were generated. In addition, PhCORh(tpp) **2** reacted with Rh(tpp)H **14** to generate [Rh(tpp)CH(OH)Ph] as intermediate. [Rh(tpp)CH(OH)Ph] appeared to be further reduced by Rh(tpp)H **14** to give BnRh(tpp) **3**.

Moreover, Rh(tpp)H **14** reacted with 4-methoxybenzaldehyde at 200°C after 0.5 hour, CHA product 4-(MeOC₆H₄CO)Rh(tpp) **16** was obtained in 21% yield. In addition, unexpected Rh(tpp)Me **10** was obtained in 15% yield. This formation of Rh(tpp)Me **10** further substantiated the formation of Rh(tpp)H **14** from Rh(tpp)Cl **1** in its reaction with 4-MeOC₆H₄CHO (Table 2.4 entry 10).

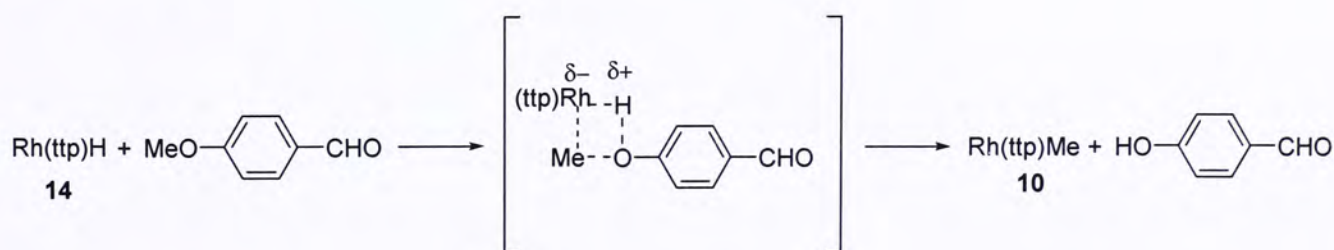
The formation of Rh(tpp)Me **10** suggested that C-O bond cleavage at the OMe group occurred. Rh(tpp)H **14** could react in two possible pathways: (1) ionic pathway and (2) neutral pathway.^{13, 25}

(1) Ionic pathway. As Rh(tpp)H **14** is a weak acid with pKa ~11^{66,73} and can dissociate at elevated temperature into Rh(tpp)⁻ and H⁺. Protonation of methoxy oxygen can assist the nucleophilic C-O cleavage by Rh(tpp)⁻ to give Rh(tpp)Me and phenol (Scheme 2.3).



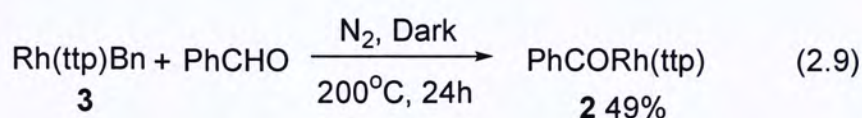
Scheme 2.3 Ionic Pathway : CHA of 4-Methoxybenzaldehyde with Rh(tpp)H **14**.

(2) Neutral pathway. Rh(tpp)H **14** directly reacts with the OMe group to give Rh(tpp)Me **10** and [4-HOC₆H₄CHO] (Scheme 2.4). However, Rh(tpp)⁻ is difficult to be generated in 4-methoxybenzaldehyde, a non-basic solvent, a neutral pathway is more favorable.



Scheme 2.4 Neutral Pathway : CHA of 4-Methoxybenzaldehyde with Rh(tpp)H **14**.

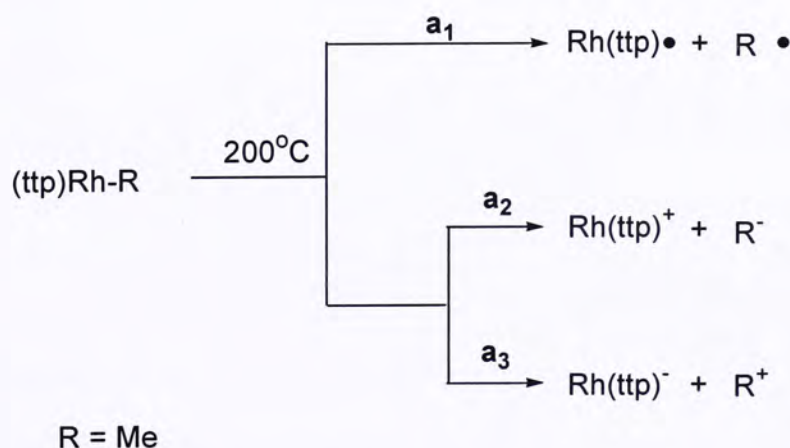
Pathway E. Rh(tpp)Bn **3** reacted with PhCHO at 200°C in 1 day to give Rh(tpp)COPh **2** in 49% yield (eq. 2.9). The sterically more hindered Rh(tpp)Bn **3** was less reactive than Rh(tpp)Me **10** in Table 2.8 entry 1 (0.5 hour, 200°C, **2** (82 %)). Not only pathway E has been established, but also possible direct CHA of [Rh(tpp)CH(OH)Ph] with PhCHO. Therefore, these experiments successfully mapped the reaction pathways shown in Scheme 2.2. Further details on the nature of the each elementary step still await further experiments.



2.4.2 CHA of Aldehydes by Rh(tpp)R

As the aldehydic CHA reaction with Rh(tpp)Me **10** did not give any reduction product. The mechanism of Rh(tpp)Me **10** seems to differ from that of Rh(tpp)X (X = Cl and OTf). The mechanistic pathways of Rh(tpp)Me **10** can be considered either as (1) non-concerted pathways or (2) concerted pathways.

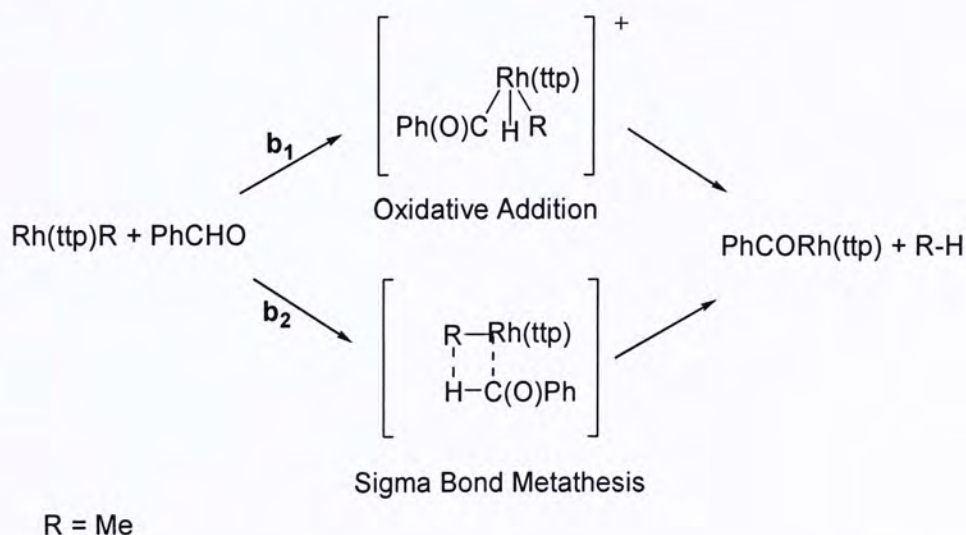
(1) Non-concerted pathways. Rh(tpp)Me **10** can form the Rh^{II}(tpp) radical homolytically (**a**₁), or undergo heterolysis to give Rh(tpp)⁻/R⁺ (**a**₂) or Rh(tpp)⁺/R⁻ (**a**₃) (Scheme 2.5).



Scheme 2.5 Non-concerted pathways of Aldehydic CHA with Rh(tpp)Me **10**

However, the non-concerted pathways are *unlikely* to proceed. Since $\text{Rh}^{\text{II}}(\text{tmp})$ (tmp = tetrakis(mesityl)porphyrin) did not react with PhCHO in benzene at 120°C to give $\text{PhCORh}(\text{tmp})$,⁶⁰ so the analogous and less reactive $\text{Rh}^{\text{II}}(\text{ttp})$ will unlikely react to give $\text{PhCORh}(\text{ttp})$ **2**. Furthermore, $\text{Rh}(\text{ttp})\text{Me}$ **10** is unlikely to generate $\text{Rh}^{\text{II}}(\text{ttp})$ radical via homolysis (**a**₁);²⁶⁻²⁸ in view of the strong Rh-C bond (BDE ~ 60 kcal mol⁻¹) in $\text{Rh}(\text{ttp})\text{Me}$ **10**. Also, heterolysis (**a**₂, **a**₃) to give R⁺ and R⁻ are also energetically costly. Therefore alternatively concerted pathways are more reasonable.

(2) Concerted Pathways. Aldehydic CHA with $\text{Rh}(\text{ttp})\text{Me}$ **10** might undergo associative pathways. The associative pathways exist in two possibilities: (1) Oxidative addition (**b**₁) (2) sigma- bond metathesis (**b**₂) (Scheme 2.6)



Scheme 2.6 Concerted pathways of Aldehydic CHA with $\text{Rh}(\text{ttp})\text{Me}$ **10**.

In the case of oxidative addition pathway, an intermediate with higher oxidation states will be involved (in this case +3 to +5). Though Bergman successfully isolated Ir(V) intermediates in silicon-hydrogen activation,²⁵ there was no supporting evidence for Rh(V) as intermediate in carbon-hydrogen activation. Furthermore, 7-coordinated intermediate is required in oxidative addition (**b**₁), while in sigma bond metathesis (**b**₂) the intermediate is only 6-coordinated. In a preliminary study, when 30 equiv. of pyridine

was added, Rh(tpp)Me **10** reacted much slower to give PhCORh(tpp) **2** (Table 2.13, entry 4). Hence, likely oxidative addition via 7-coordinated intermediate (**b**₁) is less possible than sigma bond metathesis with a 6-coordinated transition state (**b**₂).

2.4.2.1 Other experiments

Since no intermediate was isolated, further experiments were carried out to probe the nature of the CHA by Rh(tpp)R.

(1) **Hammett Plot.** The electronic effect on the CHA of aryl aldehydes by Rh(tpp)Me **10** was studied by constructing the Hammett plot.⁵⁶ Competition experiments were carried in solvent-free conditions at 200°C. Since solvent-free conditions were used, therefore only liquid aryl aldehydes were used. Benzaldehyde was mixed with a *para*-substituted aryl aldehydes in 1:1 ratio with the Rh(tpp)Me **10** at 200°C. The relative rate was obtained from the integration of ¹HNMR and plot against the para-substituent constants (σ_p) (Table 2.11).⁵⁶ The k (FG/H) ratio did not change even the competition experiments were under prolonged heating for 1 day.

Table 2.11 Competition reaction.

	FG	k (FG/H)	Log k (FG/H)	σ _p	σ _p ^{+/-}
1	CF ₃	1.5913	0.2018	0.53	0.65
2	F	0.9907	-0.0040	0.15	-0.07
3	OMe	1.0008	0.0035	-0.12	-0.78
4	^t Bu	0.7516	-0.1201	-0.15	-0.07

σ_p---para-substituent constant; σ_p^{+/-}---para-substituent constant (resonance and inductive effect)

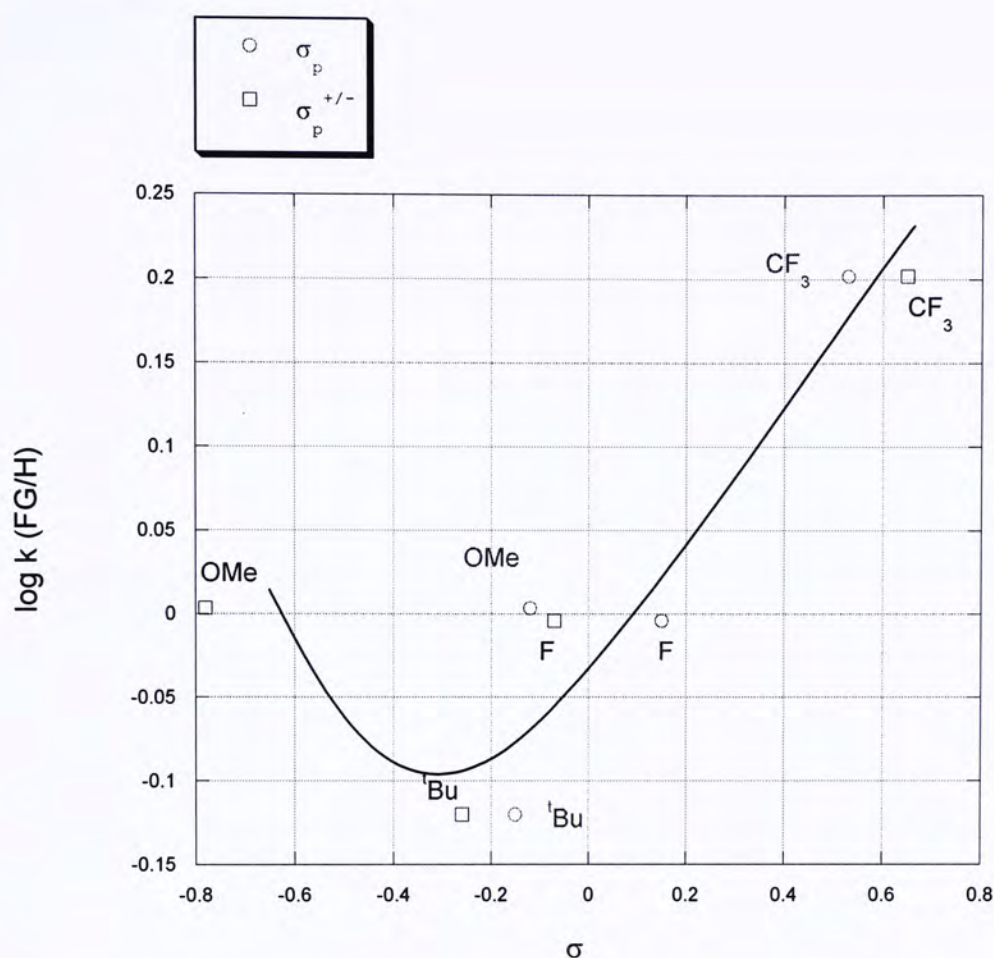


Figure 2.1 Hammett Plot of CHA of aryl aldehydes with Rh(tpp)Me **10**.

A non-linear Hammett plot was obtained (Figure 2.1). This suggests that the transition states change with substituents.⁵⁶ Alternatively, this Hammett plot was not constructed properly from the data obtained in nearly identical conditions. The solvent-free conditions of mixed aldehydes seriously differed in polarities, dielectric constants and viscosities, thus preclude conclusion to be drawn.

(2) Exchange. Rh(tpp)R (R = COAr, Ar = 4-FC₆H₄, 4- t Bu-C₆H₄) reacted with PhCHO to give PhCORh(tpp) **2** (Table 2.12). Both 4- t BuC₆H₄CORh(tpp) and 4-FC₆H₄CORh(tpp) reacted with benzaldehyde, and the aryl group (Ar = 4-FC₆H₄, 4- t Bu-C₆H₄) exchanged with the PhCHO to give PhCORh(tpp) **2**. The facile exchange might be due to the weakness of Rh-C(O)R bond (B.D.E. ~ 62 kcal mol⁻¹⁴⁷ and C(O)-H _{α} (B.D.E. \sim

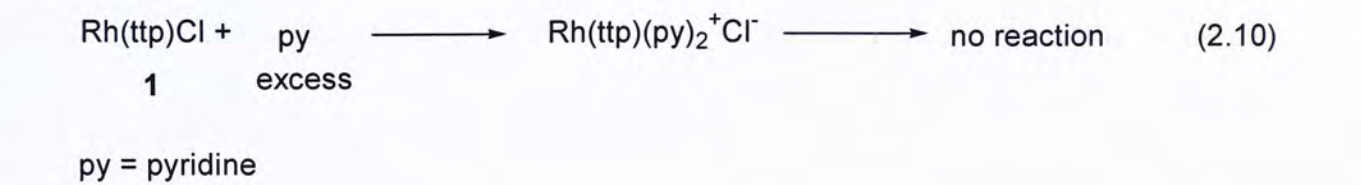
88 kcal mol⁻¹).^{10,31} In view of CHA of Rh(ttp)R (R = Me, Bn), general exchange of Rh(ttp)R with R'-H to give Rh(ttp)R' and R-H might be expected.

Table 2.12 CHA of PhCHO by Rh(ttp)R.

<div> <div>Rh(ttp)R + PhCHO</div> <div> $\xrightarrow[\text{Temp, Time}]{\text{N}_2, \text{Dark}}$ </div> <div>PhCORh(ttp)</div> <div>2</div> </div>				
Entry	R	Temp (°C)	Time (h)	2 Yield (%)
1	4- ^t BuC ₆ H ₄ CO	200	96	57 ^a
2	4-FC ₆ H ₄ CO	50	15	96 ^b
3	Me	80	120	none ^c

^a: solvent-free conditions ; ^b: 1.0 mL THF; ^c 1.0 mL THF and Rh(ttp)Me recovered.

(3) Ligand Effect and Base Effect on CHA. When pyridine (30 equiv.) was added, Rh(ttp)Cl **1** did not react with PhCHO. Presumably after 120 h, excess pyridine gave (Rh(ttp)(py)₂⁺Cl⁻) by ligand substitution which is coordination saturated to allow any CHA (eq. 2.10).⁶²⁻⁶³



When 1.0 equivalent of PPh₃ was added, aldehydic CHA required 1 day to complete at 200°C and gave PhCORh(ttp) **2** in 79% yield. Only trace amount of reduction product Rh(ttp)Bn **3** was observed. More electron rich (PPh₃)Rh(ttp)⁺ likely formed.⁶⁹ Though it is less electrophilic, it is rationalized to exist in higher concentration overall faster CHA. In addition, (PPh₃)Rh(ttp)⁺ being more electron-rich, it is less easily reduced

to give Rh(ttp)Bn **3** .When a non-coordinating base 2,4,6-trimethylpyridine was added, the rate increased with a slightly decrease in yield and no BnRh(ttp) **3** was found. Therefore, addition of coordinating ligand or bulky base would enhance the reaction rate of aldehydic CHA.

Table 2.13 Addition of 30 equiv. of pyridine.

<div> <div> <div>Rh(ttp)R+ PhCHO</div> <div> <div>Ligand, N₂, Dark</div> <div>200°C, Time</div> </div> <div> <div>PhCORh(ttp) + BnRh(ttp)</div> <div>2</div> </div> </div> </div>					
Entry	R	Ligand	Time (h)	2 Yield (%)	BnRh(ttp) (%)
1	Cl	none	24	79	0
2		Py (1.0 equiv.)	96	32	16
3		py (30 equiv.)	120	0	0
4		PPh ₃ (1 equiv.)	24	79 ^a	0
5		2,4,6-trimethylpyridine	2	65	0
6	Me	none	0.5	82	0
7		py (30 equiv.)	2	71	0
8		PPh ₃ (1 equiv.)	45 mins	51	0
^a : with trace amount of BnRh(ttp) observed by TLC analysis					

2.5 Comparison of the $\nu(\text{C}=\text{O})$

The IR stretching, $\nu(\text{C}=\text{O})$ of the benzoyl rhodium complexes do not vary much from the $\nu(\text{C}=\text{O})$ of aryl aldehydes. The $\nu(\text{C}=\text{O})$ of the benzoyl rhodium complexes lie between 1690 to 1720 cm^{-1} , where the $\nu(\text{C}=\text{O})$ of the ArCHO ranges from 1690 – 1730 cm^{-1} (Table 2.14).

Table 2.14 Carbonyl stretching vibrational data for (ttp)Rh-X

X	IR (KBr) $\nu_{\text{C}=\text{O}}$ (cm^{-1})	IR(KBr) $\nu_{\text{C}=\text{O}}$ (ArCHO) (cm^{-1})
$\text{C}_6\text{H}_5\text{C}(\text{O})$	1716	1700
4- $\text{FC}_6\text{H}_4\text{C}(\text{O})$	1711	1701
4- $\text{ClC}_6\text{H}_4\text{C}(\text{O})$	1703	1701
4- $\text{CF}_3\text{C}_6\text{H}_4\text{C}(\text{O})$	1691	1711
4-CN $\text{C}_6\text{H}_4\text{C}(\text{O})$	1694	1701
4-Me $\text{C}_6\text{H}_4\text{C}(\text{O})$	1704	1692
4- $^t\text{BuC}_6\text{H}_4\text{C}(\text{O})$	1710	1699 ^a
4-MeOC $_6\text{H}_4\text{C}(\text{O})$	1704	1688
4-N(Me) $_2\text{C}_6\text{H}_4\text{C}(\text{O})$	1602	1696
$\text{CH}_3\text{CH}_2\text{C}(\text{O})$	1717	1731
$\text{CH}_3(\text{CH}_2)_5\text{C}(\text{O})$	1716	1726
$(\text{CH}_3)_3\text{CC}(\text{O})$	1732	1725 ^a

IR data from Ref 49 and 64 ; ^a: measured at room temperature

The carbonyl stretching frequencies in $\text{RCORh}(\text{oep})$ ⁴⁶ are lower than that in $\text{RCORh}(\text{ttp})$ (Table 2.15). The IR stretching frequency of carbonyl group in rhodium (III) porphyrin complexes are generally lower than those in the aldehydes. When the porphyrins (oep) is more electron rich, the stretching frequency of the carbonyl group is lower.

Table 2.15 Comparison of carbonyl stretching vibrational data for (ttp)Rh-X and (oep)Rh-X

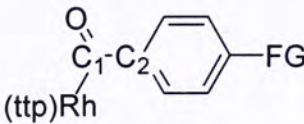
X	IR (KBr) $\nu_{\text{C=O}}$ (Rh(ttp)-X) (cm^{-1})	IR(KBr) $\nu_{\text{C=O}}$ (Rh(oep)-X) (cm^{-1}) ^a	IR(KBr) $\nu_{\text{C=O}}$ (ArCHO) (cm^{-1}) ^b
C ₆ H ₅ C(O)	1716	1684	1716
CH ₃ CH ₂ C(O)	1717	1709	1731
(CH ₃) ₃ CC(O)	1732	1687	1725 ^c

^a: Ref 46; ^b: Ref a9 and 64; ^c: measured at room temperature

2.6 X-ray Data

The para-substitutents on the benzaldehyde do not affect the bond length between Rh-C(O) as they are similar to the Rh-C(O) (1.988(5) Å) of the (oep)RhC(O)NH(C₈H₃(CH₃)₂) reported by Wayland.⁸¹ Moreover, the bond angle is not affected by the para-substitutents (Table 2.16). The aryl aldehydes does not cause any distortion of the rhodium porphyrin complexes **2**, **4** and **5** (Figure 2.2)

Table 2.16 Comparison of the bond length and bond angle of compound **2**, **4** and **5**



FG	H	F	CF ₃
Bond length (Rh-C ₁)	1.950(5) Å	1.976(7) Å	1.941(7) Å
Bond angle (Rh-C ₁ -C ₂)	117.8(4) °	117.1(5) °	118.3(5) °

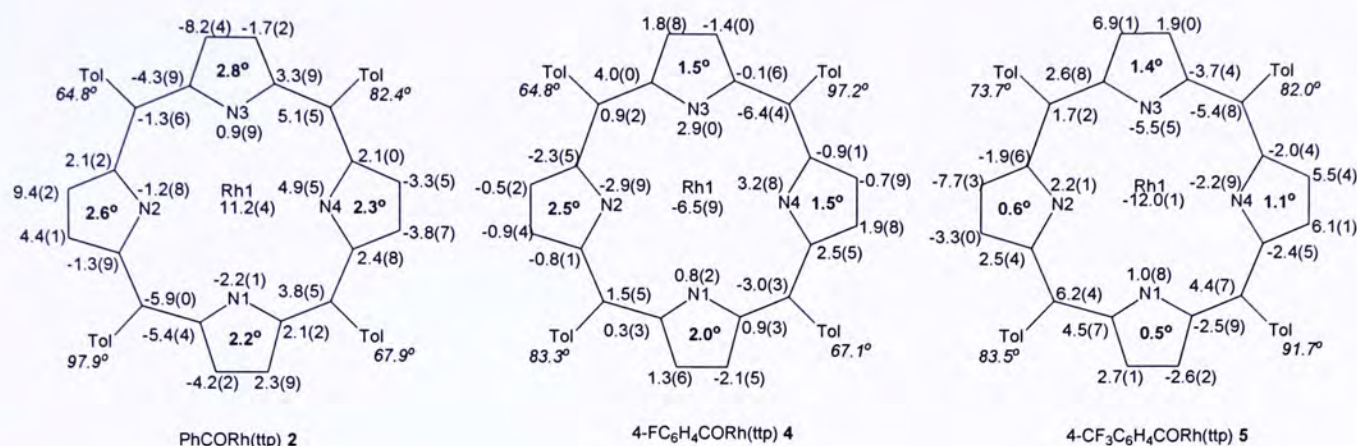


Figure 2.2 The conformation of the porphyrin in **2**, **4** and **5**, showing the displacements of the core atoms and of Rh from the 24-atom least-squares plane of the porphyrin core (in pm; positive values correspond to displacement towards the aryoyl ligands). Absolute values of the angles between the pyrrole rings and the least-squares plane of the 24-atom porphyrin core are shown in bold, and absolute values of the angles between the least-squares plane of the phenyl substituents and the 24-atom least-squares plane are shown in italics.

2.7 Summary

Selective aldehydic CHA of aryl and alkyl aldehydes have been achieved by high valent rhodium (III) complexes, Rh(tpp)Cl **1** and Rh(tpp)Me **10** in solvent-free conditions. Synthetically, this method provides an alternative and convenient preparation of an array of acyl rhodium porphyrins. Rh(tpp)Cl **1** appears to dissociate and yield Rh(tpp)⁺ which further reacts with aldehydic C-H bond through electrophilic attack, with both PhCORh(tpp) **2** and Rh(tpp)H **14** formed in a parallel manner. Rh(tpp)H **14** and Rh(tpp)Bn **3** appear to be the intermediates. On the other hand, Rh(tpp)Me **10** likely to undergo

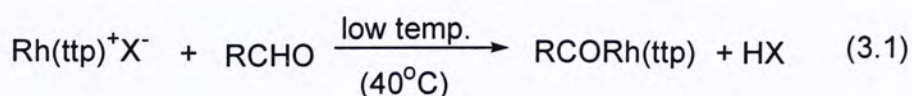
associative pathways either (1) oxidative addition or (2) sigma bond metathesis. However, from the coordination's point of view, the *cis* 6-coordinated transition state in sigma bond metathesis is more favorable. The details of the mechanism remain unclear.

Chapter 3 **CHA of Aldehydes by Rh(ttp)CH₂CH₂OH and Rh(ttp)⁺X⁻**

3.1 Introduction

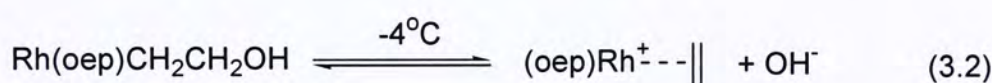
Although aldehydic CHA of aryl and alkyl aldehydes are successfully achieved by Rh(ttp)Cl **1** and Rh(ttp)Me **10**, improvements are needed to tackle the existing problems. (1) Formation of the reduction product Rh(ttp)Bn **3** in the CHA of aldehydes by Rh(ttp)Cl **1**, which sometimes results in complex mixture or loss of CHA products. (2) Though Rh(ttp)Me **10** can activate the aldehydic C-H bond with elimination of reduction products, the reaction temperature is high (200°C). (3) Solvent-free conditions restrict the range of aldehydes in aldehydic CHA. Incomplete reaction occurs due to poor solubility of rhodium porphyrin complexes in aldehydes.

The much facile aldehydic CHA by Rh(ttp)OTf **16** suggested that Rh(ttp)⁺ might be very reactive and allow the selective CHA reaction in the presence of solvent or even at low temperature. A convenient source of Rh(ttp)⁺ is sought and prepared (eq. 3.1).

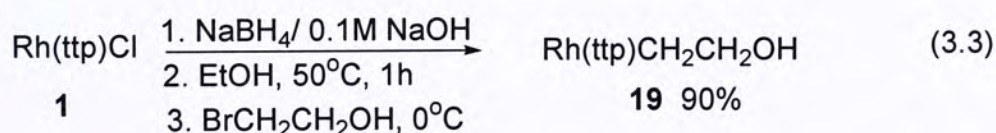


3.2 CHA of Aldehydes by Rh(tpp)CH₂CH₂OH

Indeed, Wayland reported the rapid acid dehydroxylation of the β -hydroxyethyl of Rh(oep)CH₂CH₂OH by formation of an observable intermediate, π -ethene complex, (oep)Rh(CH₂=CH₂)⁺ at low temperature (eq. 3.2).⁶⁵ Similarly, β -hydroxyethyl rhodium porphyrins might be expected to undergo β -dehydroxylation to give very reactive Rh(por)(CH₂=CH₂)⁺OH⁻. Therefore Rh(tpp)CH₂CH₂OH was prepared for the aldehydic CHA.



Rh(tpp)CH₂CH₂OH **19** was prepared by reductive alkylation of Rh(tpp)Cl **1** with NaBH₄/BrCH₂CH₂OH in 90% yield (eq. 3.3).⁵⁷ Rh(tpp)CH₂CH₂OH **19** is thermally unstable and the solvent has to be removed in the workup below 40°C.



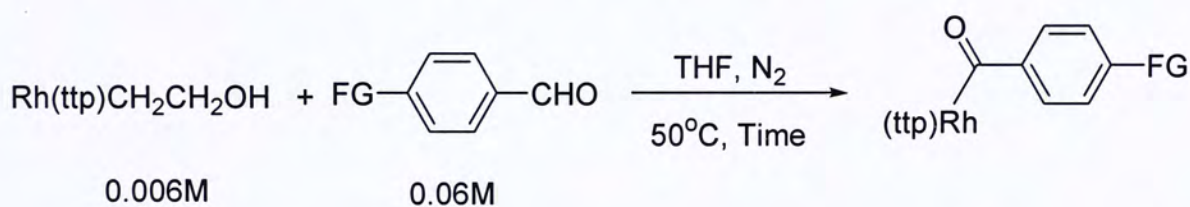
3.2.1 Results and Discussions

3.2.1.1 CHA of Aryl Aldehydes

To our delight, CHA of *para*-substituted aryl aldehydes by Rh(tpp)CH₂CH₂OH **19** were successfully carried out at 50°C in THF under N₂. Rh(tpp)CH₂CH₂OH **19** reacted with aryl aldehydes (10 equiv.) slowly and gave aldehydic CHA products generally with yields ~ 40% together with a minor unidentified side product at about 10% yield. No reduction product Rh(tpp)Bn **3** was observed (Table 3.1). Since, THF solvent was used, solid aryl aldehydes (CN and N(Me)₂) could also be employed. Higher yields were also

observed (Table 3.1, entries 7 and 8). Presumably the amine and cyano nitrogen coordinate to the rhodium and further stabilize the cationic $\text{Rh}(\text{ttp})^+$, and hence increased the yield. However, the electron rich 4-methoxybenzaldehyde did not produce aldehydic CHA product at 50°C. A higher temperature was required for the CHA of more electron-rich 4-MeOC₆H₄CHO (Table 3.1, entry 5).

Table 3.1 CHA of aryl aldehydes by $\text{Rh}(\text{ttp})\text{CH}_2\text{CH}_2\text{OH}$ **19**



Entry	FG	Time (h)	Yield (%)
1	H	72	2 (15)
2	F	72	4 (28)
3	CF ₃	72	5 (18)
4	Me	72	7 (28)
5	OMe	72	16 (none)
6	Cl	48	17 (67)
7	CN	48	20 (46)
8	NMe ₂	72	18 (42)

^a: ≤ 10% side product was obtained; ^b: No reaction, only $\text{Rh}(\text{ttp})\text{CH}_2\text{CH}_2\text{OH}$ observed by

TLC and ¹H NMR analysis

3.2.2 Increase in Concentration of Aryl Aldehydes.

To optimize the product yield, excess benzaldehyde at higher concentration (100 equiv.) was used (Table 3.2). Both reaction rate and yield were increased indeed; besides less minor side product was formed (Table 3.2, entry 1). Similar results were obtained from the aldehydic CHA of electron withdrawing substituent (F) and electron donating substituent (Me) (Table 3.2, entries 3 and 6).

Further user-friendly CHA conditions were found, Rh(ttp)CH₂CH₂OH **19** reacted with benzaldehyde(100 equiv.) in THF in air (Table 3.2, entry 2). The presence of air did not affect the selective CHA; results were similar to those obtained under N₂. Other substituents also gave selective aldehydic CHA products together with a minor side product. Since reaction rate and yield were similar in air and N₂, all subsequent CHA was run in air.

Table 3.2 CHA of aryl aldehydes (100 equiv.) by Rh(tpp)CH₂CH₂OH **19**

Entry	FG	Time (h)	Atmosphere	Yield (%)
1	H	48	N ₂	2 (62) ^a
2		60	Air	2 (81) ^a
3	F	60	N ₂	4 (65) ^a
4		24	Air	4 (74) ^a
5	CF ₃	36	Air	5 (44) ^a
6	Me	24	N ₂	7 (47) ^a
7		24	Air	7 (51) ^a
8	^t Bu	24	Air	9 (36) ^a

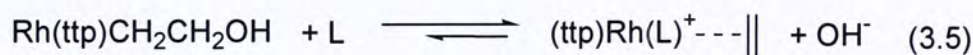
^a: ≤ 10% side product was obtained

3.2.3 Addition of Triphenylphosphine Ligand

Sufficient amounts of π -ethene complex $(\text{ttp})\text{Rh}(\text{CH}_2=\text{CH}_2)^+$ can be generated via β -dehydroxylation of the β -hydroxyethyl at low temperature which allows the CHA to occur (eq. 3.4).

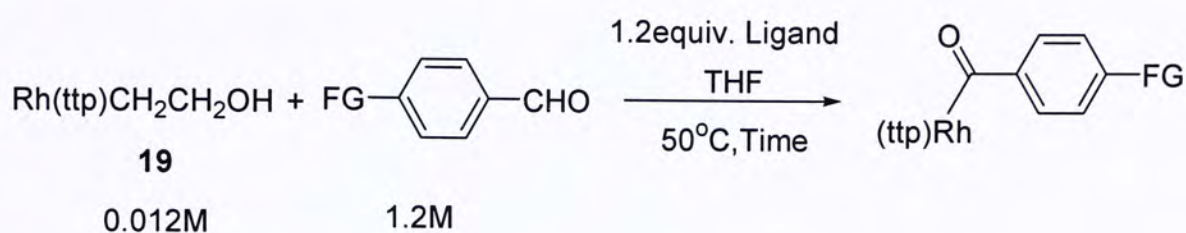


We postulated that addition of ligand will enrich the electron density of $(\text{ttp})\text{Rh}(\text{CH}_2=\text{CH}_2)\text{OH}$. The equilibrium will then shift to the right and generate a higher concentration of $[(\text{L})\text{Rh}(\text{ttp})(\text{CH}_4\text{CH}_4)]^+$ (eq. 3.5). Hopefully, aldehydic CHA will be expected to be more facile.



Triphenylphosphine (PPh_3) was therefore added to the reaction mixture in both aerobic and anaerobic conditions. Also, the concentration of $\text{Rh}(\text{ttp})\text{CH}_2\text{CH}_2\text{OH}$ **19** (0.012 M) and aryl aldehydes (1.2 M) were further increased to facilitate the CHA (Table 3.3). Indeed, no side product was observed from CHA of benzaldehyde by $\text{Rh}(\text{ttp})\text{CH}_2\text{CH}_2\text{OH}$ **19** either with PPh_3 or $\text{O}=\text{PPh}_3$.⁷² Also a significant increase in rate was observed. Similar results were obtained from CHA of 4-F- $\text{C}_6\text{H}_4\text{CHO}$. Surprisingly the CHA of 4-NMe₂- $\text{C}_6\text{H}_4\text{CHO}$ did not show any differences among the reaction rate, this might due to the coordination of a stronger sigma donor nitrogen to the rhodium instead of PPh_3 .

Table 3.3 Ligand effect on CHA



Entry	FG	Ligand	Time (h)	Atmosphere	Yield (%)
1	H	none	60	Air	2 (81) ^a
2		PPh ₃	5	Air	2 (76)
3		PPh ₃	36	N ₂	2 (76)
4		O=PPh ₃	16	Air	2 (67)
5		O=PPh ₃	46	N ₂	2 (62)
6	F	none	24	Air	4 (74) ^a
7		PPh ₃	7	Air	4 (65)
8		PPh ₃	36	N ₂	4 (56)
9	NMe ₂	none	72	N ₂	18 (42) ^a
10		PPh ₃	72	Air	18 (54)
11		PPh ₃	72	N ₂	18 (36)

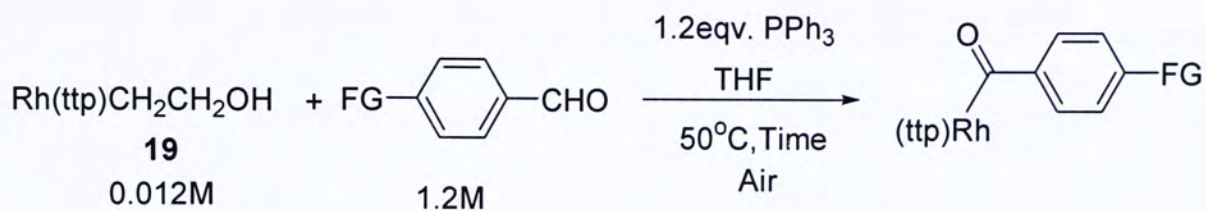
^a: ≤ 10% side product was obtained

3.2.4 Optimized Aerobic CHA of Aryl Aldehydes

Rh(ttp)CH₂CH₂OH **19** reacted with aryl aldehydes in the presence of PPh₃ in air at 50°C. Most of the substrates gave moderate to good yield of aldehydic CHA products (Table 3.4). The electron rich aldehydes, e.g. 4-MeC₆H₄CHO and 4-^tBuC₆H₄CHO (Table 3.4, entries 7 and 8), generally gave better yields of rhodium aroyl complexes than the electron deficient ones. 4-MeOC₆H₄CHO also yielded the rhodium aroyl complex **16** at

80°C. However, with unknown reasons, CHA of 4-BrC₆H₄CHO and 4-NO₂C₆H₄CHO did not give any desired products.

Table 3.4 Optimized Aerobic CHA of aldehydes by Rh(tpp)CH₂CH₂OH **21**.



Entry	FG	Time (h)	Yield (%)
1	H	5	2 (76)
2	F	7	4 (65)
3	Cl	16	17 (82)
4	Br	72	none ^b
5	CF ₃	48	5 (35)
6	CN	60	20 (46)
7	Me	7	7 (75)
8	^t Bu	36	9 (71)
9	OMe ^a	24	16 (83)
10	NMe ₂	72	18 (54)
11	NO ₂	72	none ^b

^a: yield was obtained at 80°C; ^b: No reaction, only Rh(tpp)CH₂CH₂OH

observed by TLC and ¹H NMR analysis

3.2.5 CHA of Aliphatic Aldehydes

Apart from aromatic aldehydes, Rh(ttp)CH₂CH₂OH **19** also reacted with aliphatic aldehydes in aerobic conditions (Table 3.5). Propanal reacted with Rh(ttp)CH₂CH₂OH **19** to give good yield of aldehydic CHA products EtCORh(ttp) **13** (80 % yield) within 30 min. When 1.2 equiv. of PPh₃ was added, the reaction rate was retarded. Therefore, propanal was more reactive than PhCHO (Table 3.5, entry 1). It was likely that the less sterically hindered propanal can bind to the rhodium easily and thus facilitated the reaction rate. However, after addition of ligand, [(ttp)Rh(L)(CH₂=CH₂)]⁺ becomes less electrophilic and less reactive. The reactive and strongly binding propanal will compete with PPh₃ for coordination. Therefore the rate decreased upon the addition of PPh₃. Unfortunately, ^tBuCHO did not react due to steric hindrance.

Table 3.5 CHA of aliphatic aldehydes by Rh(ttp)CH₂CH₂OH **19**.

$$\text{Rh(ttp)CH}_2\text{CH}_2\text{OH} + \text{RCHO} \xrightarrow[50^\circ\text{C, Time}]{\text{THF}} \text{RCORh(ttp)}$$

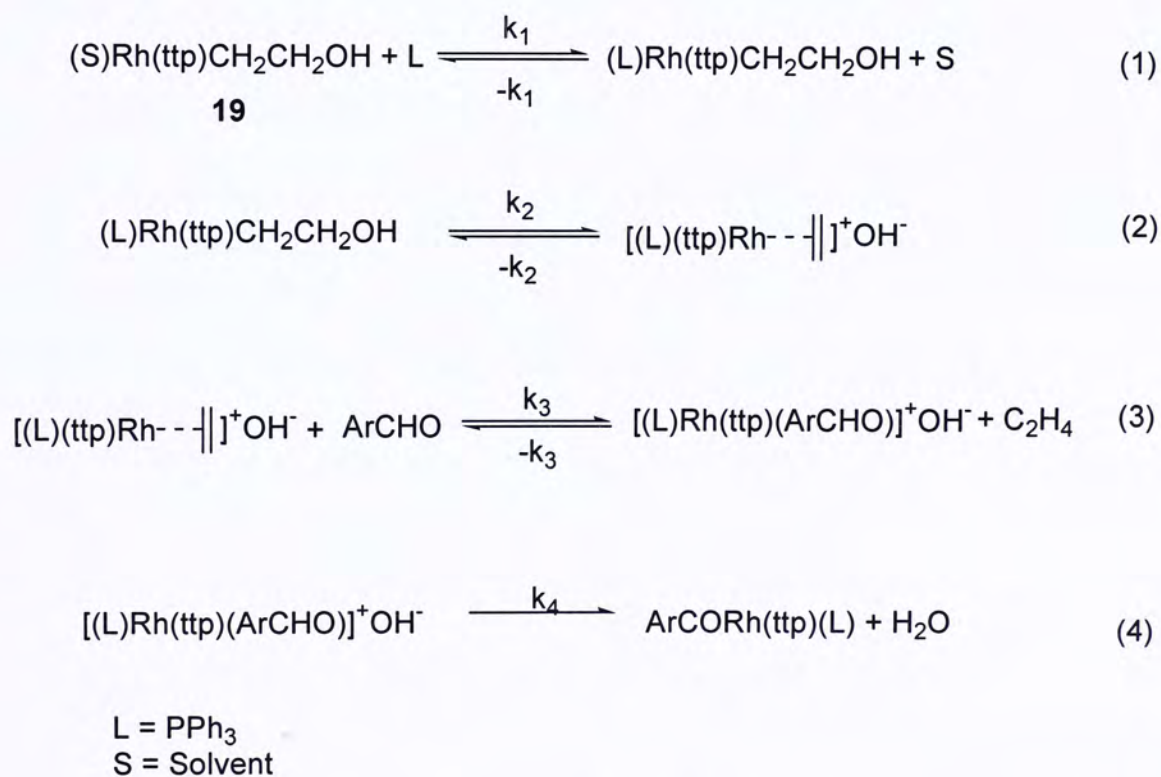
19

Entry	R	Time (h)	Yield (%)
1	C ₂ H ₅	0.5	13 (80)
2		6	13 (90) ^a
3	^t Bu	36	none ^b
4		48	none ^{a,b}

^a: 1.2 equiv. of PPh₃; ^b: No reaction, only **19** observed by TLC and ¹H NMR analysis

3.2.2 Mechanistic Studies

Scheme 3.1 depicts the proposed mechanism of CHA by Rh(ttp)CH₂CH₂OH **19**. PPh₃ undergoes ligand substitution with Rh(ttp)CH₂CH₂OH **19** and generates (L)Rh(ttp)CH₂CH₂OH in a fast pre-equilibrium (*k*₁). A fast ligand substrate reaction is attained (**1**). The (L)Rh(ttp)CH₂CH₂OH can undergo β-elimination to give stable [(L)Rh(ttp)(C₂H₄)]OH (**2**). Then the aldehydes bind to [(L)Rh(ttp)(C₂H₄)]⁺ via ligand substitution (**3**). Finally, CHA of aldehydes occurs and yields both stable aldehydic CHA product ArCORh(ttp) and H₂O (*k*₃) (**4**) (Scheme 3.2).

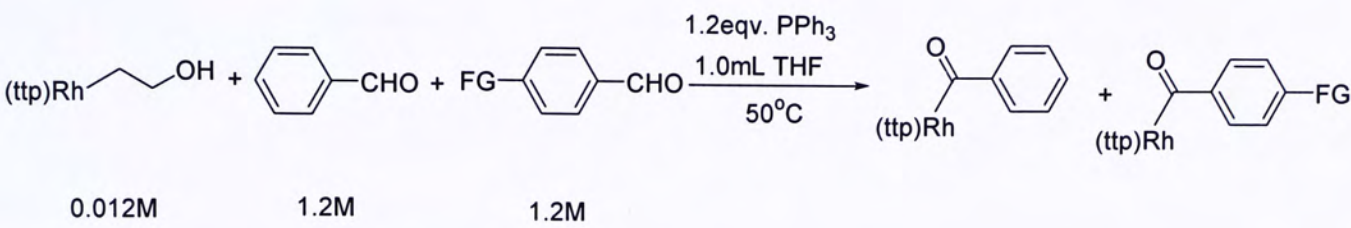


Scheme 3.1 Proposed mechanism for Aldehydic CHA by Rh(ttp)CH₂CH₂OH **19**

CHA of aldehydes by Rh(ttp)CH₂CH₂OH **19** at low temperature does not generate Rh(ttp)H **14** as Rh(ttp)Cl **1**, since no reduction product Rh(ttp)Bn **3** was found. Thus reduction of Rh(por)⁺ is only competitive with CHA at high temperature. Furthermore, the electronic effect of the *para*-substituent towards the aldehydic carbon bond was significant; the electron-rich aldehydes generally show a slower rate of CHA but with a better yield. This result was examined by the Hammett Plot.

Hammett Plot. The electronic effect on aldehydic CHA by Rh(ttp)CH₂CH₂OH **19** was examined by the Hammett plot. Competition reactions were carried out. Typically, a *para*-substituted aryl aldehyde was mixed with benzaldehyde in 1:1 ratio in THF with 1.2 equivalents of PPh₃ in aerobic conditions. The reaction was heated at 50°C and monitored till the starting material Rh(ttp)CH₂CH₂OH **19** disappeared by TLC analysis. Then the relative rate was calculated from the integration of methyl signal of the products in the crude reaction mixture in ¹H NMR and plot against the *para*-substituent constants (σ_p) (Table 3.6). The relative rate did not change even upon further heating.

Table 3.6 Competition reaction



	FG	k (FG/H)	Log k (FG/H)	σ_p	$\sigma_p^{+/-}$
1	CF ₃	1.2432	0.0946	0.53	0.65
2	Cl	2.0415	0.3099	0.34	0.11
3	F	0.8854	-0.0529	0.15	-0.07
4	CN	0.6342	-0.1978	0.71	0.99
5	Me	0.7332	-0.1348	-0.14	-0.30
6	^t Bu	0.6309	-0.2001	-0.15	-0.26
7	N(Me) ₂	0.6049	-0.2183	-0.32	-1.70

σ_p ---para-substituent constant; $\sigma_p^{+/-}$ ---para-substituent constant (resonance and inductive effect)

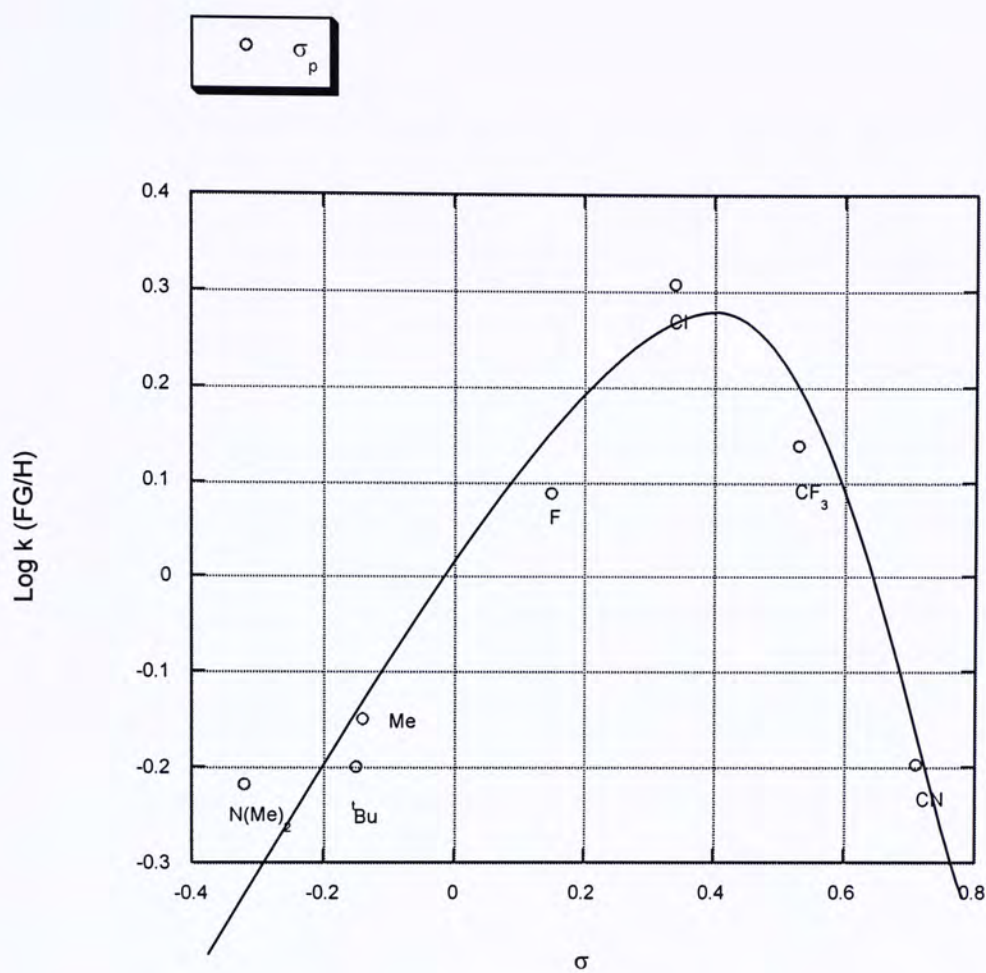


Figure 3.1 Hammett Plot of CHA of aryl aldehydes with Rh(ttp)CH₂CH₂OH **19**.

From Figure 3.1, a curve Hammett plot was observed which due to change of the rate determination steps (RDS) in the mechanism. This could be rationalized by k_3 and k_4 in Scheme 3.1. Since the transition state is highly affected by the *para*-substituents. The binding of ArCHO to $[(L)Rh(ttp)(C_2H_4)]^+$ in k_3 generates a partial positive charge on the C=O carbon and gives the aldehyde adduct $[(L)Rh(ttp)(ArCHO)]^+OH^-$. When the *para*-substituted group is an electron donating group (EDG), the transition state is stabilized.⁸⁰ While in k_4 , the aldehyde adduct will undergo CHA with the rhodium, thus the transition state will be favored by the electron withdrawing substituents and give a more thermodynamically stable aldehydic CHA product. Since k_3 and k_4 are comparable rates, so the overall effect yields a curve plot.

3.3 CHA of Aldehydes by Rh(ttp)X

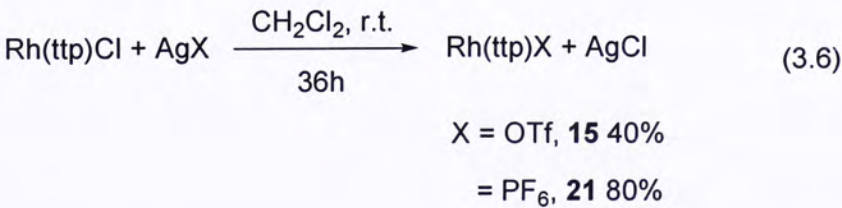
While Rh(ttp)⁺ is generated from Rh(ttp)X (X =Cl, OTf, CH₂CH₂OH (OH)) and the rates of CHA are: CH₂CH₂OH > OTf > Cl. Therefore the anions are important as CHA appears to depend on the [Rh(ttp)⁺]. The pKa of the anions are listed in Table 3.7.

Table 3.7 pKa of the inorganic acid.

Formula	pKa
H-Cl	-8.0 ^a
H-SO ₃ CF ₃	-14 ^a
H-OH	15.7 ^a
H-PF ₆	-12.6 ^b
H-BF ₄	- 15.5 ^b
^a : Ref. 75; ^b : Ref 82	

3.3.1 Preparation of Rh(ttp)X

The Rh(ttp)⁺ species were prepared by using less coordinating counteranions, for examples, OTf⁻ and PF₆⁻. According to Ogoshi, Rh(ttp)Cl **1** reacted with AgX (X = OTf and PF₆) to give Rh(ttp)X in dichloromethane at room temperature (eq. 3.6).⁴⁴



3.3.2 Results and Discussion

Rh(ttp)X (X = OTf, PF₆⁻) reacted with benzaldehyde more slowly (Table 3.7). Rh(ttp)X (X = OTf, PF₆⁻) showed either little or no reaction towards the aldehydic CHA in various solvents below 60°C. In solvent-free conditions, higher temperature was needed to give the desired CHA product (discussed in section 2.4.1). Though triflate (OTf) and hexafluorophosphate (PF₆⁻) are weaker coordinating counteranions,^{68-71,75,78} the results show that their dissociation abilities to generate Rh(ttp)⁺ are weaker than Rh(ttp)CH₂CH₂OH **19**. This could be explained by the weak Rh-OH bond (BDE ~ 64 kcal mol),⁶⁶⁻⁶⁷ in Rh(ttp)CH₂CH₂OH **19**, which eventually gives a more thermodynamically stable product, H₂O. Thus a more rapid reaction occurs. These results also suggest anion may have important role in the mechanistic step; however the details await further experiments.

Table 3.7 CHA of benzaldehydes by Rh(ttp)X.

Entry	X	FG	Solvent	Temp (°C)	Time (h)	Yield (%)
1	OTf	H	Solvent-free ^a	200	15min	2 (89)
2	OTf	OMe	Solvent-free ^a	200	15min	mixture
4	PF ₆	H	Hexafluorobenzene	60	48	0
5	PF ₆	H	1,2-dichloroethane	60	48	0
6	PF ₆	H	THF	60	48	trace ^b

^a: both in air and N₂ had the same results; ^c: no reaction, starting materials remained by TLC analysis.

3.4 Summary

$\text{Rh}(\text{ttp})\text{CH}_2\text{CH}_2\text{OH}$ **19** undergoes dehydroxylation at low temperature to give $\text{Rh}(\text{ttp})^+$ and OH^- . Selective aldehydic CHA of aldehydes is achieved by $\text{Rh}(\text{ttp})\text{CH}_2\text{CH}_2\text{OH}$ **19** in THF with addition of PPh_3 under mild, aerobic conditions. No reduction products are observed. This provides an alternative, and more efficient synthesis of aroyl rhodium complexes.

Conclusion

Selective aldehydic CHA can be achieved by high valent rhodium (III) complexes, Rh(tpp)Cl **1**, Rh(tpp)Me **10** and Rh(tpp)CH₂CH₂OH **19**. It provides a convenient synthesis of aroyl and acyl rhodium porphyrin complexes.

Aldehydic CHA were accomplished with Rh(tpp)Cl **1** and Rh(tpp)Me **10** in solvent-free conditions at 200°C. Rh(tpp)Cl reacted with aldehydes to give both CHA products and reduction products in a parallel manner, while much cleaner reaction occurred with Rh(tpp)Me without the formation of reduction product.

Improvement was made by generating a more reactive Rh(tpp)⁺ at low temperature from Rh(tpp)CH₂CH₂OH **19** in THF by β-dehydroxylation. This insitu prepared Rh(tpp)⁺ reacted with aldehydes in THF at 50°C to give rhodium porphyrin acyl complexes selectively without any reduction product. The aldehydic CHA was successfully improved to occur in aerobic conditions. Improved rate and yields were achieved with the addition of 1.2 equivalent of PPh₃.

Experimental Section

Unless otherwise noted, all reagents were purchased from commercial suppliers and used before purification. Hexane for chromatography was distilled from anhydrous calcium chloride. Tetrahydrofuran (THF) was distilled from sodium benzophenone ketyl prior to use. Benzonitrile was distilled from anhydrous P_2O_5 . $H_2(ftp)$ was prepared by the undergraduate, Mr. K. H. Lam and Mr. F. Wong. Thin layer chromatography was performed on pre-coated silica gel 60 F₂₅₄ plated. Silica gel (Merck, 70 - 230 and 230 - 400 mesh) was used for column chromatography.

1H NMR spectra were recorded on a Bruker DPX 300 (300MHz) spectrometer. Spectra were referenced internally to the residual proton resonance in C_6D_6 (δ 7.15 ppm) $CDCl_3$ (δ 7.26 ppm), or with tetramethylsilane (TMS, δ 0.00 ppm) as the internal standard. Chemical shifts (δ) were reported in part per million (ppm). ^{13}C NMR spectra were recorded on a Bruker DPX 300 (75 MHz) spectrometer and referenced to $CDCl_3$ (δ 77.10 ppm) Spectra. Coupling constants (J) were reported in Hertz (Hz). High resolution mass spectra (HRMS) were performed on a Thermofinnign MAT 95 XL (FABMS).

Unless otherwise stated, all reactions were carried at least twice, and the yields obtained were the average yields.

Preparation of Starting Materials

5, 10, 15, 20-Tetratolylporphyrinato)rhodium(III) Chloride, Rh(ttp)Cl (1).⁴⁵

H₂ttp (350 mg, 0.51 mmol) and RhCl₃·xH₂O (209 mg, 1.00 mmol) were refluxed in PhCN (30 mL) in air for 3 hours. After removal of solvent, the mixture was purified by column chromatography on silica gel eluting with CH₂Cl₂. **(1)** was then dried under vacuum at 80°C to remove the coordinated PhCN. Purplish red solid **(1)** was obtained after recrystallization from CH₂Cl₂/MeOH (368 mg, 0.39 mmol, 76% yield). *R_f* = 0.30 (CH₂Cl₂). ¹H NMR (300 MHz, CDCl₃) δ 2.71 (s, 12 H), 7.54 (d, 8 H, *J* = 8.1 Hz), 8.07 (d, 4 H, *J* = 6.9 Hz), 8.12 (d, 4 H, *J* = 6.9 Hz), 8.94 (s, 8 H).

(5, 10, 15, 20-Tetratolylporphyrinato)(methyl)rhodium(III), Rh(ttp)Me (10).⁵⁷

A suspension of Rh(ttp)Cl (98 mg, 0.11 mmol) in EtOH (50 mL) and a solution of NaBH₄ (40 mg, 1.08 mmol) in aq. NaOH (0.1 M, 2 mL) were purged with N₂ for 15 min separately. The solution of NaBH₄ was added slowly to the suspension of Rh(ttp)Cl via a cannula. The mixture was heated at 50°C under N₂ for 1 h to give a brown solution. The solution was then cooled to 0°C under N₂ and methyl iodide (0.7 mL, 10.8 mmol) was added via a syringe. A reddish orange suspension was formed. After being stirred at room temperature for another 15 min under N₂, the reaction mixture was worked up by extraction with CH₂Cl₂ and washed with H₂O. The combined organic extract was dried (anhydrous MgSO₄), filtered and rotatory evaporated. The reddish orange residue was purified by column chromatography over silica gel (250 - 400 mesh) eluting with a solvent mixture of hexane/CH₂Cl₂ (4:1). The major orange fraction was collected and gave **(2)** reddish orange solids (73 mg, 0.095 mmol, 86% yield) which were further

purified by recrystallization from CH₂Cl₂/CH₃OH. R_f = 0.72 (hexane/CH₂Cl₂ = 1:1). ¹H NMR (CDCl₃, 300 MHz) δ -5.83 (d, 3 H, J = 3.0 Hz), 2.96 (s, 12 H), 7.52 (d, 8 H, J = 8.1 Hz), 8.00 – 8.09 (m, 8 H), 8.72 (s, 8 H). HRMS (FABMS): Calcd. for (C₄₉H₃₉N₄Rh)⁺: m/z 786.2224. Found: m/z 786.2242.

(5, 10, 15, 20-Tetratolylporphyrinato)(beta-hydroxyethyl)rhodium(III), Rh(ttp)CH₂CH₂OH (19) ⁸²

A suspension of Rh(ttp)Cl (100 mg, 0.11 mmol) in EtOH (50 mL) and a solution of NaBH₄ (40 mg, 1.08 mmol) in aq. NaOH (0.1 M, 2 mL) were purged with N₂ for 15 min. The solution of NaBH₄ was added slowly to the suspension of Rh(ttp)Cl via a cannula. The solution mixture was heated at 50°C under N₂ for 1 h to give a brown suspension. The solution was then cooled to 0°C under N₂ and BrCH₂CH₂OH (0.8 mL, 10.8 mmol) was added via a syringe. A reddish orange suspension was formed. The reaction mixture was worked up by extraction with CH₂Cl₂/H₂O. The combined organic extract was dried (anhydrous MgSO₄), filtered and rotatory evaporated below 30°C to avoid decomposition. The reddish orange residue was purified by column chromatography over silica gel (250 - 400 mesh) eluting with hexane/CH₂Cl₂ (1:1). The major orange fraction was collected and gave reddish orange solids (**3**) (86 mg, 0.099 mmol, 90% yield) which was further purified by recrystallization from CH₂Cl₂/CH₃OH. R_f = 0.34 (hexane/CH₂Cl₂ = 1:1). ¹H NMR (CDCl₃, 300 MHz) δ -4.97 - -4.91 (m, 2 H), -2.74 (t, 1 H, J = 6.5 Hz), -2.20 (dd, 2 H, J = 6.3, 13.5 Hz), 2.70 (s, 12 H), 7.52 – 7.55 (d, 8 H, J = 7.8 Hz), 7.99 – 8.08 (m, 8 H), 8.75 (s, 8 H).

(5, 10, 15, 20-Tetratolylporphyrinato) rhodium(III) Triflate, Rh(ttp)OTf (15)⁴⁵

Rh(ttp)Cl (50 mg, 0.057 mmol) and the silver triflate (25.6 mg, 0.11 mmol) was put into the dried CH₂Cl₂ (100 mL), and stirred for 1.5 days at room temperature. The color of the mixture changed from red to reddish brown after 1.5 days. Then the product was isolated on silica gel eluting with CH₂Cl₂/EA (9:1). **(4)** was collected as orange solids (22 mg, 0.023 mmol, 40% yield). *R_f* = 0.32 (hexane/CH₂Cl₂ = 1:1). ¹H NMR (300 MHz, CDCl₃) δ 2.70 (s, 12 H), 7.48 – 7.61 (m, 8 H), 7.98 – 8.05 (m, 8 H), 8.76 (s, 8 H). Calcd. for (C₄₉H₃₆N₄RhO₃F₃S)⁺: *m/z* 771.1990. Found: *m/z* 771.1998.

(5, 10, 15, 20-Tetratolylporphyrinato)rhodium(III) Hexafluorophosphate, Rh(ttp)PF₆ (23)⁴⁵

Rh(ttp)Cl (50 mg, 0.057 mmol) and the silver hexafluorophosphate (32 mg, 0.11 mmol) was suspended in anhydrous CH₂Cl₂ (100 mL), and stirred for 1.5 days at room temperature. The color of the mixture remained red after 1.5 days. Then the product was isolated on silica gel eluting with CH₂Cl₂/EA (9:1). Orange fraction **5** was collected (40 mg, 0.046 mmol, 80% yield). *R_f* = 0.35 (hexane/CH₂Cl₂ = 1:1). ¹H NMR (300 MHz, CDCl₃) δ 2.71 (s, 12 H), 7.53 (d, 8 H, *J* = 8.1 Hz), 8.04 – 8.10 (m, 8 H), 8.91 (s, 8 H). ¹³C NMR (75 MHz, CDCl₃) δ 22.1, 127.8 (d, *J* = 27 Hz), 133.0, 134.4, 135.2, 137.8, 139.6, 143.7. Calcd. for (C₄₈H₃₆N₄RhPF₆)⁺: *m/z* 771.1986. Found: *m/z* 771.1990.

(5, 10, 15, 20-Tetratolylporphyrinato)rhodium(III) Hydride, Rh(ttp)H (14)⁵⁸

A suspension of Rh(ttp)Cl (100 mg, 0.11 mmol) in MeOH (50 mL) and a solution of NaBH₄ (17 mg, 0.45 mmol) in aq. NaOH (0.1 M, 2 mL) were purged with N₂ for 15 min separately. The solution of NaBH₄ was added slowly to the suspension of Rh(ttp)Cl via a cannula. The mixture was heated at 50 °C under N₂ for 1 h to give a brown solution. The solution was then cooled to 0 °C under N₂ and 0.1 M HCl (40 mL) was added via a syringe. A brick red suspension was formed. After stirred at room temperature for another 15 min under N₂, the brick red precipitate was collected after filtration and washing with water (2 x 10 mL). The brick red residue for **(6)** was obtained (80 mg, 0.10 mmol, 92% yield) and vacuum dried. ¹H NMR (C₆D₆, 300 MHz) δ -40.12 (d, 1 H, *J*_{Rh-H} = 43.5 Hz), 2.42 (s, 12 H), 7.16 (d, 4 H, *J* = 8.2 Hz), 7.35 (d, 4 H, *J* = 8.2 Hz), 7.95 (d, 4 H, *J* = 8.1 Hz), 8.22 (d, 4 H, *J* = 8.1 Hz), 9.03 (s, 8 H).

Reaction of Aromatic Aldehydes with Rh(ttp)Cl (1)

(5, 10, 15, 20-Tetratolylporphyrinato)(benzoyl)rhodium(III), $\text{C}_6\text{H}_5\text{CORh(ttp)}$ (**2**) and

(5, 10, 15, 20-Tetratolylporphyrinato)(benzyl)rhodium(III), $\text{C}_6\text{H}_5\text{CH}_2\text{Rh(ttp)}$ (**3**) :

General Procedure:

Method A1: Rh(ttp)Cl (47 mg, 0.054 mmol) was dissolved in benzaldehyde (2.0 mL) and formed a bright red reaction mixture. The bright red reaction mixture was heated at 150°C under N_2 in the dark for 1.5 days. After 1.5 days, the mixture turned into dark red. Excess benzaldehyde was removed, the dark red crude products were then isolated by column chromatography on silica gel eluting with hexane/ CH_2Cl_2 (4:1). Two fractions were collected. Red solid, $\text{C}_6\text{H}_5\text{CORh(ttp)}$ (**2**) were collected a major product (24 mg, 0.028 mmol, 52% yield). $R_f = 0.42$ (hexane: $\text{CH}_2\text{Cl}_2 = 1:1$). ^1H NMR (300 MHz, CDCl_3) δ 2.43 (dd, 2 H, $J = 1.2, 8.1$ Hz), 2.70 (s, 12 H), 5.98 – 6.00 (m, 2 H), 6.40 (t, 1 H, $J = 7.8$ Hz), 7.53 – 7.56 (m, 8 H), 7.95 – 8.07 (m, 8 H), 8.76 (s, 8 H). HRMS (FABMS): Calcd. for $(\text{C}_{55}\text{H}_{41}\text{N}_4\text{ORh})^+$: m/z 876.2330. Found: m/z 876.2303. IR (KBr, cm^{-1}) $\nu(\text{C}=\text{O})$ 1716 (s). Anal. Calcd. for $\text{C}_{55}\text{H}_{41}\text{N}_4\text{ORh}\cdot\text{H}_2\text{O}$: C, 73.82; H, 4.62; N, 6.26; Found C, 73.66; H, 4.64; N, 5.90. Single crystal for X-ray diffraction analysis was grown from $\text{CH}_2\text{Cl}_2/\text{MeOH}$. Orange red solid, $\text{C}_6\text{H}_5\text{CH}_2\text{Rh(ttp)}$ (**3**) was collected a minor product, (13 mg, 0.015 mmol, 28% yield). $R_f = 0.52$ (hexane: $\text{CH}_2\text{Cl}_2 = 1:1$). ^1H NMR (300 MHz, CDCl_3) δ -3.80 (d, 2 H, $J = 3.6$ Hz), 2.67 (s, 12 H), 2.94 (d, 2 H, $J = 6.5$ Hz), 5.84 – 5.89 (m, 2 H), 6.38 (t, 1 H, $J = 7.4$ Hz), 7.45 – 7.56 (m, 8 H), 7.98 – 8.08 (m, 8 H), 8.67 (s, 8 H).

Method A2: Rh(ttp)Cl (47 mg, 0.054 mmol) was added into benzaldehyde (2.0 mL). The bright red reaction mixture was heated at 200°C under N₂ in the dark for 1 day only (**2**) was isolated (24 mg, 0.043 mmol, 79% yield).

Method B: Rh(ttp)CH₃ (30 mg, 0.038 mmol) was mixed with benzaldehyde (1.0 mL) in a Telfon screw capped flask under nitrogen at 200°C in the dark for 30 min. Only the red solid (**2**) was obtained as the major product (20 mg, 0.027 mmol, 70% yield).

Method C: Rh(ttp)CH₂CH₂OH (10 mg, 0.012 mmol) was mixed with 100 equiv. of benzaldehyde (124 µL, 1.20 mmol) in THF (1.0 mL) at 50°C for 2.5 days to yield (**2**) (8.5 mg, 0.0097 mmol, 81% yield) .

Method D: Rh(ttp)CH₂CH₂OH (10 mg, 0.012 mmol) and 1.2 equiv. of PPh₃ (3.8 mg, 0.014 mmol) were mixed with 100 equiv. of benzaldehyde (124 µL, 1.20 mmol) in THF (1.0 mL) at 50°C for 5 hours to yield (**2**) (8.0 mg, 0.0091 mmol, 76% yield).

(5, 10, 15, 20-Tetratolyporphyrinato)(4-fluorobenzoyl)rhodium(III), 4-FC₆H₅CORh(ttp) (4**).**

Method A2: Rh(ttp)Cl (47 mg, 0.054 mmol) was mixed with 4-fluorobenzaldehyde (2.0 mL) at 200°C under N₂ in the dark for 1 day. The dark red crude product was purified by column chromatography on silica gel eluting with hexane/CH₂Cl₂ (4:1). 4-FC₆H₅CORh(ttp) (**4**) was obtained as a red solid (22 mg, 0.024 mmol, 45% yield). R_f = 0.54 (hexane: CH₂Cl₂ = 1:1). ¹H NMR (300 MHz, CDCl₃) δ 2.40 (dd, 2 H, *J* = 3.2, *J* = 8.7 Hz), 2.71 (s, 12 H), 5.65 (t, 2 H, *J* = 8.7 Hz), 7.53 (t, 8 H, *J* = 6.1 Hz), 7.95 – 7.977 (m, 4 H), 8.03 – 8.07 (m, 8 H), 8.78 (s, 8 H). HRMS (FABMS): Calcd. for (C₅₅H₄₀N₄OFRh)⁺: *m/z* 894.2236. Found: *m/z* 894.2256. IR (KBr, cm⁻¹) ν (C=O) 1711 (s). Anal. Calcd. for

C₅₅H₄₀N₄ORhF·3H₂O: C, 70.13; H, 4.28; N, 5.95; Found C, 70.39; H, 4.50; N, 5.84.

Single crystal for X-ray diffraction analysis was grown from CH₂Cl₂/MeOH.

Method B: Rh(ttp)CH₃ (30 mg, 0.038 mmol) was mixed with 4-fluorobenzaldehyde (1.0 mL) in a Telfon screw capped flask under nitrogen at 200°C in the dark for 8 hours to yield (**4**) as a red solid, (26 mg, 0.029 mmol, 76% yield).

Method C: Rh(ttp)CH₂CH₂OH (10 mg, 0.012 mmol) was mixed with 100 equiv. of 4-fluorobenzaldehyde (130 µL, 1.20 mmol) in THF (1.0 mL) at 50°C for 1 day to yield (**4**) (8.0 mg, 0.0089 mmol, 74% yield).

Method D: Rh(ttp)CH₂CH₂OH (10 mg, 0.012 mmol) and 1.2 equiv. of PPh₃ (3.8 mg, 0.014 mmol) were mixed with 4-fluorobenzaldehyde (130 µL, 1.20 mmol) in THF (1.0 mL) at 50°C for 7 hours to yield (**4**) (7.0 mg, 0.0078 mmol, 65% yield).

(5, 10, 15, 20-Tetratolyporphyrinato)(4-chlorobenzoyl)rhodium(III), 4-ClC₆H₅CORh(ttp) (17**).**

Method B: Rh(ttp)CH₃ (30 mg, 0.038 mmol) was mixed with 4-chlorobenzaldehyde (938 mg) in a Telfon screw capped flask under nitrogen at 200°C in the dark for 8 hours to yield 4-ClC₆H₅CORh(ttp) (**17**) as a red solid, (16 mg, 0.020 mmol, 53% yield).

Method C: Rh(ttp)CH₂CH₂OH (10 mg, 0.012 mmol) was mixed 100 equiv. of 4-chlorobenzaldehyde (22 mg, 0.12 mmol) in THF (1.0 mL) at 50°C for 2 day. The solvent was then removed and (**17**) was isolated by column chromatography on silica gel with hexane/CH₂Cl₂ (4:1). Red solid of (**17**) was obtained (8.5 mg, 0.0080 mmol, 67% yield).

R_f = 0.70 (hexane: CH₂Cl₂ = 1:1). ¹H NMR (300 MHz, CDCl₃) δ 2.33 (d, 2 H, *J* = 8.1 Hz), 2.71 (s, 12 H), 5.94 (d, 2 H, *J* = 8.1 Hz), 7.53 (t, 8 H, *J* = 6.6 Hz), 7.90 – 7.93 (m, 4

H), 8.03 – 8.06 (m, 4 H), 8.79 (s, 8 H). IR (KBr, cm^{-1}) $\nu(\text{C}=\text{O})$ 1703 (s). Anal. Calcd. for $\text{C}_{55}\text{H}_{40}\text{ClN}_4\text{ORh}\cdot\text{H}_2\text{O}$: C, 71.08; H, 4.56; N, 6.03; Found C, 70.68; H, 4.35; N, 5.97.

Method D: $\text{Rh}(\text{ttp})\text{CH}_2\text{CH}_2\text{OH}$ (10 mg, 0.012 mmol) and 1.2 equiv. of PPh_3 (3.8 mg, 0.014 mmol) were mixed with 4-chlorobenzaldehyde (172 mg, 1.20 mmol) in THF (1.0 mL) at 50°C for 16 hours to yield (**17**) as a red solid (9 mg, 0.0098 mmol, 82% yield).

**(5, 10, 15, 20-Tetratolyporphyrinato)(4- α,α,α -trifluoromethylbenzoyl)rhodium(III),
4- $\text{CF}_3\text{C}_6\text{H}_5\text{CORh}(\text{ttp})$ (**5**).**

Method A2: $\text{Rh}(\text{ttp})\text{Cl}$ (47 mg, 0.054 mmol) was dissolved in 4- α,α,α -trifluoromethylbenzaldehyde (2.0 mL) and heated at 200°C under N_2 in the dark for 1 day. Excess 4- α,α,α -trifluoromethylbenzaldehyde was removed, the dark red crude products were then purified by column chromatography on silica gel eluting with hexane/ CH_2Cl_2 (4:1). One fraction was collected. Reddish purple solid, 4- $\text{CF}_3\text{C}_6\text{H}_5\text{CORh}(\text{ttp})$ (**5**) (26 mg, 0.021 mmol, 38% yield) was obtained. $R_f = 0.54$ (hexane: $\text{CH}_2\text{Cl}_2 = 1:1$). ^1H NMR (300 MHz, CDCl_3) δ 2.48 (d, 2 H, $J = 8.1$ Hz), 2.71 (s, 12 H), 6.25 (d, 2 H, $J = 8.1$ Hz), 7.53 (d, 8 H, $J = 7.8$ Hz), 7.90 – 7.93 (m, 4 H), 8.03 – 8.06 (m, 4 H), 8.79 (s, 8 H). HRMS (FABMS): Calcd. for $(\text{C}_{56}\text{H}_{40}\text{N}_4\text{OF}_3\text{Rh})^+$: m/z 944.2204. Found: m/z 944.2220. IR (KBr, cm^{-1}) $\nu(\text{C}=\text{O})$ 1691 (s). Anal. Calcd. for $\text{C}_{56}\text{H}_{40}\text{N}_4\text{F}_3\text{ORh}\cdot\text{H}_2\text{O}$: C, 69.86; H, 4.19; N, 5.82; Found C, 69.96; H 4.26; N, 5.73.

Method B: Rh(ttp)CH₃ (30 mg, 0.038 mmol) was mixed with 4- α,α,α -trifluoromethylbenzaldehyde (1.0 mL) in a Teflon screw capped flask under nitrogen at 200°C in the dark for 2 days to yield **(5)** as a reddish purple solid, (14 mg, 0.015 mmol, 39% yield).

Method C: Rh(ttp)CH₂CH₂OH (10 mg, 0.012 mmol) was mixed with 100 equiv. of 4- α,α,α -trifluoromethylbenzaldehyde (167 μ L, 1.20 mmol) in THF (1.0 mL) at 50°C for 1.5 days to yield **(5)** (5.7 mg, 0.0053 mmol, 44% yield).

Method D: Rh(ttp)CH₂CH₂OH (10 mg, 0.012 mmol) and 1.2 equiv. of PPh₃ (3.8 mg, 0.014 mmol) were mixed with 4- α,α,α -trifluoromethylbenzaldehyde (167 μ L, 1.20 mmol) in THF (1.0 mL) at 50°C for 2 days to yield **(5)** (4 mg, 0.0042 mmol, 35% yield).

(5, 10, 15, 20-Tetratolyporphyrinato)(4-cyanobenzoyl)rhodium(III), 4-CNC₆H₅CORh(ttp) (20).

Method C: Rh(ttp)CH₂CH₂OH (10 mg, 0.012 mmol) was mixed 100 equiv. of 4-cyanobenzaldehyde (16 mg, 0.12 mmol) in THF (1.0 mL) at 50°C for 2 day. The solvent was then removed and 4-CNC₆H₅CORh(ttp) (**20**) was isolated by column chromatography on silica gel eluting with hexane/CH₂Cl₂ (4:1). Red solid was obtained (5 mg, 0.0054 mmol, 46% yield). R_f = 0.42 (hexane: CH₂Cl₂ = 1:1). ¹H NMR (300 MHz, CDCl₃) δ 2.44 (d, 2 H, J = 8.7 Hz), 2.71 (s, 12 H), 6.28 (d, 2 H, J = 8.7 Hz), 7.54 (t, 8 H, J = 8.9 Hz), 7.91 (dd, 4 H, J = 2.3, J = 7.8 Hz), 8.03 (dd, 4 H, J = 2.3, J = 7.8 Hz), 8.80 (s, 8 H). HRMS (FABMS): Calcd. for (C₅₆H₄₀N₅ORh)⁺: m/z 901.2288. Found: m/z 901.2282. IR (KBr, cm⁻¹) ν (C=O) 1694 (s). Anal. Calcd. for C₅₆H₄₀N₅ORh·H₂O: C, 73.12; H, 4.60; N, 7.83; Found C, 72.75; H, 4.49; N, 8.23.

Method D: Rh(ttp)CH₂CH₂OH (10 mg, 0.012 mmol) and 1.2 equiv. of PPh₃ (3.8 mg, 0.014 mmol) were mixed with 4-cyanobenzaldehyde (161 mg, 1.20 mmol) in THF (1.0 mL) at 50°C for 2.5 days to yield **(20)** as a red solid (5 mg, 0.0055 mmol, 46% yield).

(5, 10, 15, 20-Tetratolyporphyrinato)(4-methylbenzoyl)rhodium(III), 4-CH₃C₆H₅CORh(ttp) (7) and (5, 10, 15, 20-Tetratolyporphyrinato)(4-formylbenzyl)rhodium(III), 4-CHOC₆H₅CH₂Rh(ttp) (6).

Method A2: Rh(ttp)Cl (47 mg, 0.054 mmol) was dissolved in 4-methylbenzaldehyde (2.0 mL) and heated at 200°C under N₂ in the dark for 2h. Then excess 4-methylbenzaldehyde was removed, the dark red crude products were then isolated by column chromatography on silica gel eluting with hexane/CH₂Cl₂ (4:1). Red solid, 4-CH₃C₆H₅CORh(ttp) **(7)** (14 mg, 0.016 mmol, 30% yield) was collected. *R_f* = 0.45 (hexane: CH₂Cl₂ = 1:1). ¹H NMR (300 MHz, CDCl₃) δ 1.87 (s, 3 H), 2.35 (d, 2 H, *J* = 8.1 Hz), 2.70 (s, 12 H), 5.76 (d, 2 H, *J* = 8.1 Hz), 7.53 (d, 8 H, *J* = 8.1 Hz), 7.92 – 7.95 (m, 4 H), 8.05 – 8.08 (m, 4 H), 8.76 (s, 8 H). Calcd. for (C₅₆H₄₃N₄ORh)⁺: *m/z* 890.2486. Found: *m/z* 890.2472. IR (KBr, cm⁻¹) ν(C=O) 1704 (s). Anal. Calcd. for C₅₆H₄₃N₄ORh·H₂O: C, 73.28; H, 4.72; N, 6.10; Found C, 73.50; H, 4.70; N, 5.98. Orange red solid, 4-CHOC₆H₅CH₂Rh(ttp) **(6)** (26 mg, 0.030 mmol, 55% yield) was collected. *R_f* = 0.35 (hexane: CH₂Cl₂ = 1:1). ¹H NMR (300 MHz, CDCl₃) δ -3.80 (d, 2 H, *J* = 3.0 Hz), 2.70 (s, 12 H), 2.97 (d, 2 H, *J* = 7.8 Hz), 6.35 (d, 2 H, *J* = 7.8 Hz), 7.53 – 7.56 (m, 8 H), 7.94 – 8.08 (m, 8 H), 8.70 (s, 8 H), 9.44 (s, 1 H). ¹³C NMR (75 MHz, CDCl₃) δ 9.81 (d, *J*_{Rh-C} = 27 Hz), 22.0, 24.0, 123.2, 125.2, 128.0, 132.0, 132.2, 134.2, 134.4, 137.8, 139.8,

143.6, 192.3. Calcd for $(C_{56}H_{45}N_4Rh)^+$: m/z 890.2486. Found: m/z 890.2482. IR (KBr, cm^{-1}) $\nu(C=O)$ 1693 (s)

Method B: Rh(tp) CH_3 (30 mg, 0.038 mmol) was mixed with 4-methylbenzaldehyde (1.0 mL) in a Teflon screw capped flask under nitrogen at 200°C in the dark for 16 hours to yield **(12a)** (6 mg, 0.021 mmol, 54% yield).

Method C: Rh(tp) CH_2CH_2OH (10 mg, 0.012 mmol) was mixed 100 equiv. of 4-methylbenzaldehyde (144 μ L, 1.20 mmol) in THF (1.0 mL) at 50°C for 1 day. **(7)** was obtained (5.4 mg, 0.0061 mmol, 51% yield).

Method D: Rh(tp) CH_2CH_2OH (10 mg, 0.012 mmol) and 1.2 equiv. of PPh_3 (3.8 mg, 0.014 mmol) were mixed with 4-methylbenzaldehyde (144 μ L, 1.20 mmol) in THF (1.0 mL) at 50°C for 7 hours to yield **(7)** (8.0 mg, 0.0090 mmol, 75% yield).

(5, 10, 15, 20-Tetratolylporphyrinato)(4-^tButylbenzoyl)rhodium(III), 4-^tBuC₆H₅CORh(tp) (9) and (5, 10, 15, 20-Tetratolylporphyrinato)(4-Formyl-phenyl-1,1-dimethyl-ethyl)rhodium(III), 4-CHOC₆H₄(Me)₂CH₂Rh(tp) (8).

Method A2: Rh(tp)Cl (47 mg, 0.054 mmol) was dissolved in 4-tert-butylbenzaldehyde (2.0 mL) and heated at 200°C under N₂ in the dark for 1 hour. Then excess 4-tert-butylbenzaldehyde was removed, the dark red crude products were then isolated by column chromatography on silica gel eluting with hexane/ CH_2Cl_2 (4:1). Red solids of 4-^tBuC₆H₅CORh(tp) **(9)** (9 mg, 0.0092 mmol, 17% yield) was collected. R_f = 0.43 (hexane: CH_2Cl_2 = 1:1). ¹H NMR (300 MHz, $CDCl_3$) δ 0.95 (s, 9 H), 2.42 (d, 2 H, J = 8.3 Hz), 2.70 (s, 12 H), 5.96 (d, 2 H, J = 8.3 Hz), 7.52 (d, 8 H, J = 8.1 Hz), 7.95 – 7.98 (m, 4 H), 8.04 – 8.07 (m, 4 H), 8.74 (s, 8 H). Calcd. for $(C_{59}H_{49}N_4ORh)^+$: m/z 932.2956. Found:

m/z 932.2974. IR (KBr, cm^{-1}) $\nu(\text{C}=\text{O})$ 1710 (s). Anal. Calcd. for $\text{C}_{59}\text{H}_{49}\text{N}_4\text{ORh}\cdot 2\text{H}_2\text{O}$: C, 73.13; H, 5.51; N, 5.78; Found C, 73.25; H, 5.22; N, 5.69. Another orange fraction 4- $\text{CHOC}_6\text{H}_4(\text{Me})_2\text{CH}_2\text{Rh}(\text{ttp})$ (**8**) was also collected (3 mg, 0.0011 mmol, 2% yield). $R_f = 0.69$ (hexane: $\text{CH}_2\text{Cl}_2 = 1:1$). ^1H NMR (300 MHz, CDCl_3) δ -3.79 (d, 2 H, $J = 3.0$ Hz), 1.25 (s, 9 H), 2.70 (s, 12 H), 2.92 (d, 2 H, $J = 9.0$ Hz), 5.87 (d, 2 H, $J = 9.0$ Hz), 7.52 – 7.56 (m, 8 H), 8.01 (t, 8 H, $J = 7.5\text{Hz}$), 8.65 (s, 8 H). ^{13}C NMR (75 MHz, CDCl_3) δ 13.0 (d, $J_{\text{Rh-C}} = 28$ Hz), 22.1, 31.2, 122.9, 123.5, 124.6, 127.8, 127.9, 131.8, 134.3, 134.4, 137.6, 138.3, 139.9, 143.6, 194.5. Calcd. for $(\text{C}_{59}\text{H}_{49}\text{N}_4\text{O}_1\text{Rh}_1)^+$: m/z 932.3288. Found: m/z 932.2956. IR (KBr, cm^{-1}) $\nu(\text{C}=\text{O})$ 1704 (s)

Method B: $\text{Rh}(\text{ttp})\text{CH}_3$ (30 mg, 0.038 mmol) was mixed with 4- tert-butylbenzaldehyde (1.0 mL) in Telfon screw capped flask under nitrogen at 200°C in the dark for 16 hours to yield (**9**) (26 mg, 0.028 mmol, 73% yield).

Method C: $\text{Rh}(\text{ttp})\text{CH}_2\text{CH}_2\text{OH}$ (10 mg, 0.012 mmol) was mixed 100 equiv. of 4-tert-butylbenzaldehyde (150 μL , 1.20 mmol) in THF (1.0 mL) at 50°C for 1 day to yield (**9**) (5.4 mg, 0.0061 mmol, 51% yield).

Method D: $\text{Rh}(\text{ttp})\text{CH}_2\text{CH}_2\text{OH}$ (10 mg, 0.012 mmol) and 1.2 equiv. of PPh_3 (3.8 mg, 0.014 mmol) were mixed with 4-methylbenzaldehyde (150 μL , 1.20 mmol) in THF (1.0 mL) at 50°C for 7 hours to yield (**9**) (8.0 mg, 0.0085 mmol, 71 %yield).

(5, 10, 15, 20-Tetratolyporphyrinato)(4-methoxybenzoyl)rhodium(III), 4-MeOC₆H₅CORh(ttp) (16).

Method B: Rh(ttp)CH₃ (30 mg, 0.038 mmol) was dissolved in anisaldehyde (1.0 mL) in Telfon screw capped flask under nitrogen at 200°C in the dark for 16 hours to yield 4-MeOC₆H₅CORh(ttp) (**16**) (21 mg, 0.021 mmol, 56% yield) as red solid. *R_f* = 0.52 (hexane: CH₂Cl₂ = 1:1). ¹H NMR (300 MHz, CDCl₃) δ 2.42 (d, 2 H, *J* = 8.5 Hz), 2.70 (s, 12 H), 3.45 (s, 3 H), 5.47 (d, 2 H, *J* = 8.5 Hz), 7.53 (d, 8 H, *J* = 8.1 Hz), 7.95 -8.08 (m, 8 H), 8.76 (s, 8 H). Calcd for (C₅₆H₄₃N₄O₂Rh)⁺: *m/z* 906.2422. Found: 906.2436 *m/z*. IR (KBr, cm⁻¹) ν(C=O) 1704 (s). Anal. Calcd for C₅₆H₄₃N₄ORh·2H₂O: C, 71.33; H, 5.02; N, 5.94; Found C, 71.71; H, 4.72; N, 5.77.

Method D: Rh(ttp)CH₂CH₂OH (10 mg, 0.012 mmol) and 1.2 equiv. of PPh₃ (3.8 mg, 0.014 mmol) were mixed with anisaldehyde (115 μL, 1.20 mmol) in THF (1.0 mL) at 80°C for 1 day to yield (**16**) (9.0 mg, 0.010 mmol, 83% yield).

(5, 10, 15, 20-Tetratolyporphyrinato)(4-*N,N*-Dimethylbenzoyl)rhodium(III), 4-(NMe₂)C₆H₅CORh(ttp) (18)

Method C: Rh(ttp)CH₂CH₂OH (10 mg, 0.012 mmol) was mixed 100 equiv. 4-*N,N*-Dimethylbenzaldehyde (20 mg, 0.12 mmol) in THF (1.0 mL) at 50°C for 3 days. The solvent was then removed and 4-(NMe₂)C₆H₅CORh(ttp) (**18**) was isolated by column chromatography on silica gel eluting with hexane/CH₂Cl₂ (5:1), followed by CH₂Cl₂. Brick red solid was obtained (5 mg, 0.0050 mmol, 42% yield). *R_f* = 0.30 (hexane: CH₂Cl₂ = 1:1). ¹H NMR (300 MHz, CDCl₃) δ 2.44 (d, 2 H, *J* = 8.7 Hz), 2.61 (s, 6 H), 2.70 (s, 12 H), 5.24 (d, 2 H, *J* = 8.7 Hz), 7.51 (d, 8 H, *J* = 8.1 Hz), 7.945 – 7.98 (m, 4 H), 8.05 – 8.08

(m, 4 H), 8.74 (s, 8 H). Anal. Calcd for $C_{58}H_{46}N_5ORh \cdot CH_3OH$: C 73.16, H 5.30, N 7.34, Found C 72.87, H 4.91, N 7.01.

Method D: Rh(ttp)CH₂CH₂OH (10 mg, 0.012 mmol) and 1.2 equiv. of PPh₃ (3.8 mg, 0.014 mmol) were mixed with mixed 4-*N*, *N*-Dimethylbenzaldehyde (182 mg, 1.20 mmol) in THF (1.0 mL) at 50°C for 3 days to yield **(18)** (6 mg, 0.0065 mmol, 54% yield).

Reaction of Aliphatic aldehydes with Rh(ttp)Cl (1)

(5, 10, 15, 20-Tetratolylporphyrinato)(ethylformyl)rhodium(III), CH₃CH₂CORh(ttp)

(12): General Procedure.

Method A: Rh(ttp)Cl (47 mg, 0.054 mmol) was dissolved in propanal (2.0 mL) and heated at 100°C under N₂ in the dark for 2 day. Then excess propanal was removed, the dark red crude products were then isolated by column chromatography on silica gel eluting with hexane/CH₂Cl₂ (4:1). Red solid, CH₃CH₂CORh(ttp) (**12**) (1 mg, 0.0016 mmol, 3% yield) was collected. $R_f = 0.52$ (hexane: CH₂Cl₂ = 1:1). ¹H NMR (300 MHz, CDCl₃) δ -3.14 (q, 2 H, $J = 7.5$ Hz), -1.69 (t, 3 H, $J = 7.2$ Hz), 2.70 (s, 12 H), 7.26 (d, 8 H, $J = 7.8$ Hz), 8.05 (d, 8 H, $J = 6.3$ Hz), 8.80 (s, 8 H). HRMS (FABMS): Calcd. for (C₅₁H₄₁N₄ORh)⁺: m/z 828.2335. Found: m/z 828.2330. IR (KBr, cm⁻¹) ν (C=O) 1717 (s). Anal. Calcd. for C₅₁H₄₁N₄ORh·2H₂O: C, 70.83; H, 5.24; N, 6.48; Found C, 70.46; H, 4.81; N, 6.21.

Method B: Rh(ttp)Me (30 mg, 0.038 mmol) was added into propanal (1.0 mL). The bright red reaction mixture was heated at 100°C under N₂ in the dark for 1 day. Excess propanal was removed. The dark red crude products were then isolated by column chromatography on silica gel eluting with hexane/CH₂Cl₂ (4:1). Bright red solid (**12**) was collected (19 mg, 0.023 mmol, 60% yield)

Method C: Rh(ttp)CH₂CH₂OH (10 mg, 0.012 mmol) was mixed 100 equiv. of propanal (87 μ L, 0.12 mmol) in THF (2.0 mL) at 50°C for 30min. The solvent was then removed and (**12**) was isolated by column chromatography on silica gel eluting with hexane/CH₂Cl₂ (4:1), followed by CH₂Cl₂. Brick red solid was obtained (8.0 mg, 0.0096 mmol, 80% yield).

Method D: Rh(ttp)CH₂CH₂OH (10 mg, 0.012 mmol) and 1.2 equiv. of PPh₃ (3.8 mg, 0.014 mmol) were mixed with mixed 100 equiv. propanal (87 μL, 1.20 mmol) in THF (1.0 mL) at 50°C for 6 hours to yield **(12)** (6 mg, 0.011 mmol, 90% yield).

5, 10, 15, 20-Tetratolyporphyrinato)(hexylformyl)rhodium(III),
CH₃(CH₂)₅CORh(ttp) (11)

Method B: Rh(ttp)Me (30 mg, 0.038 mmol) was added into heptanal (1.0 mL). The bright red reaction mixture was heated at 200°C under N₂ in the dark for 3 days. Excess heptanal was removed. The dark red crude products were then isolated by column chromatography on silica gel eluting with hexane/CH₂Cl₂ (4:1). Bright red solids of CH₃(CH₂)₅CORh(ttp) **(11)** were collected (14 mg, 0.016 mmol, 41% yield). *R_f* = 0.67 (hexane: CH₂Cl₂ = 1:1). ¹H NMR (300 MHz, CDCl₃) δ -3.12 (t, 2 H, *J* = 7.2 Hz), -1.40 (p, 2 H, *J* = 9.0 Hz), -0.88 (q, 2 H, *J* = 9.0 Hz), 0.47 (d, 2 H, *J* = 5.7 Hz), 0.53 (m, 2 H), 0.86 (d, 3 H, *J* = 7.2 Hz), 2.70 (s, 12 H), 7.57 (d, 8 H, *J* = 7.3 Hz), 8.01 – 8.09 (m, 8 H), 8.79 (s, 8 H). HRMS (FABMS): Calcd. for (C₅₅H₄₉N₄ORh)⁺: *m/z* 884.2953. Found: *m/z* 884.2956. IR (KBr, cm⁻¹) ν(C=O) 1716 (s). Anal. Calcd. for C₅₅H₄₉N₄ORh·2H₂O: C, 71.57; H, 6.00; N, 6.07; Found C, 71.61; H, 5.60; N, 6.05.

(5, 10, 15, 20-Tetratolyporphyrinato)(tert-butylformyl)rhodium(III), ^tBuCORh(ttp)
(13)

Method A: Rh(ttp)Cl (47 mg, 0.054 mmol) was dissolved in tert-butylaldehyde (2.0 mL) and heated at 200°C under N₂ in the dark for 1 day. Then excess tert-butylaldehyde was removed, the dark red crude products were then isolated by column chromatography on

silica gel eluting with hexane/CH₂Cl₂ (4:1). Red solids of ^tBuCORh(ttp) (**18**) (11 mg, 0.013 mmol, 24% yield) were collected. *R_f* = 0.52 (hexane: CH₂Cl₂ = 1:1). ¹H NMR (300 MHz, CDCl₃) δ -2.36 (s, 9 H), 2.70 (s, 12 H), 7.53 (d, 8 H, *J* = 9.0 Hz), 7.96 – 8.05 (m, 8 H), 8.70 (s, 8 H). HRMS (FABMS): Calcd. for (C₅₃H₄₅N₄ORh)⁺: *m/z* 857.2700. Found: *m/z* 857.2721. IR (KBr, cm⁻¹) ν(C=O) 1732 (s). Anal. Calcd. for C₅₃H₄₉N₄ORh·H₂O: C, 72.75; H, 5.42; N, 6.41; Found C, 72.61; H, 5.60; N, 6.05.

Method B: Rh(ttp)Me (30 mg, 0.038 mmol) was added into tert-butylaldehyde (1.0 mL). The bright red reaction mixture was heated at 200°C under N₂ in the dark for 3 days. Excess solvent was removed. The dark red crude products were then isolated by column chromatography on silica gel eluting with hexane/CH₂Cl₂ (4:1). Bright red solid (**18**) was collected (16 mg, 0.018 mmol, 48% yield).

Competition Reaction between benzaldehyde and *p*-substituted benzaldehydes:

General Procedures

(1) Competition Reactions using Rh(ttp)Me (10) as starting materials

Rh(ttp)Me (10) (30 mg, 0.038 mmol) was mixed with benzaldehyde and *p*-substituted benzaldehydes in 1:1 ratio. The mixture was then heated at 200°C under N₂ in the dark. The reaction was monitored till the starting material Rh(ttp)Me (10) disappeared by TLC analysis. After the reaction was completed, crude ¹H NMR spectra were taken. Then the relative rate was calculated from the integration of methyl signal of the products in the crude reaction mixture in ¹H NMR

<i>p</i> -FG-PhCHO	Time (h)	Integration		Relative Rate	
		H	FG	k (H _{FG} /H _H)	log k (H _{FG} /H _H)
CF ₃	3	8.0	5.0	1.6	0.2
F	30	8.0	8.1	1.0	-0.004
^t Bu	32	8.0	10.6	0.8	-0.1
OMe	16	8.0	8.0	1.0	0.004

The relative rate did not change even upon further reactions.

(2) Competition Reactions using Rh(ttp)CH₂CH₂OH as starting materials

Rh(ttp)CH₂CH₂OH (10 mg, 0.012 mmol) and 1.2 equiv. PPh₃ (3.8 mg, 0.014 mmol) were mixed with 100 equiv. benzaldehyde and 100 equiv. *p*-substituted benzaldehyde in THF (1.0 mL) at 50°C. The reaction was monitored till the starting material Rh(ttp)CH₂CH₂OH 19 disappeared by TLC analysis. After the reaction was completed, crude ¹H NMR spectra were taken. Then the relative rate was calculated from

the integration of methyl signal of the products in the crude reaction mixture in ¹H NMR

The relative rate did not change even upon further reactions.

<i>p</i> -FG-PhCHO	Time (h)	Integration		Relative Rate	
		H	FG	k (H _{FG} /H _H)	log k (H _{FG} /H _H)
CF ₃	16	8.0	10.0	1.2	0.09
Cl	12	8.0	16.3	2.0	0.3
F	16	8.0	7.1	0.9	-0.05
CN	2.5	8.0	5.1	0.6	-0.2
Me	22	8.0	5.9	0.7	-0.1
^t Bu	16	8.0	5.1	0.6	-0.2
N(Me) ₂	48	8.0	4.8	0.6	-0.2
<i>The relative rate did not change even upon further reactions.</i>					

Reactions between Rh(ttp)H and Aldehydes: General Procedures

(1) Rh(ttp)H with benzaldehydes

Rh(ttp)H (**14**) (20 mg, 0.026 mmol) was dissolved in benzaldehydye (1.0 mL) to form a dark red solution. The solution mixture was heated at different temperature to give the reduction product:

At 50°C: When the reaction mixture was heated at 50°C for 2 days, only trace amount of the C₆H₅CORh(ttp) (**2**) was observed from TLC and ¹H NMR analysis. However, no C₆H₅CH₂Rh(ttp) (**3**) was observed.

At 200°C: When the reaction mixture was heated at 200°C for 30 min both $\text{C}_6\text{H}_5\text{CORh}(\text{ttp})$ (**2**) (8.0 mg, 0.0091 mmol, 35% yield) and $\text{C}_6\text{H}_5\text{CH}_2\text{Rh}(\text{ttp})$ (**3**) (1.0 mg, 0.0010 mmol, 4% yield) were obtained after chromatography.

(2) Rh(ttp)H with 4-methoxybenzaldehyde

Rh(ttp)H (**14**) (20 mg, 0.026 mmol) was dissolved in anisaldehyde (1.0 mL) to form the dark red solution. The solution mixture was heated at different temperature to deduce the reduction products:

At 50°C: When the reaction mixture was heated at 50°C for 2 days, no reaction was occurred.

At 200°C: When the reaction mixture was heated at 200°C for 30 min both 4-MeOC₆H₄CORh(ttp) (**16**) (5 mg, 0.0055 mmol, 21% yield) and Rh(ttp)Me (**10**) (3 mg, 0.0038 mmol, 15% yield) were obtained after chromatography.

Reactions between Rh(ttp)⁺X⁻ and Aldehydes: General Procedures

(1) Rh(ttp)OTf with benzaldehyde

Rh(ttp)OTf (**15**) (10 mg, 0.010 mmol) was dissolved in benzaldehyde (1.0 mL) and heated at 200°C under N₂ in the dark. After 15 min, $\text{C}_6\text{H}_5\text{CORh}(\text{ttp})$ (**2**) (7.8 mg, 0.0089 mmol, 89% yield) was obtained.

(2) Rh(ttp)OTf with 4-methoxybenzaldehyde

Rh(ttp)OTf (**15**) (10 mg, 0.010 mmol) was dissolved in anisaldehyde (1.0 mL) and heated at 200°C under N₂ in the dark for 15 min. No products were obtained.

(3) Rh(ttp)PF₆ with benzaldehyde

Rh(ttp)PF₆ (**23**) (11.6 mg, 0.012 mmol) with 100 equiv. of benzaldehyde (124 μ L, 1.2 mmol) were added in different solvents at different temperature. However, all of them seem no reaction occurred, Rh(ttp)PF₆ (**23**) remained from the TLC analysis.

Solvent	Temperature (°C)	Time (d)	Products (7a)
Hexafluorobenzene	40	2	No reaction
	60	2	No reaction
1,2-dichloroethane	40	2	No reaction
	60	2	No reaction
THF (under air)	60	2	Trace amount
THF (under N ₂)	60	2	Trace amount

Addition of Ligand and Base:

(1) Addition of 1.0 equiv. of pyridine

Rh(ttp)Cl (**1**) (30 mg, 0.037 mmol) was dissolved in benzaldehyde (1.0 mL) then followed by the addition of 1.0 equiv. of pyridine. The red reaction mixture was heated at 200°C for 4 days, C₆H₅CORh(ttp) (**2**) (12 mg, 0.012 mmol, 32% yield) and BnRh(ttp) (**3**) (6mg, 0.0059 mmol, 16% yield) were formed.

(2) Addition of 30 equiv. of pyridine

(a) Rh(ttp)Cl (**1**) (30 mg, 0.037 mmol) was dissolved in benzaldehyde (1.0 mL) then followed by the addition of 30 equiv. of pyridine. The red reaction mixture was heated at 200°C for 5 days, no product of C₆H₅CORh(ttp) (**2**) formed.

(b) Rh(tp)Me (**10**) (30 mg, 0.038 mmol) was dissolved in benzaldehyde (1.0 mL) then followed by the addition of 30 equiv. of pyridine. The red reaction mixture was heated at 200°C for 2 hours, C₆H₅CORh(tp) (**2**) (24 mg, 0.027 mmol, 71% yield) was obtained.

(2) Addition of 1.0 equiv of PPh₃

(a) Rh(tp)Cl (**1**) (30 mg, 0.037 mmol) was dissolved in benzaldehyde (1.0 mL) then followed by the addition of 1.0 equiv. of PPh₃. The red reaction mixture was heated at 200°C for 1 day, C₆H₅CORh(tp) (**2**) (25mg, 0.029 mmol, 79%) was formed.

(b) Rh(tp)Me (**10**) (30 mg, 0.038 mmol) was dissolved in benzaldehyde (1.0 mL) then followed by the addition of 1.0 equiv. of PPh₃. The red reaction mixture was heated at 200°C for 45 min, C₆H₅CORh(tp) (**2**) (17 mg, 0.019 mmol, 51%) was formed.

(3) Addition of 30 equiv. of 2,4,6-trimethylpyridine.

Rh(tp)Cl (**1**) (30 mg, 0.037 mmol) was dissolved in benzaldehyde (1.0 mL) then followed by the addition of 30 equiv. of 2,4,6-trimethylpyridine. The red reaction mixture was heated at 200°C for 2 h, C₆H₅CORh(tp) (**2**) (0.024 mmol, 65%) was formed.

Exchange experiments: General Procedures

Carbon-hydrogen activated rhodium complexes (0.01 mmol) was mixed with benzaldehyde and heated at different temperature. Exchange of the aromatics was observed.

Rh(ttp)Ar	Solvent	PhCHO	Temp (°C)	Time (h)	C ₆ H ₅ CORh(ttp) 2
C ₆ H ₄ CH ₂ Rh(ttp) (2)	none	1.0 mL	200	24	49%
4- ^t BuC ₆ H ₄ CORh(ttp) (9)	none	1.0 mL	200	4	57%
4-FC ₆ H ₄ CORh(ttp) (4)	1.0 mL THF	100 equiv.	50	15	96%
MeRh(ttp) (10)	1.0 mL THF	100 equiv	80	120	No reaction

Reference:

1. Olah, G. A.; Molnar, A. *Hydrocarbon chemistry, 2nd Edition*, Hoboken, N. J.: Wiley-Interscience, **1995**.
2. Shilov, A. E.; Shteinman, A. A. *Coord. Chem. Rev.* **1977**, *24*, 97-99.
3. Shul'pin, G. B.; Shilov, A. E.; Kitaigorodskii, A. N.; Zeile-Krevor, J. V. *J. Organomet. Chem.* **1980**, *201*, 319-325.
4. Janowicz, A. H.; Bergman, R. G. *J. Am. Chem. Soc.* **1983**, *105*, 3929 – 3939.
5. Bergman, R. G. *Science* **1984**, *223*, 902-922.
6. Olah, G. A.; Molnar, A. *Hydrocarbon chemistry, 2nd Edition*, Hoboken, N. J.: Wiley-Interscience, **1995**, Chapter 3.
7. Huheey, J. E.; Keiter, E. A.; Keiter, R. L. *Inorganic Chemistry Principles of Structure and Reactivity, 4th Edition*, Harper-Collins College Publishers, Chapter 16.
8. Periana, R. A.; Taube, D. J.; Gamble, S.; Taube, H.; Satoh, T.; Fujii, H. *Science* **1998**, *280*, 560-564.
9. Periana, R. A.; Mironov, O.; Taube, D.; Bhalla, G.; Jones, C. J. *Science* **2003**, *301*, 814-818.
10. Luo, Y. R. *Handbook of Bond Dissociation Energies in Organic Compounds*, CRC PRESS, **2003**.
11. (a) Bagno, A.; Bukala, J.; Olah, G. A. *J. Org. Chem.* **1990**, *55*, 4284-4289. (b) Hynes, A.; Mann, B. E.; Morris, G. E.; Maitlis, P. M. *J. Am. Chem. Soc.* **1993**, *115*, 4093-4100. (c) Haynes, A.; Maitlis, P. M.; Morris, G. E.; Sunley, G. J.; Adams, H.; Badger, P. W.; Bowers, C. M.; Cook, D. B.; Elliott, P. I. P.; Ghaffar, T.; Green, H.; Griffin, T. R.; Payne, M.; Pearson, J. M.; Taylor, M. J.; Vickers, P. W.; Watt, R. J. *J. Am. Chem. Soc.* **2004**, *126*, 2847-2861.

12. Gossage, R. A.; Koten, G. V.; Jones, W. D.; Kakiuchi, F.; Murai, S.; Sen, A.; Murakami, M.; Ito, Y.; Suginome, M.; Lin, Y. -S.; Yamamoto, A.; Grushin, V. V.; Alper, H.; Hidai, M.; Mizobe, Y.; Richmond, T.G. . *Activation of unreactive bonds and organic synthesis*, Murai, S. Ed., Springer-Verlag: Berlin Heidelberg, **1999**, Chapter 2, 3 and 4.
13. Collman, J. P.; Hegedus, L. S.,. *Principles and applications of organotransition metal chemistry*, 1ST Ed.; Kelly, A. Ed.; Mill Valley, Calif: University Science Books, **1980**, Chapter 5 (Table 5).
14. Thayer, J. S. *Organometallic Chemistry. An Overview*, New York, N. Y., Weinheim: VCH Publishers, **1987**.
15. Bulls, R. A.; Bercaw, J. E.; Manriquez, J. M.; Thompson, M. E. *Polyhedron* **1988**, 7, 1409-1428.
16. Thompson, M. E.; Baxter, S. M.; Bulls, A. R.; Burger, B. J.; Nolan, M. C.; Santarsiero, B. D.; Schaefer, W. P.; Bercaw, J. E. *J. Am. Chem. Soc.* **1987**, 109(1), 203-219.
17. Bercaw, J. E. *Pure & Appl. Chem.* **1990**, 62(6), 1151-1154.
18. Choi, J. C.; Sakakura, T. *J. Am. Chem. Soc.* **2003**, 125, 7762-7763.
19. Watson, P. L. *J. Am. Chem. Soc.* **1983**, 105, 6491-6493.
20. Thompson, M. E.; Bercaw, J. E. *Pure. Appl. Chem.* **1984**, 56, 1-10.
21. Holtcamp, M. W.; Labinger, J. A.; Bercaw, J. E. *J. Am. Chem. Soc.* **1997**, 119, 848-849.
22. Strout, D. L.; Zaric, S.; Niu, S.; Hall, M. B. *J. Am. Chem. Soc.* **1996**, 118, 6068-6069.
23. Duckett, S. B.; Haddleton, D. M.; Jackson, S. A.; Perutz, M. P.; Upmacis, R. K. *Organometallics* **1988**, 7, 1526-1532.

24. Fernandez, M. J.; Bailey, P. M.; Bentz, P. O.; Ricci, J. S.; Koetzle, T. F.; Maitlis, P. M. *J. Am. Chem. Soc.* **1984**, *106*, 5458-5463.
25. Klei, S. R.; Tilley, T. D.; Bergman, R. G. *J. Am. Chem. Soc.* **2000**, *122*, 1816-1817.
26. Sherry, A. E.; Wayland, B. B. *J. Am. Chem. Soc.* **1990**, *112*, 1259-1261.
27. Cui, W.; Zhang, X. P.; Wayland, B. B. *J. Am. Chem. Soc.* **2003**, *125*, 4994-4995.
28. Wayland, B. B.; Ba, S.; Sherry, A. E. *J. Am. Chem. Soc.* **1991**, *113*, 5305-5311.
29. Chen, H. L.; Ellis, P. E.; Wijesekera, J. T.; Hagan, T. E.; Groh, S. E.; Lyons, J. E., Ridge, D. P. *J. Am. Chem. Soc.* **1994**, *116*, 1086-1089.
30. Walsh, P. J.; Hollander, F. J.; Bergman, R. G. *J. Am. Chem. Soc.* **1988**, *110*, 8729-8731.
31. Eguillor, B.; Esteruelas, M. A.; Olivan, M.; Oriate, E. *Organometallics* **2004**, *23*, 6015-6024.
32. Marder, T. B.; Roe, D. C.; Milstein D. *Organometallics* **1988**, *7*, 1451-1453.
33. Tanaka, K.; Fu, G. C. *J. Am. Chem. Soc.* **2001**, *123*, 11492-11493.
34. Alaimo, P. J.; Arndtsen, B. A.; Bergman, R. G. *Organometallics* **2000**, *19*, 2130-2143.
35. Gomez, M.; Kisenyi, J. M.; Sunley, G. J.; Maitlis, P. M. *J. Organomet. Chem.* **1985**, *296*, 197-207.
36. Robinson, N. P.; Main, L.; Nicholson, B. K. *J. Organomet. Chem.* **1988**, *349*, 209-218.
37. Vicente, J.; Abad, J. A.; Martinez-Viviente, E.; Ramirez de Arellano, M. C.; Jones, P. G. *Organometallics* **2000**, *19*, 752-760.
38. Milstein, D. *Organometallics* **1982**, *1*, 1549-1551.

39. Bianchini, C.; Meli, A.; Perzzini, M.; Ramirez, J. A.; Vacca, A.; Vizza, F.; Zanobin, F. *Organometallics* **1989**, 8, 337-345.
40. Bernard, K. A.; Atwood, J. D. *Organometallics* **1988**, 7, 235-236.
41. Corkey, B. K.; Taw, F. L.; Bergman, R. G.; Brookhart, M. *Polyhedron* **2004**, 23, 2943-2948.
42. Smith, K. M.; Fallk, J. E. *In Porphyrins and Metalloporphyrins*, Elsevier Scientific: Amsterdam, **1975**, 1-28.
43. Wayland, B. B.; Balkus, K. J. J.; Farnos, M. D. *Organometallics*, **1989**, 8, 950-953.
44. Aoyama, Y.; Yoshida, T.; Sakurai, K. I.; Ogoshi, H. *Organometallics* **1986**, 5, 168-173.
45. Zhou, X.; Li, Q.; Mak, T. C. W.; Chan, K. S. *Inorg. Chim. Acta.* **1998**, 270, 551-553.
46. Del Rossi, K. J.; Zhang, X. X.; Wayland, B. B. *J. Organomet. Chem.* **1995**, 504, 47-56.
47. Martinho Simoes, J. A.; Beauchamp, J. L.; *Chem. Rev.*, **1990**, 90, 629-688.
48. Lide, D. R. *CRC Handbook of Chemistry and Physics*, **2002**, CRC PRESS LCC, CD-Rom.
49. The IR stretching frequencies of aldehydes ($\nu_{C=O}$) are from <http://www.acros.be>.
50. Kadish, K. M.; Royal, G.; Caemelbecke, E. V.; Gueletti, L.; Tabata, M.; Nishimoto, J. *The Porphyrin Handbook Volume 9 Database of Redox Potentials and Binding Constants*, Kadish, K. M.; Smith, K. M.; Guillard, R. Ed.; San Diego: Academic Press, **2000**, Chapter 60.
51. Wayland, B. B.; Newman, A. R. *Inorg. Chem.* **1981**, 20, 3093-3097.
52. Kadish, K. M.; Anderson, J. E.; Yao, C. L.; Guillard, R. *Inorg. Chem.* **1986**, 25, 1277-1280.

53. Kadish, K. M.; Yao, C. L.; Anderson, J. E.; Cocolios, P. *Inorg. Chem.* **1985**, *24*, 4515-4520.
54. Guillard, R.; Kadish, K. M. *Chem. Rev.* **1988**, *88*, 1121-1146.
55. Anderson, J. E.; Yao, C. L.; Kadish, K. M. *Inorg. Chem.* **1986**, *25*, 718-719.
56. Issaacs, N. S. *Physical Organic Chemistry*, ELBS, Longman: Avon, **1987**, Chapter 4.
57. Ogoshi, H.; Setsune, J.; Omura, T.; Yoshida, Z. *J. Am. Chem. Soc.* **1975**, *97*, 6461-6466.
58. Wayland, B. B.; Van Voorhees, S. L.; Wilker, C. *Inorg. Chem.* **1986**, *25*, 4039-4042.
59. Bullock, R. M. *Transition Metal Hydrides*; Dedieu, A. Ed.; VCH: New York, **1992**.
60. Tam, T. T. L. *MPhil. Thesis*, The Chinese University of Hong Kong, **2001**.
61. Wayland, B. B.; Sherry, A. E.; Bunn, A. G. *J. Am. Chem. Soc.* **1993**, *115*, 7675-7684.
62. Collman, J. P.; Boulatoy, R. *Acta. Cryst.*, **2001**, *C57*, 406-408.
63. Al-Akhdar, W. A.; Belmore, K. A.; Kendrick, M. *Inorg. Chim. Acta*, **1989**, *165*, 15-17.
64. Pretsch, E.; Buhlmann, P.; Affolter, C. *Structure Determination of Organic Compounds: Tables of Spectral Data*, Berlin, New York: Springer, **2000**.
65. Wayland, B. B.; Van Voorhees, S. L.; Del Rossi, K. J. *J. Am. Chem. Soc.* **1987**, *109*, 6513-6515.
66. Wayland, B. B.; Fu, X. *J. Am. Chem. Soc.* **2004**, *126*, 2623-2631.
67. Tobe, M. L. *Acc. Chem. Res.* **1970**, *3*, 377-385.
68. Burger, P.; Bergman, R. G. *J. Am. Chem. Soc.* **1993**, *115*, 10462-10463.
69. Tellers, D. M.; Yung, C. M.; Arndtsen, B. A.; Adamson, D. R.; Bergman, R. G. *J. Am. Chem. Soc.* **2002**, *124*, 1400-1410.
70. Sen, A.; Lai, T. W. *J. Am. Chem. Soc.* **1981**, *5*, 4627-4629.

71. Branan, D. M.; Hoffman, N. W.; McElroy, E. A.; Prokopuk, N.; Salazar, A. B. *Inorg. Chem.* **1991**, *30*, 1200-1207.
72. Kadish, K. M.; Hu, Y.; Boschi, T.; Tagliatesta, P. *Inorg. Chem.* **1993**, *32*, 2996-3002.
73. Nelson, A. P.; DiMagno, S. G. *J. Am. Chem. Soc.* **2000**, *122*, 8569-8570.
74. Sun, H.; Xue, F.; Nelson, A. P.; Redepenning, J.; DiMagno, S. G. *Inorg. Chem.* **2003**, *42*, 4507-4509.
75. pKa's Data from the <http://daeiris.harvard.edu/DavidEvans.html>
76. Lersch, M.; Tilset, M. *Chem Rev.* **2005**, *105*, 2471-2526.
77. Nolan, S. P.; Hoff, C. D.; Stoutland, P. O.; Newman, L. J.; Buchanan, J. M.; Bergman, R. G.; Yang, G. K.; Peters, K. S. *J. Am. Chem. Soc.* **1987**, *109*, 3143-3145.
78. Atkins, P. W. *Physical Chemistry ATKINS*, 6th Ed., Oxford University Press, **1998**.
79. Beck, W.; Sünkel, K. *Chem. Rev.* **1988**, *88*, 1405-1421.
80. Doherty, N. M.; Bercaw, J. E. *J. Am. Chem. Soc.* **1985**, *107*, 2670-2682.
81. Poszmik, G.; Carroll, P. J.; Wayland, B. B. *Organometallics* **1993**, *12*, 3410-3417.
82. (a) Olah, G. A.; Surya Prakash, G. K.; Sommer, J. *Superacids*, A Wiley-Interscience Publication : John Wiley & Sons, Inc., **1976**. (b) Fabre, P. L.; Devynck, J.; Tremillon, B. *Chem. Rev.* **1982**, *82*, 591-614.

Appendix I

Crystal data collection and processing parameters

$\text{C}_6\text{H}_5\text{CORh}(\text{ttp}) \mathbf{2}$

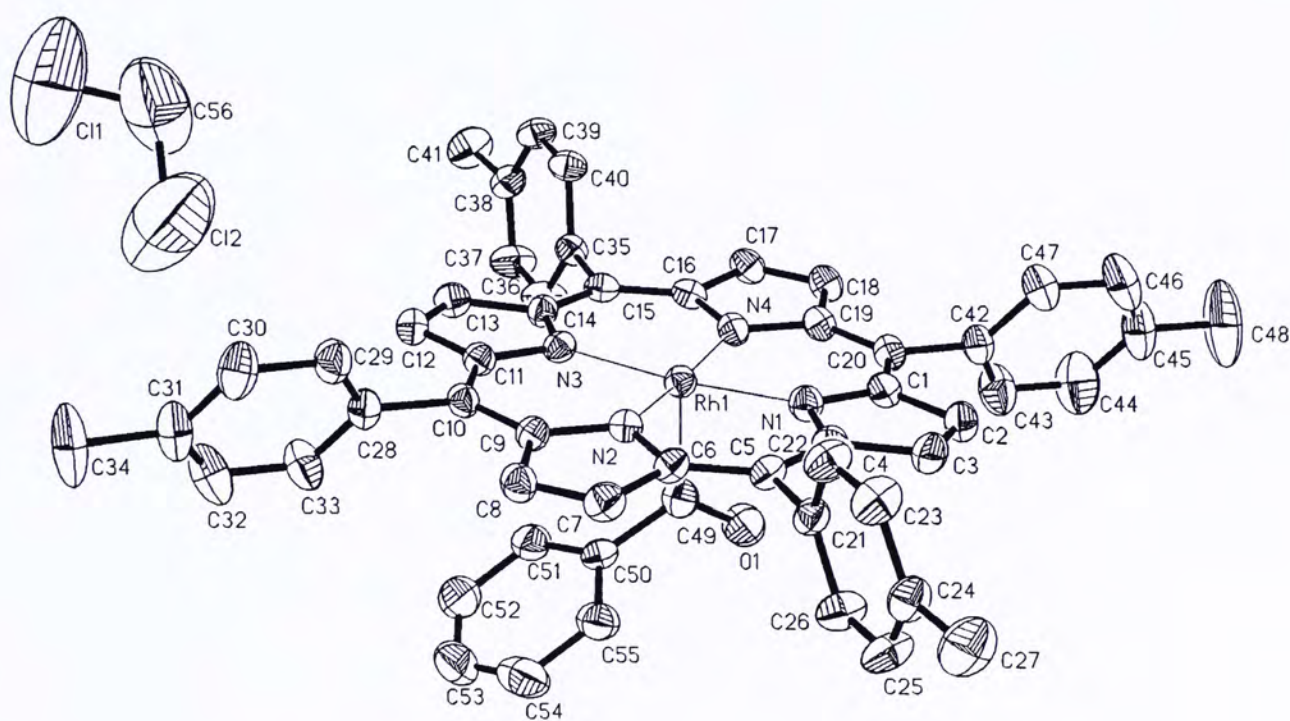


Figure 1. ORTEP of complex $\text{C}_6\text{H}_5\text{CORh}(\text{ttp}) \mathbf{2}$, showing the atomic labelling scheme and 30% probability displacement ellipsoids.

Crystal Data

Empirical Formula	C ₅₆ H ₄₃ Cl ₂ N ₄ ORh
Formula weight	961.75
Temperature	293(2) K
Wavelength	0.71073 Å
Crystal system	monoclinic
Space group	P2(1)
Unit cell dimensions	a = 13.6118(7) Å b = 22.2699(12) Å c = 15.6005(8) Å $\alpha = 90^\circ$ $\beta = 97.0330(10)^\circ$ $\gamma = 90^\circ$
Volume	4693.5(4) Å ⁻³
Z	4
Calculated density	1.361 Mg/m ⁻³
Absorption coefficient	0.522 mm ⁻¹
F(000)	1976
Crystal size	0.50 x 0.40 x 0.20 mm
θ range for data collection	1.51 to 28.02 °
Limiting indices	-17 ≤ h ≤ 16, -25 ≤ k ≤ 29, -20 ≤ l ≤ 20

Reflections collected	31881
Unique	11318 [R(int) =0.0987]
Absorption correction	SADABS
Completeness to θ	28.02 99.7%
Max. Transmission	1.0000
Min. Transmission	0.637161
Refinement method	full-matrix least-squares on F^2
Data / restraints / parameters	11318 / 0 / 577
Goodness-of-fit on F^2	0.877
Final R indices [$I > 2\sigma(I)$]	R1 = 0.0542, wR2 = 0.1152
R indices (all data)	R1 = 0.1589, wR2 = 0.1503
Absolute structure parameter	-
Largest diff. peak	0.550 eA ⁻³
Largest diff. hole	-0.485 eA ⁻³

Table 1. Crystal data and structure refinement for P.

Identification code	cml702
Empirical formula	C56 H43 Cl2 N4 O Rh
Formula weight	961.75
Temperature	293(2) K
Wavelength	0.71073 Å
Crystal system, space group	MONOCLINIC, P2(1)/c
Unit cell dimensions	a = 13.6118(7) Å b = 22.2699(12) Å c = 15.6005(8) Å alpha = 90 deg. beta = 97.0330(10) deg. gamma = 90 deg.
Volume	4693.5(4) Å ³
Z, Calculated density	4, 1.361 Mg/m ³
Absorption coefficient	0.522 mm ⁻¹
F(000)	1976
Crystal size	0.50 x 0.40 x 0.20 mm
Theta range for data collection	1.51 to 28.02 deg.
Limiting indices	-17<=h<=16, -25<=k<=29, -20<=l<=20
Reflections collected / unique	31881 / 11318 [R(int) = 0.0987]
Completeness to theta = 28.02	99.7 %
Absorption correction	SADABS

Max. and min. transmission	1.0000 and 0.637161
Refinement method	Full-matrix least-squares on F ²
Data / restraints / parameters	11318 / 0 / 577
Goodness-of-fit on F ²	0.877
Final R indices [I>2sigma(I)]	R1 = 0.0542, wR2 = 0.1152
R indices (all data)	R1 = 0.1589, wR2 = 0.1503
Largest diff. peak and hole	0.550 and -0.485 e.A ⁻³

Table 2. Atomic coordinates ($\times 10^4$) and equivalent isotropic displacement parameters ($\text{\AA}^2 \times 10^3$) for P.
 U(eq) is defined as one third of the trace of the orthogonalized Uij tensor.

	x	y	z	U(eq)
Rh(1)	15459(1)	8590(1)	1978(1)	41(1)
N(1)	16727(3)	8681(2)	1422(2)	48(1)
N(2)	14775(3)	8253(2)	855(2)	45(1)
N(3)	14241(3)	8398(2)	2562(2)	43(1)
N(4)	16190(3)	8848(2)	3128(2)	45(1)
O(1)	15695(3)	9814(2)	1745(3)	85(1)
C(1)	17611(3)	8914(2)	1809(3)	51(1)
C(2)	18291(4)	8953(2)	1175(3)	55(1)
C(3)	17827(4)	8737(2)	432(4)	59(2)
C(4)	16841(3)	8571(2)	572(3)	47(1)
C(5)	16119(3)	8352(2)	-54(3)	45(1)
C(6)	15156(3)	8217(2)	79(3)	45(1)
C(7)	14401(4)	8018(2)	-586(3)	54(1)
C(8)	13569(4)	7942(2)	-207(3)	52(1)
C(9)	13793(3)	8069(2)	694(3)	43(1)
C(10)	13137(3)	8017(2)	1309(3)	43(1)
C(11)	13367(3)	8162(2)	2178(3)	45(1)
C(12)	12698(3)	8109(2)	2822(3)	53(1)
C(13)	13155(4)	8323(2)	3556(3)	52(1)
C(14)	14126(3)	8505(2)	3416(3)	43(1)
C(15)	14839(4)	8728(2)	4044(3)	46(1)
C(16)	15812(4)	8872(2)	3911(3)	47(1)
C(17)	16567(4)	9073(2)	4573(3)	54(1)
C(18)	17392(4)	9168(2)	4188(3)	53(1)
C(19)	17164(3)	9035(2)	3287(3)	48(1)
C(20)	17820(3)	9077(2)	2670(3)	48(1)
C(21)	16423(3)	8256(2)	-937(3)	47(1)
C(22)	16720(4)	7696(2)	-1193(3)	61(1)
C(23)	17054(4)	7615(3)	-1976(4)	66(2)
C(24)	17096(4)	8077(3)	-2550(3)	57(1)
C(25)	16768(4)	8633(3)	-2301(4)	74(2)
C(26)	16452(4)	8724(2)	-1508(4)	65(2)
C(27)	17472(5)	7986(3)	-3407(4)	97(2)
C(28)	12129(3)	7759(2)	1000(3)	52(1)

C(29)	12036(4)	7181(3)	719(4)	65(2)
C(30)	11118(4)	6943(3)	405(4)	79(2)
C(31)	10270(4)	7290(4)	357(4)	80(2)
C(32)	10368(4)	7861(3)	676(4)	93(2)
C(33)	11287(4)	8110(3)	991(4)	76(2)
C(34)	9270(4)	7041(4)	-7(5)	129(3)
C(35)	14586(3)	8795(2)	4947(3)	48(1)
C(36)	14079(4)	9288(3)	5199(4)	72(2)
C(37)	13792(4)	9323(3)	6020(4)	73(2)
C(38)	14004(4)	8878(3)	6617(3)	57(1)
C(39)	14533(4)	8394(2)	6377(3)	57(1)
C(40)	14820(4)	8354(2)	5566(3)	52(1)
C(41)	13617(5)	8903(3)	7479(3)	82(2)
C(42)	18835(3)	9321(3)	2965(3)	55(1)
C(43)	18959(4)	9899(3)	3216(4)	87(2)
C(44)	19907(5)	10137(4)	3487(5)	109(3)
C(45)	20724(5)	9769(4)	3510(4)	95(2)
C(46)	20593(5)	9191(4)	3277(4)	99(2)
C(47)	19656(4)	8953(3)	3002(4)	73(2)
C(48)	21757(5)	10023(5)	3787(5)	170(5)
C(49)	15092(4)	9413(2)	1658(3)	54(1)
C(50)	14039(4)	9530(2)	1260(4)	52(1)
C(51)	13289(4)	9596(2)	1758(4)	67(2)
C(52)	12340(5)	9731(3)	1371(5)	88(2)
C(53)	12166(5)	9789(3)	506(6)	100(3)
C(54)	12894(6)	9720(3)	0(5)	95(2)
C(55)	13858(4)	9585(2)	377(4)	69(2)
C(56)	10780(10)	6280(9)	3595(8)	294(10)
C1(1)	9761(4)	5968(3)	3702(4)	364(4)
C1(2)	10570(5)	6848(3)	2812(4)	375(4)

Table 3. Bond lengths [Å] and angles [deg] for P.

Rh(1)-C(49)	1.950(5)	C(21)-C(22)	1.384(7)
Rh(1)-N(2)	2.025(4)	C(22)-C(23)	1.366(7)
Rh(1)-N(4)	2.025(4)	C(23)-C(24)	1.369(7)
Rh(1)-N(3)	2.034(4)	C(24)-C(25)	1.388(7)
Rh(1)-N(1)	2.034(4)	C(24)-C(27)	1.502(7)
N(1)-C(4)	1.376(6)	C(25)-C(26)	1.373(7)
N(1)-C(1)	1.379(6)	C(28)-C(29)	1.362(7)
N(2)-C(6)	1.376(6)	C(28)-C(33)	1.385(7)
N(2)-C(9)	1.390(5)	C(29)-C(30)	1.390(7)
N(3)-C(11)	1.371(5)	C(30)-C(31)	1.384(8)
N(3)-C(14)	1.381(6)	C(31)-C(32)	1.365(8)
N(4)-C(19)	1.383(5)	C(31)-C(34)	1.514(7)
N(4)-C(16)	1.384(6)	C(32)-C(33)	1.401(7)
O(1)-C(49)	1.207(5)	C(35)-C(36)	1.378(7)
C(1)-C(20)	1.388(6)	C(35)-C(40)	1.388(6)
C(1)-C(2)	1.438(6)	C(36)-C(37)	1.387(7)
C(2)-C(3)	1.340(6)	C(37)-C(38)	1.366(7)
C(3)-C(4)	1.435(6)	C(38)-C(39)	1.373(7)
C(4)-C(5)	1.386(6)	C(38)-C(41)	1.504(7)
C(5)-C(6)	1.386(6)	C(39)-C(40)	1.373(7)
C(5)-C(21)	1.502(6)	C(42)-C(43)	1.350(7)
C(6)-C(7)	1.438(6)	C(42)-C(47)	1.382(7)
C(7)-C(8)	1.351(6)	C(43)-C(44)	1.411(8)
C(8)-C(9)	1.429(6)	C(44)-C(45)	1.377(9)
C(9)-C(10)	1.394(6)	C(45)-C(46)	1.344(10)
C(10)-C(11)	1.391(6)	C(45)-C(48)	1.529(8)
C(10)-C(28)	1.510(6)	C(46)-C(47)	1.399(8)
C(11)-C(12)	1.441(6)	C(49)-C(50)	1.513(7)
C(12)-C(13)	1.322(6)	C(50)-C(51)	1.365(7)
C(13)-C(14)	1.424(6)	C(50)-C(55)	1.375(7)
C(14)-C(15)	1.384(6)	C(51)-C(52)	1.391(8)
C(15)-C(16)	1.402(6)	C(52)-C(53)	1.347(9)
C(15)-C(35)	1.497(6)	C(53)-C(54)	1.350(9)
C(16)-C(17)	1.437(6)	C(54)-C(55)	1.402(8)
C(17)-C(18)	1.354(6)	C(56)-C1(1)	1.579(14)
C(18)-C(19)	1.433(6)	C(56)-C1(2)	1.758(15)
C(19)-C(20)	1.394(6)	C(49)-Rh(1)-N(2)	92.89(18)
C(20)-C(42)	1.503(6)	C(49)-Rh(1)-N(4)	92.41(18)
C(21)-C(26)	1.374(7)	C(49)-Rh(1)-N(3)	96.56(18)

C(49)-Rh(1)-N(1)	90.11(19)	N(3)-C(11)-C(10)	126.5(4)
N(2)-Rh(1)-N(4)	174.67(15)	N(3)-C(11)-C(12)	108.3(4)
N(2)-Rh(1)-N(3)	89.78(15)	C(10)-C(11)-C(12)	125.1(4)
N(4)-Rh(1)-N(3)	90.10(15)	C(13)-C(12)-C(11)	107.7(4)
N(2)-Rh(1)-N(1)	89.58(15)	C(12)-C(13)-C(14)	108.5(5)
N(4)-Rh(1)-N(1)	89.92(15)	N(3)-C(14)-C(15)	126.3(4)
N(3)-Rh(1)-N(1)	173.32(15)	N(3)-C(14)-C(13)	108.4(4)
C(4)-N(1)-C(1)	107.0(4)	C(15)-C(14)-C(13)	125.3(5)
C(4)-N(1)-Rh(1)	126.5(3)	C(14)-C(15)-C(16)	124.7(5)
C(1)-N(1)-Rh(1)	126.3(3)	C(14)-C(15)-C(35)	118.7(4)
C(6)-N(2)-C(9)	106.3(4)	C(16)-C(15)-C(35)	116.5(4)
C(6)-N(2)-Rh(1)	126.9(3)	N(4)-C(16)-C(15)	125.6(4)
C(9)-N(2)-Rh(1)	126.5(3)	N(4)-C(16)-C(17)	109.6(4)
C(11)-N(3)-C(14)	107.1(4)	C(15)-C(16)-C(17)	124.7(5)
C(11)-N(3)-Rh(1)	126.6(3)	C(18)-C(17)-C(16)	106.8(5)
C(14)-N(3)-Rh(1)	126.2(3)	C(17)-C(18)-C(19)	108.1(4)
C(19)-N(4)-C(16)	106.4(4)	N(4)-C(19)-C(20)	125.3(4)
C(19)-N(4)-Rh(1)	127.0(3)	N(4)-C(19)-C(18)	109.1(4)
C(16)-N(4)-Rh(1)	126.7(3)	C(20)-C(19)-C(18)	125.7(4)
N(1)-C(1)-C(20)	125.9(5)	C(1)-C(20)-C(19)	125.3(4)
N(1)-C(1)-C(2)	108.9(4)	C(1)-C(20)-C(42)	117.6(4)
C(20)-C(1)-C(2)	125.2(5)	C(19)-C(20)-C(42)	117.1(4)
C(3)-C(2)-C(1)	107.3(4)	C(26)-C(21)-C(22)	117.6(5)
C(2)-C(3)-C(4)	108.2(5)	C(26)-C(21)-C(5)	121.3(5)
N(1)-C(4)-C(5)	126.0(4)	C(22)-C(21)-C(5)	121.0(5)
N(1)-C(4)-C(3)	108.6(4)	C(23)-C(22)-C(21)	121.1(5)
C(5)-C(4)-C(3)	125.4(5)	C(22)-C(23)-C(24)	122.1(5)
C(4)-C(5)-C(6)	125.0(5)	C(23)-C(24)-C(25)	116.4(5)
C(4)-C(5)-C(21)	116.5(4)	C(23)-C(24)-C(27)	121.9(5)
C(6)-C(5)-C(21)	118.6(4)	C(25)-C(24)-C(27)	121.7(5)
N(2)-C(6)-C(5)	125.8(4)	C(26)-C(25)-C(24)	122.1(5)
N(2)-C(6)-C(7)	109.9(4)	C(25)-C(26)-C(21)	120.5(5)
C(5)-C(6)-C(7)	124.4(5)	C(29)-C(28)-C(33)	119.1(5)
C(8)-C(7)-C(6)	106.6(4)	C(29)-C(28)-C(10)	120.4(5)
C(7)-C(8)-C(9)	108.4(4)	C(33)-C(28)-C(10)	120.5(5)
N(2)-C(9)-C(10)	125.7(4)	C(28)-C(29)-C(30)	121.2(5)
N(2)-C(9)-C(8)	108.7(4)	C(31)-C(30)-C(29)	121.0(6)
C(10)-C(9)-C(8)	125.6(4)	C(32)-C(31)-C(30)	117.1(5)
C(11)-C(10)-C(9)	124.4(4)	C(32)-C(31)-C(34)	121.4(6)
C(11)-C(10)-C(28)	119.0(4)	C(30)-C(31)-C(34)	121.4(6)
C(9)-C(10)-C(28)	116.5(4)	C(31)-C(32)-C(33)	122.7(6)

C(28)-C(33)-C(32)	118.9(6)	C(46)-C(45)-C(48)	121.2(7)
C(36)-C(35)-C(40)	116.4(5)	C(44)-C(45)-C(48)	120.0(8)
C(36)-C(35)-C(15)	122.0(5)	C(45)-C(46)-C(47)	122.1(7)
C(40)-C(35)-C(15)	121.6(4)	C(42)-C(47)-C(46)	119.3(6)
C(35)-C(36)-C(37)	121.1(5)	O(1)-C(49)-C(50)	121.0(5)
C(38)-C(37)-C(36)	121.9(5)	O(1)-C(49)-Rh(1)	121.1(4)
C(37)-C(38)-C(39)	117.2(5)	C(50)-C(49)-Rh(1)	117.8(4)
C(37)-C(38)-C(41)	120.9(5)	C(51)-C(50)-C(55)	120.4(5)
C(39)-C(38)-C(41)	121.7(5)	C(51)-C(50)-C(49)	121.5(5)
C(40)-C(39)-C(38)	121.3(5)	C(55)-C(50)-C(49)	118.1(5)
C(39)-C(40)-C(35)	121.9(5)	C(50)-C(51)-C(52)	119.8(6)
C(43)-C(42)-C(47)	118.8(5)	C(53)-C(52)-C(51)	119.7(7)
C(43)-C(42)-C(20)	120.8(5)	C(52)-C(53)-C(54)	121.6(7)
C(47)-C(42)-C(20)	120.4(5)	C(53)-C(54)-C(55)	119.7(7)
C(42)-C(43)-C(44)	121.4(6)	C(50)-C(55)-C(54)	118.9(6)
C(45)-C(44)-C(43)	119.4(7)	Cl(1)-C(56)-Cl(2)	108.6(8)
C(46)-C(45)-C(44)	118.8(6)		

Symmetry transformations used to generate equivalent atoms:

Table 4. Anisotropic displacement parameters ($\text{\AA}^2 \times 10^3$) for P.
 The anisotropic displacement factor exponent takes the form:
 $-2 \pi^2 [h^2 a^{*2} U_{11} + \dots + 2 h k a^* b^* U_{12}]$

	U11	U22	U33	U23	U13	U12
Rh(1)	41(1)	40(1)	44(1)	-1(1)	5(1)	-1(1)
N(1)	45(2)	52(3)	46(2)	-3(2)	4(2)	-2(2)
N(2)	44(2)	45(2)	46(3)	5(2)	5(2)	1(2)
N(3)	48(2)	35(2)	47(2)	-1(2)	8(2)	0(2)
N(4)	40(2)	45(2)	51(3)	-2(2)	3(2)	1(2)
O(1)	77(3)	48(2)	125(4)	5(2)	-7(3)	-9(2)
C(1)	43(3)	53(3)	56(3)	2(3)	3(3)	2(2)
C(2)	44(3)	66(4)	56(3)	-2(3)	9(3)	-2(3)
C(3)	54(3)	67(4)	59(4)	4(3)	21(3)	-1(3)
C(4)	48(3)	41(3)	54(3)	1(3)	8(2)	0(3)
C(5)	51(3)	40(3)	45(3)	1(2)	10(2)	-4(2)
C(6)	50(3)	41(3)	46(3)	1(2)	8(2)	-6(2)
C(7)	63(3)	55(3)	42(3)	-2(2)	4(3)	-4(3)
C(8)	46(3)	52(3)	54(3)	-3(3)	-1(3)	-4(3)
C(9)	44(3)	37(3)	48(3)	-4(2)	2(2)	-5(2)
C(10)	38(3)	39(3)	51(3)	-3(2)	1(2)	-1(2)
C(11)	41(3)	38(3)	53(3)	-2(2)	1(2)	-3(2)
C(12)	44(3)	57(3)	58(3)	2(3)	5(3)	-6(3)
C(13)	56(3)	58(3)	41(3)	-1(3)	6(3)	0(3)
C(14)	41(3)	45(3)	44(3)	1(2)	9(2)	-1(2)
C(15)	54(3)	40(3)	45(3)	3(2)	4(2)	6(2)
C(16)	49(3)	47(3)	43(3)	2(2)	0(2)	8(2)
C(17)	52(3)	63(4)	45(3)	-6(3)	-2(3)	6(3)
C(18)	48(3)	60(4)	50(3)	-9(3)	0(3)	3(3)
C(19)	43(3)	52(3)	49(3)	-5(2)	1(2)	1(2)
C(20)	38(3)	48(3)	57(3)	-4(3)	4(2)	1(2)
C(21)	49(3)	47(3)	46(3)	1(2)	5(2)	-10(2)
C(22)	80(4)	48(3)	59(4)	-2(3)	21(3)	-1(3)
C(23)	85(4)	53(4)	64(4)	-10(3)	22(3)	-3(3)
C(24)	63(3)	66(4)	45(3)	-5(3)	16(3)	-5(3)
C(25)	98(4)	65(4)	65(4)	18(3)	28(3)	-5(4)
C(26)	91(4)	51(4)	57(4)	4(3)	18(3)	5(3)
C(27)	114(5)	119(6)	65(4)	-3(4)	35(4)	-6(5)
C(28)	42(3)	60(4)	54(3)	-2(3)	7(2)	-8(3)
C(29)	53(3)	61(4)	80(4)	-5(3)	0(3)	-10(3)

C(30)	69(4)	86(5)	83(5)	-29(4)	16(4)	-28(4)
C(31)	47(3)	122(6)	72(4)	-26(4)	12(3)	-19(4)
C(32)	50(4)	127(7)	99(5)	-35(5)	0(4)	15(4)
C(33)	48(3)	80(4)	97(5)	-19(4)	0(3)	8(3)
C(34)	52(4)	208(9)	127(7)	-70(6)	13(4)	-43(5)
C(35)	46(3)	51(3)	45(3)	0(2)	2(2)	3(2)
C(36)	99(5)	62(4)	58(4)	16(3)	19(3)	26(3)
C(37)	99(5)	63(4)	62(4)	7(3)	29(3)	29(3)
C(38)	65(3)	56(4)	49(3)	1(3)	7(3)	-10(3)
C(39)	78(4)	50(3)	42(3)	4(2)	2(3)	-3(3)
C(40)	65(3)	40(3)	49(3)	-3(2)	1(3)	8(3)
C(41)	112(5)	86(5)	53(4)	-6(3)	27(4)	-4(4)
C(42)	41(3)	65(4)	57(3)	-7(3)	1(2)	-5(3)
C(43)	56(4)	82(5)	121(6)	-25(4)	6(4)	-9(3)
C(44)	84(5)	117(6)	124(7)	-58(5)	7(5)	-30(5)
C(45)	51(4)	156(8)	79(5)	-42(5)	11(3)	-16(5)
C(46)	47(4)	154(8)	93(5)	-24(5)	-3(3)	15(4)
C(47)	49(3)	88(4)	81(4)	-11(4)	1(3)	4(3)
C(48)	64(5)	290(13)	154(8)	-114(8)	8(5)	-56(6)
C(49)	55(3)	53(3)	53(3)	-7(3)	4(3)	-5(3)
C(50)	59(3)	37(3)	60(4)	10(2)	7(3)	0(2)
C(51)	65(4)	60(4)	79(4)	13(3)	18(3)	10(3)
C(52)	72(5)	78(5)	118(6)	19(5)	31(4)	18(4)
C(53)	69(5)	87(5)	139(8)	21(5)	-9(5)	12(4)
C(54)	101(6)	83(5)	93(6)	10(4)	-28(5)	6(4)
C(55)	71(4)	61(4)	71(4)	8(3)	1(3)	5(3)
C(56)	170(12)	560(30)	149(12)	77(15)	10(9)	-22(16)
C1(1)	312(6)	481(9)	326(7)	-123(6)	151(5)	-179(6)
C1(2)	429(8)	400(8)	293(7)	52(6)	36(6)	-191(7)

Table 5. Hydrogen coordinates ($\times 10^4$) and isotropic displacement parameters ($\text{\AA}^2 \times 10^3$) for P.

	x	y	z	U(eq)
H(2A)	18935	9102	1264	66
H(3A)	18098	8700	-85	70
H(7A)	14472	7953	-1164	64
H(8A)	12955	7826	-484	62
H(12A)	12060	7953	2738	63
H(13A)	12888	8350	4075	62
H(17A)	16502	9127	5154	65
H(18A)	18001	9297	4461	64
H(22A)	16691	7370	-825	73
H(23A)	17259	7235	-2123	79
H(25A)	16761	8954	-2683	89
H(26A)	16257	9106	-1356	78
H(27A)	17448	8361	-3713	146
H(27B)	17065	7697	-3739	146
H(27C)	18142	7844	-3316	146
H(29A)	12597	6941	737	78
H(30A)	11073	6545	225	95
H(32A)	9802	8093	684	111
H(33A)	11331	8503	1191	91
H(34A)	8774	7346	11	194
H(34B)	9112	6703	332	194
H(34C)	9290	6917	-594	194
H(36A)	13927	9601	4812	86
H(37A)	13445	9659	6169	88
H(39A)	14701	8087	6773	69
H(40A)	15183	8021	5427	62
H(41A)	13266	9273	7526	123
H(41B)	14160	8881	7932	123
H(41C)	13177	8571	7528	123
H(43A)	18408	10147	3209	104
H(44A)	19981	10538	3648	131
H(46A)	21143	8941	3299	119
H(47A)	19587	8550	2847	88
H(48A)	22240	9711	3768	255
H(48B)	21791	10176	4366	255
H(48C)	21890	10342	3403	255

H(51A)	13413	9552	2354	81
H(52A)	11827	9781	1708	105
H(53A)	11529	9879	252	120
H(54A)	12758	9761	-596	115
H(55A)	14365	9534	35	82
H(56A)	11241	5986	3417	353
H(56B)	11064	6451	4142	353

4-FC₆H₄CORh(ttp) 4

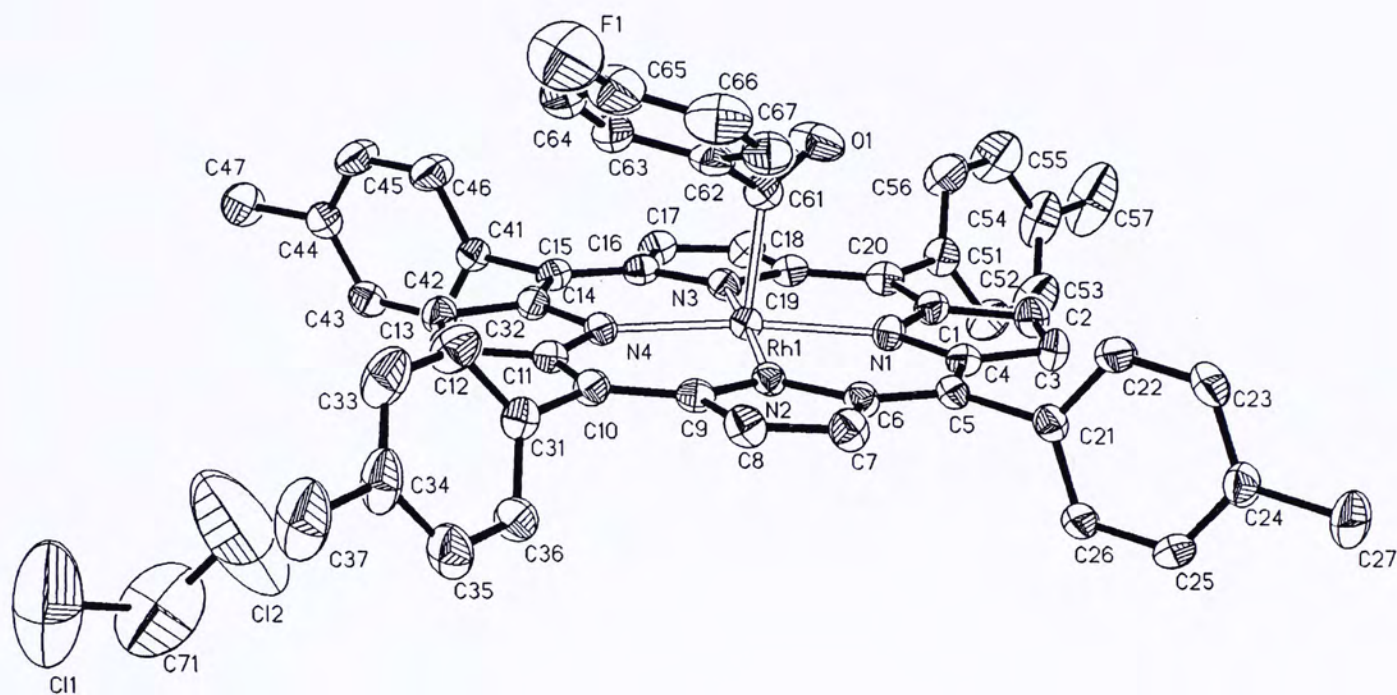


Figure 2. ORTEP of complex 4-FC₆H₄CORh(ttp) 4, showing the atomic labelling scheme and 30% probability displacement ellipsoids.

Crystal Data

Empirical Formula	C ₅₆ H ₄₂ Cl ₂ FN ₄ ORh
Formula weight	979.75
Temperature	293(2) K
Wavelength	0.71073 Å
Crystal system	monoclinic
Space group	P2(1)
Unit cell dimensions	a = 13.705(17) Å b = 22.17(2) Å c = 15.746(18) Å $\alpha = 90^\circ$ $\beta = 96.93(3)^\circ$ $\gamma = 90^\circ$
Volume	4750(10) Å ⁻³
Z	4
Calculated density	1.370 Mg/m ⁻³
Absorption coefficient	0.520 mm ⁻¹
F(000)	2008
Crystal size	0.30 x 0.20 x 0.10 mm
θ range for data collection	1.50 to 25.00°
Limiting indices	-16 ≤ h ≤ 9, -21 ≤ k ≤ 25, -18 ≤ l ≤ 18

Reflections collected	12264
Unique	8057 [R(int) = 0.0848]
Absorption correction	SADABS
Completeness to θ	25.00 96.2 %
Max. Transmission	1.0000
Min. Transmission	0.461514
Refinement method	full-matrix least-squares on F^2
Data / restraints / parameters	8057 / 0 / 586
Goodness-of-fit on F^2	0.937
Final R indices [$I > 2\sigma(I)$]	R1 = 0.0648, wR2 = 0.1480
R indices (all data)	R1 = 0.1194, wR2 = 0.1480
Absolute structure parameter	-
Largest diff. peak	0.956 eA ⁻³
Largest diff. hole	-0.682 eA ⁻³

Table 1. Crystal data and structure refinement for P.

Identification code	all492
Empirical formula	C ₅₆ H ₄₂ Cl ₂ F N ₄ O Rh
Formula weight	979.75
Temperature	293(2) K
Wavelength	0.71073 Å
Crystal system, space group	MONOCLINIC, P2(1)/c
Unit cell dimensions	a = 13.705(17) Å b = 22.17(2) Å c = 15.746(18) Å alpha = 90 deg. beta = 96.93(3) deg. gamma = 90 deg.
Volume	4750(10) Å ³
Z, Calculated density	4, 1.370 Mg/m ³
Absorption coefficient	0.520 mm ⁻¹
F(000)	2008
Crystal size	0.30 x 0.20 x 0.10 mm
Theta range for data collection	1.50 to 25.00 deg.
Limiting indices	-16<=h<=9, -21<=k<=25, -18<=l<=18
Reflections collected / unique	12264 / 8057 [R(int) = 0.0848]
Completeness to theta = 25.00	96.2 %
Absorption correction	SADABS

Max. and min. transmission	1.0000 and 0.461514
Refinement method	Full-matrix least-squares on F^2
Data / restraints / parameters	8057 / 0 / 586
Goodness-of-fit on F^2	0.937
Final R indices [$I > 2\sigma(I)$]	$R_1 = 0.0648$, $wR_2 = 0.1480$
R indices (all data)	$R_1 = 0.1194$, $wR_2 = 0.1701$
Largest diff. peak and hole	0.956 and -0.682 e. \AA^{-3}

Table 2. Atomic coordinates ($\times 10^4$) and equivalent isotropic displacement parameters ($\text{\AA}^2 \times 10^3$) for P.
 $U(\text{eq})$ is defined as one third of the trace of the orthogonalized U_{ij} tensor.

	x	y	z	$U(\text{eq})$
Rh(1)	5438(1)	6403(1)	1938(1)	37(1)
O(1)	5672(4)	5176(2)	1676(4)	79(2)
N(1)	6700(3)	6310(2)	1389(3)	40(1)
N(2)	4754(3)	6747(2)	815(3)	37(1)
N(3)	6170(3)	6145(2)	3095(3)	39(1)
N(4)	4221(3)	6592(2)	2520(3)	38(1)
F(1)	1211(4)	5135(3)	98(4)	140(2)
C(1)	7577(4)	6082(3)	1768(4)	45(2)
C(2)	8257(4)	6043(3)	1143(4)	50(2)
C(3)	7799(4)	6253(3)	396(4)	50(2)
C(4)	6815(4)	6422(3)	537(4)	42(1)
C(5)	6092(4)	6645(3)	-89(4)	40(1)
C(6)	5134(4)	6785(3)	36(4)	40(1)
C(7)	4381(5)	6982(3)	-622(4)	49(2)
C(8)	3554(4)	7061(3)	-250(4)	49(2)
C(9)	3778(4)	6926(3)	655(4)	39(1)
C(10)	3126(4)	6980(3)	1268(4)	42(1)
C(11)	3344(4)	6827(3)	2136(4)	43(2)
C(12)	2684(4)	6881(3)	2776(4)	47(2)
C(13)	3149(4)	6671(3)	3526(4)	47(2)
C(14)	4108(4)	6489(3)	3386(4)	41(1)
C(15)	4835(4)	6264(3)	4011(4)	42(2)
C(16)	5797(4)	6123(3)	3880(4)	42(1)
C(17)	6560(4)	5932(3)	4538(4)	49(2)
C(18)	7379(4)	5837(3)	4161(4)	47(2)
C(19)	7139(4)	5961(3)	3258(4)	41(2)
C(20)	7799(4)	5915(3)	2645(4)	45(2)
C(21)	6393(4)	6742(3)	-986(4)	41(2)
C(22)	6404(5)	6278(3)	-1559(4)	54(2)
C(23)	6720(5)	6373(3)	-2355(5)	64(2)
C(24)	7046(5)	6927(3)	-2598(4)	56(2)
C(25)	7023(5)	7386(3)	-2023(4)	58(2)
C(26)	6701(5)	7301(3)	-1226(4)	54(2)
C(27)	7433(6)	7026(4)	-3458(4)	83(3)

C(31)	2116(4)	7231(3)	955(4)	46(2)
C(32)	1283(5)	6890(4)	944(5)	67(2)
C(33)	361(5)	7118(4)	632(5)	81(3)
C(34)	256(5)	7698(5)	328(5)	77(3)
C(35)	1102(5)	8044(4)	353(5)	75(2)
C(36)	2016(5)	7820(3)	674(4)	59(2)
C(37)	-745(6)	7958(5)	-38(6)	123(4)
C(41)	4570(4)	6205(3)	4922(4)	42(2)
C(42)	4800(4)	6652(3)	5517(4)	48(2)
C(43)	4503(5)	6607(3)	6345(4)	52(2)
C(44)	3985(5)	6113(3)	6582(4)	50(2)
C(45)	3793(6)	5669(3)	5985(5)	68(2)
C(46)	4077(6)	5705(3)	5161(4)	68(2)
C(47)	3609(6)	6085(4)	7440(4)	73(2)
C(51)	8809(4)	5676(3)	2940(4)	51(2)
C(52)	9632(5)	6045(4)	2961(5)	66(2)
C(53)	10555(5)	5819(5)	3238(5)	84(3)
C(54)	10701(5)	5238(5)	3497(5)	85(3)
C(55)	9892(6)	4870(5)	3476(6)	104(3)
C(56)	8938(5)	5095(4)	3195(6)	80(2)
C(57)	11736(6)	4993(6)	3802(7)	151(6)
C(61)	5062(5)	5566(3)	1614(4)	47(2)
C(62)	4022(5)	5461(3)	1223(5)	53(2)
C(63)	3270(5)	5398(3)	1727(5)	61(2)
C(64)	2321(6)	5273(4)	1355(7)	83(3)
C(65)	2145(6)	5229(4)	487(8)	89(3)
C(66)	2857(7)	5302(4)	-36(6)	87(3)
C(67)	3806(5)	5411(3)	323(5)	65(2)
C(71)	625(13)	8752(9)	3518(10)	216(8)
C1(1)	-626(5)	8782(4)	3404(4)	321(4)
C1(2)	785(8)	8190(5)	2783(6)	431(7)

Table 3. Bond lengths [Å] and angles [deg] for P.

Rh(1)-C(61)	1.976(7)	C(21)-C(22)	1.370(8)
Rh(1)-N(1)	2.035(5)	C(21)-C(26)	1.376(9)
Rh(1)-N(4)	2.042(5)	C(22)-C(23)	1.390(9)
Rh(1)-N(2)	2.047(5)	C(23)-C(24)	1.377(10)
Rh(1)-N(3)	2.052(5)	C(24)-C(25)	1.366(9)
O(1)-C(61)	1.199(7)	C(24)-C(27)	1.528(8)
N(1)-C(1)	1.373(7)	C(25)-C(26)	1.391(8)
N(1)-C(4)	1.393(7)	C(31)-C(32)	1.369(9)
N(2)-C(9)	1.389(7)	C(31)-C(36)	1.379(9)
N(2)-C(6)	1.391(7)	C(32)-C(33)	1.394(10)
N(3)-C(19)	1.383(7)	C(33)-C(34)	1.375(11)
N(3)-C(16)	1.395(7)	C(34)-C(35)	1.386(11)
N(4)-C(11)	1.380(7)	C(34)-C(37)	1.535(10)
N(4)-C(14)	1.410(7)	C(35)-C(36)	1.386(9)
F(1)-C(65)	1.367(9)	C(41)-C(42)	1.373(8)
C(1)-C(20)	1.426(8)	C(41)-C(46)	1.375(9)
C(1)-C(2)	1.438(8)	C(42)-C(43)	1.417(8)
C(2)-C(3)	1.346(8)	C(43)-C(44)	1.381(9)
C(3)-C(4)	1.443(8)	C(44)-C(45)	1.366(9)
C(4)-C(5)	1.401(8)	C(44)-C(47)	1.504(9)
C(5)-C(6)	1.386(8)	C(45)-C(46)	1.401(9)
C(5)-C(21)	1.534(8)	C(51)-C(56)	1.356(10)
C(6)-C(7)	1.441(8)	C(51)-C(52)	1.391(9)
C(7)-C(8)	1.349(8)	C(52)-C(53)	1.381(10)
C(8)-C(9)	1.452(8)	C(53)-C(54)	1.360(12)
C(9)-C(10)	1.398(8)	C(54)-C(55)	1.373(12)
C(10)-C(11)	1.405(8)	C(54)-C(57)	1.541(10)
C(10)-C(31)	1.518(8)	C(55)-C(56)	1.419(11)
C(11)-C(12)	1.438(8)	C(61)-C(62)	1.501(9)
C(12)-C(13)	1.355(8)	C(62)-C(63)	1.381(9)
C(13)-C(14)	1.417(8)	C(62)-C(67)	1.417(10)
C(14)-C(15)	1.405(8)	C(63)-C(64)	1.388(11)
C(15)-C(16)	1.395(8)	C(64)-C(65)	1.364(12)
C(15)-C(41)	1.527(8)	C(65)-C(66)	1.360(12)
C(16)-C(17)	1.443(8)	C(66)-C(67)	1.375(10)
C(17)-C(18)	1.349(8)	C(71)-Cl(1)	1.704(17)
C(18)-C(19)	1.445(8)	C(71)-Cl(2)	1.732(18)
C(19)-C(20)	1.404(8)	C(61)-Rh(1)-N(1)	90.2(2)
C(20)-C(51)	1.502(8)	C(61)-Rh(1)-N(4)	96.2(2)

N(1)-Rh(1)-N(4)	173.58(19)	C(11)-C(10)-C(31)	118.9(5)
C(61)-Rh(1)-N(2)	92.8(2)	N(4)-C(11)-C(10)	126.1(5)
N(1)-Rh(1)-N(2)	89.71(19)	N(4)-C(11)-C(12)	108.2(5)
N(4)-Rh(1)-N(2)	89.86(19)	C(10)-C(11)-C(12)	125.7(5)
C(61)-Rh(1)-N(3)	93.0(2)	C(13)-C(12)-C(11)	108.2(5)
N(1)-Rh(1)-N(3)	89.9(2)	C(12)-C(13)-C(14)	108.1(5)
N(4)-Rh(1)-N(3)	89.8(2)	C(15)-C(14)-N(4)	125.7(5)
N(2)-Rh(1)-N(3)	174.21(18)	C(15)-C(14)-C(13)	125.8(5)
C(1)-N(1)-C(4)	106.9(5)	N(4)-C(14)-C(13)	108.4(5)
C(1)-N(1)-Rh(1)	126.7(4)	C(16)-C(15)-C(14)	125.4(5)
C(4)-N(1)-Rh(1)	126.3(4)	C(16)-C(15)-C(41)	117.1(5)
C(9)-N(2)-C(6)	106.1(5)	C(14)-C(15)-C(41)	117.4(5)
C(9)-N(2)-Rh(1)	126.4(4)	N(3)-C(16)-C(15)	125.3(5)
C(6)-N(2)-Rh(1)	127.1(4)	N(3)-C(16)-C(17)	109.6(5)
C(19)-N(3)-C(16)	105.7(5)	C(15)-C(16)-C(17)	125.1(6)
C(19)-N(3)-Rh(1)	127.1(4)	C(18)-C(17)-C(16)	107.4(5)
C(16)-N(3)-Rh(1)	127.2(4)	C(17)-C(18)-C(19)	107.5(5)
C(11)-N(4)-C(14)	107.1(4)	N(3)-C(19)-C(20)	125.2(5)
C(11)-N(4)-Rh(1)	126.6(4)	N(3)-C(19)-C(18)	109.8(5)
C(14)-N(4)-Rh(1)	126.3(4)	C(20)-C(19)-C(18)	125.0(5)
N(1)-C(1)-C(20)	126.2(5)	C(19)-C(20)-C(1)	124.5(5)
N(1)-C(1)-C(2)	109.3(5)	C(19)-C(20)-C(51)	117.3(5)
C(20)-C(1)-C(2)	124.6(5)	C(1)-C(20)-C(51)	118.1(5)
C(3)-C(2)-C(1)	107.8(5)	C(22)-C(21)-C(26)	117.9(6)
C(2)-C(3)-C(4)	107.5(5)	C(22)-C(21)-C(5)	121.8(6)
N(1)-C(4)-C(5)	126.0(5)	C(26)-C(21)-C(5)	120.3(5)
N(1)-C(4)-C(3)	108.5(5)	C(21)-C(22)-C(23)	120.6(6)
C(5)-C(4)-C(3)	125.4(5)	C(24)-C(23)-C(22)	122.2(7)
C(6)-C(5)-C(4)	125.5(5)	C(25)-C(24)-C(23)	116.4(6)
C(6)-C(5)-C(21)	117.7(5)	C(25)-C(24)-C(27)	121.3(7)
C(4)-C(5)-C(21)	116.8(5)	C(23)-C(24)-C(27)	122.3(7)
C(5)-C(6)-N(2)	125.0(5)	C(24)-C(25)-C(26)	122.2(6)
C(5)-C(6)-C(7)	125.1(5)	C(21)-C(26)-C(25)	120.6(6)
N(2)-C(6)-C(7)	109.9(5)	C(32)-C(31)-C(36)	118.0(6)
C(8)-C(7)-C(6)	107.1(5)	C(32)-C(31)-C(10)	121.8(6)
C(7)-C(8)-C(9)	108.1(5)	C(36)-C(31)-C(10)	120.2(6)
N(2)-C(9)-C(10)	125.6(5)	C(31)-C(32)-C(33)	121.5(7)
N(2)-C(9)-C(8)	108.8(5)	C(34)-C(33)-C(32)	121.0(7)
C(10)-C(9)-C(8)	125.6(5)	C(33)-C(34)-C(35)	117.1(7)
C(9)-C(10)-C(11)	124.9(5)	C(33)-C(34)-C(37)	122.3(8)
C(9)-C(10)-C(31)	116.2(5)	C(35)-C(34)-C(37)	120.6(9)

C(36)-C(35)-C(34)	121.9(8)	C(53)-C(54)-C(57)	121.6(9)
C(31)-C(36)-C(35)	120.4(7)	C(55)-C(54)-C(57)	120.6(10)
C(42)-C(41)-C(46)	118.4(6)	C(54)-C(55)-C(56)	120.7(9)
C(42)-C(41)-C(15)	121.1(5)	C(51)-C(56)-C(55)	120.6(8)
C(46)-C(41)-C(15)	120.4(6)	O(1)-C(61)-C(62)	122.7(6)
C(41)-C(42)-C(43)	120.6(6)	O(1)-C(61)-Rh(1)	119.9(5)
C(44)-C(43)-C(42)	121.3(6)	C(62)-C(61)-Rh(1)	117.1(5)
C(45)-C(44)-C(43)	116.7(6)	C(63)-C(62)-C(67)	119.1(7)
C(45)-C(44)-C(47)	122.0(7)	C(63)-C(62)-C(61)	121.2(6)
C(43)-C(44)-C(47)	121.3(7)	C(67)-C(62)-C(61)	119.7(6)
C(44)-C(45)-C(46)	123.0(6)	C(62)-C(63)-C(64)	120.3(8)
C(41)-C(46)-C(45)	120.0(7)	C(65)-C(64)-C(63)	118.7(8)
C(56)-C(51)-C(52)	118.4(6)	C(66)-C(65)-C(64)	123.1(8)
C(56)-C(51)-C(20)	120.6(6)	C(66)-C(65)-F(1)	116.7(10)
C(52)-C(51)-C(20)	121.0(6)	C(64)-C(65)-F(1)	120.2(9)
C(53)-C(52)-C(51)	120.3(8)	C(65)-C(66)-C(67)	119.0(9)
C(54)-C(53)-C(52)	122.3(8)	C(66)-C(67)-C(62)	119.8(8)
C(53)-C(54)-C(55)	117.8(7)	Cl(1)-C(71)-Cl(2)	99.4(9)

Symmetry transformations used to generate equivalent atoms:

Table 4. Anisotropic displacement parameters ($\text{\AA}^2 \times 10^3$) for P.
 The anisotropic displacement factor exponent takes the form:
 $-2 \pi^2 [h^2 a^{*2} U_{11} + \dots + 2 h k a^* b^* U_{12}]$

	U11	U22	U33	U23	U13	U12
Rh(1)	36(1)	38(1)	35(1)	1(1)	3(1)	0(1)
O(1)	74(3)	48(3)	110(5)	-8(3)	-6(3)	10(3)
N(1)	38(3)	47(3)	33(3)	0(2)	5(2)	-1(2)
N(2)	40(3)	37(3)	35(3)	-2(2)	5(2)	1(2)
N(3)	38(3)	39(3)	41(3)	-1(2)	2(2)	3(2)
N(4)	43(3)	38(3)	33(3)	-4(2)	7(2)	-1(2)
F(1)	64(3)	143(5)	203(7)	-35(5)	-30(4)	-19(3)
C(1)	41(3)	43(4)	50(4)	3(3)	8(3)	1(3)
C(2)	44(4)	60(5)	48(4)	1(4)	6(3)	8(3)
C(3)	39(3)	65(5)	47(4)	1(3)	16(3)	2(3)
C(4)	44(3)	37(3)	46(4)	3(3)	8(3)	2(3)
C(5)	46(3)	36(3)	38(3)	-5(3)	9(3)	1(3)
C(6)	44(3)	41(4)	35(3)	-3(3)	6(3)	2(3)
C(7)	57(4)	55(4)	35(3)	1(3)	5(3)	7(3)
C(8)	47(4)	53(4)	44(4)	4(3)	-4(3)	11(3)
C(9)	42(3)	35(3)	39(3)	5(3)	0(3)	3(3)
C(10)	38(3)	43(4)	44(4)	4(3)	4(3)	1(3)
C(11)	42(3)	35(4)	51(4)	0(3)	8(3)	0(3)
C(12)	38(3)	54(4)	49(4)	-2(3)	7(3)	5(3)
C(13)	50(4)	50(4)	43(4)	-1(3)	11(3)	-2(3)
C(14)	40(3)	42(4)	41(3)	-1(3)	7(3)	-2(3)
C(15)	48(3)	40(4)	39(3)	1(3)	4(3)	-6(3)
C(16)	47(3)	39(4)	40(4)	1(3)	1(3)	-5(3)
C(17)	54(4)	52(4)	39(4)	5(3)	-3(3)	-3(3)
C(18)	39(3)	57(4)	44(4)	11(3)	-4(3)	-2(3)
C(19)	38(3)	41(4)	42(4)	4(3)	-7(3)	-3(3)
C(20)	43(3)	46(4)	43(4)	-2(3)	-3(3)	-2(3)
C(21)	43(3)	43(4)	38(3)	1(3)	6(3)	9(3)
C(22)	77(5)	40(4)	49(4)	0(3)	18(3)	-5(3)
C(23)	81(5)	56(5)	57(4)	-16(4)	22(4)	7(4)
C(24)	64(4)	61(5)	44(4)	3(4)	17(3)	6(4)
C(25)	78(5)	40(4)	61(5)	14(4)	22(4)	1(3)
C(26)	79(5)	40(4)	48(4)	-4(3)	25(4)	1(3)
C(27)	110(7)	100(7)	47(5)	-2(5)	35(4)	-5(5)
C(31)	43(3)	57(4)	37(3)	4(3)	3(3)	1(3)

C(32)	48(4)	76(5)	76(5)	21(4)	-3(4)	-7(4)
C(33)	43(4)	114(8)	87(6)	24(6)	5(4)	-7(4)
C(34)	42(4)	126(8)	64(5)	30(5)	10(4)	26(4)
C(35)	61(5)	87(6)	77(5)	23(5)	12(4)	31(4)
C(36)	47(4)	59(5)	71(5)	12(4)	5(3)	13(3)
C(37)	56(5)	188(11)	125(8)	63(8)	12(5)	45(6)
C(41)	42(3)	44(4)	40(4)	3(3)	4(3)	0(3)
C(42)	52(4)	45(4)	44(4)	0(3)	-3(3)	-3(3)
C(43)	62(4)	51(4)	41(4)	-11(3)	2(3)	0(3)
C(44)	57(4)	53(4)	40(4)	6(4)	5(3)	8(3)
C(45)	93(6)	62(5)	54(5)	-3(4)	23(4)	-30(4)
C(46)	97(6)	60(5)	51(4)	-16(4)	23(4)	-29(4)
C(47)	96(6)	80(6)	45(4)	9(4)	17(4)	3(5)
C(51)	43(3)	62(5)	46(4)	7(4)	1(3)	7(3)
C(52)	47(4)	79(5)	68(5)	6(4)	-3(3)	-16(4)
C(53)	48(5)	121(8)	79(6)	17(6)	-8(4)	-15(5)
C(54)	42(4)	145(9)	67(5)	37(6)	-2(4)	15(5)
C(55)	73(6)	113(8)	123(8)	58(7)	5(6)	29(6)
C(56)	56(5)	75(6)	112(7)	35(5)	18(5)	9(4)
C(57)	51(5)	255(15)	147(10)	105(10)	11(6)	50(7)
C(61)	54(4)	47(4)	38(4)	8(3)	3(3)	5(3)
C(62)	60(4)	34(4)	64(5)	-10(3)	3(4)	-7(3)
C(63)	61(4)	53(5)	71(5)	-12(4)	19(4)	-12(4)
C(64)	69(5)	64(5)	119(8)	-22(6)	29(5)	-14(4)
C(65)	57(5)	76(6)	130(9)	-24(6)	-8(6)	-11(4)
C(66)	86(6)	80(6)	86(6)	-10(5)	-29(5)	-16(5)
C(67)	70(5)	60(5)	64(5)	-4(4)	-1(4)	-7(4)
C(71)	193(17)	300(30)	142(13)	-15(14)	-25(12)	-81(17)
Cl(1)	214(6)	509(13)	258(7)	65(7)	105(5)	89(7)
Cl(2)	524(15)	432(13)	366(11)	25(9)	169(11)	306(12)

Table 5. Hydrogen coordinates ($\times 10^4$) and isotropic displacement parameters ($\text{\AA}^2 \times 10^3$) for P.

	x	y	z	U(eq)
H(2A)	8898	5899	1237	60
H(3A)	8069	6283	-117	59
H(7A)	4451	7044	-1196	59
H(8A)	2946	7181	-525	58
H(12A)	2048	7034	2690	56
H(13A)	2885	6651	4042	56
H(17A)	6498	5884	5115	59
H(18A)	7987	5714	4431	57
H(22A)	6198	5896	-1414	65
H(23A)	6711	6051	-2735	77
H(25A)	7229	7768	-2168	70
H(26A)	6693	7626	-852	65
H(27A)	7637	7438	-3500	125
H(27B)	6923	6937	-3914	125
H(27C)	7983	6764	-3500	125
H(32A)	1333	6496	1149	81
H(33A)	-191	6874	630	98
H(35A)	1054	8437	148	90
H(36A)	2566	8068	700	71
H(37A)	-1246	7660	-5	185
H(37B)	-727	8070	-625	185
H(37C)	-888	8307	286	185
H(42A)	5154	6987	5374	57
H(43A)	4661	6916	6738	62
H(45A)	3458	5327	6131	82
H(46A)	3932	5390	4775	82
H(47A)	3270	5710	7491	109
H(47B)	3164	6414	7491	109
H(47C)	4151	6112	7885	109
H(52A)	9561	6445	2789	79
H(53A)	11095	6074	3247	101
H(55)	9970	4470	3648	124
H(56A)	8397	4841	3187	96
H(57A)	12211	5308	3770	227
H(57B)	11882	4663	3443	227
H(57C)	11761	4856	4382	227

H(63A)	3400	5440	2318	73
H(64A)	1815	5221	1692	99
H(66A)	2705	5278	-627	104
H(67A)	4305	5452	-25	78
H(71A)	894	8638	4094	260
H(71B)	912	9132	3367	260

4-CF₃C₆H₄CORh(ttp) **5**

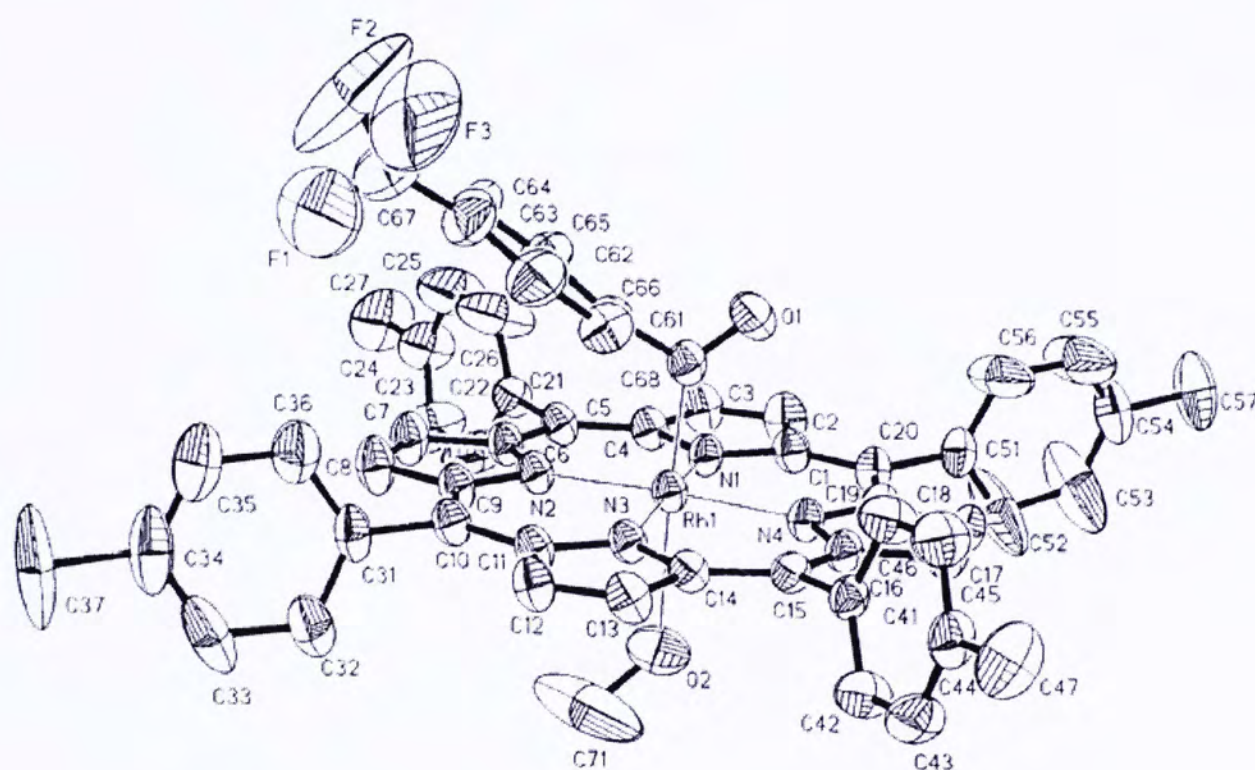


Figure 2. ORTEP of complex 4-CF₃C₆H₄CORh(ttp) **5**, showing the atomic labelling scheme and 30% probability displacement ellipsoids.

Crystal Data

Empirical Formula	C ₅₇ H ₄₄ F ₃ N ₄ ORh
Formula weight	976.87
Temperature	293(2) K
Wavelength	0.71073 Å
Crystal system	monoclinic
Space group	C2/c
Unit cell dimensions	a = 34.69 (18) Å b = 13.33 (7) Å c = 22.78 (11) Å $\alpha = 90^\circ$ $\beta = 116.96 (10)^\circ$ $\gamma = 90^\circ$
Volume	9384 (8) Å ⁻³
Z	8
Calculated density	1.383 Mg/m ⁻³
Absorption coefficient	0.424 mm ⁻¹
F(000)	4016
Crystal size	0.40 x 0.30 x 0.20 mm
θ range for data collection	1.32 to 28.70 °
Limiting indices	-45 ≤ h ≤ 46, -17 ≤ k ≤ 17, -28 ≤ l ≤ 30

Reflections collected	32798
Unique	12061 [R(int) = 0.0956]
Absorption correction	SADABS
Completeness to θ	28.70 99.4 %
Max. Transmission	1.0000
Min. Transmission	0.756103
Refinement method	full-matrix least-squares on F^2
Data / restraints / parameters	12061 / 0 / 604
Goodness-of-fit on F^2	0.912
Final R indices [$I > 2\sigma(I)$]	R1 = 0.0655, wR2 = 0.1559
R indices (all data)	R1 = 0.1977, wR2 = 0.2214
Absolute structure parameter	-
Largest diff. peak	0.568 eA ⁻³
Largest diff. hole	-0.612 eA ⁻³

Table 1. Crystal data and structure refinement for p.

Identification code	a12131
Empirical formula	C57 H44 F3 N4 O2 Rh
Formula weight	976.87
Temperature	293(2) K
Wavelength	0.71073 Å
Crystal system, space group	MONOCLINIC, C2/c
Unit cell dimensions	a = 34.6870(18) Å b = 13.3266(7) Å c = 22.7762(11) Å alpha = 90 deg. beta = 116.9640(10) deg. gamma = 90 deg.
Volume	9384.0(8) Å ³
Z, Calculated density	8, 1.383 Mg/m ³
Absorption coefficient	0.424 mm ⁻¹
F(000)	4016
Crystal size	0.40 x 0.30 x 0.20 mm
Theta range for data collection	1.32 to 28.70 deg.
Limiting indices	-45<=h<=46, -17<=k<=17, -28<=l<=30
Reflections collected / unique	32798 / 12061 [R(int) = 0.0956]
Completeness to theta = 28.70	99.4 %
Absorption correction	SADABS

Max. and min. transmission	1.0000 and 0.756103
Refinement method	Full-matrix least-squares on F ²
Data / restraints / parameters	12061 / 0 / 604
Goodness-of-fit on F ²	0.912
Final R indices [I>2sigma(I)]	R1 = 0.0655, wR2 = 0.1559
R indices (all data)	R1 = 0.1977, wR2 = 0.2214
Largest diff. peak and hole	0.568 and -0.612 e.A ⁻³

Table 2. Atomic coordinates ($\times 10^4$) and equivalent isotropic displacement parameters ($\text{\AA}^2 \times 10^3$) for p.
 U(eq) is defined as one third of the trace of the orthogonalized Uij tensor.

	x	y	z	U(eq)
Rh(1)	3473(1)	4605(1)	7455(1)	51(1)
O(1)	3476(2)	4900(4)	6240(3)	89(2)
O(2)	3347(2)	5084(5)	8398(3)	111(2)
N(1)	3740(2)	5990(4)	7519(2)	58(1)
N(2)	4065(2)	4081(4)	8099(2)	55(1)
N(3)	3210(2)	3250(4)	7467(2)	54(1)
N(4)	2876(2)	5163(4)	6863(2)	56(1)
C(1)	3517(2)	6833(5)	7183(3)	62(2)
C(2)	3828(2)	7637(5)	7330(4)	82(2)
C(3)	4215(2)	7294(5)	7756(3)	76(2)
C(4)	4170(2)	6243(5)	7874(3)	59(2)
C(5)	4497(2)	5623(5)	8278(3)	59(2)
C(6)	4448(2)	4607(5)	8380(3)	61(2)
C(7)	4787(2)	3960(6)	8793(3)	79(2)
C(8)	4620(2)	3045(6)	8784(3)	82(2)
C(9)	4162(2)	3122(5)	8341(3)	62(2)
C(10)	3869(2)	2321(5)	8211(3)	61(2)
C(11)	3421(2)	2405(5)	7799(3)	60(2)
C(12)	3118(2)	1590(5)	7637(3)	69(2)
C(13)	2733(2)	1941(5)	7212(3)	67(2)
C(14)	2779(2)	2972(5)	7099(3)	53(2)
C(15)	2449(2)	3595(5)	6670(3)	53(2)
C(16)	2492(2)	4610(5)	6576(3)	55(2)
C(17)	2151(2)	5275(5)	6159(3)	65(2)
C(18)	2323(2)	6181(5)	6188(3)	65(2)
C(19)	2779(2)	6116(5)	6621(3)	58(2)
C(20)	3073(2)	6896(5)	6745(3)	64(2)
C(21)	4949(2)	6036(5)	8645(3)	64(2)
C(22)	5119(3)	6281(8)	9274(5)	127(4)
C(23)	5550(3)	6625(9)	9628(5)	141(4)
C(24)	5799(3)	6750(8)	9319(5)	108(3)
C(25)	5650(3)	6381(11)	8725(5)	157(5)
C(26)	5227(3)	6039(12)	8388(5)	180(6)
C(27)	6264(3)	7131(10)	9685(6)	163(5)

C(31)	4047(2)	1342(5)	8526(4)	71(2)
C(32)	3981(3)	1018(7)	9051(4)	100(3)
C(33)	4190(4)	118(9)	9379(5)	132(4)
C(34)	4454(3)	-412(8)	9183(7)	128(5)
C(35)	4498(3)	-83(8)	8670(6)	126(4)
C(36)	4301(3)	761(7)	8329(5)	106(3)
C(37)	4690(4)	-1348(7)	9603(6)	218(8)
C(41)	2016(2)	3117(5)	6258(3)	55(2)
C(42)	1730(2)	2910(6)	6491(3)	81(2)
C(43)	1344(2)	2393(6)	6111(4)	88(2)
C(44)	1253(2)	2063(6)	5497(4)	73(2)
C(45)	1528(2)	2304(6)	5252(4)	88(2)
C(46)	1913(2)	2817(6)	5628(3)	83(2)
C(47)	847(2)	1457(7)	5074(4)	115(3)
C(51)	2912(2)	7873(5)	6392(4)	70(2)
C(52)	2755(6)	8602(8)	6612(5)	221(9)
C(53)	2618(6)	9511(8)	6238(6)	240(10)
C(54)	2613(3)	9653(7)	5670(5)	101(3)
C(55)	2730(5)	8917(10)	5461(7)	209(8)
C(56)	2885(5)	8013(8)	5806(6)	183(7)
C(57)	2442(4)	10624(6)	5268(5)	148(5)
C(61)	3746(2)	3306(5)	6648(3)	66(2)
C(62)	4181(3)	3222(7)	6794(4)	96(3)
C(63)	4342(3)	2295(10)	6721(5)	118(3)
C(64)	4085(4)	1466(8)	6513(5)	106(3)
C(65)	3658(3)	1545(7)	6368(4)	103(3)
C(66)	3492(3)	2443(6)	6442(4)	81(2)
C(67)	4259(7)	485(15)	6475(11)	176(7)
C(68)	3558(2)	4314(5)	6687(3)	63(2)
C(71)	3426(8)	4469(11)	8907(8)	306(14)
F(1)	4314(8)	-117(9)	6850(9)	343(12)
F(2)	4606(5)	552(9)	6417(16)	381(13)
F(3)	4072(6)	83(11)	5950(8)	343(11)

Table 3. Bond lengths [Å] and angles [deg] for p.

Rh(1)-C(68)	1.941(7)	C(20)-C(51)	1.499(9)
Rh(1)-N(3)	2.030(5)	C(21)-C(22)	1.319(9)
Rh(1)-N(2)	2.032(5)	C(21)-C(26)	1.337(11)
Rh(1)-N(4)	2.033(5)	C(22)-C(23)	1.414(11)
Rh(1)-N(1)	2.040(5)	C(23)-C(24)	1.353(12)
O(1)-C(68)	1.209(7)	C(24)-C(25)	1.304(12)
O(2)-C(71)	1.342(13)	C(24)-C(27)	1.527(11)
N(1)-C(4)	1.377(7)	C(25)-C(26)	1.389(12)
N(1)-C(1)	1.383(8)	C(31)-C(32)	1.385(10)
N(2)-C(9)	1.372(8)	C(31)-C(36)	1.390(11)
N(2)-C(6)	1.375(7)	C(32)-C(33)	1.425(13)
N(3)-C(11)	1.369(7)	C(33)-C(34)	1.382(17)
N(3)-C(14)	1.392(7)	C(34)-C(35)	1.321(16)
N(4)-C(19)	1.365(8)	C(34)-C(37)	1.559(13)
N(4)-C(16)	1.397(7)	C(35)-C(36)	1.363(12)
C(1)-C(20)	1.408(8)	C(41)-C(42)	1.347(8)
C(1)-C(2)	1.449(9)	C(41)-C(46)	1.371(8)
C(2)-C(3)	1.330(9)	C(42)-C(43)	1.402(9)
C(3)-C(4)	1.448(9)	C(43)-C(44)	1.358(9)
C(4)-C(5)	1.368(8)	C(44)-C(45)	1.345(9)
C(5)-C(6)	1.397(9)	C(44)-C(47)	1.527(9)
C(5)-C(21)	1.507(8)	C(45)-C(46)	1.394(9)
C(6)-C(7)	1.416(9)	C(51)-C(56)	1.309(11)
C(7)-C(8)	1.346(9)	C(51)-C(52)	1.319(12)
C(8)-C(9)	1.448(8)	C(52)-C(53)	1.432(13)
C(9)-C(10)	1.408(8)	C(53)-C(54)	1.299(15)
C(10)-C(11)	1.409(8)	C(54)-C(55)	1.236(13)
C(10)-C(31)	1.482(9)	C(54)-C(57)	1.541(11)
C(11)-C(12)	1.440(8)	C(55)-C(56)	1.405(13)
C(12)-C(13)	1.328(8)	C(61)-C(66)	1.394(9)
C(13)-C(14)	1.421(8)	C(61)-C(62)	1.397(10)
C(14)-C(15)	1.392(8)	C(61)-C(68)	1.512(9)
C(15)-C(16)	1.386(8)	C(62)-C(63)	1.396(12)
C(15)-C(41)	1.506(8)	C(63)-C(64)	1.364(13)
C(16)-C(17)	1.439(8)	C(64)-C(65)	1.367(12)
C(17)-C(18)	1.335(8)	C(64)-C(67)	1.458(17)
C(18)-C(19)	1.437(8)	C(65)-C(66)	1.371(10)
C(19)-C(20)	1.391(8)	C(67)-F(1)	1.124(18)

C(67)-F(3)	1.20(2)	N(2)-C(9)-C(10)	126.9(5)
C(67)-F(2)	1.27(2)	N(2)-C(9)-C(8)	109.6(6)
F(2)-F(3)	1.778(19)	C(10)-C(9)-C(8)	123.5(6)
C(68)-Rh(1)-N(3)	95.1(2)	C(9)-C(10)-C(11)	123.5(6)
C(68)-Rh(1)-N(2)	93.7(2)	C(9)-C(10)-C(31)	117.6(5)
N(3)-Rh(1)-N(2)	89.89(19)	C(11)-C(10)-C(31)	118.9(6)
C(68)-Rh(1)-N(4)	90.0(2)	N(3)-C(11)-C(10)	125.9(6)
N(3)-Rh(1)-N(4)	90.26(19)	N(3)-C(11)-C(12)	109.3(5)
N(2)-Rh(1)-N(4)	176.2(2)	C(10)-C(11)-C(12)	124.7(6)
C(68)-Rh(1)-N(1)	89.8(2)	C(13)-C(12)-C(11)	107.4(6)
N(3)-Rh(1)-N(1)	175.12(19)	C(12)-C(13)-C(14)	108.3(6)
N(2)-Rh(1)-N(1)	88.96(19)	C(15)-C(14)-N(3)	125.4(5)
N(4)-Rh(1)-N(1)	90.57(19)	C(15)-C(14)-C(13)	125.5(5)
C(4)-N(1)-C(1)	108.1(5)	N(3)-C(14)-C(13)	109.0(5)
C(4)-N(1)-Rh(1)	126.8(4)	C(16)-C(15)-C(14)	125.4(5)
C(1)-N(1)-Rh(1)	125.0(4)	C(16)-C(15)-C(41)	117.6(5)
C(9)-N(2)-C(6)	106.2(5)	C(14)-C(15)-C(41)	117.0(5)
C(9)-N(2)-Rh(1)	126.4(4)	C(15)-C(16)-N(4)	126.0(5)
C(6)-N(2)-Rh(1)	127.4(4)	C(15)-C(16)-C(17)	126.1(6)
C(11)-N(3)-C(14)	106.0(5)	N(4)-C(16)-C(17)	107.9(6)
C(11)-N(3)-Rh(1)	127.4(4)	C(18)-C(17)-C(16)	108.0(6)
C(14)-N(3)-Rh(1)	126.5(4)	C(17)-C(18)-C(19)	107.9(6)
C(19)-N(4)-C(16)	107.2(5)	N(4)-C(19)-C(20)	126.1(6)
C(19)-N(4)-Rh(1)	126.8(4)	N(4)-C(19)-C(18)	109.0(6)
C(16)-N(4)-Rh(1)	125.8(4)	C(20)-C(19)-C(18)	124.8(6)
N(1)-C(1)-C(20)	126.8(6)	C(19)-C(20)-C(1)	124.4(6)
N(1)-C(1)-C(2)	107.5(6)	C(19)-C(20)-C(51)	118.7(6)
C(20)-C(1)-C(2)	125.6(6)	C(1)-C(20)-C(51)	116.9(6)
C(3)-C(2)-C(1)	108.3(6)	C(22)-C(21)-C(26)	114.8(7)
C(2)-C(3)-C(4)	108.0(6)	C(22)-C(21)-C(5)	122.2(6)
C(5)-C(4)-N(1)	126.4(6)	C(26)-C(21)-C(5)	122.2(7)
C(5)-C(4)-C(3)	125.7(6)	C(21)-C(22)-C(23)	122.4(8)
N(1)-C(4)-C(3)	107.9(6)	C(24)-C(23)-C(22)	120.2(9)
C(4)-C(5)-C(6)	124.8(5)	C(25)-C(24)-C(23)	116.6(8)
C(4)-C(5)-C(21)	119.3(6)	C(25)-C(24)-C(27)	121.1(9)
C(6)-C(5)-C(21)	115.9(6)	C(23)-C(24)-C(27)	121.5(9)
N(2)-C(6)-C(5)	125.5(5)	C(24)-C(25)-C(26)	121.3(9)
N(2)-C(6)-C(7)	109.5(6)	C(21)-C(26)-C(25)	123.3(9)
C(5)-C(6)-C(7)	125.0(6)	C(32)-C(31)-C(36)	118.9(7)
C(8)-C(7)-C(6)	108.6(6)	C(32)-C(31)-C(10)	119.7(8)
C(7)-C(8)-C(9)	106.0(6)	C(36)-C(31)-C(10)	121.3(7)

C(31)-C(32)-C(33)	118.1(10)	C(53)-C(54)-C(57)	122.8(11)
C(34)-C(33)-C(32)	121.0(11)	C(54)-C(55)-C(56)	124.9(11)
C(35)-C(34)-C(33)	118.4(10)	C(51)-C(56)-C(55)	121.7(10)
C(35)-C(34)-C(37)	124.7(14)	C(66)-C(61)-C(62)	117.6(7)
C(33)-C(34)-C(37)	116.9(14)	C(66)-C(61)-C(68)	122.0(6)
C(34)-C(35)-C(36)	123.3(12)	C(62)-C(61)-C(68)	120.3(7)
C(35)-C(36)-C(31)	120.2(10)	C(63)-C(62)-C(61)	119.5(9)
C(42)-C(41)-C(46)	117.5(6)	C(64)-C(63)-C(62)	121.5(9)
C(42)-C(41)-C(15)	123.1(6)	C(63)-C(64)-C(65)	119.2(9)
C(46)-C(41)-C(15)	119.2(6)	C(63)-C(64)-C(67)	121.6(14)
C(41)-C(42)-C(43)	121.6(7)	C(65)-C(64)-C(67)	119.1(14)
C(44)-C(43)-C(42)	120.5(7)	C(64)-C(65)-C(66)	120.5(9)
C(45)-C(44)-C(43)	118.1(6)	C(65)-C(66)-C(61)	121.7(8)
C(45)-C(44)-C(47)	119.3(7)	F(1)-C(67)-F(3)	106(2)
C(43)-C(44)-C(47)	122.6(7)	F(1)-C(67)-F(2)	107(2)
C(44)-C(45)-C(46)	121.6(7)	F(3)-C(67)-F(2)	92.1(16)
C(41)-C(46)-C(45)	120.6(7)	F(1)-C(67)-C(64)	121.9(16)
C(56)-C(51)-C(52)	115.6(8)	F(3)-C(67)-C(64)	114.2(18)
C(56)-C(51)-C(20)	120.5(7)	F(2)-C(67)-C(64)	112(2)
C(52)-C(51)-C(20)	123.6(8)	O(1)-C(68)-C(61)	118.0(6)
C(51)-C(52)-C(53)	118.6(11)	O(1)-C(68)-Rh(1)	123.7(5)
C(54)-C(53)-C(52)	124.5(11)	C(61)-C(68)-Rh(1)	118.3(5)
C(55)-C(54)-C(53)	114.2(9)	C(67)-F(2)-F(3)	42.3(10)
C(55)-C(54)-C(57)	122.8(11)	C(67)-F(3)-F(2)	45.6(12)

Symmetry transformations used to generate equivalent atoms:

Table 4. Anisotropic displacement parameters ($\text{\AA}^2 \times 10^3$) for p.
 The anisotropic displacement factor exponent takes the form:
 $-2 \pi^2 [h^2 a^{*2} U_{11} + \dots + 2 h k a^* b^* U_{12}]$

	U11	U22	U33	U23	U13	U12
Rh(1)	41(1)	53(1)	46(1)	1(1)	9(1)	-5(1)
O(1)	102(4)	96(4)	68(3)	18(3)	36(3)	8(3)
O(2)	143(6)	112(5)	94(4)	-22(4)	67(4)	-22(4)
N(1)	41(3)	62(3)	59(3)	4(3)	11(2)	-1(2)
N(2)	46(3)	58(3)	48(3)	3(2)	9(2)	-8(2)
N(3)	48(3)	58(3)	44(3)	2(2)	10(2)	-5(2)
N(4)	46(3)	55(3)	57(3)	2(2)	15(2)	-1(2)
C(1)	64(4)	48(4)	66(4)	8(3)	21(3)	-5(3)
C(2)	76(5)	55(4)	98(6)	6(4)	22(4)	-17(4)
C(3)	59(4)	71(5)	76(5)	-1(4)	11(4)	-19(4)
C(4)	49(4)	59(4)	56(4)	-1(3)	12(3)	-13(3)
C(5)	49(4)	64(5)	44(3)	0(3)	6(3)	-12(3)
C(6)	44(3)	67(4)	57(4)	8(3)	11(3)	-1(3)
C(7)	40(4)	85(5)	86(5)	16(4)	6(3)	-5(4)
C(8)	52(4)	75(5)	84(5)	17(4)	0(4)	-7(4)
C(9)	50(4)	68(5)	48(4)	7(3)	6(3)	-1(3)
C(10)	55(4)	63(4)	49(4)	4(3)	9(3)	-3(3)
C(11)	55(4)	61(4)	49(4)	3(3)	10(3)	-8(3)
C(12)	64(4)	58(4)	64(4)	8(3)	11(3)	-8(3)
C(13)	59(4)	64(4)	61(4)	3(3)	13(3)	-20(3)
C(14)	46(3)	57(4)	47(3)	-2(3)	14(3)	-12(3)
C(15)	42(3)	60(4)	53(4)	-1(3)	17(3)	-7(3)
C(16)	39(3)	69(4)	48(3)	-4(3)	10(3)	0(3)
C(17)	42(3)	75(5)	68(4)	1(4)	16(3)	-2(3)
C(18)	48(4)	60(4)	76(4)	8(4)	19(3)	6(3)
C(19)	54(4)	52(4)	61(4)	-2(3)	20(3)	1(3)
C(20)	58(4)	55(4)	68(4)	5(3)	17(3)	7(3)
C(21)	46(4)	80(5)	54(4)	-1(4)	13(3)	-16(3)
C(22)	63(5)	208(11)	115(7)	-77(7)	46(5)	-49(6)
C(23)	74(6)	217(13)	122(8)	-84(8)	36(6)	-52(7)
C(24)	62(5)	145(9)	109(7)	-22(6)	31(5)	-49(5)
C(25)	81(7)	285(17)	105(8)	-11(9)	41(6)	-55(9)
C(26)	90(7)	370(20)	74(6)	-32(9)	37(6)	-90(10)
C(27)	63(6)	212(13)	193(11)	-24(9)	39(7)	-57(7)
C(31)	48(4)	59(4)	77(5)	20(4)	4(3)	-6(3)

C(32)	81(6)	105(7)	86(6)	31(5)	15(4)	-3(5)
C(33)	108(8)	129(9)	107(8)	68(7)	3(6)	-33(7)
C(34)	75(6)	71(6)	156(11)	26(7)	-18(7)	-9(5)
C(35)	105(8)	77(7)	159(11)	9(7)	27(8)	18(6)
C(36)	100(7)	86(6)	121(7)	21(6)	41(6)	15(5)
C(37)	133(9)	90(7)	264(15)	94(9)	-56(9)	-7(7)
C(41)	38(3)	64(4)	53(4)	0(3)	12(3)	-1(3)
C(42)	61(4)	119(6)	60(4)	-15(4)	23(4)	-27(4)
C(43)	58(5)	125(7)	83(6)	-6(5)	33(4)	-27(5)
C(44)	45(4)	82(5)	72(5)	-3(4)	8(3)	-13(3)
C(45)	70(5)	115(7)	66(5)	-24(4)	18(4)	-20(5)
C(46)	62(4)	124(7)	58(4)	-17(4)	21(4)	-35(4)
C(47)	62(5)	119(7)	135(8)	-30(6)	19(5)	-35(5)
C(51)	64(4)	55(4)	72(5)	-1(4)	14(4)	8(3)
C(52)	430(20)	98(8)	67(6)	9(6)	48(10)	117(11)
C(53)	460(30)	85(8)	90(8)	1(7)	53(12)	128(12)
C(54)	96(6)	65(5)	88(6)	16(5)	-5(5)	-8(5)
C(55)	380(20)	142(11)	223(14)	112(11)	236(16)	133(13)
C(56)	335(19)	126(9)	201(12)	100(9)	219(14)	136(11)
C(57)	158(10)	71(6)	143(9)	42(6)	6(8)	17(6)
C(61)	62(4)	82(5)	50(4)	-6(3)	22(3)	0(4)
C(62)	59(5)	128(8)	97(6)	-25(5)	32(4)	-3(5)
C(63)	81(7)	152(10)	112(7)	-12(7)	35(6)	39(7)
C(64)	114(8)	96(7)	108(7)	-9(6)	50(6)	28(6)
C(65)	112(8)	91(7)	112(7)	-18(5)	54(6)	3(6)
C(66)	78(5)	77(5)	85(5)	-16(4)	36(4)	-10(4)
C(67)	217(18)	175(16)	166(15)	-9(12)	114(14)	83(14)
C(68)	45(4)	72(5)	59(4)	5(3)	12(3)	-7(3)
C(71)	650(40)	170(15)	246(18)	17(13)	330(30)	-19(19)
F(1)	610(30)	172(10)	352(18)	101(11)	320(20)	216(15)
F(2)	265(15)	200(11)	800(40)	-109(18)	350(20)	25(10)
F(3)	450(30)	259(14)	254(14)	-100(11)	100(14)	169(15)

Table 5. Hydrogen coordinates ($\times 10^4$) and isotropic displacement parameters ($\text{\AA}^2 \times 10^3$) for p.

	x	y	z	U(eq)
H(2)	3403	4794	8129	167
H(2A)	3768	8283	7157	99
H(3A)	4470	7665	7946	91
H(7A)	5076	4138	9031	95
H(8A)	4768	2479	9014	99
H(12A)	3179	939	7799	82
H(13A)	2477	1574	7021	80
H(17A)	1862	5104	5911	78
H(18A)	2174	6753	5968	78
H(22A)	4949	6226	9493	152
H(23A)	5662	6766	10075	169
H(25A)	5831	6345	8525	189
H(26A)	5132	5801	7961	216
H(27A)	6387	7177	9384	245
H(27B)	6431	6674	10034	245
H(27C)	6265	7782	9866	245
H(32A)	3804	1377	9185	120
H(33A)	4148	-115	9730	158
H(35A)	4672	-447	8534	151
H(36A)	4336	950	7963	127
H(37A)	4865	-1651	9424	326
H(37B)	4480	-1824	9595	326
H(37C)	4871	-1144	10049	326
H(42A)	1791	3116	6914	98
H(43A)	1150	2276	6280	106
H(45A)	1461	2124	4822	106
H(46A)	2101	2958	5450	100
H(47A)	845	1295	4662	173
H(47B)	595	1847	4994	173
H(47C)	846	850	5300	173
H(52A)	2733	8528	7002	265
H(53A)	2527	10036	6413	288
H(55A)	2714	8965	5043	251
H(56A)	2971	7502	5613	220
H(57A)	2465	10574	4865	222
H(57B)	2609	11185	5519	222

H(57C)	2144	10718	5169	222
H(62A)	4362	3778	6938	115
H(63A)	4632	2243	6816	142
H(65A)	3479	986	6219	124
H(66A)	3203	2477	6352	97
H(71A)	3355	4805	9219	459
H(71B)	3726	4288	9117	459
H(71C)	3253	3875	8750	459

Appendix I

Crystal data collection and processing parameters

$\text{C}_6\text{H}_5\text{CORh}(\text{ttp}) \mathbf{2}$

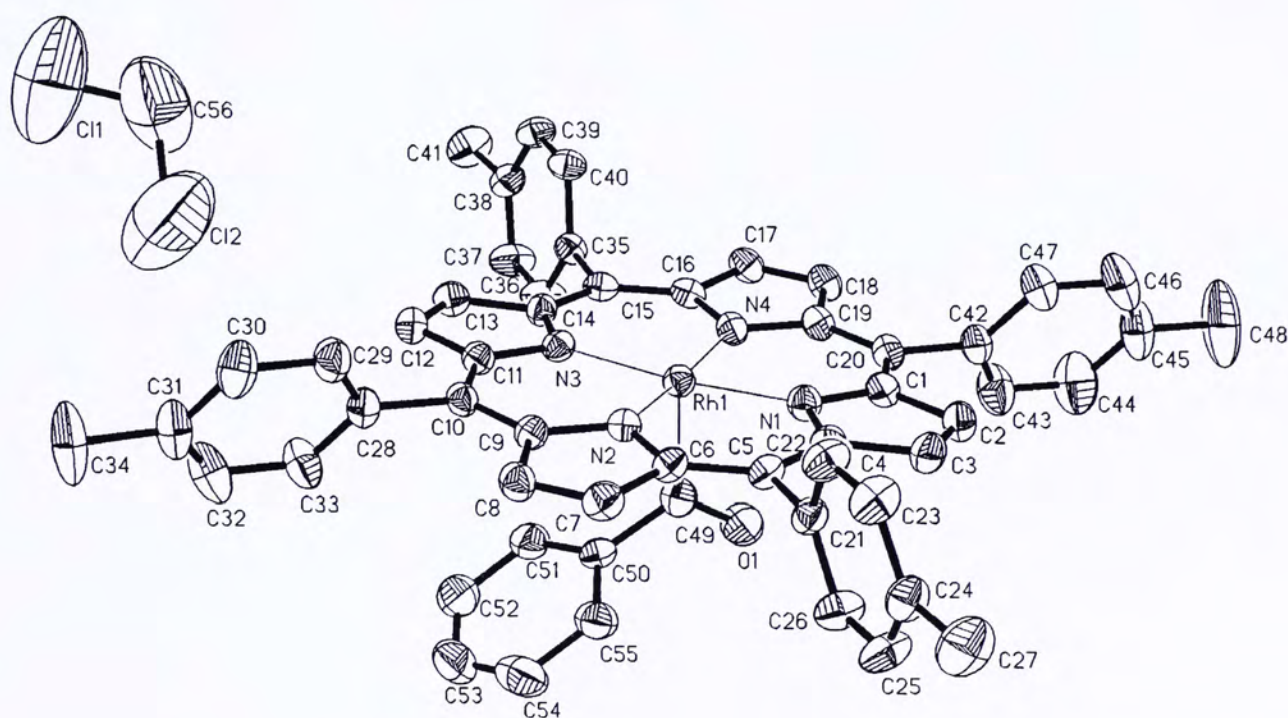


Figure 1. ORTEP of complex $\text{C}_6\text{H}_5\text{CORh}(\text{ttp}) \mathbf{2}$, showing the atomic labelling scheme and 30% probability displacement ellipsoids.

Crystal Data

Empirical Formula	C ₅₆ H ₄₃ Cl ₂ N ₄ ORh
Formula weight	961.75
Temperature	293(2) K
Wavelength	0.71073 Å
Crystal system	monoclinic
Space group	P2(1)
Unit cell dimensions	a = 13.6118(7) Å b = 22.2699(12) Å c = 15.6005(8) Å $\alpha = 90^\circ$ $\beta = 97.0330(10)^\circ$ $\gamma = 90^\circ$
Volume	4693.5(4) Å ⁻³
Z	4
Calculated density	1.361 Mg/m ⁻³
Absorption coefficient	0.522 mm ⁻¹
F(000)	1976
Crystal size	0.50 x 0.40 x 0.20 mm
θ range for data collection	1.51 to 28.02 °
Limiting indices	-17 ≤ h ≤ 16, -25 ≤ k ≤ 29, -20 ≤ l ≤ 20

Reflections collected	31881
Unique	11318 [R(int) =0.0987]
Absorption correction	SADABS
Completeness to θ	28.02 99.7%
Max. Transmission	1.0000
Min. Transmission	0.637161
Refinement method	full-matrix least-squares on F^2
Data / restraints / parameters	11318 / 0 / 577
Goodness-of-fit on F^2	0.877
Final R indices [$I > 2\sigma(I)$]	R1 = 0.0542, wR2 = 0.1152
R indices (all data)	R1 = 0.1589, wR2 = 0.1503
Absolute structure parameter	-
Largest diff. peak	0.550 eA ⁻³
Largest diff. hole	-0.485 eA ⁻³

Table 1. Crystal data and structure refinement for P.

Identification code	cm1702
Empirical formula	C56 H43 Cl2 N4 O Rh
Formula weight	961.75
Temperature	293(2) K
Wavelength	0.71073 Å
Crystal system, space group	MONOCLINIC, P2(1)/c
Unit cell dimensions	a = 13.6118(7) Å b = 22.2699(12) Å c = 15.6005(8) Å alpha = 90 deg. beta = 97.0330(10) deg. gamma = 90 deg.
Volume	4693.5(4) Å ³
Z, Calculated density	4, 1.361 Mg/m ³
Absorption coefficient	0.522 mm ⁻¹
F(000)	1976
Crystal size	0.50 x 0.40 x 0.20 mm
Theta range for data collection	1.51 to 28.02 deg.
Limiting indices	-17<=h<=16, -25<=k<=29, -20<=l<=20
Reflections collected / unique	31881 / 11318 [R(int) = 0.0987]
Completeness to theta = 28.02	99.7 %
Absorption correction	SADABS

Max. and min. transmission	1.0000 and 0.637161
Refinement method	Full-matrix least-squares on F ²
Data / restraints / parameters	11318 / 0 / 577
Goodness-of-fit on F ²	0.877
Final R indices [I>2sigma(I)]	R1 = 0.0542, wR2 = 0.1152
R indices (all data)	R1 = 0.1589, wR2 = 0.1503
Largest diff. peak and hole	0.550 and -0.485 e.A ⁻³

Table 2. Atomic coordinates ($\times 10^4$) and equivalent isotropic displacement parameters ($\text{\AA}^2 \times 10^3$) for P.
 U(eq) is defined as one third of the trace of the orthogonalized U_{ij} tensor.

	x	y	z	U(eq)
Rh(1)	15459(1)	8590(1)	1978(1)	41(1)
N(1)	16727(3)	8681(2)	1422(2)	48(1)
N(2)	14775(3)	8253(2)	855(2)	45(1)
N(3)	14241(3)	8398(2)	2562(2)	43(1)
N(4)	16190(3)	8848(2)	3128(2)	45(1)
O(1)	15695(3)	9814(2)	1745(3)	85(1)
C(1)	17611(3)	8914(2)	1809(3)	51(1)
C(2)	18291(4)	8953(2)	1175(3)	55(1)
C(3)	17827(4)	8737(2)	432(4)	59(2)
C(4)	16841(3)	8571(2)	572(3)	47(1)
C(5)	16119(3)	8352(2)	-54(3)	45(1)
C(6)	15156(3)	8217(2)	79(3)	45(1)
C(7)	14401(4)	8018(2)	-586(3)	54(1)
C(8)	13569(4)	7942(2)	-207(3)	52(1)
C(9)	13793(3)	8069(2)	694(3)	43(1)
C(10)	13137(3)	8017(2)	1309(3)	43(1)
C(11)	13367(3)	8162(2)	2178(3)	45(1)
C(12)	12698(3)	8109(2)	2822(3)	53(1)
C(13)	13155(4)	8323(2)	3556(3)	52(1)
C(14)	14126(3)	8505(2)	3416(3)	43(1)
C(15)	14839(4)	8728(2)	4044(3)	46(1)
C(16)	15812(4)	8872(2)	3911(3)	47(1)
C(17)	16567(4)	9073(2)	4573(3)	54(1)
C(18)	17392(4)	9168(2)	4188(3)	53(1)
C(19)	17164(3)	9035(2)	3287(3)	48(1)
C(20)	17820(3)	9077(2)	2670(3)	48(1)
C(21)	16423(3)	8256(2)	-937(3)	47(1)
C(22)	16720(4)	7696(2)	-1193(3)	61(1)
C(23)	17054(4)	7615(3)	-1976(4)	66(2)
C(24)	17096(4)	8077(3)	-2550(3)	57(1)
C(25)	16768(4)	8633(3)	-2301(4)	74(2)
C(26)	16452(4)	8724(2)	-1508(4)	65(2)
C(27)	17472(5)	7986(3)	-3407(4)	97(2)
C(28)	12129(3)	7759(2)	1000(3)	52(1)

C(29)	12036(4)	7181(3)	719(4)	65(2)
C(30)	11118(4)	6943(3)	405(4)	79(2)
C(31)	10270(4)	7290(4)	357(4)	80(2)
C(32)	10368(4)	7861(3)	676(4)	93(2)
C(33)	11287(4)	8110(3)	991(4)	76(2)
C(34)	9270(4)	7041(4)	-7(5)	129(3)
C(35)	14586(3)	8795(2)	4947(3)	48(1)
C(36)	14079(4)	9288(3)	5199(4)	72(2)
C(37)	13792(4)	9323(3)	6020(4)	73(2)
C(38)	14004(4)	8878(3)	6617(3)	57(1)
C(39)	14533(4)	8394(2)	6377(3)	57(1)
C(40)	14820(4)	8354(2)	5566(3)	52(1)
C(41)	13617(5)	8903(3)	7479(3)	82(2)
C(42)	18835(3)	9321(3)	2965(3)	55(1)
C(43)	18959(4)	9899(3)	3216(4)	87(2)
C(44)	19907(5)	10137(4)	3487(5)	109(3)
C(45)	20724(5)	9769(4)	3510(4)	95(2)
C(46)	20593(5)	9191(4)	3277(4)	99(2)
C(47)	19656(4)	8953(3)	3002(4)	73(2)
C(48)	21757(5)	10023(5)	3787(5)	170(5)
C(49)	15092(4)	9413(2)	1658(3)	54(1)
C(50)	14039(4)	9530(2)	1260(4)	52(1)
C(51)	13289(4)	9596(2)	1758(4)	67(2)
C(52)	12340(5)	9731(3)	1371(5)	88(2)
C(53)	12166(5)	9789(3)	506(6)	100(3)
C(54)	12894(6)	9720(3)	0(5)	95(2)
C(55)	13858(4)	9585(2)	377(4)	69(2)
C(56)	10780(10)	6280(9)	3595(8)	294(10)
C1(1)	9761(4)	5968(3)	3702(4)	364(4)
C1(2)	10570(5)	6848(3)	2812(4)	375(4)

Table 3. Bond lengths [Å] and angles [deg] for P.

Rh(1)-C(49)	1.950(5)	C(21)-C(22)	1.384(7)
Rh(1)-N(2)	2.025(4)	C(22)-C(23)	1.366(7)
Rh(1)-N(4)	2.025(4)	C(23)-C(24)	1.369(7)
Rh(1)-N(3)	2.034(4)	C(24)-C(25)	1.388(7)
Rh(1)-N(1)	2.034(4)	C(24)-C(27)	1.502(7)
N(1)-C(4)	1.376(6)	C(25)-C(26)	1.373(7)
N(1)-C(1)	1.379(6)	C(28)-C(29)	1.362(7)
N(2)-C(6)	1.376(6)	C(28)-C(33)	1.385(7)
N(2)-C(9)	1.390(5)	C(29)-C(30)	1.390(7)
N(3)-C(11)	1.371(5)	C(30)-C(31)	1.384(8)
N(3)-C(14)	1.381(6)	C(31)-C(32)	1.365(8)
N(4)-C(19)	1.383(5)	C(31)-C(34)	1.514(7)
N(4)-C(16)	1.384(6)	C(32)-C(33)	1.401(7)
O(1)-C(49)	1.207(5)	C(35)-C(36)	1.378(7)
C(1)-C(20)	1.388(6)	C(35)-C(40)	1.388(6)
C(1)-C(2)	1.438(6)	C(36)-C(37)	1.387(7)
C(2)-C(3)	1.340(6)	C(37)-C(38)	1.366(7)
C(3)-C(4)	1.435(6)	C(38)-C(39)	1.373(7)
C(4)-C(5)	1.386(6)	C(38)-C(41)	1.504(7)
C(5)-C(6)	1.386(6)	C(39)-C(40)	1.373(7)
C(5)-C(21)	1.502(6)	C(42)-C(43)	1.350(7)
C(6)-C(7)	1.438(6)	C(42)-C(47)	1.382(7)
C(7)-C(8)	1.351(6)	C(43)-C(44)	1.411(8)
C(8)-C(9)	1.429(6)	C(44)-C(45)	1.377(9)
C(9)-C(10)	1.394(6)	C(45)-C(46)	1.344(10)
C(10)-C(11)	1.391(6)	C(45)-C(48)	1.529(8)
C(10)-C(28)	1.510(6)	C(46)-C(47)	1.399(8)
C(11)-C(12)	1.441(6)	C(49)-C(50)	1.513(7)
C(12)-C(13)	1.322(6)	C(50)-C(51)	1.365(7)
C(13)-C(14)	1.424(6)	C(50)-C(55)	1.375(7)
C(14)-C(15)	1.384(6)	C(51)-C(52)	1.391(8)
C(15)-C(16)	1.402(6)	C(52)-C(53)	1.347(9)
C(15)-C(35)	1.497(6)	C(53)-C(54)	1.350(9)
C(16)-C(17)	1.437(6)	C(54)-C(55)	1.402(8)
C(17)-C(18)	1.354(6)	C(56)-Cl(1)	1.579(14)
C(18)-C(19)	1.433(6)	C(56)-Cl(2)	1.758(15)
C(19)-C(20)	1.394(6)	C(49)-Rh(1)-N(2)	92.89(18)
C(20)-C(42)	1.503(6)	C(49)-Rh(1)-N(4)	92.41(18)
C(21)-C(26)	1.374(7)	C(49)-Rh(1)-N(3)	96.56(18)

C(49)-Rh(1)-N(1)	90.11(19)	N(3)-C(11)-C(10)	126.5(4)
N(2)-Rh(1)-N(4)	174.67(15)	N(3)-C(11)-C(12)	108.3(4)
N(2)-Rh(1)-N(3)	89.78(15)	C(10)-C(11)-C(12)	125.1(4)
N(4)-Rh(1)-N(3)	90.10(15)	C(13)-C(12)-C(11)	107.7(4)
N(2)-Rh(1)-N(1)	89.58(15)	C(12)-C(13)-C(14)	108.5(5)
N(4)-Rh(1)-N(1)	89.92(15)	N(3)-C(14)-C(15)	126.3(4)
N(3)-Rh(1)-N(1)	173.32(15)	N(3)-C(14)-C(13)	108.4(4)
C(4)-N(1)-C(1)	107.0(4)	C(15)-C(14)-C(13)	125.3(5)
C(4)-N(1)-Rh(1)	126.5(3)	C(14)-C(15)-C(16)	124.7(5)
C(1)-N(1)-Rh(1)	126.3(3)	C(14)-C(15)-C(35)	118.7(4)
C(6)-N(2)-C(9)	106.3(4)	C(16)-C(15)-C(35)	116.5(4)
C(6)-N(2)-Rh(1)	126.9(3)	N(4)-C(16)-C(15)	125.6(4)
C(9)-N(2)-Rh(1)	126.5(3)	N(4)-C(16)-C(17)	109.6(4)
C(11)-N(3)-C(14)	107.1(4)	C(15)-C(16)-C(17)	124.7(5)
C(11)-N(3)-Rh(1)	126.6(3)	C(18)-C(17)-C(16)	106.8(5)
C(14)-N(3)-Rh(1)	126.2(3)	C(17)-C(18)-C(19)	108.1(4)
C(19)-N(4)-C(16)	106.4(4)	N(4)-C(19)-C(20)	125.3(4)
C(19)-N(4)-Rh(1)	127.0(3)	N(4)-C(19)-C(18)	109.1(4)
C(16)-N(4)-Rh(1)	126.7(3)	C(20)-C(19)-C(18)	125.7(4)
N(1)-C(1)-C(20)	125.9(5)	C(1)-C(20)-C(19)	125.3(4)
N(1)-C(1)-C(2)	108.9(4)	C(1)-C(20)-C(42)	117.6(4)
C(20)-C(1)-C(2)	125.2(5)	C(19)-C(20)-C(42)	117.1(4)
C(3)-C(2)-C(1)	107.3(4)	C(26)-C(21)-C(22)	117.6(5)
C(2)-C(3)-C(4)	108.2(5)	C(26)-C(21)-C(5)	121.3(5)
N(1)-C(4)-C(5)	126.0(4)	C(22)-C(21)-C(5)	121.0(5)
N(1)-C(4)-C(3)	108.6(4)	C(23)-C(22)-C(21)	121.1(5)
C(5)-C(4)-C(3)	125.4(5)	C(22)-C(23)-C(24)	122.1(5)
C(4)-C(5)-C(6)	125.0(5)	C(23)-C(24)-C(25)	116.4(5)
C(4)-C(5)-C(21)	116.5(4)	C(23)-C(24)-C(27)	121.9(5)
C(6)-C(5)-C(21)	118.6(4)	C(25)-C(24)-C(27)	121.7(5)
N(2)-C(6)-C(5)	125.8(4)	C(26)-C(25)-C(24)	122.1(5)
N(2)-C(6)-C(7)	109.9(4)	C(25)-C(26)-C(21)	120.5(5)
C(5)-C(6)-C(7)	124.4(5)	C(29)-C(28)-C(33)	119.1(5)
C(8)-C(7)-C(6)	106.6(4)	C(29)-C(28)-C(10)	120.4(5)
C(7)-C(8)-C(9)	108.4(4)	C(33)-C(28)-C(10)	120.5(5)
N(2)-C(9)-C(10)	125.7(4)	C(28)-C(29)-C(30)	121.2(5)
N(2)-C(9)-C(8)	108.7(4)	C(31)-C(30)-C(29)	121.0(6)
C(10)-C(9)-C(8)	125.6(4)	C(32)-C(31)-C(30)	117.1(5)
C(11)-C(10)-C(9)	124.4(4)	C(32)-C(31)-C(34)	121.4(6)
C(11)-C(10)-C(28)	119.0(4)	C(30)-C(31)-C(34)	121.4(6)
C(9)-C(10)-C(28)	116.5(4)	C(31)-C(32)-C(33)	122.7(6)

C(28)-C(33)-C(32)	118.9(6)	C(46)-C(45)-C(48)	121.2(7)
C(36)-C(35)-C(40)	116.4(5)	C(44)-C(45)-C(48)	120.0(8)
C(36)-C(35)-C(15)	122.0(5)	C(45)-C(46)-C(47)	122.1(7)
C(40)-C(35)-C(15)	121.6(4)	C(42)-C(47)-C(46)	119.3(6)
C(35)-C(36)-C(37)	121.1(5)	O(1)-C(49)-C(50)	121.0(5)
C(38)-C(37)-C(36)	121.9(5)	O(1)-C(49)-Rh(1)	121.1(4)
C(37)-C(38)-C(39)	117.2(5)	C(50)-C(49)-Rh(1)	117.8(4)
C(37)-C(38)-C(41)	120.9(5)	C(51)-C(50)-C(55)	120.4(5)
C(39)-C(38)-C(41)	121.7(5)	C(51)-C(50)-C(49)	121.5(5)
C(40)-C(39)-C(38)	121.3(5)	C(55)-C(50)-C(49)	118.1(5)
C(39)-C(40)-C(35)	121.9(5)	C(50)-C(51)-C(52)	119.8(6)
C(43)-C(42)-C(47)	118.8(5)	C(53)-C(52)-C(51)	119.7(7)
C(43)-C(42)-C(20)	120.8(5)	C(52)-C(53)-C(54)	121.6(7)
C(47)-C(42)-C(20)	120.4(5)	C(53)-C(54)-C(55)	119.7(7)
C(42)-C(43)-C(44)	121.4(6)	C(50)-C(55)-C(54)	118.9(6)
C(45)-C(44)-C(43)	119.4(7)	Cl(1)-C(56)-Cl(2)	108.6(8)
C(46)-C(45)-C(44)	118.8(6)		

Symmetry transformations used to generate equivalent atoms:

Table 4. Anisotropic displacement parameters ($\text{\AA}^2 \times 10^3$) for P.
 The anisotropic displacement factor exponent takes the form:
 $-2 \pi^2 [h^2 a^{*2} U_{11} + \dots + 2 h k a^* b^* U_{12}]$

	U11	U22	U33	U23	U13	U12
Rh(1)	41(1)	40(1)	44(1)	-1(1)	5(1)	-1(1)
N(1)	45(2)	52(3)	46(2)	-3(2)	4(2)	-2(2)
N(2)	44(2)	45(2)	46(3)	5(2)	5(2)	1(2)
N(3)	48(2)	35(2)	47(2)	-1(2)	8(2)	0(2)
N(4)	40(2)	45(2)	51(3)	-2(2)	3(2)	1(2)
O(1)	77(3)	48(2)	125(4)	5(2)	-7(3)	-9(2)
C(1)	43(3)	53(3)	56(3)	2(3)	3(3)	2(2)
C(2)	44(3)	66(4)	56(3)	-2(3)	9(3)	-2(3)
C(3)	54(3)	67(4)	59(4)	4(3)	21(3)	-1(3)
C(4)	48(3)	41(3)	54(3)	1(3)	8(2)	0(3)
C(5)	51(3)	40(3)	45(3)	1(2)	10(2)	-4(2)
C(6)	50(3)	41(3)	46(3)	1(2)	8(2)	-6(2)
C(7)	63(3)	55(3)	42(3)	-2(2)	4(3)	-4(3)
C(8)	46(3)	52(3)	54(3)	-3(3)	-1(3)	-4(3)
C(9)	44(3)	37(3)	48(3)	-4(2)	2(2)	-5(2)
C(10)	38(3)	39(3)	51(3)	-3(2)	1(2)	-1(2)
C(11)	41(3)	38(3)	53(3)	-2(2)	1(2)	-3(2)
C(12)	44(3)	57(3)	58(3)	2(3)	5(3)	-6(3)
C(13)	56(3)	58(3)	41(3)	-1(3)	6(3)	0(3)
C(14)	41(3)	45(3)	44(3)	1(2)	9(2)	-1(2)
C(15)	54(3)	40(3)	45(3)	3(2)	4(2)	6(2)
C(16)	49(3)	47(3)	43(3)	2(2)	0(2)	8(2)
C(17)	52(3)	63(4)	45(3)	-6(3)	-2(3)	6(3)
C(18)	48(3)	60(4)	50(3)	-9(3)	0(3)	3(3)
C(19)	43(3)	52(3)	49(3)	-5(2)	1(2)	1(2)
C(20)	38(3)	48(3)	57(3)	-4(3)	4(2)	1(2)
C(21)	49(3)	47(3)	46(3)	1(2)	5(2)	-10(2)
C(22)	80(4)	48(3)	59(4)	-2(3)	21(3)	-1(3)
C(23)	85(4)	53(4)	64(4)	-10(3)	22(3)	-3(3)
C(24)	63(3)	66(4)	45(3)	-5(3)	16(3)	-5(3)
C(25)	98(4)	65(4)	65(4)	18(3)	28(3)	-5(4)
C(26)	91(4)	51(4)	57(4)	4(3)	18(3)	5(3)
C(27)	114(5)	119(6)	65(4)	-3(4)	35(4)	-6(5)
C(28)	42(3)	60(4)	54(3)	-2(3)	7(2)	-8(3)
C(29)	53(3)	61(4)	80(4)	-5(3)	0(3)	-10(3)

C(30)	69(4)	86(5)	83(5)	-29(4)	16(4)	-28(4)
C(31)	47(3)	122(6)	72(4)	-26(4)	12(3)	-19(4)
C(32)	50(4)	127(7)	99(5)	-35(5)	0(4)	15(4)
C(33)	48(3)	80(4)	97(5)	-19(4)	0(3)	8(3)
C(34)	52(4)	208(9)	127(7)	-70(6)	13(4)	-43(5)
C(35)	46(3)	51(3)	45(3)	0(2)	2(2)	3(2)
C(36)	99(5)	62(4)	58(4)	16(3)	19(3)	26(3)
C(37)	99(5)	63(4)	62(4)	7(3)	29(3)	29(3)
C(38)	65(3)	56(4)	49(3)	1(3)	7(3)	-10(3)
C(39)	78(4)	50(3)	42(3)	4(2)	2(3)	-3(3)
C(40)	65(3)	40(3)	49(3)	-3(2)	1(3)	8(3)
C(41)	112(5)	86(5)	53(4)	-6(3)	27(4)	-4(4)
C(42)	41(3)	65(4)	57(3)	-7(3)	1(2)	-5(3)
C(43)	56(4)	82(5)	121(6)	-25(4)	6(4)	-9(3)
C(44)	84(5)	117(6)	124(7)	-58(5)	7(5)	-30(5)
C(45)	51(4)	156(8)	79(5)	-42(5)	11(3)	-16(5)
C(46)	47(4)	154(8)	93(5)	-24(5)	-3(3)	15(4)
C(47)	49(3)	88(4)	81(4)	-11(4)	1(3)	4(3)
C(48)	64(5)	290(13)	154(8)	-114(8)	8(5)	-56(6)
C(49)	55(3)	53(3)	53(3)	-7(3)	4(3)	-5(3)
C(50)	59(3)	37(3)	60(4)	10(2)	7(3)	0(2)
C(51)	65(4)	60(4)	79(4)	13(3)	18(3)	10(3)
C(52)	72(5)	78(5)	118(6)	19(5)	31(4)	18(4)
C(53)	69(5)	87(5)	139(8)	21(5)	-9(5)	12(4)
C(54)	101(6)	83(5)	93(6)	10(4)	-28(5)	6(4)
C(55)	71(4)	61(4)	71(4)	8(3)	1(3)	5(3)
C(56)	170(12)	560(30)	149(12)	77(15)	10(9)	-22(16)
Cl(1)	312(6)	481(9)	326(7)	-123(6)	151(5)	-179(6)
Cl(2)	429(8)	400(8)	293(7)	52(6)	36(6)	-191(7)

Table 5. Hydrogen coordinates ($\times 10^4$) and isotropic displacement parameters ($\text{\AA}^2 \times 10^3$) for P.

	x	y	z	U(eq)
H(2A)	18935	9102	1264	66
H(3A)	18098	8700	-85	70
H(7A)	14472	7953	-1164	64
H(8A)	12955	7826	-484	62
H(12A)	12060	7953	2738	63
H(13A)	12888	8350	4075	62
H(17A)	16502	9127	5154	65
H(18A)	18001	9297	4461	64
H(22A)	16691	7370	-825	73
H(23A)	17259	7235	-2123	79
H(25A)	16761	8954	-2683	89
H(26A)	16257	9106	-1356	78
H(27A)	17448	8361	-3713	146
H(27B)	17065	7697	-3739	146
H(27C)	18142	7844	-3316	146
H(29A)	12597	6941	737	78
H(30A)	11073	6545	225	95
H(32A)	9802	8093	684	111
H(33A)	11331	8503	1191	91
H(34A)	8774	7346	11	194
H(34B)	9112	6703	332	194
H(34C)	9290	6917	-594	194
H(36A)	13927	9601	4812	86
H(37A)	13445	9659	6169	88
H(39A)	14701	8087	6773	69
H(40A)	15183	8021	5427	62
H(41A)	13266	9273	7526	123
H(41B)	14160	8881	7932	123
H(41C)	13177	8571	7528	123
H(43A)	18408	10147	3209	104
H(44A)	19981	10538	3648	131
H(46A)	21143	8941	3299	119
H(47A)	19587	8550	2847	88
H(48A)	22240	9711	3768	255
H(48B)	21791	10176	4366	255
H(48C)	21890	10342	3403	255

H(51A)	13413	9552	2354	81
H(52A)	11827	9781	1708	105
H(53A)	11529	9879	252	120
H(54A)	12758	9761	-596	115
H(55A)	14365	9534	35	82
H(56A)	11241	5986	3417	353
H(56B)	11064	6451	4142	353

4-FC₆H₄CORh(ttp) 4

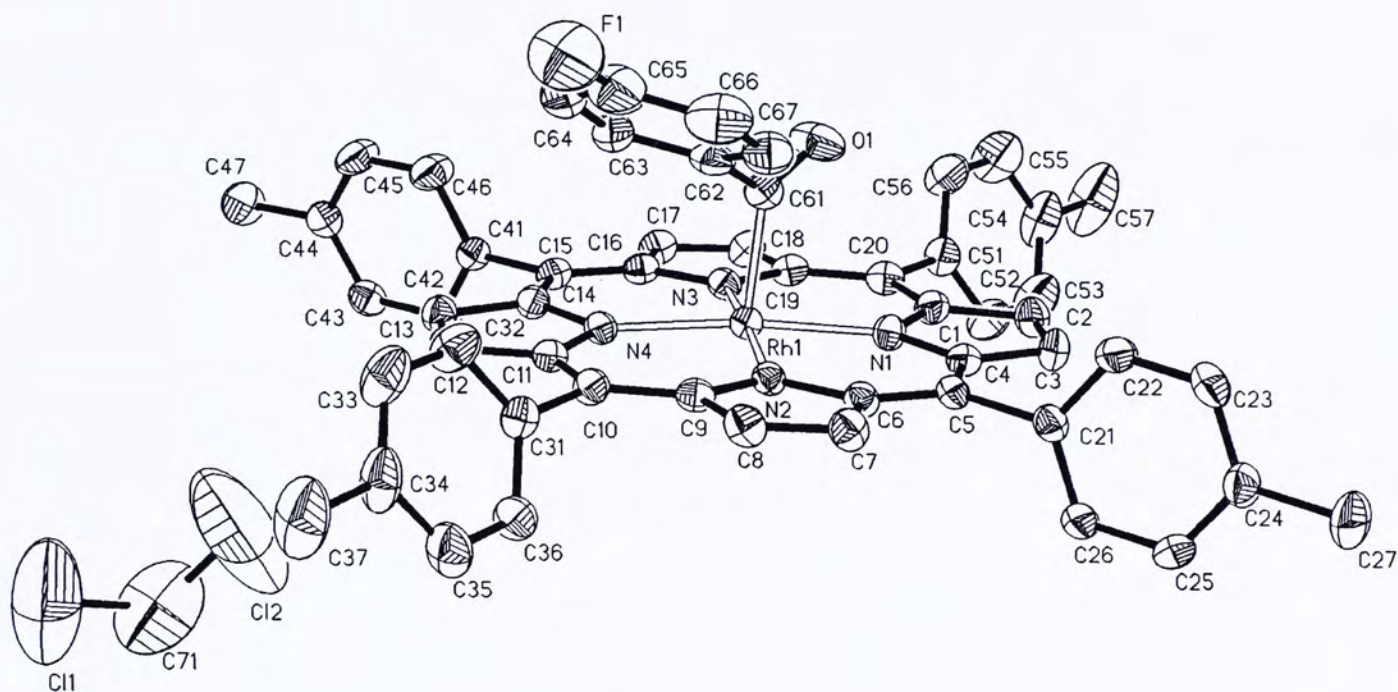


Figure 2. ORTEP of complex 4-FC₆H₄CORh(ttp) **4**, showing the atomic labelling scheme and 30% probability displacement ellipsoids.

Crystal Data

Empirical Formula	C ₅₆ H ₄₂ Cl ₂ FN ₄ ORh
Formula weight	979.75
Temperature	293(2) K
Wavelength	0.71073 Å
Crystal system	monoclinic
Space group	P2(1)
Unit cell dimensions	a = 13.705(17) Å b = 22.17(2) Å c = 15.746(18) Å $\alpha = 90^\circ$ $\beta = 96.93(3)^\circ$ $\gamma = 90^\circ$
Volume	4750(10) Å ⁻³
Z	4
Calculated density	1.370 Mg/m ⁻³
Absorption coefficient	0.520 mm ⁻¹
F(000)	2008
Crystal size	0.30 x 0.20 x 0.10 mm
θ range for data collection	1.50 to 25.00°
Limiting indices	-16 ≤ h ≤ 9, -21 ≤ k ≤ 25, -18 ≤ l ≤ 18

Reflections collected	12264
Unique	8057 [R(int) = 0.0848]
Absorption correction	SADABS
Completeness to θ	25.00 96.2 %
Max. Transmission	1.0000
Min. Transmission	0.461514
Refinement method	full-matrix least-squares on F^2
Data / restraints / parameters	8057 / 0 / 586
Goodness-of-fit on F^2	0.937
Final R indices [$I > 2\sigma(I)$]	R1 = 0.0648, wR2 = 0.1480
R indices (all data)	R1 = 0.1194, wR2 = 0.1480
Absolute structure parameter	-
Largest diff. peak	0.956 eA ⁻³
Largest diff. hole	-0.682 eA ⁻³

Table 1. Crystal data and structure refinement for P.

Identification code	al1492
Empirical formula	C56 H42 Cl2 F N4 O Rh
Formula weight	979.75
Temperature	293(2) K
Wavelength	0.71073 Å
Crystal system, space group	MONOCLINIC, P2(1)/c
Unit cell dimensions	a = 13.705(17) Å b = 22.17(2) Å c = 15.746(18) Å alpha = 90 deg. beta = 96.93(3) deg. gamma = 90 deg.
Volume	4750(10) Å ³
Z, Calculated density	4, 1.370 Mg/m ³
Absorption coefficient	0.520 mm ⁻¹
F(000)	2008
Crystal size	0.30 x 0.20 x 0.10 mm
Theta range for data collection	1.50 to 25.00 deg.
Limiting indices	-16<=h<=9, -21<=k<=25, -18<=l<=18
Reflections collected / unique	12264 / 8057 [R(int) = 0.0848]
Completeness to theta = 25.00	96.2 %
Absorption correction	SADABS

Max. and min. transmission	1.0000 and 0.461514
Refinement method	Full-matrix least-squares on F^2
Data / restraints / parameters	8057 / 0 / 586
Goodness-of-fit on F^2	0.937
Final R indices [$I > 2\sigma(I)$]	$R_1 = 0.0648$, $wR_2 = 0.1480$
R indices (all data)	$R_1 = 0.1194$, $wR_2 = 0.1701$
Largest diff. peak and hole	0.956 and -0.682 e. \AA^{-3}

Table 2. Atomic coordinates ($\times 10^4$) and equivalent isotropic displacement parameters ($\text{\AA}^2 \times 10^3$) for P.
 U(eq) is defined as one third of the trace of the orthogonalized Uij tensor.

	x	y	z	U(eq)
Rh(1)	5438(1)	6403(1)	1938(1)	37(1)
O(1)	5672(4)	5176(2)	1676(4)	79(2)
N(1)	6700(3)	6310(2)	1389(3)	40(1)
N(2)	4754(3)	6747(2)	815(3)	37(1)
N(3)	6170(3)	6145(2)	3095(3)	39(1)
N(4)	4221(3)	6592(2)	2520(3)	38(1)
F(1)	1211(4)	5135(3)	98(4)	140(2)
C(1)	7577(4)	6082(3)	1768(4)	45(2)
C(2)	8257(4)	6043(3)	1143(4)	50(2)
C(3)	7799(4)	6253(3)	396(4)	50(2)
C(4)	6815(4)	6422(3)	537(4)	42(1)
C(5)	6092(4)	6645(3)	-89(4)	40(1)
C(6)	5134(4)	6785(3)	36(4)	40(1)
C(7)	4381(5)	6982(3)	-622(4)	49(2)
C(8)	3554(4)	7061(3)	-250(4)	49(2)
C(9)	3778(4)	6926(3)	655(4)	39(1)
C(10)	3126(4)	6980(3)	1268(4)	42(1)
C(11)	3344(4)	6827(3)	2136(4)	43(2)
C(12)	2684(4)	6881(3)	2776(4)	47(2)
C(13)	3149(4)	6671(3)	3526(4)	47(2)
C(14)	4108(4)	6489(3)	3386(4)	41(1)
C(15)	4835(4)	6264(3)	4011(4)	42(2)
C(16)	5797(4)	6123(3)	3880(4)	42(1)
C(17)	6560(4)	5932(3)	4538(4)	49(2)
C(18)	7379(4)	5837(3)	4161(4)	47(2)
C(19)	7139(4)	5961(3)	3258(4)	41(2)
C(20)	7799(4)	5915(3)	2645(4)	45(2)
C(21)	6393(4)	6742(3)	-986(4)	41(2)
C(22)	6404(5)	6278(3)	-1559(4)	54(2)
C(23)	6720(5)	6373(3)	-2355(5)	64(2)
C(24)	7046(5)	6927(3)	-2598(4)	56(2)
C(25)	7023(5)	7386(3)	-2023(4)	58(2)
C(26)	6701(5)	7301(3)	-1226(4)	54(2)
C(27)	7433(6)	7026(4)	-3458(4)	83(3)

C(31)	2116(4)	7231(3)	955(4)	46(2)
C(32)	1283(5)	6890(4)	944(5)	67(2)
C(33)	361(5)	7118(4)	632(5)	81(3)
C(34)	256(5)	7698(5)	328(5)	77(3)
C(35)	1102(5)	8044(4)	353(5)	75(2)
C(36)	2016(5)	7820(3)	674(4)	59(2)
C(37)	-745(6)	7958(5)	-38(6)	123(4)
C(41)	4570(4)	6205(3)	4922(4)	42(2)
C(42)	4800(4)	6652(3)	5517(4)	48(2)
C(43)	4503(5)	6607(3)	6345(4)	52(2)
C(44)	3985(5)	6113(3)	6582(4)	50(2)
C(45)	3793(6)	5669(3)	5985(5)	68(2)
C(46)	4077(6)	5705(3)	5161(4)	68(2)
C(47)	3609(6)	6085(4)	7440(4)	73(2)
C(51)	8809(4)	5676(3)	2940(4)	51(2)
C(52)	9632(5)	6045(4)	2961(5)	66(2)
C(53)	10555(5)	5819(5)	3238(5)	84(3)
C(54)	10701(5)	5238(5)	3497(5)	85(3)
C(55)	9892(6)	4870(5)	3476(6)	104(3)
C(56)	8938(5)	5095(4)	3195(6)	80(2)
C(57)	11736(6)	4993(6)	3802(7)	151(6)
C(61)	5062(5)	5566(3)	1614(4)	47(2)
C(62)	4022(5)	5461(3)	1223(5)	53(2)
C(63)	3270(5)	5398(3)	1727(5)	61(2)
C(64)	2321(6)	5273(4)	1355(7)	83(3)
C(65)	2145(6)	5229(4)	487(8)	89(3)
C(66)	2857(7)	5302(4)	-36(6)	87(3)
C(67)	3806(5)	5411(3)	323(5)	65(2)
C(71)	625(13)	8752(9)	3518(10)	216(8)
C1(1)	-626(5)	8782(4)	3404(4)	321(4)
C1(2)	785(8)	8190(5)	2783(6)	431(7)

Table 3. Bond lengths [Å] and angles [deg] for P.

Rh(1)-C(61)	1.976(7)	C(21)-C(22)	1.370(8)
Rh(1)-N(1)	2.035(5)	C(21)-C(26)	1.376(9)
Rh(1)-N(4)	2.042(5)	C(22)-C(23)	1.390(9)
Rh(1)-N(2)	2.047(5)	C(23)-C(24)	1.377(10)
Rh(1)-N(3)	2.052(5)	C(24)-C(25)	1.366(9)
O(1)-C(61)	1.199(7)	C(24)-C(27)	1.528(8)
N(1)-C(1)	1.373(7)	C(25)-C(26)	1.391(8)
N(1)-C(4)	1.393(7)	C(31)-C(32)	1.369(9)
N(2)-C(9)	1.389(7)	C(31)-C(36)	1.379(9)
N(2)-C(6)	1.391(7)	C(32)-C(33)	1.394(10)
N(3)-C(19)	1.383(7)	C(33)-C(34)	1.375(11)
N(3)-C(16)	1.395(7)	C(34)-C(35)	1.386(11)
N(4)-C(11)	1.380(7)	C(34)-C(37)	1.535(10)
N(4)-C(14)	1.410(7)	C(35)-C(36)	1.386(9)
F(1)-C(65)	1.367(9)	C(41)-C(42)	1.373(8)
C(1)-C(20)	1.426(8)	C(41)-C(46)	1.375(9)
C(1)-C(2)	1.438(8)	C(42)-C(43)	1.417(8)
C(2)-C(3)	1.346(8)	C(43)-C(44)	1.381(9)
C(3)-C(4)	1.443(8)	C(44)-C(45)	1.366(9)
C(4)-C(5)	1.401(8)	C(44)-C(47)	1.504(9)
C(5)-C(6)	1.386(8)	C(45)-C(46)	1.401(9)
C(5)-C(21)	1.534(8)	C(51)-C(56)	1.356(10)
C(6)-C(7)	1.441(8)	C(51)-C(52)	1.391(9)
C(7)-C(8)	1.349(8)	C(52)-C(53)	1.381(10)
C(8)-C(9)	1.452(8)	C(53)-C(54)	1.360(12)
C(9)-C(10)	1.398(8)	C(54)-C(55)	1.373(12)
C(10)-C(11)	1.405(8)	C(54)-C(57)	1.541(10)
C(10)-C(31)	1.518(8)	C(55)-C(56)	1.419(11)
C(11)-C(12)	1.438(8)	C(61)-C(62)	1.501(9)
C(12)-C(13)	1.355(8)	C(62)-C(63)	1.381(9)
C(13)-C(14)	1.417(8)	C(62)-C(67)	1.417(10)
C(14)-C(15)	1.405(8)	C(63)-C(64)	1.388(11)
C(15)-C(16)	1.395(8)	C(64)-C(65)	1.364(12)
C(15)-C(41)	1.527(8)	C(65)-C(66)	1.360(12)
C(16)-C(17)	1.443(8)	C(66)-C(67)	1.375(10)
C(17)-C(18)	1.349(8)	C(71)-Cl(1)	1.704(17)
C(18)-C(19)	1.445(8)	C(71)-Cl(2)	1.732(18)
C(19)-C(20)	1.404(8)	C(61)-Rh(1)-N(1)	90.2(2)
C(20)-C(51)	1.502(8)	C(61)-Rh(1)-N(4)	96.2(2)

N(1)-Rh(1)-N(4)	173.58(19)	C(11)-C(10)-C(31)	118.9(5)
C(61)-Rh(1)-N(2)	92.8(2)	N(4)-C(11)-C(10)	126.1(5)
N(1)-Rh(1)-N(2)	89.71(19)	N(4)-C(11)-C(12)	108.2(5)
N(4)-Rh(1)-N(2)	89.86(19)	C(10)-C(11)-C(12)	125.7(5)
C(61)-Rh(1)-N(3)	93.0(2)	C(13)-C(12)-C(11)	108.2(5)
N(1)-Rh(1)-N(3)	89.9(2)	C(12)-C(13)-C(14)	108.1(5)
N(4)-Rh(1)-N(3)	89.8(2)	C(15)-C(14)-N(4)	125.7(5)
N(2)-Rh(1)-N(3)	174.21(18)	C(15)-C(14)-C(13)	125.8(5)
C(1)-N(1)-C(4)	106.9(5)	N(4)-C(14)-C(13)	108.4(5)
C(1)-N(1)-Rh(1)	126.7(4)	C(16)-C(15)-C(14)	125.4(5)
C(4)-N(1)-Rh(1)	126.3(4)	C(16)-C(15)-C(41)	117.1(5)
C(9)-N(2)-C(6)	106.1(5)	C(14)-C(15)-C(41)	117.4(5)
C(9)-N(2)-Rh(1)	126.4(4)	N(3)-C(16)-C(15)	125.3(5)
C(6)-N(2)-Rh(1)	127.1(4)	N(3)-C(16)-C(17)	109.6(5)
C(19)-N(3)-C(16)	105.7(5)	C(15)-C(16)-C(17)	125.1(6)
C(19)-N(3)-Rh(1)	127.1(4)	C(18)-C(17)-C(16)	107.4(5)
C(16)-N(3)-Rh(1)	127.2(4)	C(17)-C(18)-C(19)	107.5(5)
C(11)-N(4)-C(14)	107.1(4)	N(3)-C(19)-C(20)	125.2(5)
C(11)-N(4)-Rh(1)	126.6(4)	N(3)-C(19)-C(18)	109.8(5)
C(14)-N(4)-Rh(1)	126.3(4)	C(20)-C(19)-C(18)	125.0(5)
N(1)-C(1)-C(20)	126.2(5)	C(19)-C(20)-C(1)	124.5(5)
N(1)-C(1)-C(2)	109.3(5)	C(19)-C(20)-C(51)	117.3(5)
C(20)-C(1)-C(2)	124.6(5)	C(1)-C(20)-C(51)	118.1(5)
C(3)-C(2)-C(1)	107.8(5)	C(22)-C(21)-C(26)	117.9(6)
C(2)-C(3)-C(4)	107.5(5)	C(22)-C(21)-C(5)	121.8(6)
N(1)-C(4)-C(5)	126.0(5)	C(26)-C(21)-C(5)	120.3(5)
N(1)-C(4)-C(3)	108.5(5)	C(21)-C(22)-C(23)	120.6(6)
C(5)-C(4)-C(3)	125.4(5)	C(24)-C(23)-C(22)	122.2(7)
C(6)-C(5)-C(4)	125.5(5)	C(25)-C(24)-C(23)	116.4(6)
C(6)-C(5)-C(21)	117.7(5)	C(25)-C(24)-C(27)	121.3(7)
C(4)-C(5)-C(21)	116.8(5)	C(23)-C(24)-C(27)	122.3(7)
C(5)-C(6)-N(2)	125.0(5)	C(24)-C(25)-C(26)	122.2(6)
C(5)-C(6)-C(7)	125.1(5)	C(21)-C(26)-C(25)	120.6(6)
N(2)-C(6)-C(7)	109.9(5)	C(32)-C(31)-C(36)	118.0(6)
C(8)-C(7)-C(6)	107.1(5)	C(32)-C(31)-C(10)	121.8(6)
C(7)-C(8)-C(9)	108.1(5)	C(36)-C(31)-C(10)	120.2(6)
N(2)-C(9)-C(10)	125.6(5)	C(31)-C(32)-C(33)	121.5(7)
N(2)-C(9)-C(8)	108.8(5)	C(34)-C(33)-C(32)	121.0(7)
C(10)-C(9)-C(8)	125.6(5)	C(33)-C(34)-C(35)	117.1(7)
C(9)-C(10)-C(11)	124.9(5)	C(33)-C(34)-C(37)	122.3(8)
C(9)-C(10)-C(31)	116.2(5)	C(35)-C(34)-C(37)	120.6(9)

C(36)-C(35)-C(34)	121.9(8)	C(53)-C(54)-C(57)	121.6(9)
C(31)-C(36)-C(35)	120.4(7)	C(55)-C(54)-C(57)	120.6(10)
C(42)-C(41)-C(46)	118.4(6)	C(54)-C(55)-C(56)	120.7(9)
C(42)-C(41)-C(15)	121.1(5)	C(51)-C(56)-C(55)	120.6(8)
C(46)-C(41)-C(15)	120.4(6)	O(1)-C(61)-C(62)	122.7(6)
C(41)-C(42)-C(43)	120.6(6)	O(1)-C(61)-Rh(1)	119.9(5)
C(44)-C(43)-C(42)	121.3(6)	C(62)-C(61)-Rh(1)	117.1(5)
C(45)-C(44)-C(43)	116.7(6)	C(63)-C(62)-C(67)	119.1(7)
C(45)-C(44)-C(47)	122.0(7)	C(63)-C(62)-C(61)	121.2(6)
C(43)-C(44)-C(47)	121.3(7)	C(67)-C(62)-C(61)	119.7(6)
C(44)-C(45)-C(46)	123.0(6)	C(62)-C(63)-C(64)	120.3(8)
C(41)-C(46)-C(45)	120.0(7)	C(65)-C(64)-C(63)	118.7(8)
C(56)-C(51)-C(52)	118.4(6)	C(66)-C(65)-C(64)	123.1(8)
C(56)-C(51)-C(20)	120.6(6)	C(66)-C(65)-F(1)	116.7(10)
C(52)-C(51)-C(20)	121.0(6)	C(64)-C(65)-F(1)	120.2(9)
C(53)-C(52)-C(51)	120.3(8)	C(65)-C(66)-C(67)	119.0(9)
C(54)-C(53)-C(52)	122.3(8)	C(66)-C(67)-C(62)	119.8(8)
C(53)-C(54)-C(55)	117.8(7)	Cl(1)-C(71)-Cl(2)	99.4(9)

Symmetry transformations used to generate equivalent atoms:

Table 4. Anisotropic displacement parameters ($\text{\AA}^2 \times 10^3$) for P.
The anisotropic displacement factor exponent takes the form:
 $-2 \pi^2 [h^2 a^{*2} U_{11} + \dots + 2 h k a^* b^* U_{12}]$

	U11	U22	U33	U23	U13	U12
Rh(1)	36(1)	38(1)	35(1)	1(1)	3(1)	0(1)
O(1)	74(3)	48(3)	110(5)	-8(3)	-6(3)	10(3)
N(1)	38(3)	47(3)	33(3)	0(2)	5(2)	-1(2)
N(2)	40(3)	37(3)	35(3)	-2(2)	5(2)	1(2)
N(3)	38(3)	39(3)	41(3)	-1(2)	2(2)	3(2)
N(4)	43(3)	38(3)	33(3)	-4(2)	7(2)	-1(2)
F(1)	64(3)	143(5)	203(7)	-35(5)	-30(4)	-19(3)
C(1)	41(3)	43(4)	50(4)	3(3)	8(3)	1(3)
C(2)	44(4)	60(5)	48(4)	1(4)	6(3)	8(3)
C(3)	39(3)	65(5)	47(4)	1(3)	16(3)	2(3)
C(4)	44(3)	37(3)	46(4)	3(3)	8(3)	2(3)
C(5)	46(3)	36(3)	38(3)	-5(3)	9(3)	1(3)
C(6)	44(3)	41(4)	35(3)	-3(3)	6(3)	2(3)
C(7)	57(4)	55(4)	35(3)	1(3)	5(3)	7(3)
C(8)	47(4)	53(4)	44(4)	4(3)	-4(3)	11(3)
C(9)	42(3)	35(3)	39(3)	5(3)	0(3)	3(3)
C(10)	38(3)	43(4)	44(4)	4(3)	4(3)	1(3)
C(11)	42(3)	35(4)	51(4)	0(3)	8(3)	0(3)
C(12)	38(3)	54(4)	49(4)	-2(3)	7(3)	5(3)
C(13)	50(4)	50(4)	43(4)	-1(3)	11(3)	-2(3)
C(14)	40(3)	42(4)	41(3)	-1(3)	7(3)	-2(3)
C(15)	48(3)	40(4)	39(3)	1(3)	4(3)	-6(3)
C(16)	47(3)	39(4)	40(4)	1(3)	1(3)	-5(3)
C(17)	54(4)	52(4)	39(4)	5(3)	-3(3)	-3(3)
C(18)	39(3)	57(4)	44(4)	11(3)	-4(3)	-2(3)
C(19)	38(3)	41(4)	42(4)	4(3)	-7(3)	-3(3)
C(20)	43(3)	46(4)	43(4)	-2(3)	-3(3)	-2(3)
C(21)	43(3)	43(4)	38(3)	1(3)	6(3)	9(3)
C(22)	77(5)	40(4)	49(4)	0(3)	18(3)	-5(3)
C(23)	81(5)	56(5)	57(4)	-16(4)	22(4)	7(4)
C(24)	64(4)	61(5)	44(4)	3(4)	17(3)	6(4)
C(25)	78(5)	40(4)	61(5)	14(4)	22(4)	1(3)
C(26)	79(5)	40(4)	48(4)	-4(3)	25(4)	1(3)
C(27)	110(7)	100(7)	47(5)	-2(5)	35(4)	-5(5)
C(31)	43(3)	57(4)	37(3)	4(3)	3(3)	1(3)

C(32)	48(4)	76(5)	76(5)	21(4)	-3(4)	-7(4)
C(33)	43(4)	114(8)	87(6)	24(6)	5(4)	-7(4)
C(34)	42(4)	126(8)	64(5)	30(5)	10(4)	26(4)
C(35)	61(5)	87(6)	77(5)	23(5)	12(4)	31(4)
C(36)	47(4)	59(5)	71(5)	12(4)	5(3)	13(3)
C(37)	56(5)	188(11)	125(8)	63(8)	12(5)	45(6)
C(41)	42(3)	44(4)	40(4)	3(3)	4(3)	0(3)
C(42)	52(4)	45(4)	44(4)	0(3)	-3(3)	-3(3)
C(43)	62(4)	51(4)	41(4)	-11(3)	2(3)	0(3)
C(44)	57(4)	53(4)	40(4)	6(4)	5(3)	8(3)
C(45)	93(6)	62(5)	54(5)	-3(4)	23(4)	-30(4)
C(46)	97(6)	60(5)	51(4)	-16(4)	23(4)	-29(4)
C(47)	96(6)	80(6)	45(4)	9(4)	17(4)	3(5)
C(51)	43(3)	62(5)	46(4)	7(4)	1(3)	7(3)
C(52)	47(4)	79(5)	68(5)	6(4)	-3(3)	-16(4)
C(53)	48(5)	121(8)	79(6)	17(6)	-8(4)	-15(5)
C(54)	42(4)	145(9)	67(5)	37(6)	-2(4)	15(5)
C(55)	73(6)	113(8)	123(8)	58(7)	5(6)	29(6)
C(56)	56(5)	75(6)	112(7)	35(5)	18(5)	9(4)
C(57)	51(5)	255(15)	147(10)	105(10)	11(6)	50(7)
C(61)	54(4)	47(4)	38(4)	8(3)	3(3)	5(3)
C(62)	60(4)	34(4)	64(5)	-10(3)	3(4)	-7(3)
C(63)	61(4)	53(5)	71(5)	-12(4)	19(4)	-12(4)
C(64)	69(5)	64(5)	119(8)	-22(6)	29(5)	-14(4)
C(65)	57(5)	76(6)	130(9)	-24(6)	-8(6)	-11(4)
C(66)	86(6)	80(6)	86(6)	-10(5)	-29(5)	-16(5)
C(67)	70(5)	60(5)	64(5)	-4(4)	-1(4)	-7(4)
C(71)	193(17)	300(30)	142(13)	-15(14)	-25(12)	-81(17)
C1(1)	214(6)	509(13)	258(7)	65(7)	105(5)	89(7)
C1(2)	524(15)	432(13)	366(11)	25(9)	169(11)	306(12)

Table 5. Hydrogen coordinates ($\times 10^4$) and isotropic displacement parameters ($\text{\AA}^2 \times 10^3$) for P.

	x	y	z	U(eq)
H(2A)	8898	5899	1237	60
H(3A)	8069	6283	-117	59
H(7A)	4451	7044	-1196	59
H(8A)	2946	7181	-525	58
H(12A)	2048	7034	2690	56
H(13A)	2885	6651	4042	56
H(17A)	6498	5884	5115	59
H(18A)	7987	5714	4431	57
H(22A)	6198	5896	-1414	65
H(23A)	6711	6051	-2735	77
H(25A)	7229	7768	-2168	70
H(26A)	6693	7626	-852	65
H(27A)	7637	7438	-3500	125
H(27B)	6923	6937	-3914	125
H(27C)	7983	6764	-3500	125
H(32A)	1333	6496	1149	81
H(33A)	-191	6874	630	98
H(35A)	1054	8437	148	90
H(36A)	2566	8068	700	71
H(37A)	-1246	7660	-5	185
H(37B)	-727	8070	-625	185
H(37C)	-888	8307	286	185
H(42A)	5154	6987	5374	57
H(43A)	4661	6916	6738	62
H(45A)	3458	5327	6131	82
H(46A)	3932	5390	4775	82
H(47A)	3270	5710	7491	109
H(47B)	3164	6414	7491	109
H(47C)	4151	6112	7885	109
H(52A)	9561	6445	2789	79
H(53A)	11095	6074	3247	101
H(55)	9970	4470	3648	124
H(56A)	8397	4841	3187	96
H(57A)	12211	5308	3770	227
H(57B)	11882	4663	3443	227
H(57C)	11761	4856	4382	227

H(63A)	3400	5440	2318	73
H(64A)	1815	5221	1692	99
H(66A)	2705	5278	-627	104
H(67A)	4305	5452	-25	78
H(71A)	894	8638	4094	260
H(71B)	912	9132	3367	260

4-CF₃C₆H₄CORh(ttp) **5**

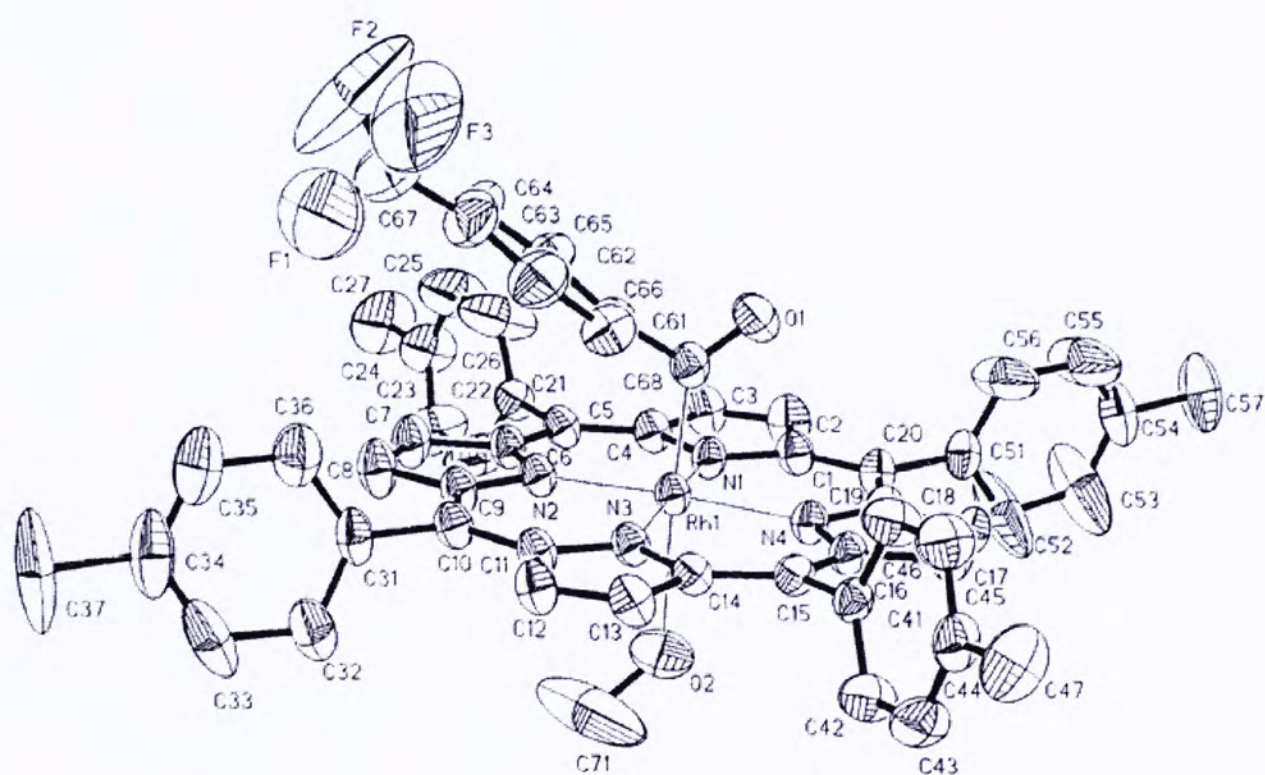


Figure 2. ORTEP of complex 4-CF₃C₆H₄CORh(ttp) **5**, showing the atomic labelling scheme and 30% probability displacement ellipsoids.

Crystal Data

Empirical Formula	C ₅₇ H ₄₄ F ₃ N ₄ ORh
Formula weight	976.87
Temperature	293(2) K
Wavelength	0.71073 Å
Crystal system	monoclinic
Space group	C2/c
Unit cell dimensions	a = 34.69 (18) Å b = 13.33 (7) Å c = 22.78 (11) Å $\alpha = 90^\circ$ $\beta = 116.96 (10)^\circ$ $\gamma = 90^\circ$
Volume	9384 (8) Å ⁻³
Z	8
Calculated density	1.383 Mg/m ⁻³
Absorption coefficient	0.424 mm ⁻¹
F(000)	4016
Crystal size	0.40 x 0.30 x 0.20 mm
θ range for data collection	1.32 to 28.70 °
Limiting indices	-45 ≤ h ≤ 46, -17 ≤ k ≤ 17, -28 ≤ l ≤ 30

Reflections collected	32798
Unique	12061 [R(int) = 0.0956]
Absorption correction	SADABS
Completeness to θ	28.70 99.4 %
Max. Transmission	1.0000
Min. Transmission	0.756103
Refinement method	full-matrix least-squares on F^2
Data / restraints / parameters	12061 / 0 / 604
Goodness-of-fit on F^2	0.912
Final R indices [$I > 2\sigma(I)$]	R1 = 0.0655, wR2 = 0.1559
R indices (all data)	R1 = 0.1977, wR2 = 0.2214
Absolute structure parameter	-
Largest diff. peak	0.568 eA ⁻³
Largest diff. hole	-0.612 eA ⁻³

Table 1. Crystal data and structure refinement for p.

Identification code	a12131
Empirical formula	C57 H44 F3 N4 O2 Rh
Formula weight	976.87
Temperature	293(2) K
Wavelength	0.71073 Å
Crystal system, space group	MONOCLINIC, C2/c
Unit cell dimensions	a = 34.6870(18) Å b = 13.3266(7) Å c = 22.7762(11) Å alpha = 90 deg. beta = 116.9640(10) deg. gamma = 90 deg.
Volume	9384.0(8) Å ³
Z, Calculated density	8, 1.383 Mg/m ³
Absorption coefficient	0.424 mm ⁻¹
F(000)	4016
Crystal size	0.40 x 0.30 x 0.20 mm
Theta range for data collection	1.32 to 28.70 deg.
Limiting indices	-45<=h<=46, -17<=k<=17, -28<=l<=30
Reflections collected / unique	32798 / 12061 [R(int) = 0.0956]
Completeness to theta = 28.70	99.4 %
Absorption correction	SADABS

Max. and min. transmission	1.0000 and 0.756103
Refinement method	Full-matrix least-squares on F^2
Data / restraints / parameters	12061 / 0 / 604
Goodness-of-fit on F^2	0.912
Final R indices [$I > 2\sigma(I)$]	$R_1 = 0.0655$, $wR_2 = 0.1559$
R indices (all data)	$R_1 = 0.1977$, $wR_2 = 0.2214$
Largest diff. peak and hole	0.568 and -0.612 e. \AA^{-3}

Table 2. Atomic coordinates ($\times 10^4$) and equivalent isotropic displacement parameters ($\text{\AA}^2 \times 10^3$) for p.
 $U(\text{eq})$ is defined as one third of the trace of the orthogonalized U_{ij} tensor.

	x	y	z	U(eq)
Rh(1)	3473(1)	4605(1)	7455(1)	51(1)
O(1)	3476(2)	4900(4)	6240(3)	89(2)
O(2)	3347(2)	5084(5)	8398(3)	111(2)
N(1)	3740(2)	5990(4)	7519(2)	58(1)
N(2)	4065(2)	4081(4)	8099(2)	55(1)
N(3)	3210(2)	3250(4)	7467(2)	54(1)
N(4)	2876(2)	5163(4)	6863(2)	56(1)
C(1)	3517(2)	6833(5)	7183(3)	62(2)
C(2)	3828(2)	7637(5)	7330(4)	82(2)
C(3)	4215(2)	7294(5)	7756(3)	76(2)
C(4)	4170(2)	6243(5)	7874(3)	59(2)
C(5)	4497(2)	5623(5)	8278(3)	59(2)
C(6)	4448(2)	4607(5)	8380(3)	61(2)
C(7)	4787(2)	3960(6)	8793(3)	79(2)
C(8)	4620(2)	3045(6)	8784(3)	82(2)
C(9)	4162(2)	3122(5)	8341(3)	62(2)
C(10)	3869(2)	2321(5)	8211(3)	61(2)
C(11)	3421(2)	2405(5)	7799(3)	60(2)
C(12)	3118(2)	1590(5)	7637(3)	69(2)
C(13)	2733(2)	1941(5)	7212(3)	67(2)
C(14)	2779(2)	2972(5)	7099(3)	53(2)
C(15)	2449(2)	3595(5)	6670(3)	53(2)
C(16)	2492(2)	4610(5)	6576(3)	55(2)
C(17)	2151(2)	5275(5)	6159(3)	65(2)
C(18)	2323(2)	6181(5)	6188(3)	65(2)
C(19)	2779(2)	6116(5)	6621(3)	58(2)
C(20)	3073(2)	6896(5)	6745(3)	64(2)
C(21)	4949(2)	6036(5)	8645(3)	64(2)
C(22)	5119(3)	6281(8)	9274(5)	127(4)
C(23)	5550(3)	6625(9)	9628(5)	141(4)
C(24)	5799(3)	6750(8)	9319(5)	108(3)
C(25)	5650(3)	6381(11)	8725(5)	157(5)
C(26)	5227(3)	6039(12)	8388(5)	180(6)
C(27)	6264(3)	7131(10)	9685(6)	163(5)

C(31)	4047(2)	1342(5)	8526(4)	71(2)
C(32)	3981(3)	1018(7)	9051(4)	100(3)
C(33)	4190(4)	118(9)	9379(5)	132(4)
C(34)	4454(3)	-412(8)	9183(7)	128(5)
C(35)	4498(3)	-83(8)	8670(6)	126(4)
C(36)	4301(3)	761(7)	8329(5)	106(3)
C(37)	4690(4)	-1348(7)	9603(6)	218(8)
C(41)	2016(2)	3117(5)	6258(3)	55(2)
C(42)	1730(2)	2910(6)	6491(3)	81(2)
C(43)	1344(2)	2393(6)	6111(4)	88(2)
C(44)	1253(2)	2063(6)	5497(4)	73(2)
C(45)	1528(2)	2304(6)	5252(4)	88(2)
C(46)	1913(2)	2817(6)	5628(3)	83(2)
C(47)	847(2)	1457(7)	5074(4)	115(3)
C(51)	2912(2)	7873(5)	6392(4)	70(2)
C(52)	2755(6)	8602(8)	6612(5)	221(9)
C(53)	2618(6)	9511(8)	6238(6)	240(10)
C(54)	2613(3)	9653(7)	5670(5)	101(3)
C(55)	2730(5)	8917(10)	5461(7)	209(8)
C(56)	2885(5)	8013(8)	5806(6)	183(7)
C(57)	2442(4)	10624(6)	5268(5)	148(5)
C(61)	3746(2)	3306(5)	6648(3)	66(2)
C(62)	4181(3)	3222(7)	6794(4)	96(3)
C(63)	4342(3)	2295(10)	6721(5)	118(3)
C(64)	4085(4)	1466(8)	6513(5)	106(3)
C(65)	3658(3)	1545(7)	6368(4)	103(3)
C(66)	3492(3)	2443(6)	6442(4)	81(2)
C(67)	4259(7)	485(15)	6475(11)	176(7)
C(68)	3558(2)	4314(5)	6687(3)	63(2)
C(71)	3426(8)	4469(11)	8907(8)	306(14)
F(1)	4314(8)	-117(9)	6850(9)	343(12)
F(2)	4606(5)	552(9)	6417(16)	381(13)
F(3)	4072(6)	83(11)	5950(8)	343(11)

Table 3. Bond lengths [Å] and angles [deg] for p.

Rh(1)-C(68)	1.941(7)	C(20)-C(51)	1.499(9)
Rh(1)-N(3)	2.030(5)	C(21)-C(22)	1.319(9)
Rh(1)-N(2)	2.032(5)	C(21)-C(26)	1.337(11)
Rh(1)-N(4)	2.033(5)	C(22)-C(23)	1.414(11)
Rh(1)-N(1)	2.040(5)	C(23)-C(24)	1.353(12)
O(1)-C(68)	1.209(7)	C(24)-C(25)	1.304(12)
O(2)-C(71)	1.342(13)	C(24)-C(27)	1.527(11)
N(1)-C(4)	1.377(7)	C(25)-C(26)	1.389(12)
N(1)-C(1)	1.383(8)	C(31)-C(32)	1.385(10)
N(2)-C(9)	1.372(8)	C(31)-C(36)	1.390(11)
N(2)-C(6)	1.375(7)	C(32)-C(33)	1.425(13)
N(3)-C(11)	1.369(7)	C(33)-C(34)	1.382(17)
N(3)-C(14)	1.392(7)	C(34)-C(35)	1.321(16)
N(4)-C(19)	1.365(8)	C(34)-C(37)	1.559(13)
N(4)-C(16)	1.397(7)	C(35)-C(36)	1.363(12)
C(1)-C(20)	1.408(8)	C(41)-C(42)	1.347(8)
C(1)-C(2)	1.449(9)	C(41)-C(46)	1.371(8)
C(2)-C(3)	1.330(9)	C(42)-C(43)	1.402(9)
C(3)-C(4)	1.448(9)	C(43)-C(44)	1.358(9)
C(4)-C(5)	1.368(8)	C(44)-C(45)	1.345(9)
C(5)-C(6)	1.397(9)	C(44)-C(47)	1.527(9)
C(5)-C(21)	1.507(8)	C(45)-C(46)	1.394(9)
C(6)-C(7)	1.416(9)	C(51)-C(56)	1.309(11)
C(7)-C(8)	1.346(9)	C(51)-C(52)	1.319(12)
C(8)-C(9)	1.448(8)	C(52)-C(53)	1.432(13)
C(9)-C(10)	1.408(8)	C(53)-C(54)	1.299(15)
C(10)-C(11)	1.409(8)	C(54)-C(55)	1.236(13)
C(10)-C(31)	1.482(9)	C(54)-C(57)	1.541(11)
C(11)-C(12)	1.440(8)	C(55)-C(56)	1.405(13)
C(12)-C(13)	1.328(8)	C(61)-C(66)	1.394(9)
C(13)-C(14)	1.421(8)	C(61)-C(62)	1.397(10)
C(14)-C(15)	1.392(8)	C(61)-C(68)	1.512(9)
C(15)-C(16)	1.386(8)	C(62)-C(63)	1.396(12)
C(15)-C(41)	1.506(8)	C(63)-C(64)	1.364(13)
C(16)-C(17)	1.439(8)	C(64)-C(65)	1.367(12)
C(17)-C(18)	1.335(8)	C(64)-C(67)	1.458(17)
C(18)-C(19)	1.437(8)	C(65)-C(66)	1.371(10)
C(19)-C(20)	1.391(8)	C(67)-F(1)	1.124(18)

C(67)-F(3)	1.20(2)	N(2)-C(9)-C(10)	126.9(5)
C(67)-F(2)	1.27(2)	N(2)-C(9)-C(8)	109.6(6)
F(2)-F(3)	1.778(19)	C(10)-C(9)-C(8)	123.5(6)
C(68)-Rh(1)-N(3)	95.1(2)	C(9)-C(10)-C(11)	123.5(6)
C(68)-Rh(1)-N(2)	93.7(2)	C(9)-C(10)-C(31)	117.6(5)
N(3)-Rh(1)-N(2)	89.89(19)	C(11)-C(10)-C(31)	118.9(6)
C(68)-Rh(1)-N(4)	90.0(2)	N(3)-C(11)-C(10)	125.9(6)
N(3)-Rh(1)-N(4)	90.26(19)	N(3)-C(11)-C(12)	109.3(5)
N(2)-Rh(1)-N(4)	176.2(2)	C(10)-C(11)-C(12)	124.7(6)
C(68)-Rh(1)-N(1)	89.8(2)	C(13)-C(12)-C(11)	107.4(6)
N(3)-Rh(1)-N(1)	175.12(19)	C(12)-C(13)-C(14)	108.3(6)
N(2)-Rh(1)-N(1)	88.96(19)	C(15)-C(14)-N(3)	125.4(5)
N(4)-Rh(1)-N(1)	90.57(19)	C(15)-C(14)-C(13)	125.5(5)
C(4)-N(1)-C(1)	108.1(5)	N(3)-C(14)-C(13)	109.0(5)
C(4)-N(1)-Rh(1)	126.8(4)	C(16)-C(15)-C(14)	125.4(5)
C(1)-N(1)-Rh(1)	125.0(4)	C(16)-C(15)-C(41)	117.6(5)
C(9)-N(2)-C(6)	106.2(5)	C(14)-C(15)-C(41)	117.0(5)
C(9)-N(2)-Rh(1)	126.4(4)	C(15)-C(16)-N(4)	126.0(5)
C(6)-N(2)-Rh(1)	127.4(4)	C(15)-C(16)-C(17)	126.1(6)
C(11)-N(3)-C(14)	106.0(5)	N(4)-C(16)-C(17)	107.9(6)
C(11)-N(3)-Rh(1)	127.4(4)	C(18)-C(17)-C(16)	108.0(6)
C(14)-N(3)-Rh(1)	126.5(4)	C(17)-C(18)-C(19)	107.9(6)
C(19)-N(4)-C(16)	107.2(5)	N(4)-C(19)-C(20)	126.1(6)
C(19)-N(4)-Rh(1)	126.8(4)	N(4)-C(19)-C(18)	109.0(6)
C(16)-N(4)-Rh(1)	125.8(4)	C(20)-C(19)-C(18)	124.8(6)
N(1)-C(1)-C(20)	126.8(6)	C(19)-C(20)-C(1)	124.4(6)
N(1)-C(1)-C(2)	107.5(6)	C(19)-C(20)-C(51)	118.7(6)
C(20)-C(1)-C(2)	125.6(6)	C(1)-C(20)-C(51)	116.9(6)
C(3)-C(2)-C(1)	108.3(6)	C(22)-C(21)-C(26)	114.8(7)
C(2)-C(3)-C(4)	108.0(6)	C(22)-C(21)-C(5)	122.2(6)
C(5)-C(4)-N(1)	126.4(6)	C(26)-C(21)-C(5)	122.2(7)
C(5)-C(4)-C(3)	125.7(6)	C(21)-C(22)-C(23)	122.4(8)
N(1)-C(4)-C(3)	107.9(6)	C(24)-C(23)-C(22)	120.2(9)
C(4)-C(5)-C(6)	124.8(5)	C(25)-C(24)-C(23)	116.6(8)
C(4)-C(5)-C(21)	119.3(6)	C(25)-C(24)-C(27)	121.1(9)
C(6)-C(5)-C(21)	115.9(6)	C(23)-C(24)-C(27)	121.5(9)
N(2)-C(6)-C(5)	125.5(5)	C(24)-C(25)-C(26)	121.3(9)
N(2)-C(6)-C(7)	109.5(6)	C(21)-C(26)-C(25)	123.3(9)
C(5)-C(6)-C(7)	125.0(6)	C(32)-C(31)-C(36)	118.9(7)
C(8)-C(7)-C(6)	108.6(6)	C(32)-C(31)-C(10)	119.7(8)
C(7)-C(8)-C(9)	106.0(6)	C(36)-C(31)-C(10)	121.3(7)

C(31)-C(32)-C(33)	118.1(10)	C(53)-C(54)-C(57)	122.8(11)
C(34)-C(33)-C(32)	121.0(11)	C(54)-C(55)-C(56)	124.9(11)
C(35)-C(34)-C(33)	118.4(10)	C(51)-C(56)-C(55)	121.7(10)
C(35)-C(34)-C(37)	124.7(14)	C(66)-C(61)-C(62)	117.6(7)
C(33)-C(34)-C(37)	116.9(14)	C(66)-C(61)-C(68)	122.0(6)
C(34)-C(35)-C(36)	123.3(12)	C(62)-C(61)-C(68)	120.3(7)
C(35)-C(36)-C(31)	120.2(10)	C(63)-C(62)-C(61)	119.5(9)
C(42)-C(41)-C(46)	117.5(6)	C(64)-C(63)-C(62)	121.5(9)
C(42)-C(41)-C(15)	123.1(6)	C(63)-C(64)-C(65)	119.2(9)
C(46)-C(41)-C(15)	119.2(6)	C(63)-C(64)-C(67)	121.6(14)
C(41)-C(42)-C(43)	121.6(7)	C(65)-C(64)-C(67)	119.1(14)
C(44)-C(43)-C(42)	120.5(7)	C(64)-C(65)-C(66)	120.5(9)
C(45)-C(44)-C(43)	118.1(6)	C(65)-C(66)-C(61)	121.7(8)
C(45)-C(44)-C(47)	119.3(7)	F(1)-C(67)-F(3)	106(2)
C(43)-C(44)-C(47)	122.6(7)	F(1)-C(67)-F(2)	107(2)
C(44)-C(45)-C(46)	121.6(7)	F(3)-C(67)-F(2)	92.1(16)
C(41)-C(46)-C(45)	120.6(7)	F(1)-C(67)-C(64)	121.9(16)
C(56)-C(51)-C(52)	115.6(8)	F(3)-C(67)-C(64)	114.2(18)
C(56)-C(51)-C(20)	120.5(7)	F(2)-C(67)-C(64)	112(2)
C(52)-C(51)-C(20)	123.6(8)	O(1)-C(68)-C(61)	118.0(6)
C(51)-C(52)-C(53)	118.6(11)	O(1)-C(68)-Rh(1)	123.7(5)
C(54)-C(53)-C(52)	124.5(11)	C(61)-C(68)-Rh(1)	118.3(5)
C(55)-C(54)-C(53)	114.2(9)	C(67)-F(2)-F(3)	42.3(10)
C(55)-C(54)-C(57)	122.8(11)	C(67)-F(3)-F(2)	45.6(12)

Symmetry transformations used to generate equivalent atoms:

Table 4. Anisotropic displacement parameters ($\text{\AA}^2 \times 10^3$) for p.
 The anisotropic displacement factor exponent takes the form:
 $-2 \pi^2 [h^2 a^{*2} U_{11} + \dots + 2 h k a^* b^* U_{12}]$

	U11	U22	U33	U23	U13	U12
Rh(1)	41(1)	53(1)	46(1)	1(1)	9(1)	-5(1)
O(1)	102(4)	96(4)	68(3)	18(3)	36(3)	8(3)
O(2)	143(6)	112(5)	94(4)	-22(4)	67(4)	-22(4)
N(1)	41(3)	62(3)	59(3)	4(3)	11(2)	-1(2)
N(2)	46(3)	58(3)	48(3)	3(2)	9(2)	-8(2)
N(3)	48(3)	58(3)	44(3)	2(2)	10(2)	-5(2)
N(4)	46(3)	55(3)	57(3)	2(2)	15(2)	-1(2)
C(1)	64(4)	48(4)	66(4)	8(3)	21(3)	-5(3)
C(2)	76(5)	55(4)	98(6)	6(4)	22(4)	-17(4)
C(3)	59(4)	71(5)	76(5)	-1(4)	11(4)	-19(4)
C(4)	49(4)	59(4)	56(4)	-1(3)	12(3)	-13(3)
C(5)	49(4)	64(5)	44(3)	0(3)	6(3)	-12(3)
C(6)	44(3)	67(4)	57(4)	8(3)	11(3)	-1(3)
C(7)	40(4)	85(5)	86(5)	16(4)	6(3)	-5(4)
C(8)	52(4)	75(5)	84(5)	17(4)	0(4)	-7(4)
C(9)	50(4)	68(5)	48(4)	7(3)	6(3)	-1(3)
C(10)	55(4)	63(4)	49(4)	4(3)	9(3)	-3(3)
C(11)	55(4)	61(4)	49(4)	3(3)	10(3)	-8(3)
C(12)	64(4)	58(4)	64(4)	8(3)	11(3)	-8(3)
C(13)	59(4)	64(4)	61(4)	3(3)	13(3)	-20(3)
C(14)	46(3)	57(4)	47(3)	-2(3)	14(3)	-12(3)
C(15)	42(3)	60(4)	53(4)	-1(3)	17(3)	-7(3)
C(16)	39(3)	69(4)	48(3)	-4(3)	10(3)	0(3)
C(17)	42(3)	75(5)	68(4)	1(4)	16(3)	-2(3)
C(18)	48(4)	60(4)	76(4)	8(4)	19(3)	6(3)
C(19)	54(4)	52(4)	61(4)	-2(3)	20(3)	1(3)
C(20)	58(4)	55(4)	68(4)	5(3)	17(3)	7(3)
C(21)	46(4)	80(5)	54(4)	-1(4)	13(3)	-16(3)
C(22)	63(5)	208(11)	115(7)	-77(7)	46(5)	-49(6)
C(23)	74(6)	217(13)	122(8)	-84(8)	36(6)	-52(7)
C(24)	62(5)	145(9)	109(7)	-22(6)	31(5)	-49(5)
C(25)	81(7)	285(17)	105(8)	-11(9)	41(6)	-55(9)
C(26)	90(7)	370(20)	74(6)	-32(9)	37(6)	-90(10)
C(27)	63(6)	212(13)	193(11)	-24(9)	39(7)	-57(7)
C(31)	48(4)	59(4)	77(5)	20(4)	4(3)	-6(3)

C(32)	81(6)	105(7)	86(6)	31(5)	15(4)	-3(5)
C(33)	108(8)	129(9)	107(8)	68(7)	3(6)	-33(7)
C(34)	75(6)	71(6)	156(11)	26(7)	-18(7)	-9(5)
C(35)	105(8)	77(7)	159(11)	9(7)	27(8)	18(6)
C(36)	100(7)	86(6)	121(7)	21(6)	41(6)	15(5)
C(37)	133(9)	90(7)	264(15)	94(9)	-56(9)	-7(7)
C(41)	38(3)	64(4)	53(4)	0(3)	12(3)	-1(3)
C(42)	61(4)	119(6)	60(4)	-15(4)	23(4)	-27(4)
C(43)	58(5)	125(7)	83(6)	-6(5)	33(4)	-27(5)
C(44)	45(4)	82(5)	72(5)	-3(4)	8(3)	-13(3)
C(45)	70(5)	115(7)	66(5)	-24(4)	18(4)	-20(5)
C(46)	62(4)	124(7)	58(4)	-17(4)	21(4)	-35(4)
C(47)	62(5)	119(7)	135(8)	-30(6)	19(5)	-35(5)
C(51)	64(4)	55(4)	72(5)	-1(4)	14(4)	8(3)
C(52)	430(20)	98(8)	67(6)	9(6)	48(10)	117(11)
C(53)	460(30)	85(8)	90(8)	1(7)	53(12)	128(12)
C(54)	96(6)	65(5)	88(6)	16(5)	-5(5)	-8(5)
C(55)	380(20)	142(11)	223(14)	112(11)	236(16)	133(13)
C(56)	335(19)	126(9)	201(12)	100(9)	219(14)	136(11)
C(57)	158(10)	71(6)	143(9)	42(6)	6(8)	17(6)
C(61)	62(4)	82(5)	50(4)	-6(3)	22(3)	0(4)
C(62)	59(5)	128(8)	97(6)	-25(5)	32(4)	-3(5)
C(63)	81(7)	152(10)	112(7)	-12(7)	35(6)	39(7)
C(64)	114(8)	96(7)	108(7)	-9(6)	50(6)	28(6)
C(65)	112(8)	91(7)	112(7)	-18(5)	54(6)	3(6)
C(66)	78(5)	77(5)	85(5)	-16(4)	36(4)	-10(4)
C(67)	217(18)	175(16)	166(15)	-9(12)	114(14)	83(14)
C(68)	45(4)	72(5)	59(4)	5(3)	12(3)	-7(3)
C(71)	650(40)	170(15)	246(18)	17(13)	330(30)	-19(19)
F(1)	610(30)	172(10)	352(18)	101(11)	320(20)	216(15)
F(2)	265(15)	200(11)	800(40)	-109(18)	350(20)	25(10)
F(3)	450(30)	259(14)	254(14)	-100(11)	100(14)	169(15)

Table 5. Hydrogen coordinates ($\times 10^4$) and isotropic displacement parameters ($\text{\AA}^2 \times 10^3$) for p.

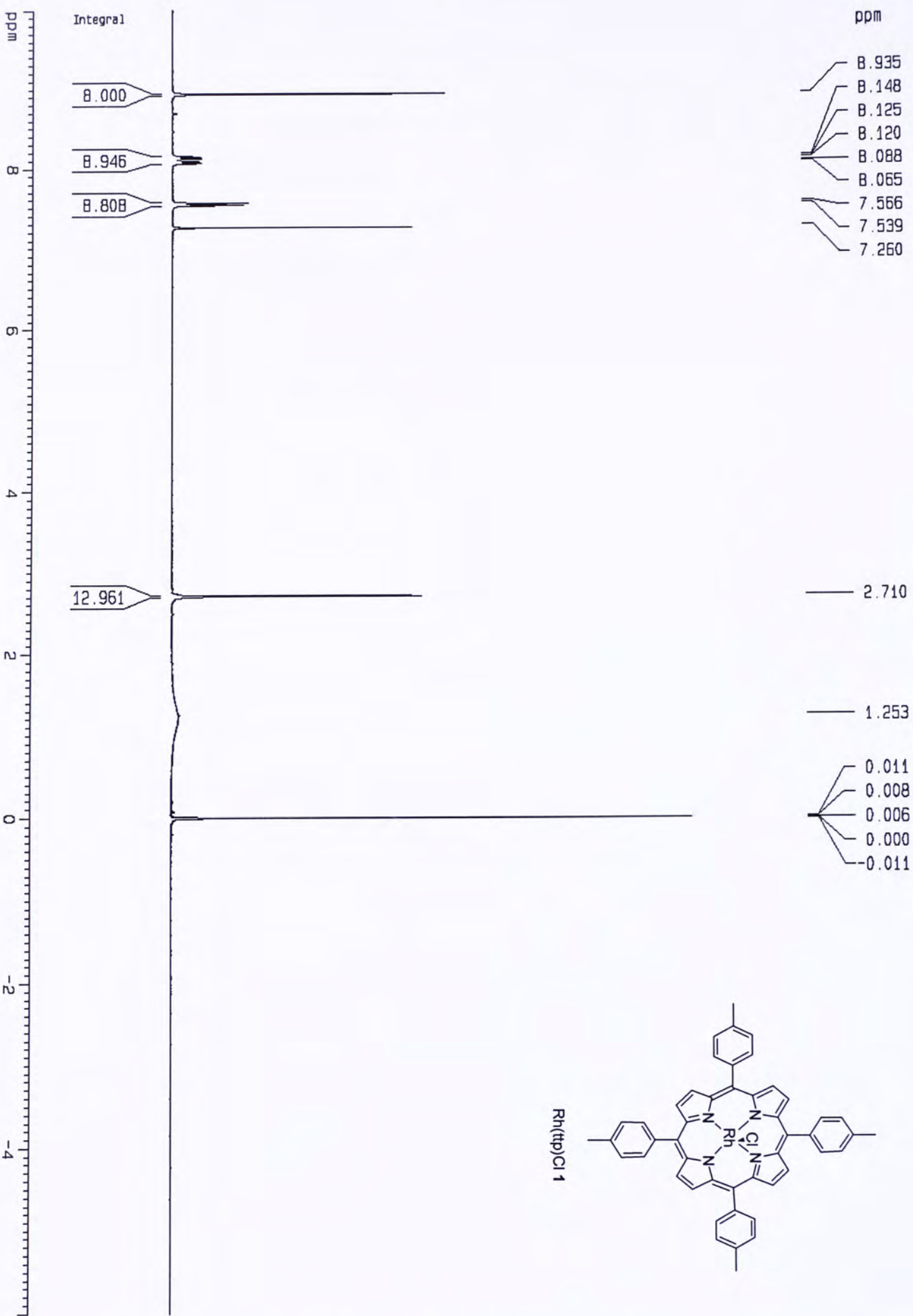
	x	y	z	U(eq)
H(2)	3403	4794	8129	167
H(2A)	3768	8283	7157	99
H(3A)	4470	7665	7946	91
H(7A)	5076	4138	9031	95
H(8A)	4768	2479	9014	99
H(12A)	3179	939	7799	82
H(13A)	2477	1574	7021	80
H(17A)	1862	5104	5911	78
H(18A)	2174	6753	5968	78
H(22A)	4949	6226	9493	152
H(23A)	5662	6766	10075	169
H(25A)	5831	6345	8525	189
H(26A)	5132	5801	7961	216
H(27A)	6387	7177	9384	245
H(27B)	6431	6674	10034	245
H(27C)	6265	7782	9866	245
H(32A)	3804	1377	9185	120
H(33A)	4148	-115	9730	158
H(35A)	4672	-447	8534	151
H(36A)	4336	950	7963	127
H(37A)	4865	-1651	9424	326
H(37B)	4480	-1824	9595	326
H(37C)	4871	-1144	10049	326
H(42A)	1791	3116	6914	98
H(43A)	1150	2276	6280	106
H(45A)	1461	2124	4822	106
H(46A)	2101	2958	5450	100
H(47A)	845	1295	4662	173
H(47B)	595	1847	4994	173
H(47C)	846	850	5300	173
H(52A)	2733	8528	7002	265
H(53A)	2527	10036	6413	288
H(55A)	2714	8965	5043	251
H(56A)	2971	7502	5613	220
H(57A)	2465	10574	4865	222
H(57B)	2609	11185	5519	222

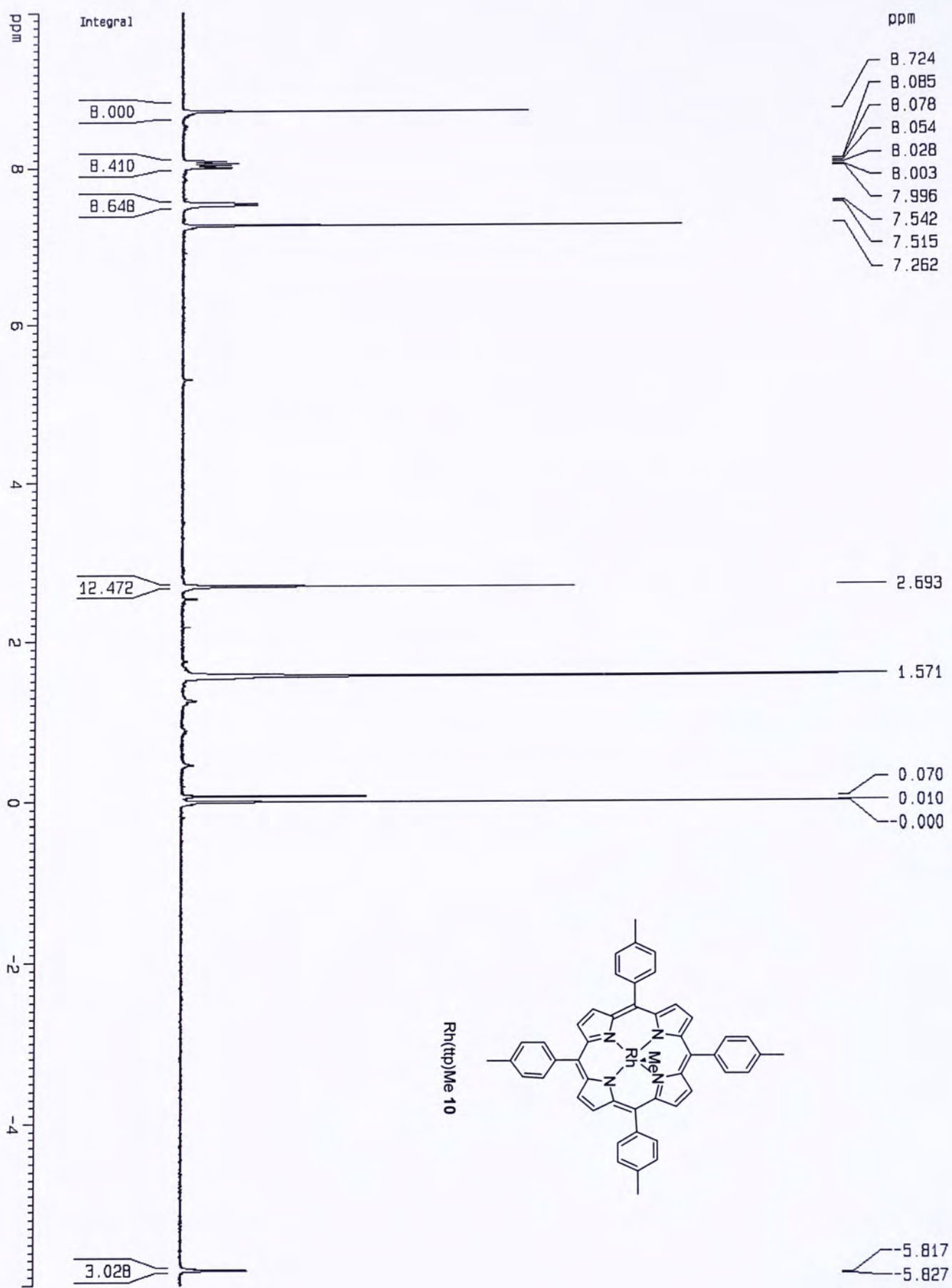
H(57C)	2144	10718	5169	222
H(62A)	4362	3778	6938	115
H(63A)	4632	2243	6816	142
H(65A)	3479	986	6219	124
H(66A)	3203	2477	6352	97
H(71A)	3355	4805	9219	459
H(71B)	3726	4288	9117	459
H(71C)	3253	3875	8750	459

List of Spectra

No	Spectra	Page
1	^1H NMR Spectrum of $\text{Rh}(\text{ttp})\text{Cl}$ (1)	142
2	^1H NMR Spectrum of $\text{Rh}(\text{ttp})\text{Me}$ (10)	143
3	^1H NMR Spectrum of $\text{Rh}(\text{ttp})\text{CH}_2\text{CH}_2\text{OH}$ (19)	144
4	^1H NMR Spectrum of $\text{Rh}(\text{ttp})\text{OTf}$ (15)	145
5	^1H NMR Spectrum of $\text{Rh}(\text{ttp})\text{PF}_6$ (21)	146
6	^{13}C NMR Spectrum of $\text{Rh}(\text{ttp})\text{PF}_6$ (21)	147
7	^1H NMR Spectrum of $\text{Rh}(\text{ttp})\text{H}$ (14)	148
8	^1H NMR Spectrum of $\text{C}_6\text{H}_5\text{CORh}(\text{ttp})$ (2)	149
9	^1H NMR Spectrum of $\text{C}_6\text{H}_5\text{CH}_2\text{Rh}(\text{ttp})$ (3)	150
10	^1H NMR Spectrum of $4\text{-FC}_6\text{H}_4\text{CORh}(\text{ttp})$ (4)	151
11	^1H NMR Spectrum of $4\text{-ClC}_6\text{H}_4\text{CORh}(\text{ttp})$ (17)	152
12	^1H NMR Spectrum of $4\text{-CF}_3\text{C}_6\text{H}_4\text{CORh}(\text{ttp})$ (5)	153
13	^1H NMR Spectrum of $4\text{-CNC}_6\text{H}_4\text{CORh}(\text{ttp})$ (20)	154
14	^1H NMR Spectrum of $4\text{-MeC}_6\text{H}_4\text{CORh}(\text{ttp})$ (7)	155
15	^1H NMR Spectrum of $4\text{-CHOC}_6\text{H}_4\text{CH}_2\text{Rh}(\text{ttp})$ (6)	156
16	^{13}C NMR Spectrum of $4\text{-CHOC}_6\text{H}_4\text{CH}_2\text{Rh}(\text{ttp})$ (6)	157
17	^1H NMR Spectrum of $4\text{-}^t\text{BuC}_6\text{H}_4\text{CORh}(\text{ttp})$ (9)	158
18	^1H NMR Spectrum of $4\text{-CHOC}_6\text{H}_4\text{C}(\text{Me})_2\text{CH}_2\text{Rh}(\text{ttp})$ (8)	159
19	^{13}C NMR Spectrum of $4\text{-CHOC}_6\text{H}_4\text{C}(\text{Me})_2\text{CH}_2\text{Rh}(\text{ttp})$ (8)	160
20	^1H NMR Spectrum of $4\text{-MeOC}_6\text{H}_4\text{CORh}(\text{ttp})$ (16)	161
21	^1H NMR Spectrum of $4\text{-N}(\text{Me})_2\text{C}_6\text{H}_4\text{CORh}(\text{ttp})$ (18)	162
22	^1H NMR Spectrum of $4\text{-CH}_3\text{CH}_2\text{CORh}(\text{ttp})$ (12)	163

23	^1H NMR Spectrum of 4- $\text{CH}_3(\text{CH}_2)_5\text{CORh}(\text{ttp})$ (11)	164
24	^1H NMR Spectrum of 4- $^t\text{BuCORh}(\text{ttp})$ (13)	165





Current Data Parameters
NAME CML091-F1-1
EXPNO 1
PROCNO 1

F2 - Acquisition Parameters
Date_ 20040325

Time 14.24
INSTRUM dpx300
PROBHD 5 mm BBO BB-1H
PULPRDG 2g
TD 32768
SOLVENT CDCl3
NS 64
DS 0

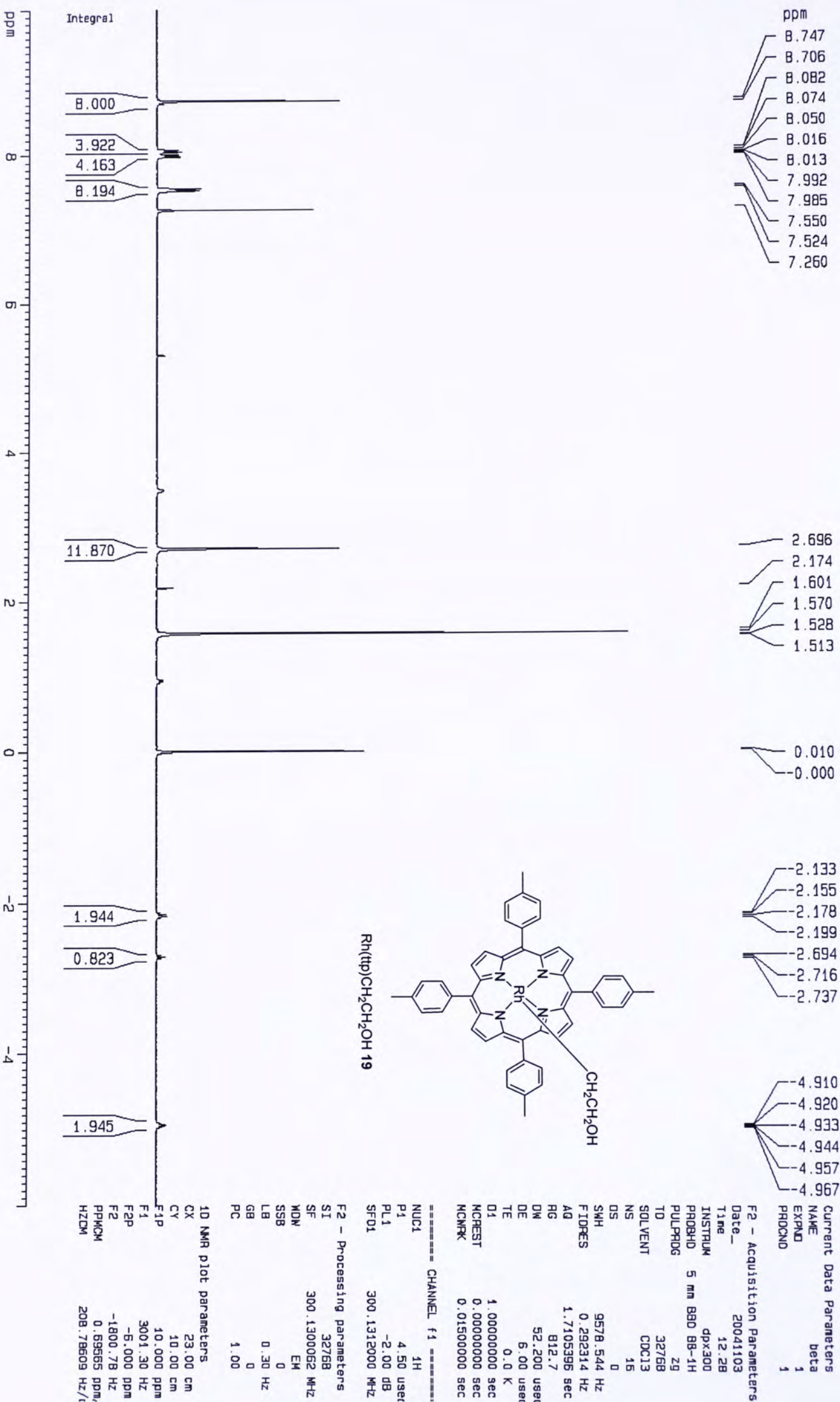
SWH 8992.806 Hz
FIDRES 0.27439 Hz
AQ 1.8219508 sec
RG 1625.5
DW 55.600 usec
DE 79.43 usec
TE 297.2 K

D1 1.00000000 sec
MCREST 0.00000000 sec
MCNMRK 0.01500000 sec

===== CHANNEL f1 =====
NUC1 1H
P1 9.00 usec
PL1 -2.00 dB
SF01 300.1312000 MHz

F2 - Processing parameters
SI 32768
SF 300.1300056 MHz
WDW EM
SSB 0
LB 0.30 Hz
GB 0
PC 1.00

1D NMR plot parameters
CX 22.00 cm
CY 50.00 cm
F1P 10.000 ppm
F1 3001.30 Hz
F2P -5.000 ppm
F2 -1800.78 Hz
PPMCM 0.72727 ppm/
HZCM 218.27637 Hz/1





Current Data Parameters
NAME CML194-F2-1
EXPNO 1
PROCNO 1

F2 - Acquisition Parameters
Date_ 20040826
Time 15.01
INSTRUM dpx300
PROBHD 5 mm BBO BB-1H
PULPRDG 29
TD 32768
SOLVENT CDCl3
NS 64
DS 0
SMH 8992.806 Hz
FIDRES 0.274439 Hz
AQ 1.8219508 sec
RG 2298.8
DM 55.600 usec
DE 79.43 usec
TE 683.2 K
D1 1.00000000 sec
MCREST 0.00000000 sec
MCNPK 0.01500000 sec

----- CHANNEL f1 -----
NUC1 1H
P1 9.00 usec
PL1 -2.00 dB
SFO1 300.1312000 MHz

F2 - Processing parameters
SI 32768
SF 300.1300055 MHz
WDW EM
SSB 0
LB 0.30 Hz
GB 0
PC 1.00

1D NMR plot parameters
CX 22.00 cm
CY 80.00 cm
F1P 10.000 ppm
F1 3001.30 Hz
F2P -6.000 ppm
F2 -1800.78 Hz
PPMCM 0.72727 ppm/
HZCM 218.27637 Hz/1

ppm

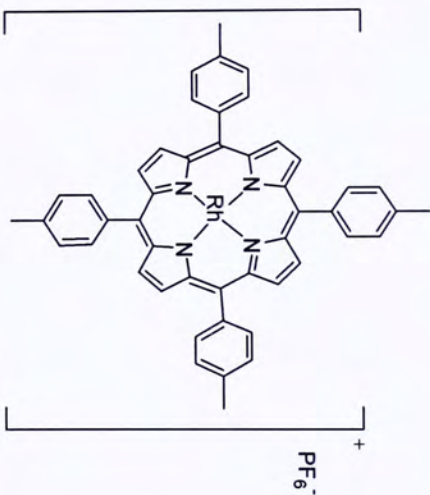
8.909
8.102
8.078
8.059
8.036
7.555
7.528
7.254

5.292

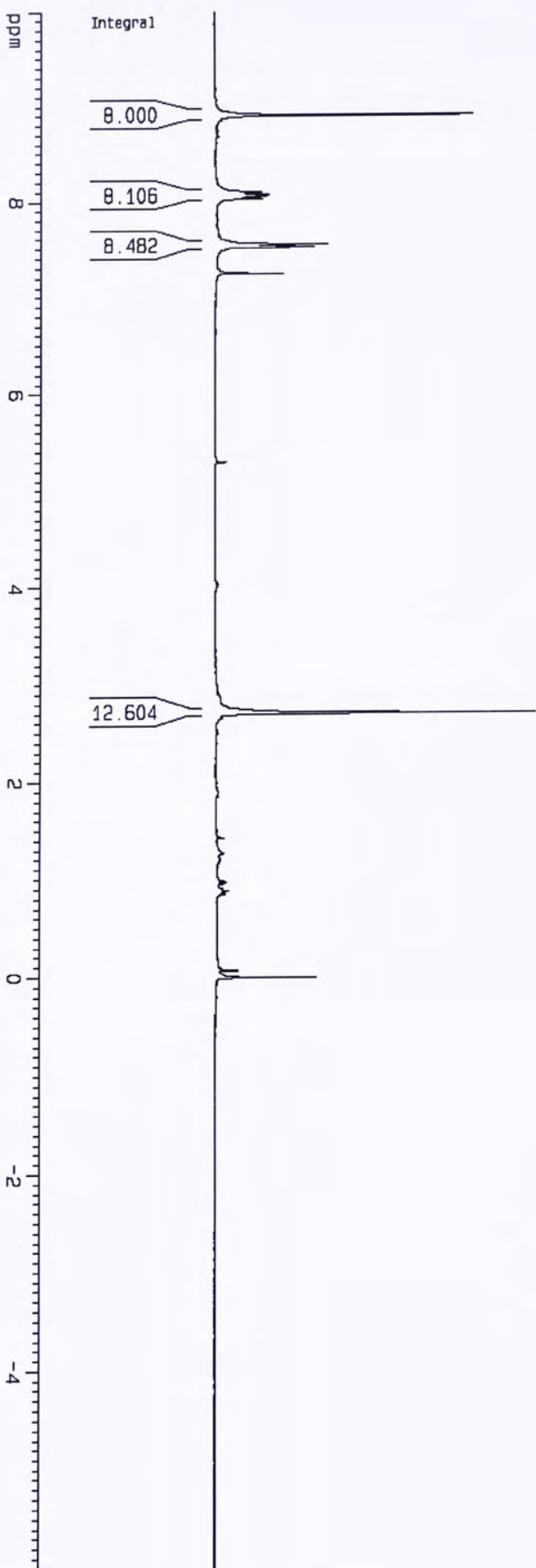
2.708

0.981
0.883

0.071
-0.000



Rh(ttp)PF₆ 21



Current Data Parameters
NAME CML375-1
EXPNO 1
PROCNO 1

F2 - Acquisition Parameters
Date_ 20050303

Time 15.50

INSTRUM dpx300

PROBHD 5 mm BBO BB-1H

PULPROG zg

TD 32768

SOLVENT CDCl3

NS 32

DS 0

SWH 8992.806 Hz

FIDRES 0.274439 Hz

AQ 1.8219508 sec

RG 512

DW 55.600 usec

DE 79.43 usec

TE 297.2 K

D1 1.00000000 sec

MCREST 0.00000000 sec

MCNPK 0.01500000 sec

----- CHANNEL f1 -----

NUC1 1H

P1 9.00 usec

PL1 -2.00 dB

SFO1 300.1312000 MHz

F2 - Processing parameters

SI 32768

SF 300.1300078 MHz

WDW EM

SSB 0

LB 0.30 Hz

GB 0

PC 1.00

1D NMR plot parameters

CX 22.00 cm

CY 5.00 cm

F1P 10.000 ppm

F1 3001.30 Hz

F2P -5.000 ppm

F2 -1800.78 Hz

PPMCM 0.72727 ppm

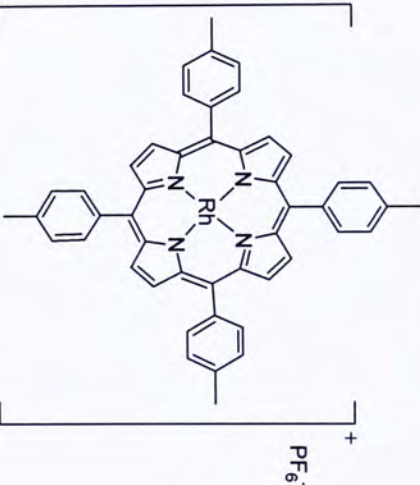
HZCM 218.27637 Hz/1

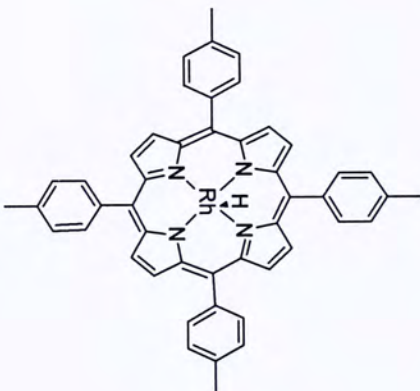
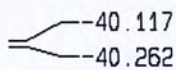
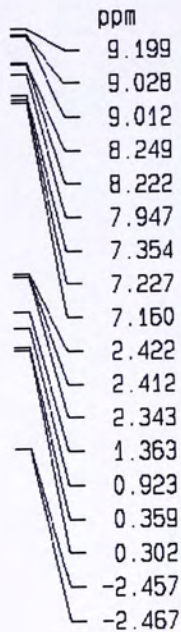
ppm

143.738
139.658
137.824
135.216
134.432
133.036
128.131
127.769

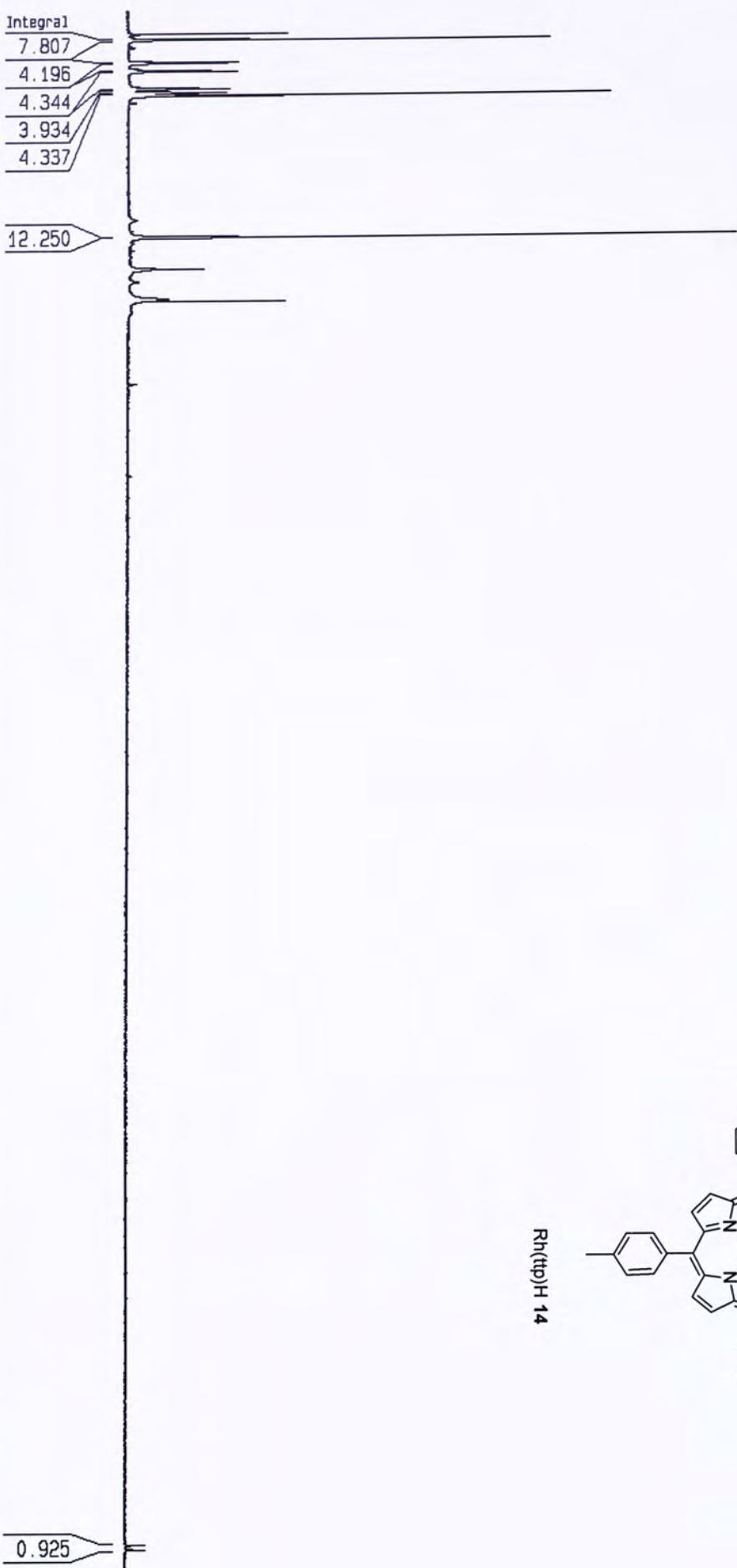
77.962
77.732
77.539
77.115

22.068



$Rh(ttp)H$ 

Rh(ttp)H 14



Current Data	Parameters
NAME	PH (http)H-1
EXPNO	1
PROCNO	1

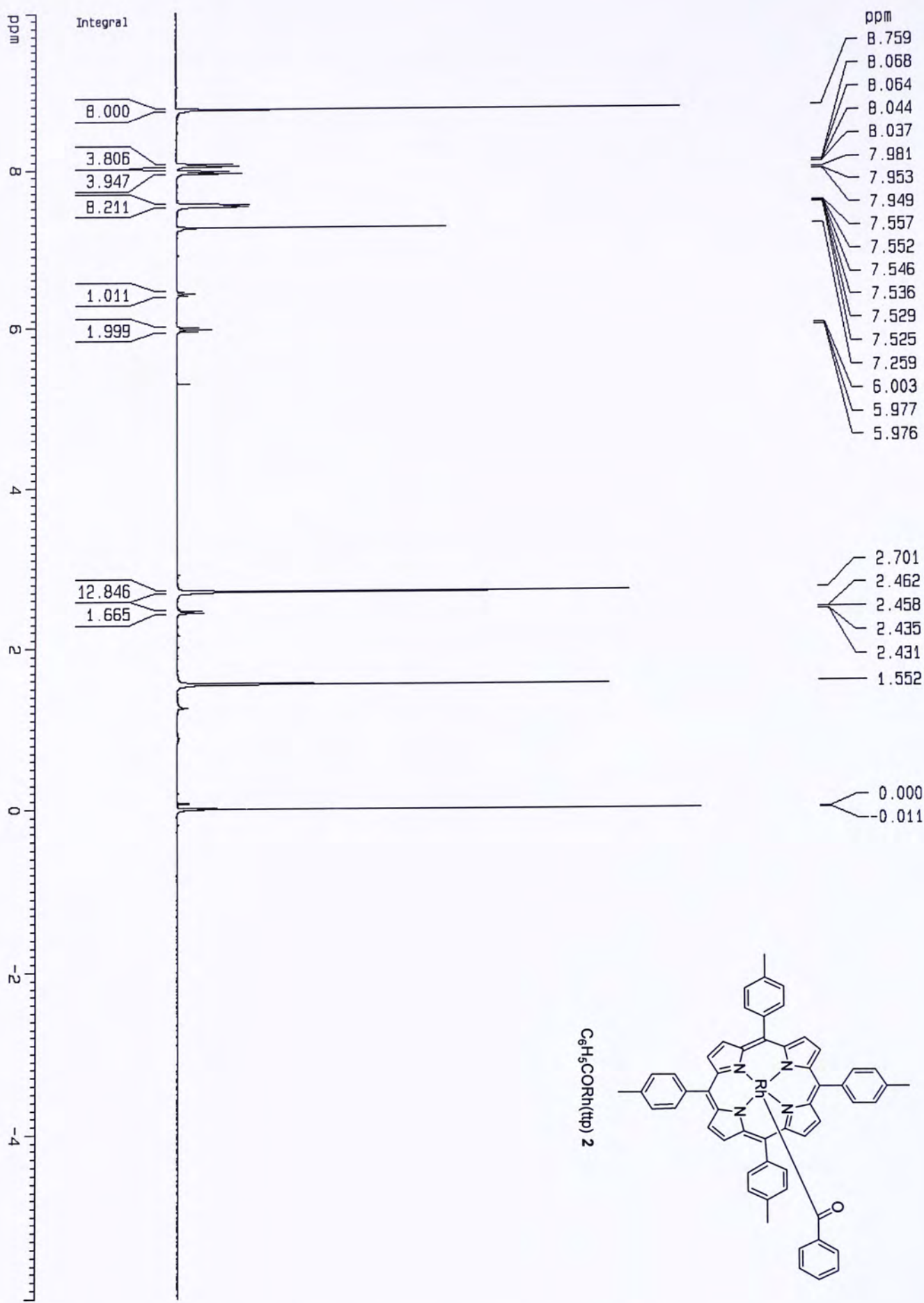
F2 - Acquisition Parameters
Date_ 20050628

TIME	22.36
INSTRUM	dpX300
PROBHD	5 mm B80 B8-1H
PULPR06	29
T0	327.76
SOLVENT	CD05
NS	300
D5	0
SWH	30030.029 Hz
FIDRES	0.915444 Hz
AQ	0.5456372 sec
R6	1024
DW	15.650 usec
DE	23.79 usec
TE	297.2 K
D1	1.00000000 sec
MCREST	0.00000000 sec
MCNPK	0.01500000 sec

```
===== CHANNEL f1 =====
NUC1          1H
P1            9.00 usec
PL1           -2.00 dB
SFD1          300.1312000 MHz
```

F2 - Processing parameters	
SI	32768
SF	300.1300317 MHz
NMK	EM
SSB	0
LB	0.30 Hz
GB	0
PC	1.00

1D NMR plot	parameters
CX	22.00 cm
CY	10.00 cm
F1P	10.000 ppm
F1	3001.30 Hz
F2P	-41.000 ppm
F2	-12305.33 Hz
PPMCM	2.31818 ppm/cm
HZCM	695.75598 Hz/cm



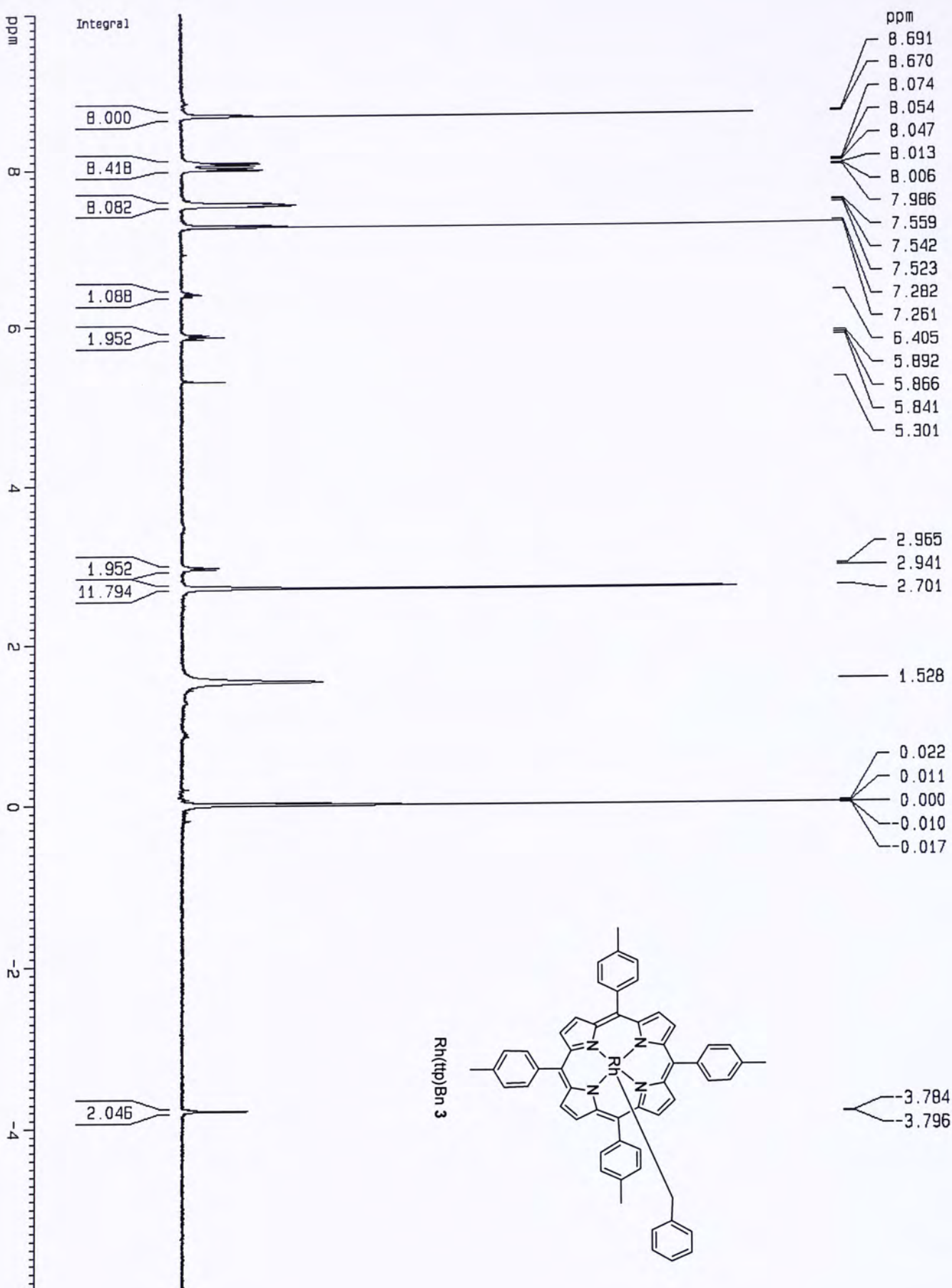
Current Data Parameters
NAME CML300-F1-1
EXPNO 1
PROCNO 1

F2 - Acquisition Parameters
Date_ 20041229
Time 15.48
INSTRUM dpx300
PROBHD 5 mm BBO BB-1H
PULPROG zg
TD 32768
SOLVENT CDCl3
NS 32
DS 0
SWH 8992.806 Hz
FIDRES 0.274439 Hz
AQ 1.8219608 sec
RG 912.3
OW 55.600 usec
DE 79.43 usec
TE 0.0 K
D1 1.00000000 sec
MCREST 0.00000000 sec
MCMRK 0.01500000 sec

===== CHANNEL f1 =====
NUC1 1H
P1 9.00 usec
PL1 -2.00 dB
SFO1 300.131200 MHz

F2 - Processing parameters
SI 32768
SF 300.130065 MHz
WDW EM
SSB 0
LB 0.30 Hz
GB 0
PC 1.00

1D NMR plot parameters
CX 22.00 cm
CY 10.00 cm
F1P 10.000 ppm
F1 3001.30 Hz
F2P -5.000 ppm
F2 -1800.78 Hz
PPMCM 0.72727 ppm/
HZCM 218.27637 Hz/1



Current Data Parameters

NAME	Bn
EXPNO	1
PROCNO	1

F2 - Acquisition Parameters

Date_	Time
20050201	9.17
INSTRUM	dpX300
PROBHD	5 mm BBO BB-1H
PULPROG	zg
TD	32768
SOLVENT	CDCl3
NS	32
DS	0
SWH	8992.806 Hz
FIDRES	0.274439 Hz
AQ	1.8219508 sec
RG	1149.4
DW	55.600 usec
DE	79.43 usec
TE	0.0 K
D1	1.00000000 sec
MCREST	0.00000000 sec
MCWRR	0.01500000 sec

===== CHANNEL f1 =====

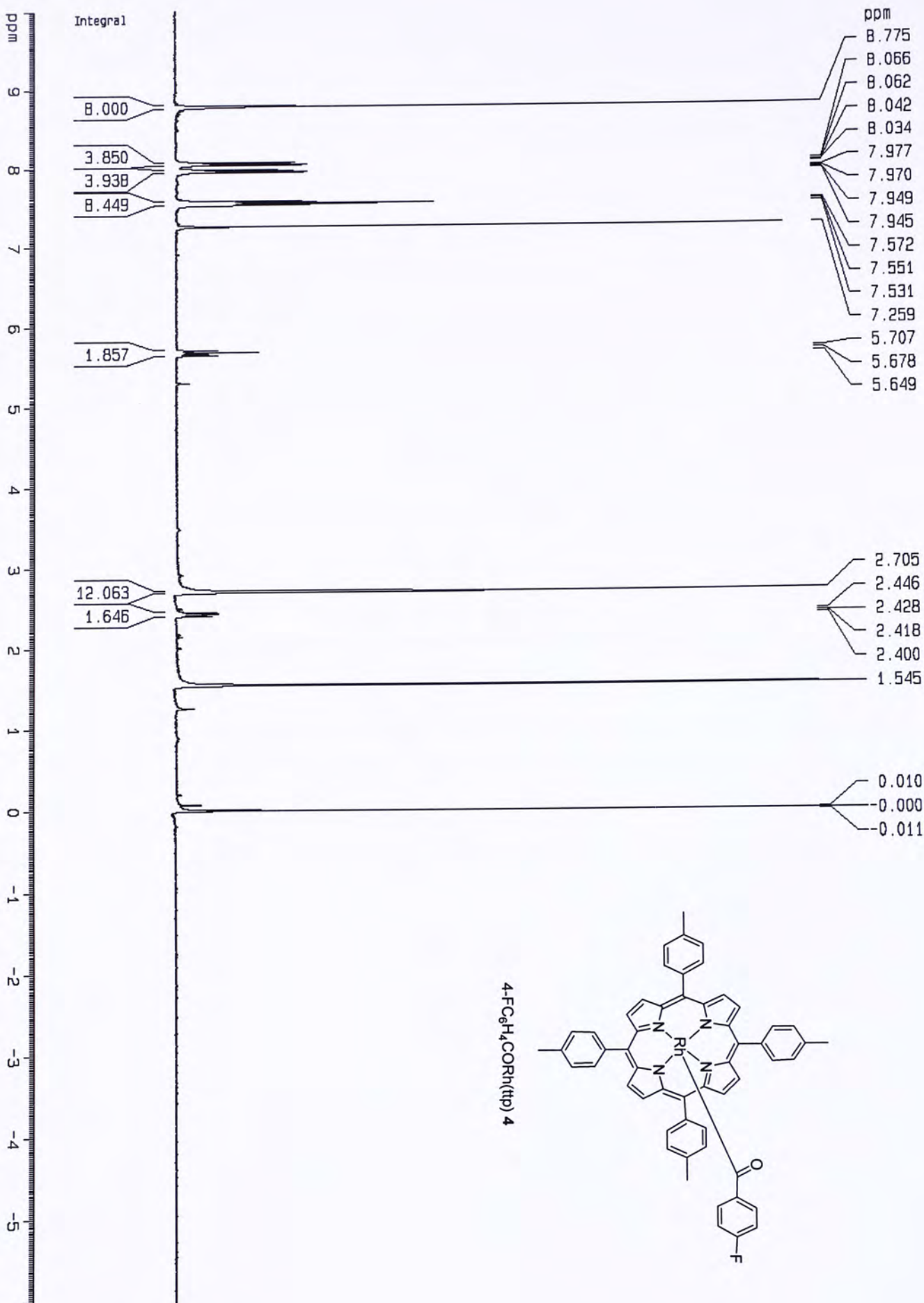
NUC1	1H
P1	5.00 usec
PL1	-2.00 dB
SFO1	300.1312000 MHz

F2 - Processing parameters

SI	32768
SF	300.1300059 MHz
WDW	EM
SSB	0
LB	0.30 Hz
GB	0
PC	1.00

1D NMR plot parameters

CX	22.00 cm
CY <td>30.00 cm</td>	30.00 cm
F1P <td>10.000 ppm</td>	10.000 ppm
F1 <td>3001.30 Hz</td>	3001.30 Hz
F2P <td>-5.000 ppm</td>	-5.000 ppm
F2 <td>-1800.78 Hz</td>	-1800.78 Hz
PPMCM <td>0.72727 ppm</td>	0.72727 ppm
HZCM <td>218.27637 Hz</td>	218.27637 Hz



Current Data Parameters

NAME	A'sf10r0
EXPNO	1
PROCNO	1

F2 - Acquisition Parameters

Date_	20050612
Time	22.58
INSTRUM	dpX300
PROBHD	5 mm BBO BB-1H
PULPROG	zg
TD	32768
SOLVENT	CDCl3
NS	32
DS	0
SWH	8992.806 Hz
FIDRES	0.274439 Hz
AQ	1.8219508 sec
RG	912.3
DW	55.600 usec
DE	79.43 usec
TE	297.2 K
D1	1.00000000 sec
MCREST	0.0000000 sec
MCNPK	0.01500000 sec

===== CHANNEL f1 =====

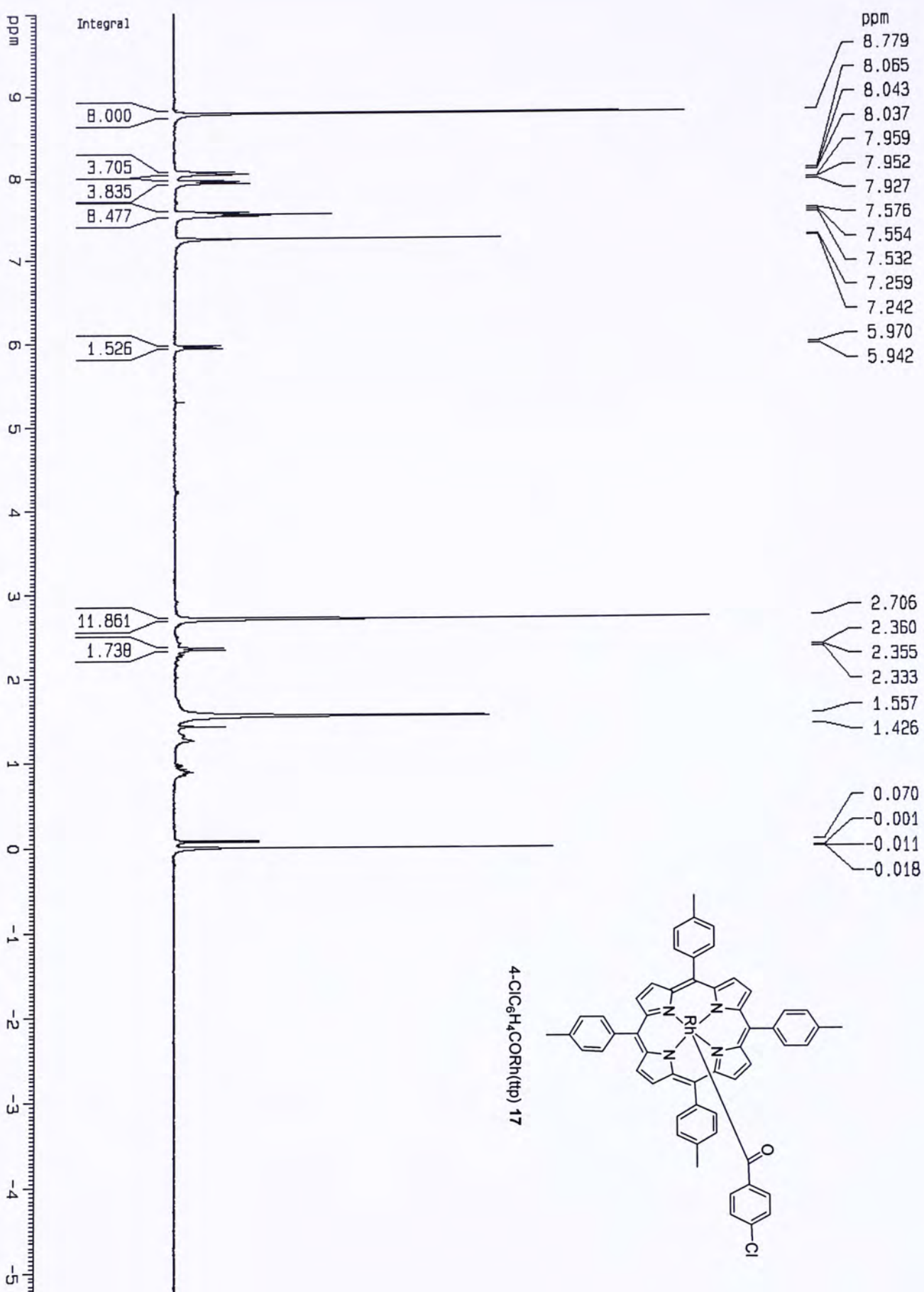
NUC1	¹ H
P1	9.00 usec
PL1	-2.00 dB
SFO1	300.1312000 MHz

F2 - Processing parameters

SI	32768
SF	300.1300065 MHz
WDW	EM
SSB	0
LB	0.30 Hz
GB	0
PC	1.00

1D NMR plot parameters

CX	22.00 cm
CY	20.00 cm
F1P	10.000 ppm
F1	3001.30 Hz
F2P	-6.000 ppm
F2	-1800.78 Hz
PPMCM	0.72727 ppm/Hz
HZCM	218.27637 Hz/Hz



Current Data Parameters
NAME CML273-F1-1
EXPNO 1
PROCNO 1

F2 - Acquisition Parameters
Date_ 20041206
Time 13.58

INSTRUM dpx300
PROBHD 5 mm BBO BB-1H
PULPROG zg

TD 32768
SOLVENT CDCl3
NS 32

DS 0
SWH 8992.806 Hz
FIDRES 0.274439 Hz

AQ 1.8219508 sec
RG 1024
DM 55.600 usec

DE 79.43 usec
TE 0.0 K
D1 1.00000000 sec

MCREST 0.00000000 sec
MCNMR 0.01500000 sec

===== CHANNEL f1 =====
NUC1 1H
P1 9.00 usec

PL1 -2.00 dB
SFO1 300.1312000 MHz

F2 - Processing parameters
SI 32768
SF 300.1300065 MHz

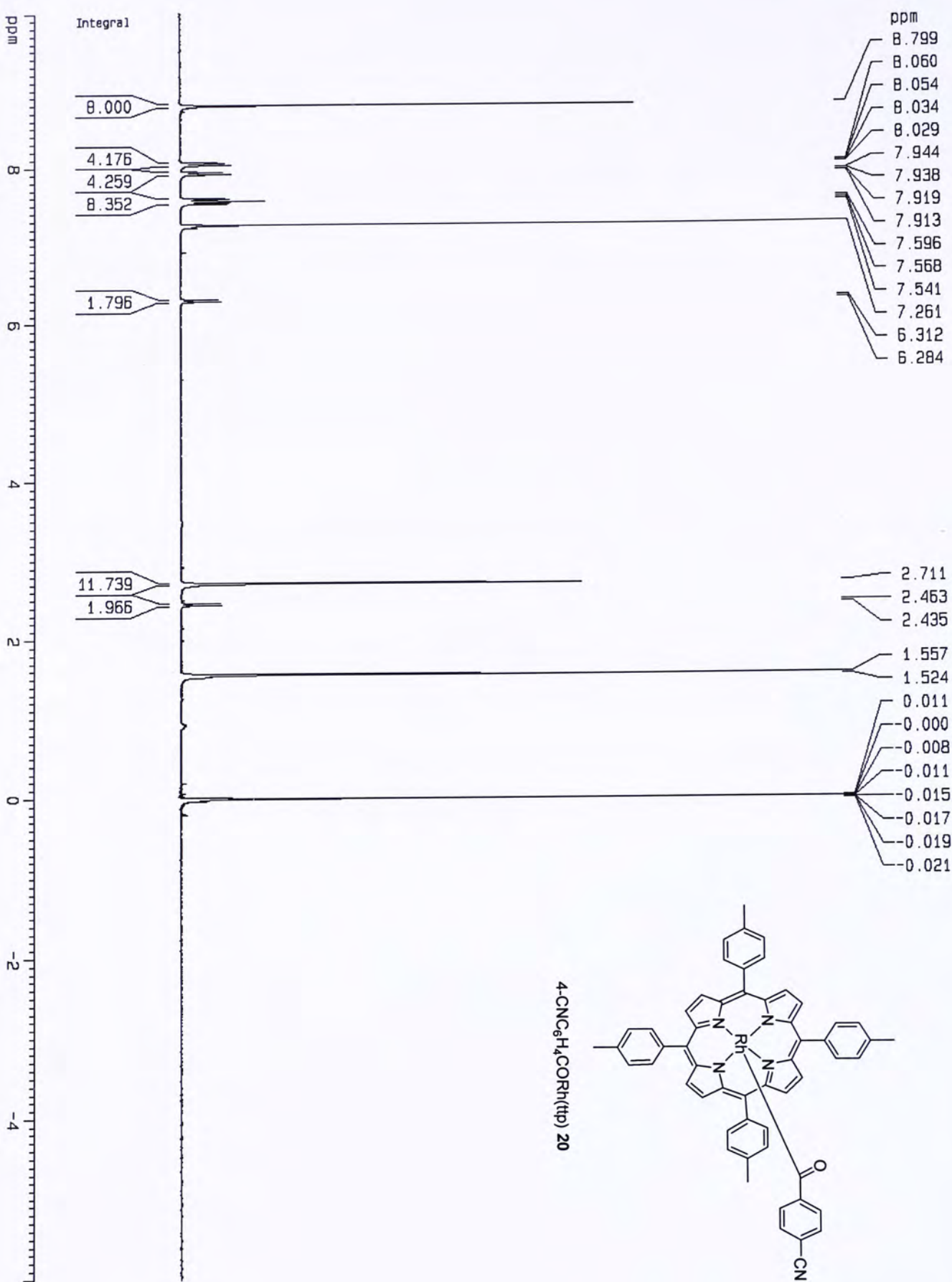
MDM EM
SSB 0
LB 0.30 Hz

GB 0
PC 1.00

1D NMR Plot parameters
CX 22.00 cm
CY 10.00 cm

F1 10.000 ppm
F2 3001.30 Hz
F2P -6.000 ppm

F2 -1800.78 Hz
PPMCM 0.72727 ppm/cm
HZCM 218.27637 Hz/cm



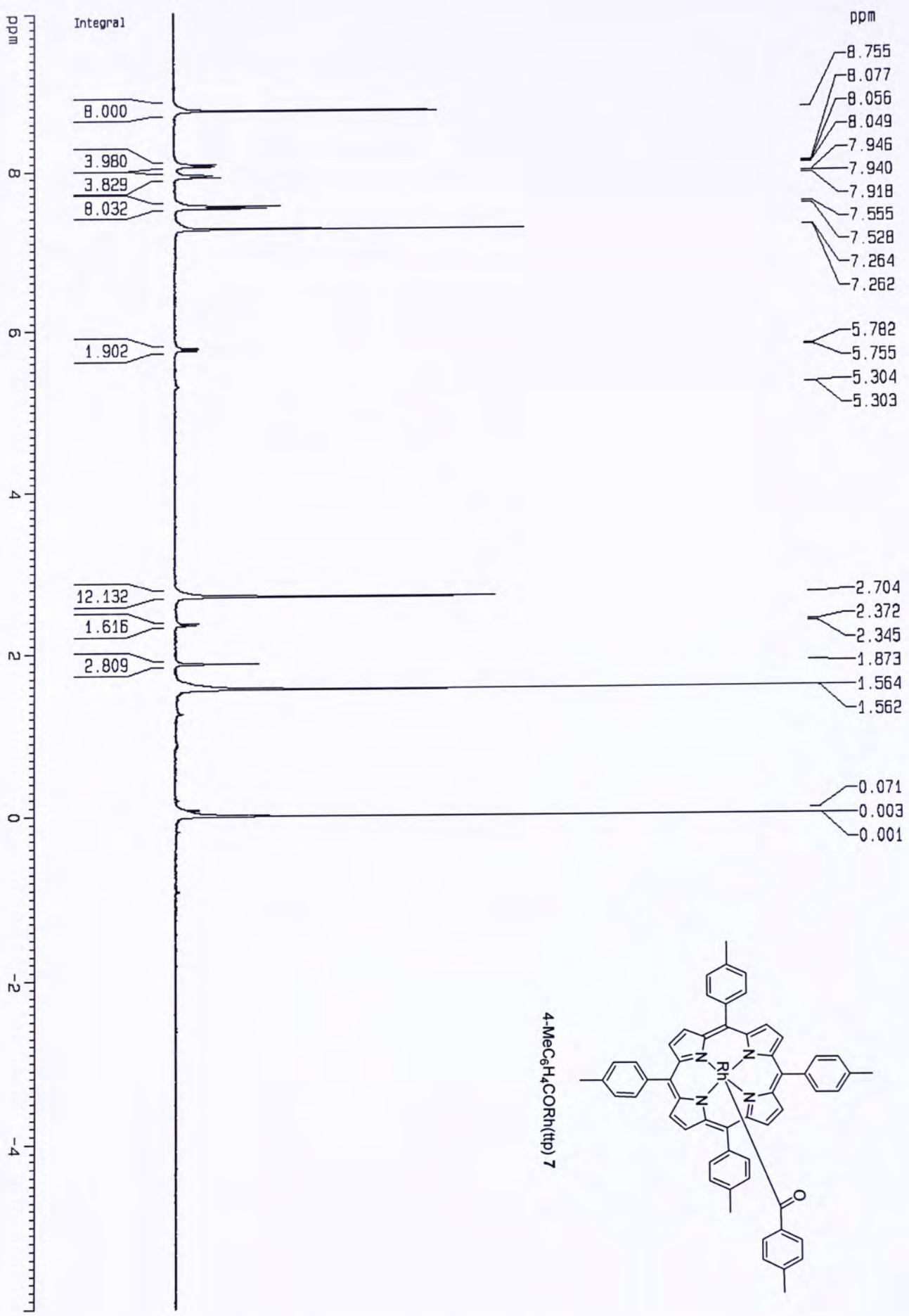
Current Data Parameters
NAME CWL362-F2-1
EXPNO 1
PROCNO 1

F2 - Acquisition Parameters
Date_ 20050223
Time 17.45
INSTRUM dpX300
PROBHD 5 mm BBO BB-1H
PULPROG zg
TD 32768
SOLVENT CDCl3
NS 64
DS 0
SWH 8992.806 Hz
FIDRES 0.274439 Hz
AQ 1.8219508 sec
RG 1149.4
DW 55.600 usec
DE 79.43 usec
TE 297.2 K
D1 1.00000000 sec
MCREST 0.00000000 sec
MCMRK 0.01500000 sec

===== CHANNEL f1 =====
NUC1 1H
P1 9.00 usec
PL1 -2.00 dB
SFO1 300.131200 MHz

F2 - Processing parameters
SI 32768
SF 300.130059 MHz
WDW EM
SSB 0
LB 0.30 Hz
GB 0
PC 1.00

1D NMR plot parameters
CX 22.00 cm
CY 30.00 cm
F1P 10.000 ppm
F1 3001.30 Hz
F2P -5.000 ppm
F2 -1800.78 Hz
PPMCM 0.72727 ppm/
HZCM 218.27637 Hz/1



Current Data Parameters

NAME	CML186-F2-1
EXPNO	1
PROCNO	1

F2 - Acquisition Parameters

Date_	20040817
Time	15.17
INSTRUM	dpX300
PROBHD	5 mm BBO BB-1H
PULPROG	zg
TD	32768
SOLVENT	CDCl3
NS	64
DS	0
SWH	8992.806 Hz
FIDRES	0.274439 Hz
AQ	1.8219508 sec
RG	2298.8
DW	55.600 usec
DE	79.43 usec
TE	297.2 K
D1	1.00000000 sec
MCHEST	0.00000000 sec
MCNMR	0.01500000 sec

===== CHANNEL f1 =====

NUC1	1H
P1	9.00 usec
PL1	-2.00 dB
SFO1	300.1312000 MHz

F2 - Processing parameters

SI	32768
SF	300.1300048 MHz
WDW	EM
SSB	0
LB	0.30 Hz
GB	0
PC	1.00

1D NMR plot parameters

CX	22.00 cm
CY	20.00 cm
F1P	10.000 ppm
F1	3001.30 Hz
F2P	-5.000 ppm
F2	-1800.78 Hz
PPMCM	0.72727 ppm/Hz
HZCM	218.27637 Hz/Hz

Current Data Parameters
NAME CML186-F3-1
EXPNO 1
PROCNO 1

F2 - Acquisition Parameters
Date_ 20040817
Time 15.28

INSTRUM dpx300
PROBHD 5 mm BBO BB-1H
PULPROG zg

TD 32768
SOLVENT CDCl3
NS 64

DS 0
SWH 8992.806 Hz
FIDRES 0.274439 Hz

AQ 1.8219508 sec
RG 2896.3
DW 55.600 usec

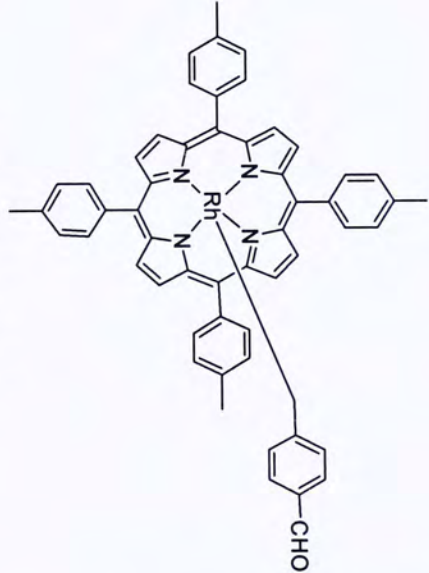
DE 79.43 usec
TE 297.2 K
D1 1.00000000 sec

MCREST 0.00000000 sec
MCWPRK 0.01500000 sec

----- CHANNEL f1 -----
NUC1 1H
P1 9.00 usec
PL1 -2.00 dB
SFO1 300.1312000 MHz

F2 - Processing parameters
SI 32768
SF 300.1300051 MHz
WDW EM
SSB 0
LB 0.30 Hz
GB 0
PC 1.00

1D NMR plot parameters
CX 22.00 cm
CY 50.00 cm
F1P 10.000 ppm
F1 3001.30 Hz
F2P -5.000 ppm
F2 -1800.78 Hz
PPMCM 0.78727 ppm,
HZCM 218.27637 Hz/1

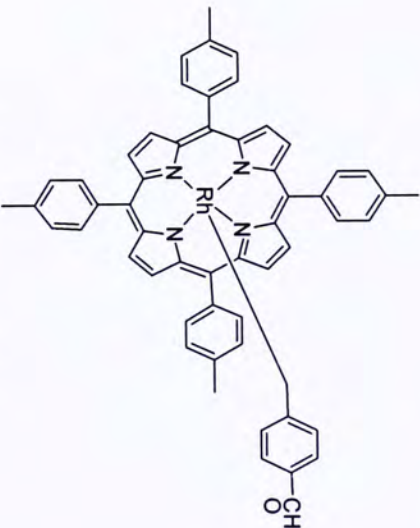


ppm

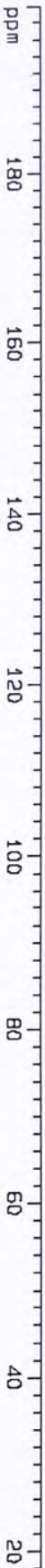
143.614
139.573
137.816
134.356
132.179
132.019
128.000
125.231
123.152

90.149
77.945
77.723
77.521
77.098

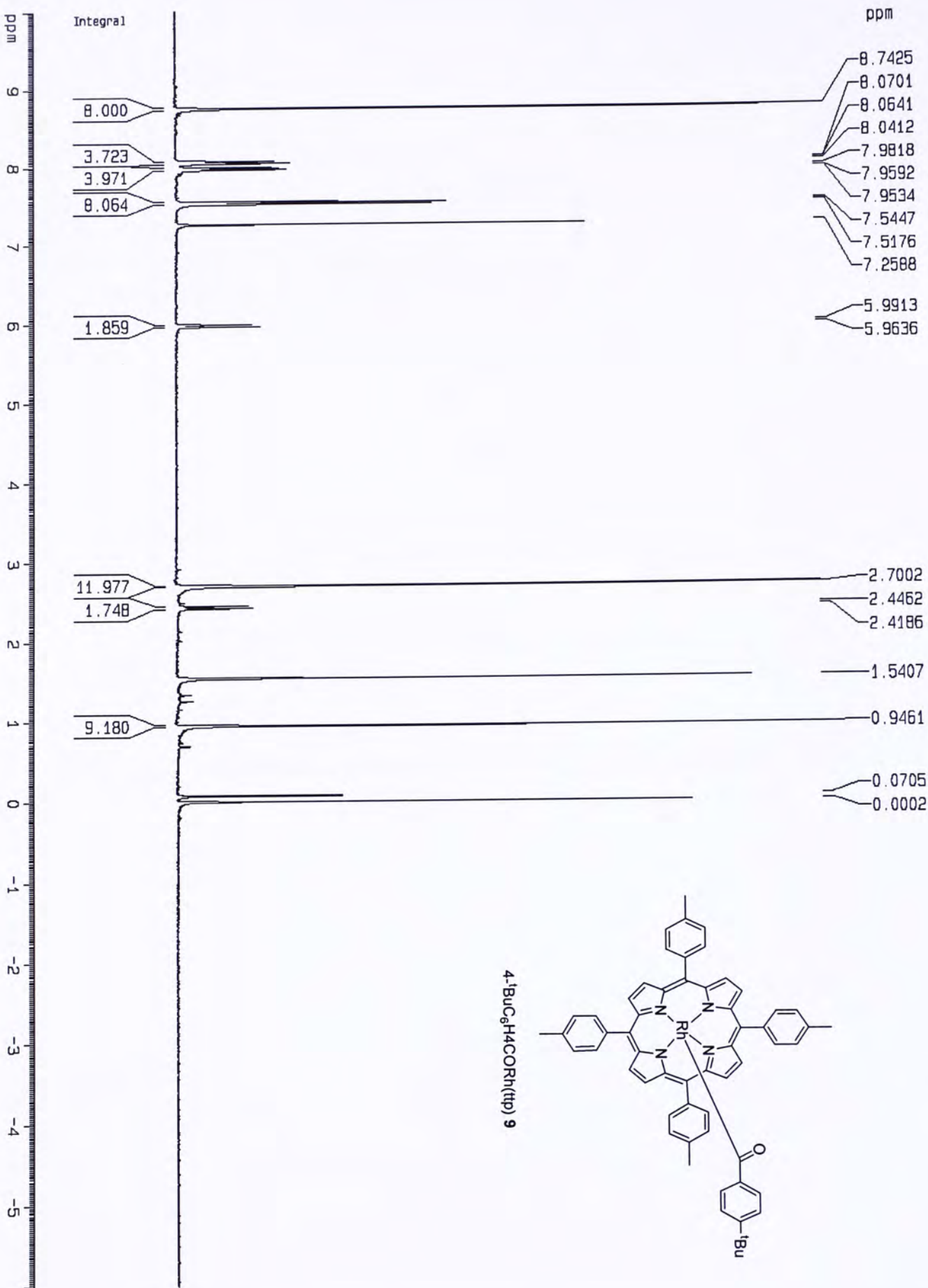
22.048



4-CHOC₆H₄CH₂Rh(tp)₃
¹³C NMR



Current Data Parameters	
NAME	CML186-3-C
EXPNO	1
PROCNO	1
F2 - Acquisition Parameters	
Date_	20050510
Time	22.06
INSTRUM	dpv300
PROBHD	5 mm BBO BB-1H
PULPROG	zgpg30
TD	65536
SOLVENT	CDCl3
NS	16876
DS	0
SWH	30120.482 Hz
FIDRES	0.459602 Hz
AQ	1.0879476 sec
RG	2298.8
DW	16.800 usec
DE	6.00 usec
TE	297.2 K
D1	1.00000000 sec
d11	0.03000000 sec
MCREST	0.00000000 sec
MCPRK	0.01500000 sec
CHANNEL f1	
NUC1	¹³ C
P1	3.00 usec
PL1	-6.00 dB
SFO1	75.4745111 MHz
CHANNEL f2	
CPDPRG2	waltz16
NUC2	¹ H
PCPD2	100.00 usec
PL2	120.00 dB
PL12	19.00 dB
SFO2	300.1315007 MHz
F2 - Processing parameters	
SI	65536
SF	75.4677113 MHz
MDW	EM
SSB	0
LB	3.00 Hz
GB	0
PC	1.40
1D NMR plot parameters	
CX	23.00 cm
CV	80.00 cm
F1P	200.000 ppm
F1	15093.54 Hz
F2P	0.000 ppm
F2	0.00 Hz
BPNCM	8.65965 ppm
HZCM	656.24097 Hz/c



Current Data Parameters

NAME	A'stubby1
EXPNO	1
PROCNO	1

F2 - Acquisition Parameters

Date_	20050612
Time	23.09
INSTRUM	dp300
PROBHD	5 mm BBO BB-1H
PULPROG	zg
TD	32768
SOLVENT	CDCl3
NS	32
DS	0
SWH	8992.806 Hz
FIDRES	0.274439 Hz
AQ	1.8219508 sec
RG	812.7
DM	55.600 usec
DE	79.43 usec
TE	297.2 K
D1	1.00000000 sec
MCREST	0.00000000 sec
MCNRC	0.01500000 sec

----- CHANNEL f1 -----

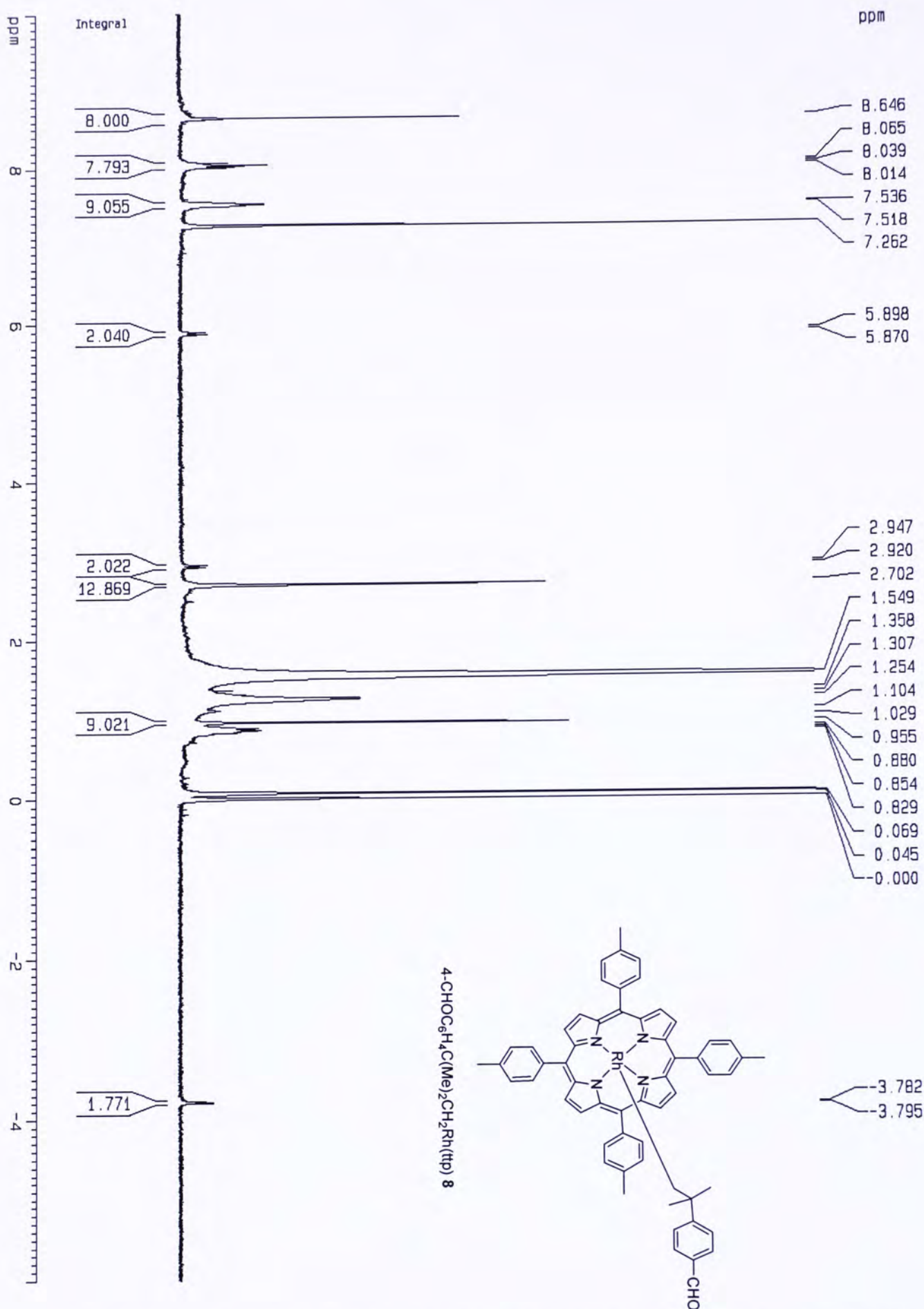
NUC1	1H
P1	9.00 usec
PL1	-2.00 dB
SFO1	300.1312000 MHz

F2 - Processing parameters

SI	32768
SF	300.1300065 MHz
WDW	EM
SSB	0
LB	0.30 Hz
GB	0
PC	1.00

1D NMR plot parameters

CX	22.00 cm
CY	20.00 cm
F1P	10.000 ppm
F1	3001.30 Hz
F2P	-6.000 ppm
F2	-1800.78 Hz
PPMCM	0.72727 ppm/1
HZCM	218.27637 Hz/1



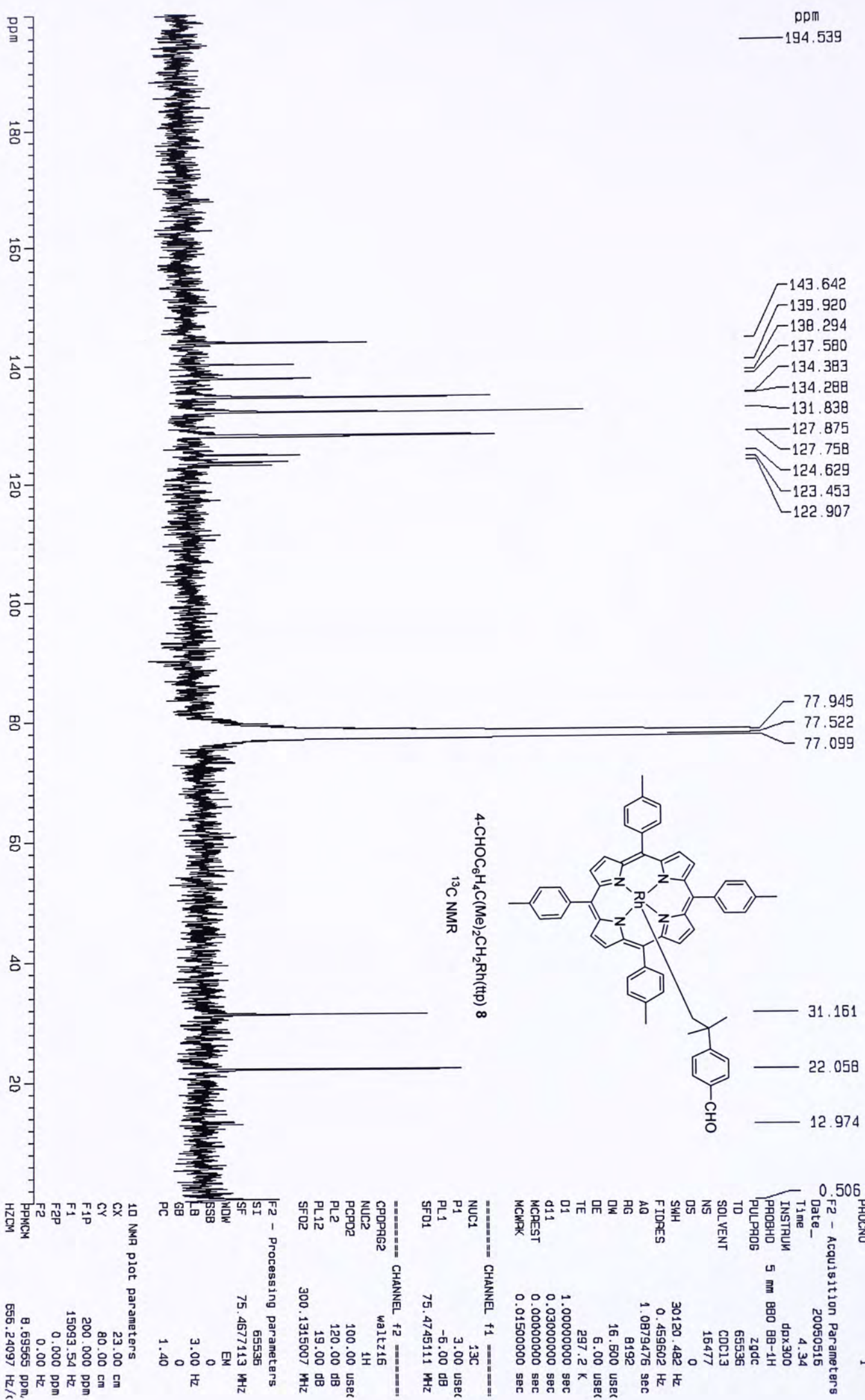
Current Data Parameters
NAME CML095-F1-1
EXPNO 1
PROCNO 1

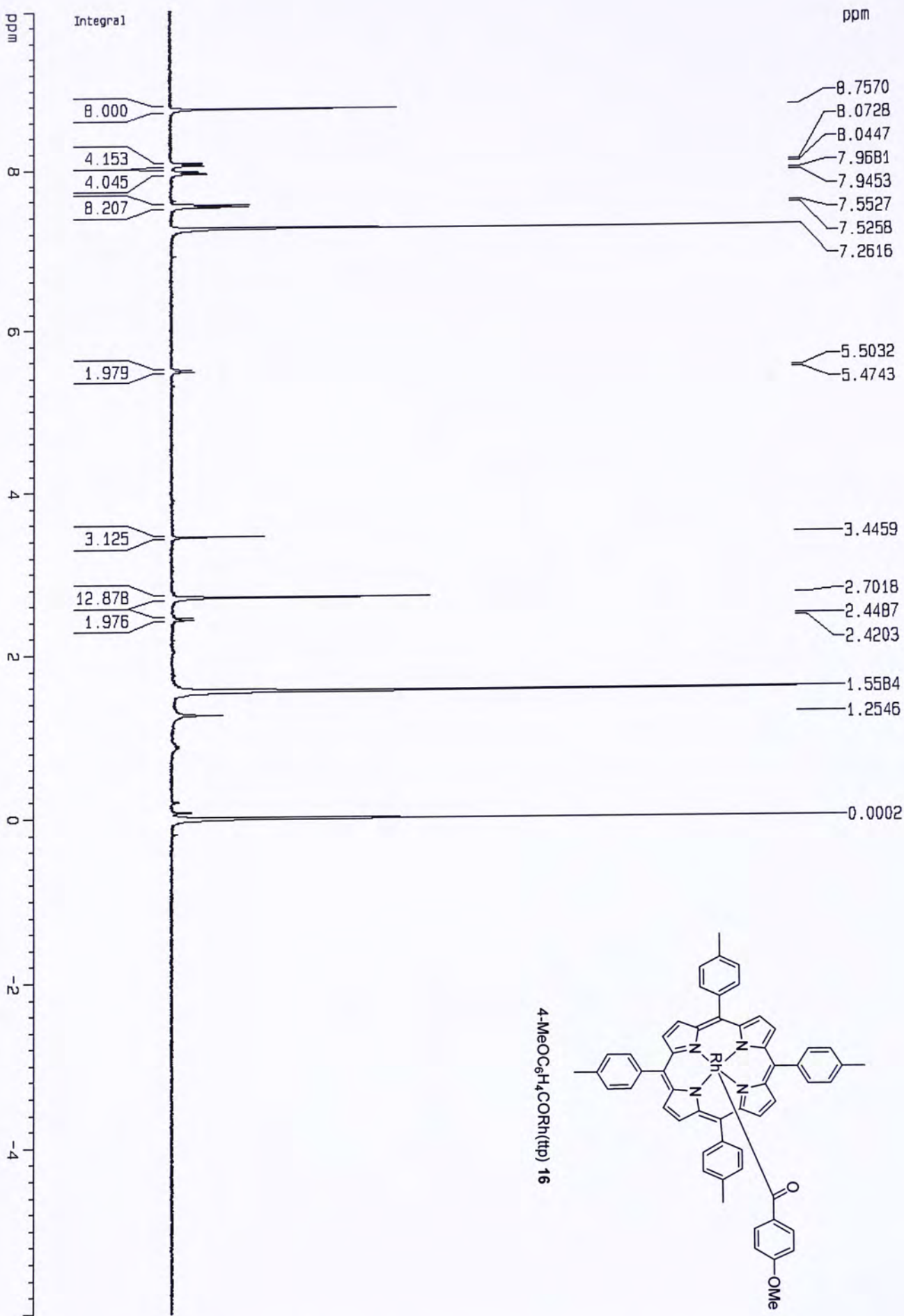
F2 - Acquisition Parameters
Date_ 20040330
Time 13.45
INSTRUM dpx300
PROBHD 5 mm BBO BB-1H
PULPROG zg
TD 32768
SOLVENT CDCl3
NS 64
DS 0
SWH 8992.806 Hz
FIDRES 0.274439 Hz
AQ 1.8219508 sec
RG 1024
DE 55.600 usec
TE 298.2 K
D1 1.00000000 sec
MCREST 0.00000000 sec
MCMRK 0.01500000 sec

----- CHANNEL f1 -----
NUC1 1H
P1 9.00 usec
PL1 -2.00 dB
SFO1 300.131200 MHz

F2 - Processing parameters
SI 32768
SF 300.130054 MHz
WDW EM
SSB 0
LB 0.30 Hz
GB 0
PC 1.00

1D NMR plot parameters
CX 22.00 cm
CY 30.00 cm
F1P 10.000 ppm
F1 3001.30 Hz
F2P -5.000 ppm
F2 -1800.78 Hz
PPMCM 0.78727 ppm/
HZCM 218.27637 Hz/1





Current Data Parameters

NAME	CML215-F2-1
EXPNO	1
PROCNO	1

F2 - Acquisition Parameters

Date_	20041021
Time	14.09
INSTRUM	dpX300
PROBHD	5 mm BBO BB-1H
PULPRDG	zg
TD	32768
SOLVENT	CDCl3
NS	64
DS	0
SWH	8992.806 Hz
FIDRES	0.274439 Hz
AQ	1.8219608 sec
RG	1149.4
DW	55.600 usec
DE	79.43 usec
TE	0.0 K
D1	1.00000000 sec
MCREST	0.00000000 sec
MCNMRK	0.01500000 sec

===== CHANNEL f1 =====

NUC1 1H

P1 9.00 usec

PL1 -2.00 dB

SFO1 300.131200 MHz

F2 - Processing parameters

SI	32768
SF <td>300.1300056 MHz</td>	300.1300056 MHz
MDW <td>EM</td>	EM
SSB <td>0</td>	0
LB <td>0.30 Hz</td>	0.30 Hz
GB <td>0</td>	0
PC <td>1.00</td>	1.00

1D NMR plot parameters

CX	22.00 cm
CY <th>30.00 cm</th>	30.00 cm
F1P <th>10.000 ppm</th>	10.000 ppm
F4 <th>3001.30 Hz</th>	3001.30 Hz
F2P <th>-5.000 ppm</th>	-5.000 ppm
F2 <th>-1800.78 Hz</th>	-1800.78 Hz
PPMCM <th>0.72727 ppm,</th>	0.72727 ppm,
HZCM <th>218.27637 Hz/t</th>	218.27637 Hz/t

Current Data Parameters
 NAME CML272-F1-1
 EXPNO 1
 PROCNO 1

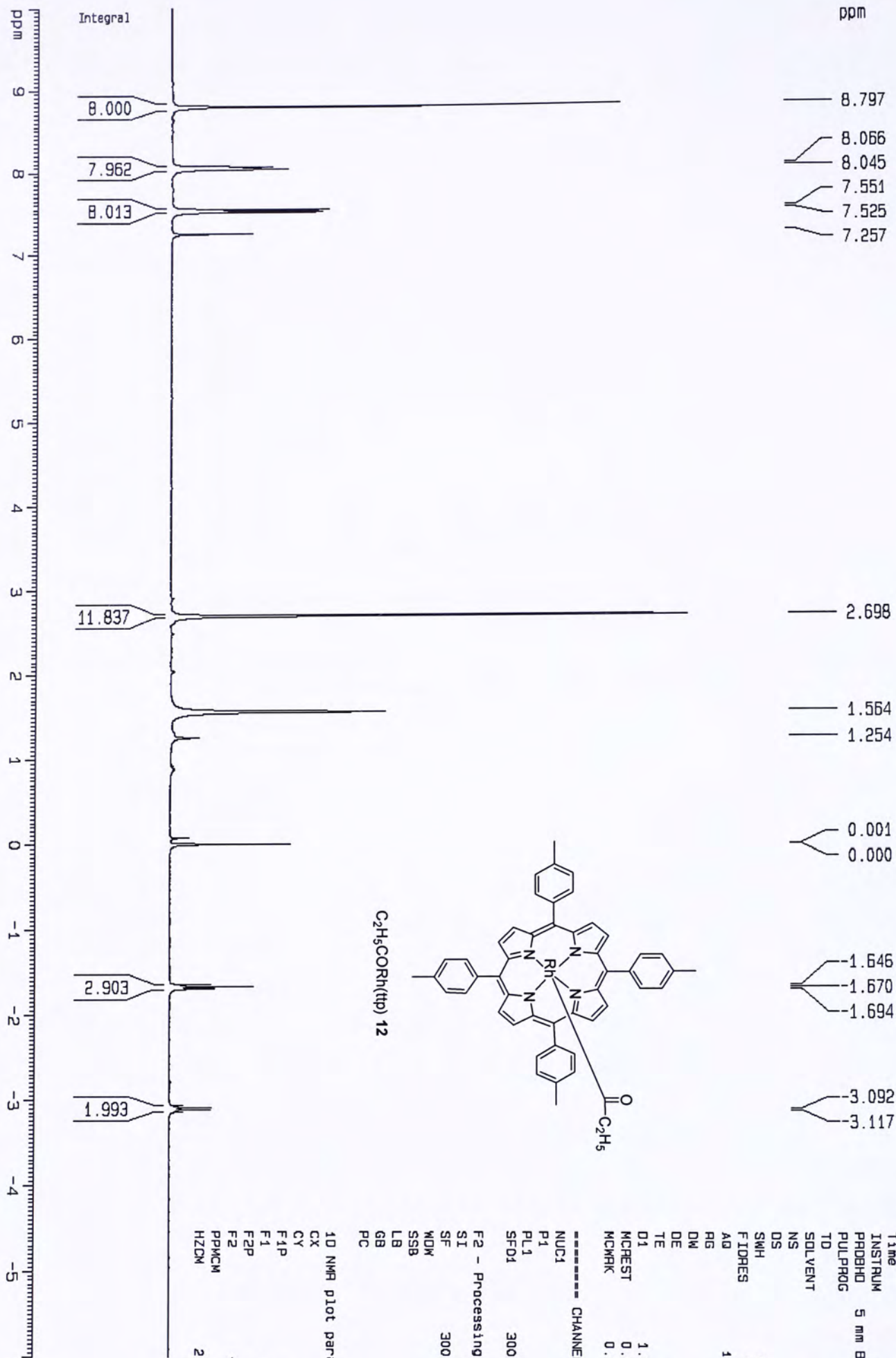
F2 - Acquisition Parameters

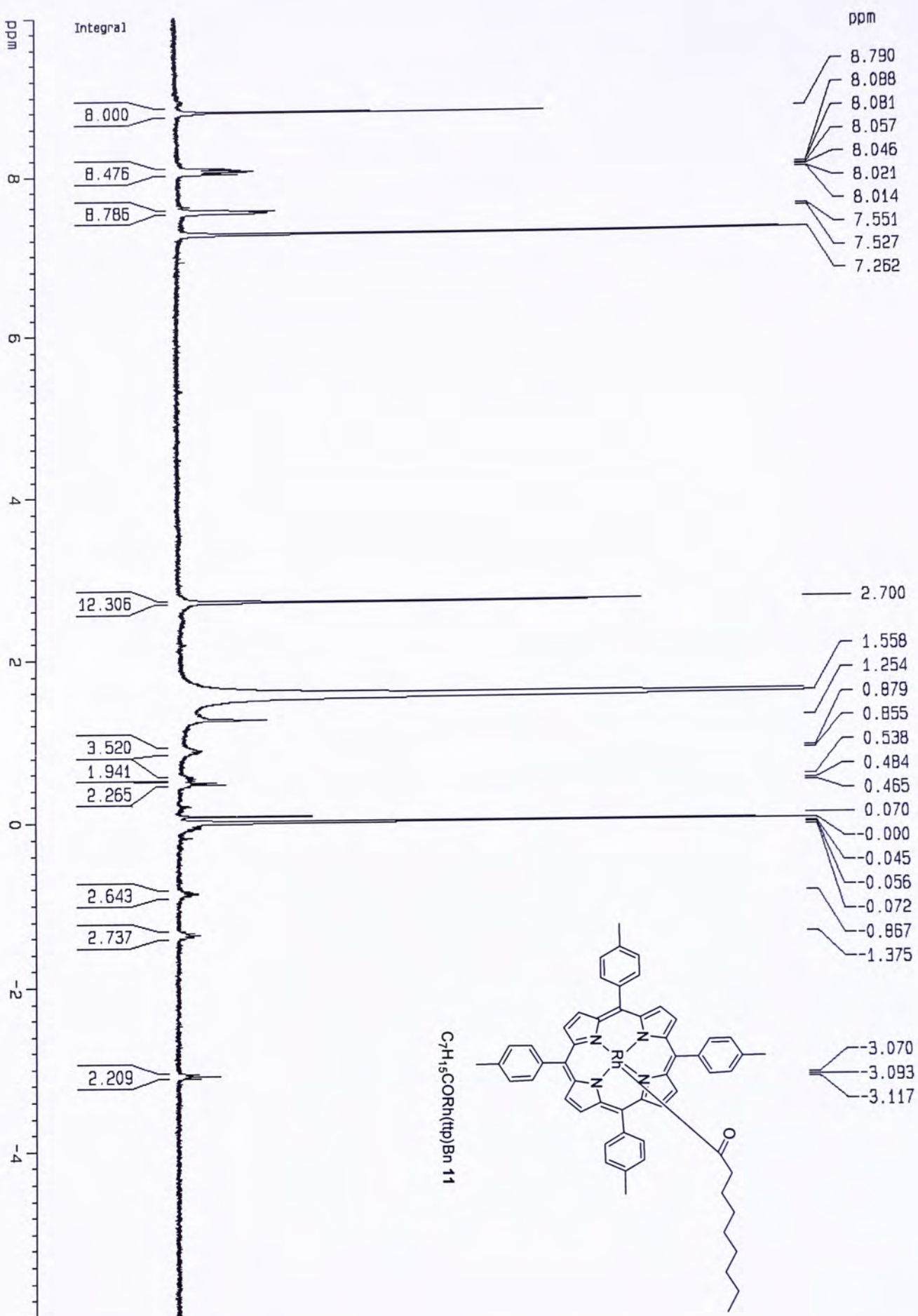
Date_ 20041205
 Time 13.49
 INSTRUM dpx300
 PROBHD 5 mm BBO BB-1H
 PULPROG zg
 TD 32768
 SOLVENT CDCl3
 NS 32
 DS 0
 SWH 8992.605 Hz
 FIDRES 0.274439 Hz
 AQ 1.8219508 sec
 RG 322.5
 DW 55.600 usec
 DE 79.43 usec
 TE 0.0 K
 D1 1.00000000 sec
 MCREST 0.00000000 sec
 MCMRK 0.01500000 sec

===== CHANNEL f1 =====
 NUC1 1H
 P1 9.00 usec
 PL1 -2.00 dB
 SFO1 300.131200 MHz

F2 - Processing parameters
 SI 32768
 SF 300.130070 MHz
 WDW EM
 SSB 0
 LB 0.30 Hz
 GB 0
 PC 1.00

1D NMR plot parameters
 CX 22.00 cm
 CY 10.00 cm
 F1P 10.000 ppm
 F1 3001.30 Hz
 F2P -6.000 ppm
 F2 -1800.78 Hz
 PPMCM 0.72727 ppm/cm
 HZCM 218.27637 Hz/cm





Current Data Parameters
NAME CML224-f2-2
EXPNO 1
PROCNO 1

F2 - Acquisition Parameters
Date_ 20041029
Time 14.29
INSTRUM dpx300
PROBHD 5 mm BBO BB-1H
PULPROG zg
TD 32768
SOLVENT CDCl3
NS 64
DS 0
SWH 8992.806 Hz
FIDRES 0.274439 Hz
AQ 1.8219508 sec
RG 1024
DW 55.600 usec
DE 79.43 usec
TE 0.0 K
D1 1.00000000 sec
MCREST 0.00000000 sec
MCMRK 0.01500000 sec

CHANNEL f1
NUC1 1H
P1 9.00 usec
PL1 -2.00 dB
SFO1 300.1312000 MHz

F2 - Processing parameters
SI 32768
SF 300.1300054 MHz
WDW EM
SSB 0
LB 0.30 Hz
GB 0
PC 1.00

1D NMR plot parameters
CX 22.00 cm
CY 50.00 cm
F1P 10.000 ppm
F1 3001.30 Hz
F2P -6.000 ppm
F2 -1800.78 Hz
PPMCH 0.72727 ppm,
HZCH 218.27637 Hz/i

ppm

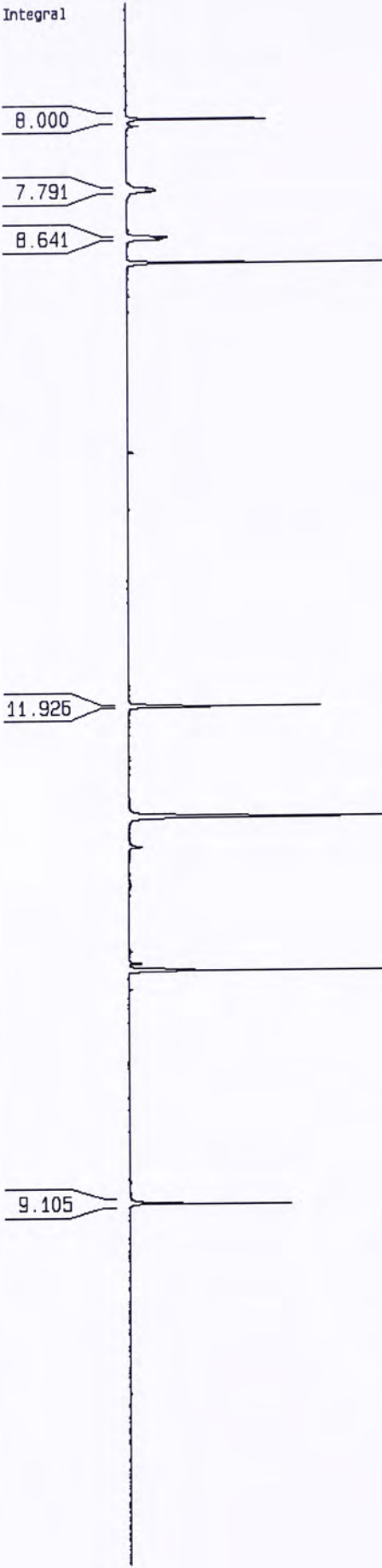
8.769
8.049
8.026
8.012
7.539
7.516
7.263

2.694

1.564

0.071
0.011
0.000

-2.333
-2.358



¹BuRh(ttp) 13

Current Data Parameters
NAME CML172-F2-1
EXPNO 1
PROCNO 1

F2 - Acquisition Parameters
Date_ 20040817
Time 14.40

INSTRUM dpx300
PROBHD 5 mm BBO BB-1H
PULPRDG zg
TD 32768
SOLVENT CDCl3
NS 64
DS 0

SMH 8992.806 Hz
FIDRES 0.274439 Hz
AQ 1.8219508 sec
RG 1625.5

DM 55.600 usec
DE 79.43 usec
TE 297.2 K

D1 1.00000000 sec
MCREST 0.00000000 sec
MCMRK 0.01500000 sec

===== CHANNEL f1 =====

NUC1 1H
P1 9.00 usec
PL1 -2.00 dB
SFO1 300.131200 MHz

F2 - Processing parameters

SI 32768
SF 300.130048 MHz
WDW EM
SSB 0
LB 0.30 Hz
GB 0
PC 1.00

1D NMR plot parameters

CX 22.00 cm
CY 10.00 cm
F1P 10.000 ppm
F1 3001.30 Hz
F2P -6.000 ppm
F2 -1800.78 Hz
PPMCM 0.72727 ppm/
HZCM 218.27637 Hz/1

CUHK Libraries



004278929